U.S. Department of the Interior
U.S. Geological Survey

HYDROGEOLOGIC FRAMEWORK, WATER LEVELS, AND TRICHLOROETHYLENE CONTAMINATION, NAVAL AIR WARFARE CENTER, WEST TRENTON, NEW JERSEY, 1993-97

Water-Resources Investigations Report 98-4167

Prepared in cooperation with the

U.S. NAVY

USGS
science for a changing world

HYDROGEOLOGIC FRAMEWORK, WATER LEVELS, AND TRICHLOROETHYLENE CONTAMINATION, NAVAL AIR WARFARE CENTER, WEST TRENTON, NEW JERSEY, 1993-97

By Pierre J. Lacombe

U.S. Geological Survey

Water-Resources Investigations Report 98-4167

Prepared in cooperation with the

U.S. NAVY

West Trenton, New Jersey

2000

USGS

science for a changing world

U.S. DEPARTMENT OF THE INTERIOR

BRUCE BABBITT, *Secretary*

U.S. GEOLOGICAL SURVEY

Charles G. Groat, *Director*

For additional information
write to:

District Chief
U.S Geological Survey
Mountain View Office Park
810 Bear Tavern Road, Suite 206
West Trenton, NJ 08628

Copies of this report can be
purchased from:

U.S. Geological Survey
Branch of Information Services
Box 25286
Denver, CO 80225-0286

CONTENTS

CONTENTS--Continued

ILLUSTRATIONS

ILLUSTRATIONS--Continued

ILLUSTRATIONS--Continued

ILLUSTRATIONS--Continued

ILLUSTRATIONS--Continued

ILLUSTRATIONS--Continued

ILLUSTRATIONS--Continued

TABLES

CONVERSION FACTORS, VERTICAL DATUM, AND ABBREVIATED WATER-QUALITY UNITS

Multiply	By	To obtain
	Length	
inch (in)	2.54	centimeter
inch (in)	25.4	millimeter
foot (ft)	0.3048	meter
mile (mi)	1.609	kilometer
	Area	
acre	4047	square meter
square mile (mi^2)	2.59	square kilometer
square mile	640	acre
	Volume	
gallon (gal)	3.785	liter
gallon (gal)	7.48	cubic foot
cubic foot (ft^3)	.02832	cubic meter
	Flow	
cubic feet per second (ft^3/s)	.02832	cubic meter per second
cubic feet per second (ft^3/s)	449	gallons per minute
gallons per minute (gal/min)	0.06309	liter per second

Altitude In this report, "altitude" refers to distance above or below the National Geodetic Vertical Datum of 1929 (NVGD of 1929. Its use is not affected by whether the distance is above of below land surface.

Sea level: In this report, "sea level" refers to the National Geodetic Vertical Datum of 1929 (NGVD of 1929)—a geodetic datum derived from a general adjustment of the first-order level nets of both the United States and Canada, formerly called Sea Level Datum of 1929.

Concentrations of chemical constituents in water are given either in milligrams per liter (mg/L) or micrograms per liter (mg/L).

HYDROGEOLOGIC FRAMEWORK, WATER LEVELS, AND TRICHLOROETHYLENE CONTAMINATION, NAVAL AIR WARFARE CENTER, WEST TRENTON, NEW JERSEY, 1993-97

By Pierre J. Lacombe

Abstract

Geophysical, drillers, and geologist logs from 48 bedrock wells at the Naval Air Warfare Center (NAWC) in West Trenton, N.J., were examined and interpreted to prepare structure maps and sections of the hydrogeologic framework. The maps and sections show the geometry of the Stockton aquifer with 5 bedding units and Lockatong aquifer with 14 bedding units. Each bedding unit consists of water-bearing zones and semi-confining zones. An east/west-trending fault crosses the southern part of NAWC and acts as a confining unit.

A 1913 topographic map shows the West Branch of Gold Run flowed along Parkway Avenue from the west side to the east side of NAWC. A 1942 roadway construction map shows that the stream was confined in a culvert under Parkway Avenue. The stream/culvert is still active as a ground-water/surface-water discharge area.

Static water levels from the 48 wells indicated that the ground-water-flow direction in the Lockatong aquifer is along bedding strike and to the west with discharge into the West Branch of Gold Run. Drawdown water levels during three aquifer tests indicated that the Lockatong aquifer is anisotropic. The water-bearing zones in the aquifer are isotropic or nearly so in the plane of the zone. Stressed water levels for 48 bedrock wells show that the recovery well causes a local anisotropic cone of depression, which probably does not capture the whole TCE contamination plume.

Analysis of water-quality data from the 48 wells indicate the extent of plumes of trichloroethylene (TCE) and its degradation products, cis-1,2-dichloroethylene (cis-DCE) and vinyl chloride (VC). The TCE plume emanating from a waste lagoon and sludge-disposal area (Site 3) is moving along strike to the west along the north side of the fault. The TCE plume emanating from a brine-handing area (Site 1) is interpreted for two scenarios. Scenario 1 assumes that dense non-aqueous phase liquid (DNAPL) TCE has sunk into the Lockatong aquifer to a depth of more than 200 ft. Scenario 2 assumes that the DNAPL TCE has dissolved by a depth of 100 ft below land surface. cis-DCE and VC concentrations indicate that degradation of TCE is occurring at depths of 0 to 100 ft below land surface but that degradation is not occurring to a significant extent at greater depths. The cis-DCE and VC plumes appear to be moving west of Site 1 as a result of ground-water flow. Centers of the cis-DCE and VC plumes are 100 and 200 ft, respectively, west of the center of the TCE plume.

INTRODUCTION

The U.S. Naval Air Warfare Center (NAWC) in West Trenton, N.J., was a jet engine testing facility for military aircraft from the mid-1950's until the late 1990's. As a result of the activities at the facility, trichloroethylene (TCE) and other chemicals have leaked onto the ground surface. TCE and other compounds have been detected in ground water at two sites at the NAWC (figs. 1 and 2). During a remedial investigation, high concentrations of TCE, as well as its degradation products, cis 1,2-dichloroethylene (cis-DCE) and vinyl chloride (VC), and other contaminants were detected in ground water at the NAWC (International Technology Corp., 1994). Reported concentrations of TCE dissolved in ground water in a brine-handling area (Site 1) during 1992-93 ranged from less than 10 mg/L to more than 20,000 mg/L. The latter concentrations strongly indicate the presence of non-aqueous phase TCE. At the same time, reported concentrations of TCE dissolved in ground water in a wastewater lagoon and sludge disposal-area (Site 3) ranged from less than the detection limit of 10 mg/L to 320 mg/L (International Technology Corp., 1994).

During 1993-97 the USGS, in cooperation with the U.S. Navy, conducted several studies to determine the hydrogeologic framework of the site, measure and map ground-water levels, collect samples for water-quality analysis, and map ground-water contamination plumes at the NAWC. The USGS also provided technical oversight and assistance to the U.S. Navy. During the same time, the US. Navy contracted EA Engineering, Science, and Technology Inc. to provide drilling services, collect water- quality samples for analysis, and measure water levels.

Purpose and Scope

This report presents an integrated interpretation of the hydrogeologic data collected at Sites 1 and 3 at the U.S. Naval Air Warfare Center (NAWC). This report includes maps and sections that describe and show the hydrogeologic framework of the bedrock, the distribution of ground-water levels, and the extent and distribution of contamination by TCE, cis-DCE, and VC. The USGS collected geophysical logs from 48 bedrock wells at the NAWC. Geologists' logs, core logs, water-level data, drawdown data from aquifer tests, and water-quality data are from published remedial investigation reports (International Technology Corp., 1994) and site interim action reports (EA Engineering, Science, and Technology Inc., 1995, 1996a, 1996b, 1996c, and 1997.

Previous Investigations

International Technology Corporation (1994) conducted a remedial investigation of the NAWC. The final report is in 6 volumes, and it covers the hydrogeologic framework, ground-water levels, ground-water quality, and surface-water quality. EA Engineering, Science, and Technology, Inc. (1995, February 1996, June 1996, July 1996, and August 1997) continued the framework, water-level, and water-quality investigation. Unpublished geologic maps (Hugh Houghton, N.J. Department of Environmental Protection, written commun., 1985) and published reports (Lyttle and Epstein, 1987; Vecchioli and Palmer, 1962) show the regional geology for areas that surround the NAWC.

Description of Study Area

The U.S. Naval Air Warfare Center (NAWC) is a 65-acre site in west central New Jersey. During World War II, the base was much larger and included what is in 1997 the Mercer County Airport (fig. 1). Currently, the

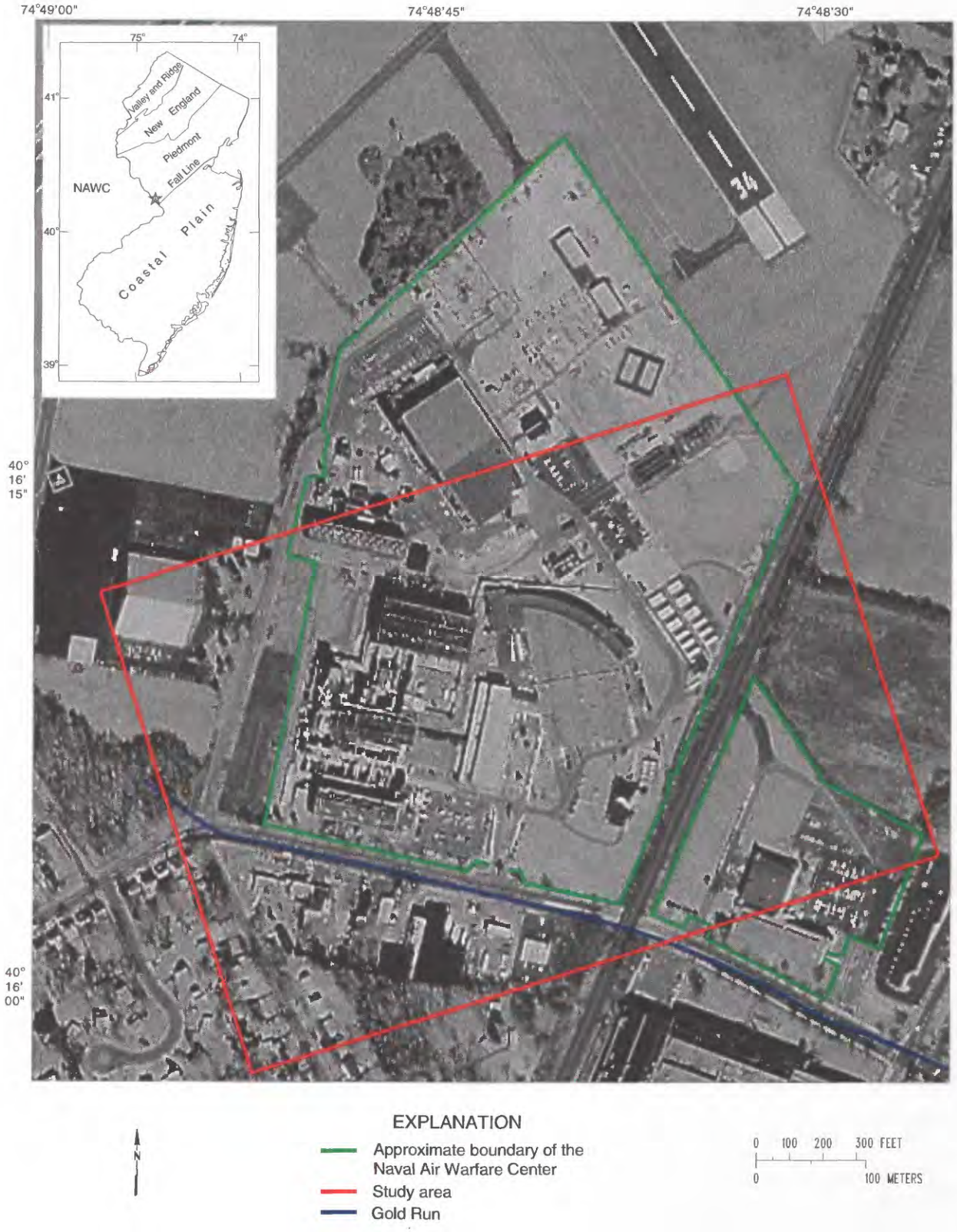

Figure 1. Digital orthophoto showing the location of the study area, Naval Air Warfare Center, West Trenton, N.J.

base is bordered by the Mercer County Airport on the north, west, and east and by Parkway Avenue on the south (fig. 2). Commercial and industrial firms occupy the south side of Parkway Avenue. Freight train tracks separate the eastern part of the base from the western part of the base.

The base is in the Piedmont physiographic province. Bedrock in the region consists of the Lockatong Formation, which is predominantly a shale, and the Stockton Formation which is predominantly a sandstone. A thrust fault runs diagonally across the southern part of the base. The natural topography in this physiographic province is usually characterized by low rolling hills; however, much of the land has been leveled or terraced to accommodate the NAWC and airport runway. Therefore, small hills have been leveled, and small depressions have been filled. The NAWC has been terraced so that the northern part of the base has an altitude of about 170 ft, and the southern part of the base has an altitude of about 150 ft.

A spring in the wooded area near the southwest corner of NAWC flows nearly all year. The spring forms the headwaters for the West Branch of Gold Run (fig. 2). During colonial times, a trail or dirt road ran along the West Branch of Gold Run. By the early 1900's, the West Branch of Gold Run flowed in a ditch along Parkway Avenue. Sometime before 1940 the West Branch of Gold Run was confined to a culvert underneath Parkway Avenue. Today (1998), flow in the West Branch of Gold Run is visible through storm grates and at the entrance and exit culverts along Parkway Avenue.

Acknowledgments

The author would like to thank Steven Feldman and Joel Dadepogu of EA Engineering, Science, and Technology, Inc. for assistance in collection of field data during this investigation and for the technical review of the hydrogeologic interpretations. In addition, the author would like to thank Jeffery Dale, Edward Boyle, and Kenneth Smith of the U.S. Navy for guidance, direction, and historical perspective of the site. Finally, the author would like to thank Jean Brown, Otto Zapecza, Donald Rice, Thomas Imbrigiotta, and Theodore Ehlke of the USGS. These coworkers provided technical and scientific guidance, expertise, and advice on many facets of this investigation.

DATA COLLECTION AND ANALYSES

This investigation is divided into three components: hydrogeologic framework of the bedrock; ground-water levels during static, drawdown, and stressed conditions; and water-quality analysis for TCE, cis-DCE, and VC contamination. The above components are analyzed collectively so that the discussions of the framework; static, drawdown, and stressed water levels; ground-water-flow gradients and directions; surface-water flow; and water quality complement one another.

Hydrogeologic Framework Development

The hydrogeologic framework is based on geologic field observations, natural gamma-ray logs, and drilling observations at bedrock wells, hydrologic analysis of the geology, static water levels, drawdown water levels that are computed during aquifer tests, stressed water-levels measured during operation of the recovery well, water-quality data, and interpreted surface-water/ground-water interactions. The geologic component of the hydrogeologic framework was developed by mapping outcrops within 1 mile of the NAWC and from published and unpublished geologic and aero-radiometric maps of the area (Vecchioli and Palmer, 1962; Hugh Houghton, written commun., 1985; U.S. Geological

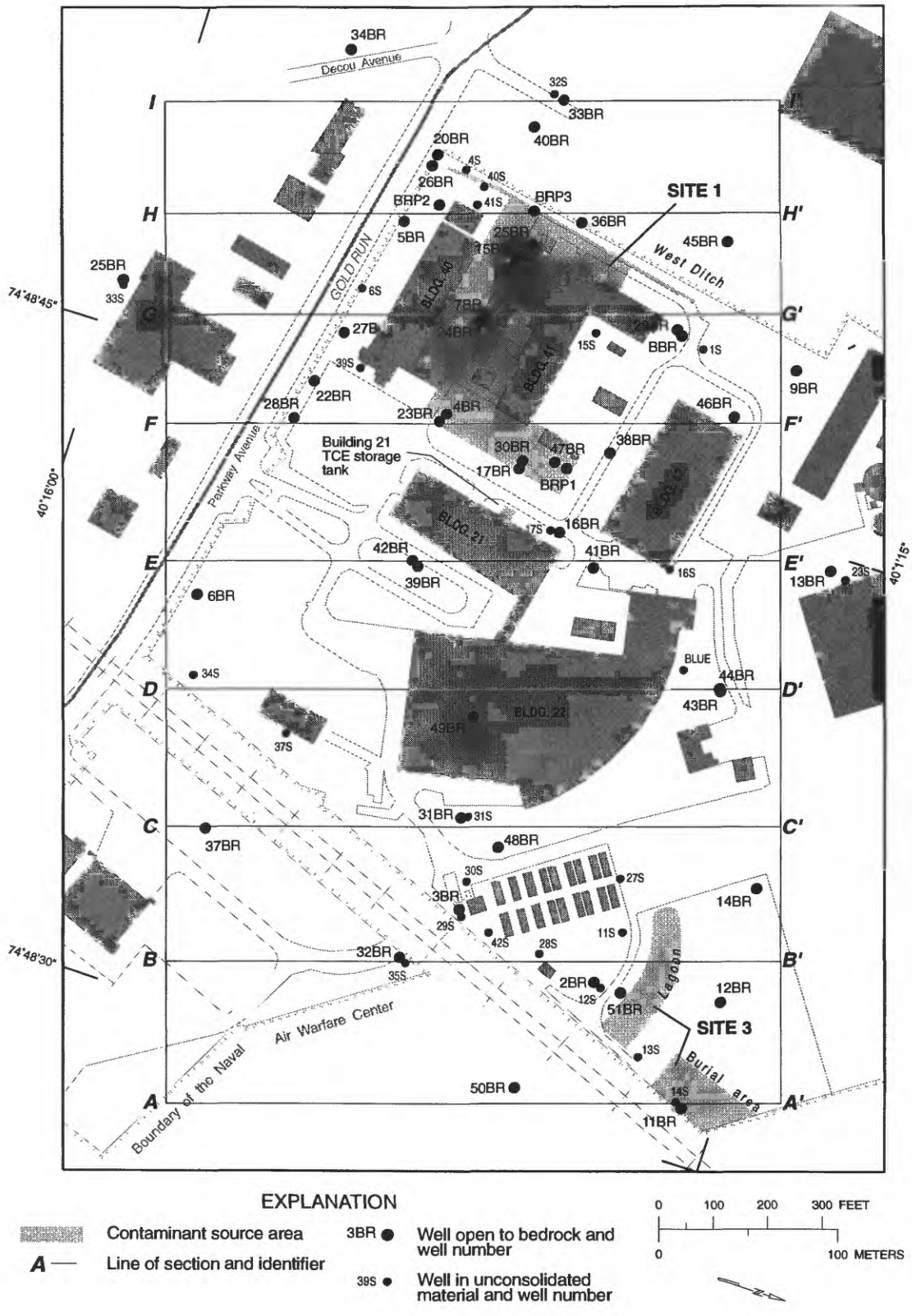

Figure 2. Study area showing location of contamination Sites 1 and 3 and location of bedrock well, Naval Air Warfare Center, West Trenton, N.J.

Survey, 1979). The regional geologic data were enhanced on the NAWC property by review and reevaluation of geologists' and drillers' logs collected from about 50 bedrock monitoring wells (International Technology Corporation, 1994, Appendix A; EA Engineering, Science, and Technology, Inc., 1997, Appendix A), examination of short rock cores from 20 monitoring wells, examination of complete rock cores from 3 wells, and analyses of natural gamma-ray logs collected by the USGS at 25 bedrock monitoring wells.

Water-Level Analyses

The hydrologic component of the hydrogeologic framework was developed from analysis of interpreted ground-water gradients and flowpaths in the bedrock aquifer based on static water-level data collected during December 1995 (EA Engineering, Science, and Technology, Inc., February 1996, table 3-1). In addition, drawdown water levels computed at the end of three aquifer tests were analyzed. The aquifer tests were conducted while pumping wells 15BR, BRP1, and 5BR and measuring the water-level drawdown in 8 to 23 nearby wells (International Technology Corporation, 1994, table 2-2; EA Engineering, Science, and Technology, Inc., July 1996, table 5-2). The static and drawdown water-level data are complemented with stressed water-level data collected during operation of the recovery well (15BR) during August 25-27, 1997. All water-level data were collected with a chalked steel tape or an electric tape. The altitude of the measuring point was leveled in by licensed surveyors.

Water-Quality Analyses

Water quality is evaluated only with respect to TCE, cis-DCE, and VC. TCE, cis-DCE, and VC values are from water samples collected during June 1997 by EA Engineering, Science, and Technology, Inc. (1997, table 1). EA Engineering, Science, and Technology, Inc., adhered to all quality assurance and quality control parameters established at the time of collection by the New Jersey Department of Environmental Protection and by the U.S. Environmental Protection Agency.

Water-Level and Water-Quality Contouring Methods

The techniques used in this study to contour water levels are significantly different from typically used "map view" techniques of contouring the potentiometric surface. In this report, water levels from monitoring wells are plotted in map and section view. Then, the maps and sections are contoured and iteratively modified until the configuration of a potentiometric surface is true in both the map view and section view. The potentiometric surface is, in part, controlled by the estimated water levels for the West Branch of Gold Run and for the spring that is west of the NAWC.

This data display and contouring method results in the following apparent discrepancies. (1) Each measurement point is at the screen interval but in the map views the data are presented so that the measurement point appears to be at land surface. (2) The potentiometric-surface contour lines appear offset in map view because the contours reflect the potentiometric surface in three dimensions. (3) More potentiometric-surface lines are shown in some section views than can be supported by available data because the contours reflect the potentiometric surface in three dimensions. If all the maps and sections are viewed as three-dimensional space, the new contouring technique defines the potentiometric surfaces more accurately than the standard technique of contouring water levels in map view only.

To show how these contouring methods were applied at the NAWC, definitions and discussion, including some fundamental ground-water concepts, are provided for (1) a

gently dipping bedrock aquifer system underlying a small valley and (2) a gently dipping bedrock aquifer system in an area cut by a fault that acts as a confining unit.

The static water level in a monitoring well is controlled by the topography and by the hydrogeologic framework. A potentiometric surface plane encompasses zones of similar ground-water levels. The hydraulic gradients indicate the maximum difference in potentiometric surfaces irrespective of the hydraulic conductivity, whereas ground-water flowpaths indicate differences in potentiometric surface respective of the hydraulic conductivity.

A schematic map and section (figs. 3a1 and 3a2) show a hypothetical small valley underlain by gently dipping sedimentary rocks. The strike of the bedrock in the valley is sub-parallel to the flow direction of the stream, and the dip direction of the bedrock is to the right. Bedding units are labeled A through G, and each bedding unit is composed of many water-bearing zones and semi-confining zones. Wells a to g are screened in their respective bedding unit. Water levels decrease in wells a, b, and c with increasing well depth, and water levels increase in wells e, f, and g with increasing well depth. Wells d, e, f, and g are possibly flowing wells. The water level in each well reflects the water level of the outcrop area of the bedding unit in which the well is screened.

This pattern of water-level decreases on one side of the stream and water-level increases on the other side of the stream invokes a symmetric potentiometric surface map (fig. 3b1) but an asymmetric potentiometric surface section (fig. 3b2). The equipotential planes of the section are skewed to the right so that in the shallow bedrock, the equipotential planes are parallel to the bedding units, but in deep bedrock the equipotential planes are perpendicular to the bedding units. The asymmetric potentiometric surface section indicates an anisotropic bedrock aquifer that consists of (a) numerous thin strata that act as semi-confining zones with few bedding-plane and vertical partings and that have a relatively low hydraulic conductivity and (b) numerous thin strata that act as water-bearing zones with many bedding-plane partings and that have a relatively high hydraulic conductivity.

A flow net usually is depicted as a series of orthorhombic equipotential lines and hydraulic-gradient lines. In three dimensions, a flow net is a series of orthorhombic equipotential planes and hydraulic-gradient planes. The fine-scale hydrogeologic schematic drawing (fig. 4) can be either a map view or a section view of a bedding unit. The schematic diagram depicts a suite of bedding units that are 100's of feet long and only 5 to 25 ft. across. The map/section shows that the bedrock in an anisotropic aquifer consists of the numerous thin semi-confining zones and water-bearing zones. The hydraulic conductivity of the semi-confining zone is much less than the hydraulic conductivity of the water-bearing zone. As a result of this anisotropic nature of the aquifer system, the maximum hydraulic gradient is from A to B, whereas the preferred flowpath is from C to D with a minor flowpath that is from E to F. This two-dimensional schematic analysis is significantly simplified. A three-dimensional analysis, which is the function of a ground-water-flow model, is necessary to qualify and quantify gradient and flowpaths in a fractured-rock aquifer.

Figure 5 is a map and section view of a small valley similar to the example shown in figure 3; in this instance, however, a fault acts as a cross-cutting confining unit. The strike of the bedrock and the fault are parallel with the long axis of the valley, although in the upstream area the stream crosses the fault. Water levels in wells b, c, and d show decreasing water levels with depth. At the fault/confining unit, water will tend to flow in any high conductance zone such that it will flow over, under, or around the confining unit.

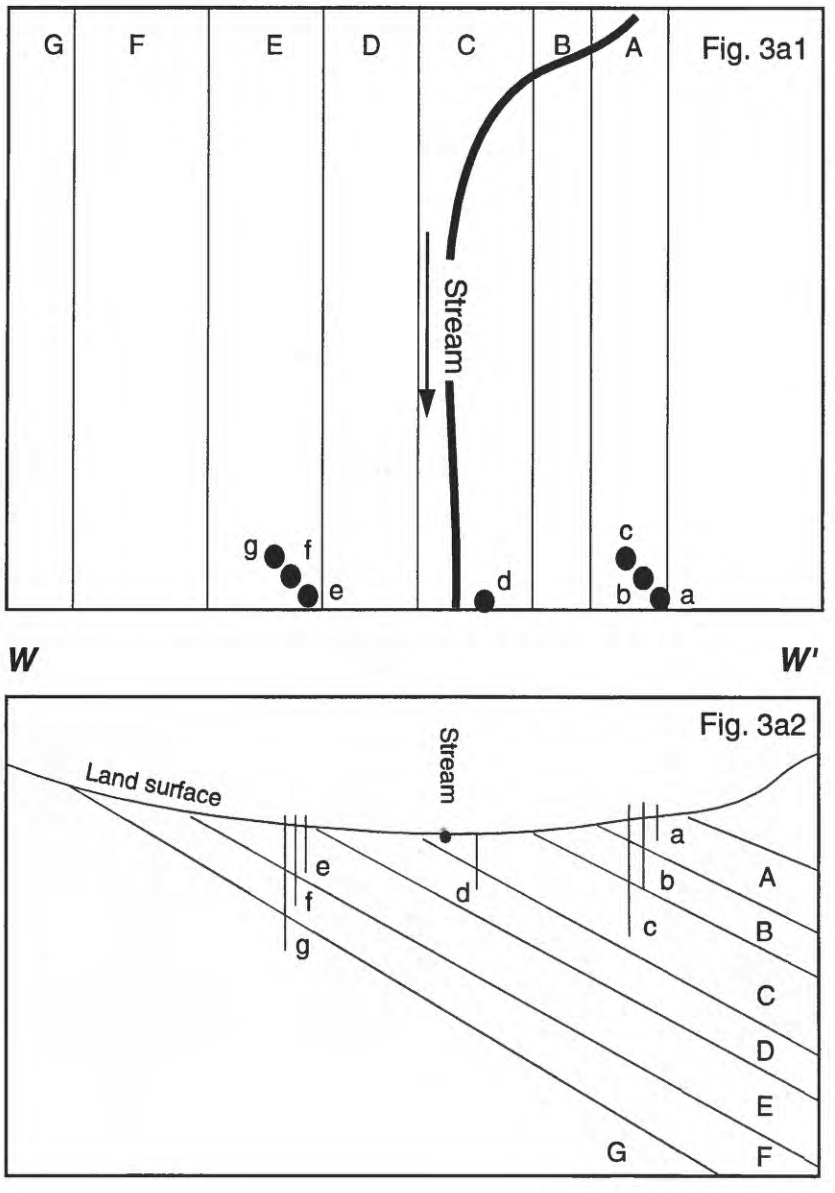

Figures 3a. Map and section *W-W'* showing a hypothetical small valley, strike and dip of bedrock, stream, and wells.

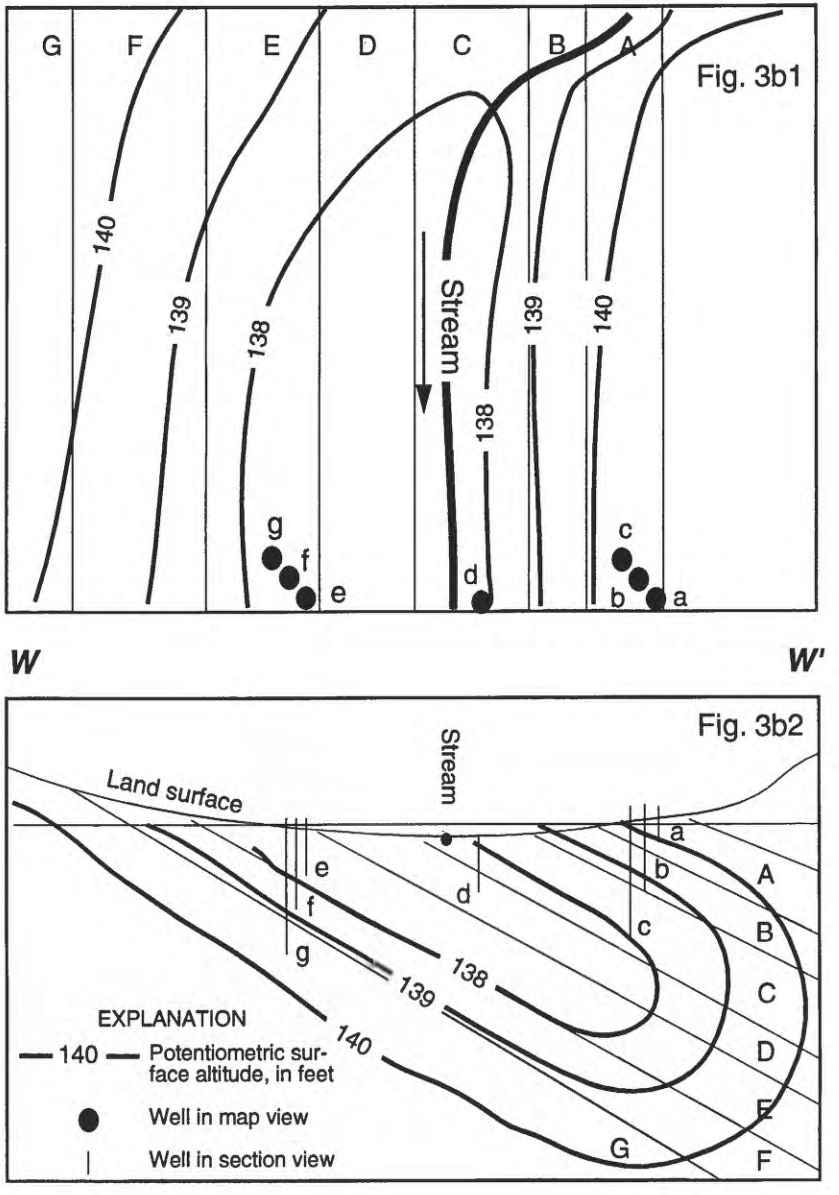

Figures 3b. Map and section *W-W'* showing static potentiometric surface.

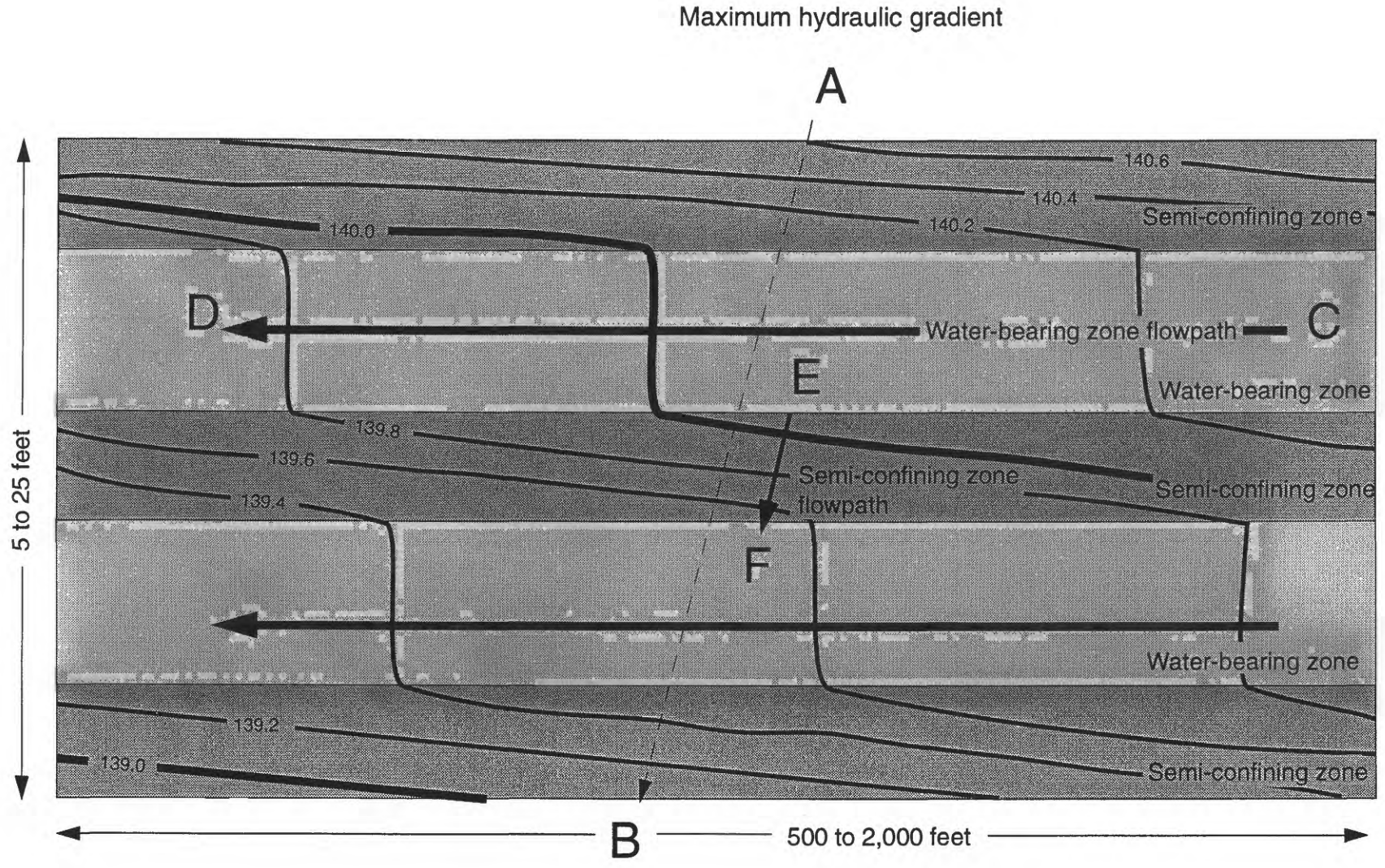

Figure 4. Bedding unit in a hypothetical bedrock aquifer that shows fine-scale water-bearing zones and semi-confining zones. [Potentiometric surface contours are constructed to reflect hydraulic conductivity of the zones. Thin dashed arrow indicates maximum hydraulic gradient (A-B). Thick arrows indicate maximum flow in water-bearing zone (C-D) and limited flow through semi-confining zone (E-F).]

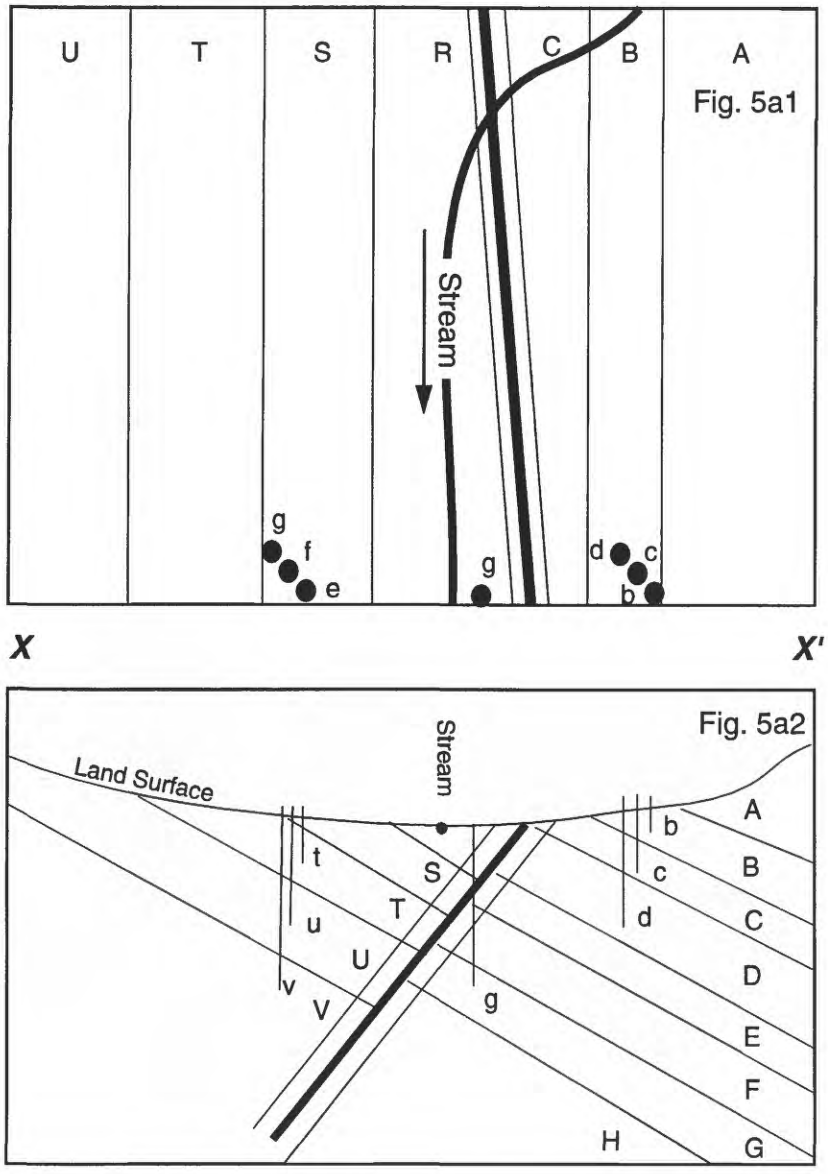

Figure 5a. Map and section *X-X'* showing a small valley, strike and dip of bedrock, stream, streamflow direction, fault, and wells.

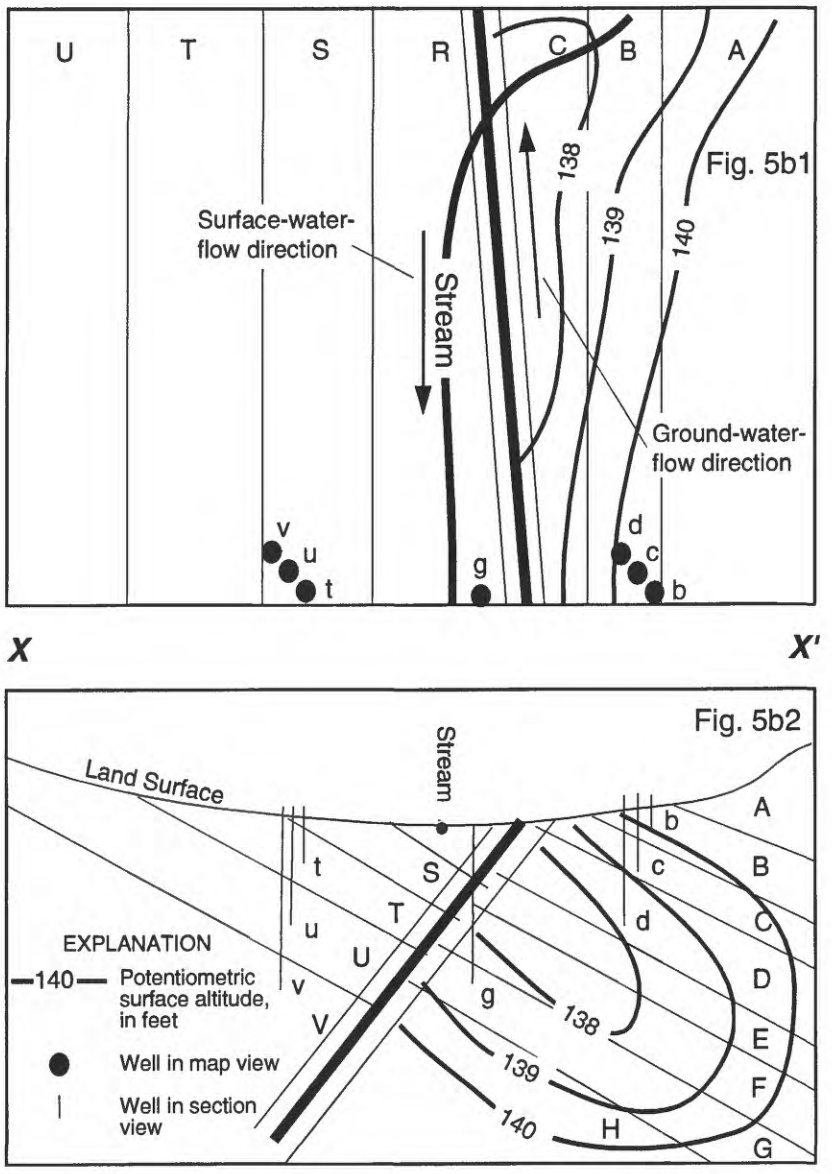

Figure 5b. Map and section *X-X'* showing static potentiometric surface on one side of the fault and ground-water-flow direction along the fault.

Because most bedding-plane partings close with depth in most viable bedrock aquifers, it is unlikely that water will flow under the fault. A more probable flow direction is upward; if water cannot rise high enough to flow directly over the confining unit, however, it will flow parallel to the fault/confining unit to a point of low topography, such as a spring or a stream channel, and then it will flow over the fault/confining unit as surface water. As a result, the ground-water-flow direction will be parallel to the fault/confining unit and towards the stream. Much like the fine-scale map/section shown in figure 4, the flowpath will exist in the high conductive water-bearing zones in the bedding units, whereas the maximum hydraulic gradient will cut across many bedding units.

Drawing a potentiometric surface plane that is highly contorted in a three-dimensional space requires abandoning the typical map view contouring methods. Typical map contouring methods show a specific water-level altitude associated with a well and then assume the screen interval of the well is at land surface. This method of contouring may be appropriate in certain types of aquifers, but it is not accurate in the fractured bedrock aquifer at the NAWC. At the NAWC, water-level contours were drawn in three-dimensions collectively using a map at land surface, a map at 100 ft below land surface and nine sections (sections A to I). Water-level contours were then drawn so that they show the highly contorted potentiometric surface. A residual effect of this contouring method for a map at land surface is that the water-level altitude for each well screen is printed near the well but the contours at the land surface will not reflect the printed water level. The residual of a section view is that the section will contain water-level contours but no data because the wells are not in the specific section. Typically, such maps and sections are drawn as fence diagrams, but in this study area, with the large number of wells and data points it is better to show maps and sections as individual figures. The reader will obtain the most useful information if the maps and sections are looked at as a single unit.

HYDROGEOLOGIC FRAMEWORK

The description of the hydrogeologic framework at the NAWC is based predominantly on borehole geophysical logs, rock type, and color from rock cores and information recorded in drillers' and geologists' logs. The identification of the fault zone is based on geologic offsets in rock cores and zones of deep weathering of the bedrock. The stratigraphic framework and the fault location is further refined on the basis of static, drawdown, and stressed water levels and concentrations of TCE, cis-DCE, and VC.

Bedrock Geology

The NAWC is located along the southern flank of the Newark Basin. The basin forms a rolling lowland underlain by a thick succession of sedimentary rocks and basalt flows of Early Jurassic and Late Triassic age. The rocks generally dip gently to moderately to the north towards a large fault zone that forms the basin's northern boundary. Rocks in the Newark Basin are divided into 15 units. The Stockton and Lockatong Formations of Upper Triassic age are the only units present at the NAWC (Hugh Houghton, written commun., 1984). In this report, the author correlates the Stockton Formation with the Stockton aquifer and the Lockatong Formation with the Lockatong aquifer.

Several generations of folds affect the rocks of the Newark Basin. The basin may have formed as a pull-apart structure with significant strike-slip movement along the larger faults. This could account for the compressional regime that produced local

folds and thrust faults (Lyttle and Epstein, 1987). An unpublished geologic map of the Pennington Quadrangle shows that the contact between the Stockton and Lockatong Formations passes through the southern half of the NAWC (fig. 6) (Hugh Houghton, written commun., 1984). Immediately west of NAWC, the map shows a single, short northeast-trending normal fault. The fault contact was observed in a ditch that was dug to repair a fire hydrant (Donald Monteverde, N.J. Geological Survey, oral commun., 1996). Numerous faults were mapped in the bottom of Villa Victoria Brook[1] about 1 mile west-southwest of NAWC. The strikes of the faults are north to northeast, but the dip directions and dip angle of each fault were not noted. The faults are interpreted to be thrust faults.

The bedrock geology at the NAWC consists of the upper strata of the Stockton Formation and lower strata of the Lockatong Formation. Regionally and at NAWC, the contact between the two formations is gradational. In this report, a thrust fault is mapped very close to the contact between the two formations at NAWC. Bedding units in each formation (table 1) are defined on the basis of natural gamma-ray logs (figs. 7a and 7b) and reinterpretation of the lithology based on rock cores and geologists' and drillers' logs (International Technology Corporation, 1994; EA Engineering, Science and Technology Inc., 1997). The strike of the bedrock at NAWC ranges from N65°E to N70°E. The dip ranges from about 70° NW near the fault to about 15° NW at a distance of more than 300 ft from the fault. The structure of the bedding units and the thrust fault are shown in map view (figs. 8 and 9) and in sections (figs. 10 to 18). A generic block diagram shows the synform of the Lockatong Formation, antiform of the Stockton Formation and the thrust fault (fig. 19).

The bedding units in each formation consist of numerous layers or hydrogeologic zones referred to as water-bearing zones and semi-confining zones. The water-bearing zones are areally extensive and have interconnected bedding-plane partings and vertical partings that produce water, whereas the semi-confining zones have a limited number of partings or poorly connected partings that produce little water. It is not possible to accurately map the water-bearing and semi-confining zones in each bedding unit, because the screened interval in a well typically crosses more than one zone.

Stockton Formation

Regionally, the Stockton Formation is a light to medium gray to pale reddish brown, thin- to thick-bedded, fine- to coarse-grained sandstone interbedded with conglomerate and shale (Lyttle and Epstein, 1987). At NAWC, the Stockton Formation is interbedded light reddish-gray sandstone and reddish mudstones that are divided into five bedding units. The bedding units are labeled S-11 through S-15[2] (table 1, figs. 8 to 18). The bedding units are based on major changes in lithotype and in color. Changes in gamma-ray signature at NAWC are not as diagnostic in the Stockton Formation as they are in the Lockatong Formation because there are not distinct layers that produce strong gamma-ray anomalies in the Stockton Formation (fig. 7a). As a result of the limited number of wells and shallow depth of the wells that are in the Stockton Formation, there is little information to confirm the characteristic of a bedding unit or generate well-defined structure maps of the unit.

[1]Villa Victoria Brook in this report refers to the unnamed brook that flows through the hamlet of Scudders Falls and Villa Victoria Academy (fig. 6).

[2] 'S' is a prefix for Stockton Formation strata and 'L' is prefix for Lockatong Formation.

On the basis of the change in rock color and sediment grain size, the contact of the Stockton with the Lockatong Formation at NAWC probably is conformable and located at the contact of bedding units S-15 and L-1. The transition represents a change in the environment of deposition from a shallow near-shore environment to a deep water, far from shore environment.

Lockatong Formation

Regionally, the Lockatong Formation consists of laminated to thick-bedded, gray and black siltstones and shales (Lyttle and Epstein, 1987). At NAWC, the Lockatong Formation consists of laminated to thick-bedded gray, greenish-gray, reddish, and black mudstones. In the study area, the formation is divided into bedding units L-1 and L-2 on the south side of the thrust fault and bedding units L-13 to L-23 on the north side of the fault (table 1, figs. 8 to 18). Bedding units L-13 to L-23 are divided on the basis of the magnitude of the natural gamma-ray signature (fig. 7b). Bedding units L-14, L-16, L-18, and L-20 have high gamma-ray counts that result from uranium enrichment of strata within the unit. Bedding units L-13, L-15, L-17, and L-19 have low gamma-ray counts. Bedding units L-21 to L-23 also have low gamma-ray counts but are divided into 3 units based on the greenish rock color of strata L-22 and dark grayish color of strata L-21 and L-23.

Bedding units close to the fault appear to be thicker than the same bedding units at a distance from the fault because of the steeper dip of the beds where measured near the fault. Bedding unit L-20 (fig. 7b) in wells 38BR, 40BR, 41BR, 43BR, 44BR, 45BR, and 46BR show a thin high-amplitude gamma-ray anomaly, whereas wells 2BR and 51BR show a very broad anomaly that results from steeply dipping beds. Bedding units near land surface typically lose the high-amplitude gamma-ray signature when uranium is mobilized in an oxidizing environment. The high gamma-ray count in bedding unit L-20 does not appear in the top of well 30BR because the uranium was dissolved from this unit sometime in the geologic past.

The Lockatong Formation consists of a basal section identified as L-1 and L-2. Because of the fault, the relation of bedding units L-1 and L-2 on the south side of the fault and bedding units L-13 to L-23 on the north side of the fault is unclear. The units on the north side of the fault are interpreted to be stratigraphically higher in the section. Bedding units L-13, L-14, L-16, L-18, L-19, L-20, and L-21 are predominantly dark gray mudstone with minor beds of green gray mudstones. Bedding units L-15 and L-17 are predominantly red mudstones and bedding unit L-22 is a greenish gray mudstone.

Fault Zone

Based on bedrock core data from monitoring well sites at NAWC, a thrust fault cuts across the facility. The trace of the thrust fault closely follows the contact of the Lockatong and Stockton Formations as mapped by the New Jersey Department of Environmental Protection (Hugh Houghton, written commun., 1985), and the fault is subparallel with the strike of the two formations. (fig. 6).

The best evidence of a fault zone is in rock cores from well 42BR at depths of 68, 111, and 127 ft below land surface (figs. 20, 21, and 22). Evidence of faulting consists of stratigraphic layers showing bedding offsets, brecciated zones, and slickensides. Rock core from a depth of 68 ft below land surface (fig. 20) shows a brecciated rock zone cemented with calcite. Bedding above and below the fault has a measured dip angle of 45° and an interpreted dip direction of N20°W. The fault has a measured dip angle of 50° and an interpreted dip direction of about S20°E. Rock core from a depth of 111 ft below land surface

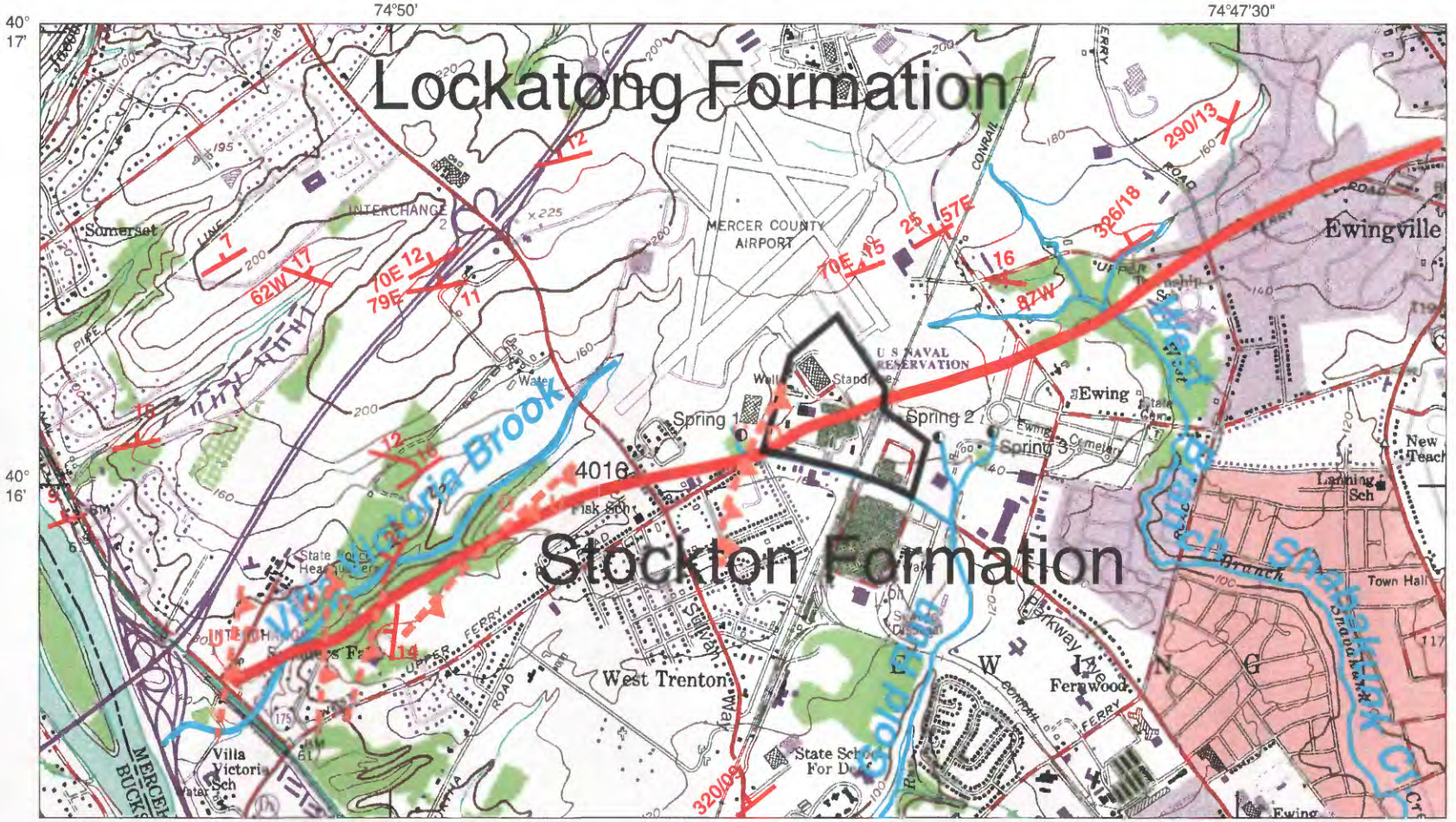

Figure 6. Geology in the area of the Naval Air Warfare Center, West Trenton, New Jersey.

Table 1. Bedding units at the Naval Air Warfare Center based on the natural gamma-ray logs, driller's logs, and core logs

Era	Series	Geologic units	Aquifers	Bedding unit	Predominate lithology and hydrology	Hydraulic character
Mesozoic	Upper Triassic	Lockatong Formation	Lockatong Aquifer	L-23	MUDSTONE. light to dark gray, laminated slightly calcareous, low gamma count	Not applicable
				L-22	MUDSTONE, dark gray and green-gray, low gamma count	Not applicable
				L-21	MUDSTONE, gray, platy, massive, interbedded, medium hard, low gamma zone	Not applicable
				L-20	MUDSTONE, gray, high gamma count	Semi-confining unit
				L-19	MUDSTONE, gray, hard to medium hard, with calcareous and soft brown mudstone seams low gamma zone	Not applicable
				L-18	SILTSTONE, MUDSTONE light to dark olive green or black, massive, bioturbidation, pyrite, fracture zone, some finely laminated, strongly calcareous, high gamma count	Not applicable
				L-17	MUDSTONE, red brown to green-gray brown, low gamma zone	Not applicable
				L-16	MUDSTONE, ARGILLITE, and SHALE, light green to gray and black, high gamma zone	Not applicable
				L-15	MUDSTONE, red brown and green-gray, soft, slightly broken, massive bedded, calcareous, low gamma zone	Not applicable
				L-14	MUDSTONE, dark gray to green-gray, high gamma zone	Not applicable
				L-13	MUDSTONE, dark gray, low gamma zone	Not applicable
					Stratigraphic relation unknown	Not applicable
				L-3	No data	Not applicable
				L-2	MUDSTONE, greenish gray, low gamma zone	Not applicable
				L-1	MUDSTONE, medium to dark gray, laminated, high gamma zone	Not applicable
		Stockton Formation	Stockton Aquifer	S-15	SANDSTONE, brown, medium hard	Not applicable
				S-14	SANDSTONE, gray white, medium hard	Not applicable
				S-13	MUDSTONE red, hard, massive	Not applicable
				S-12	SANDSTONE, gray white	Not applicable
				S-11	MUDSTONE, red	Not applicable

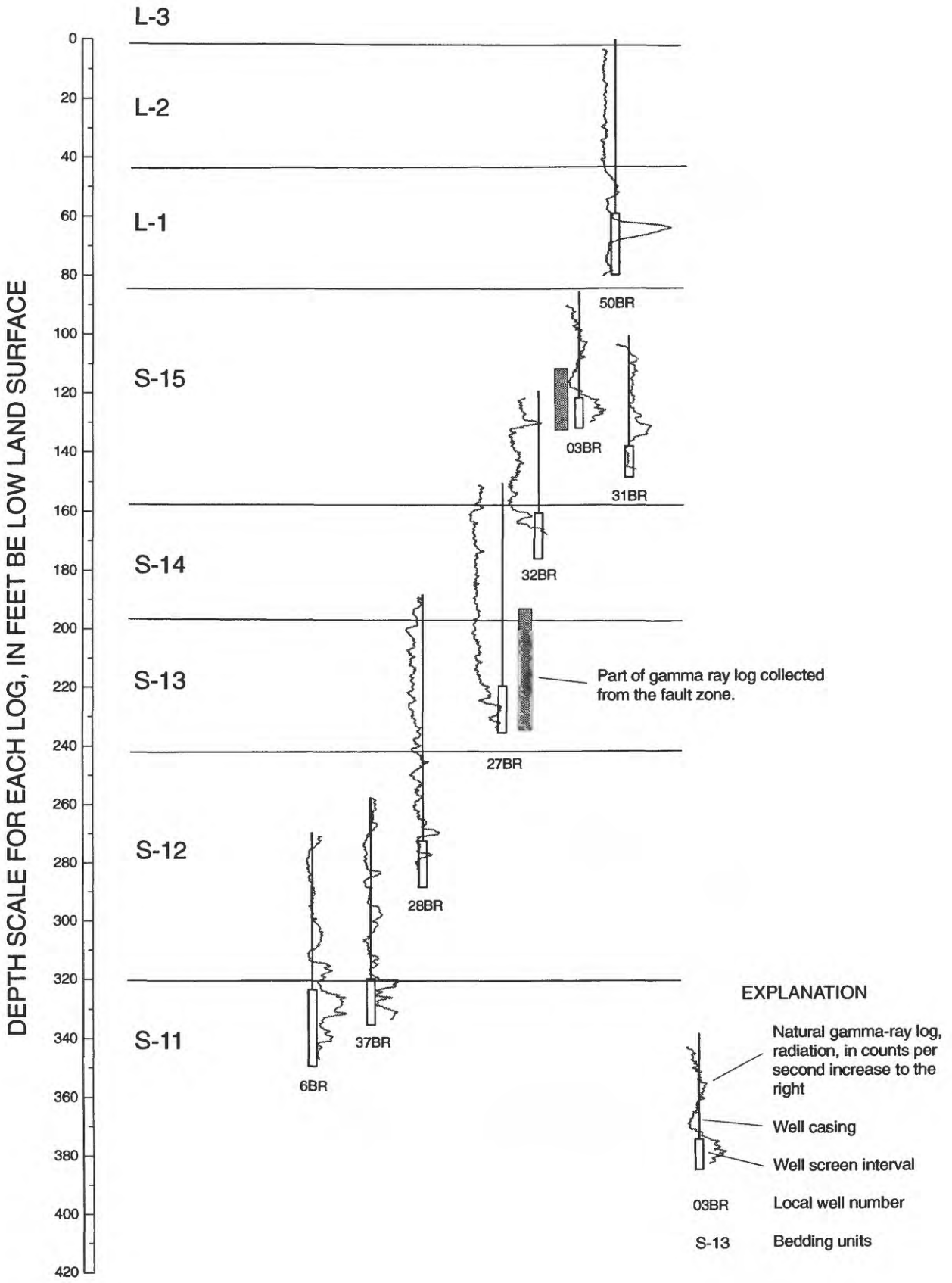

Figure 7a. Bedding units of the Stockton and Lockatong Formations south of the fault, Naval Air Warfare Center, West Trenton, N.J. [Bedding units based on natural gamma-ray logs, rock type, and rock color.]

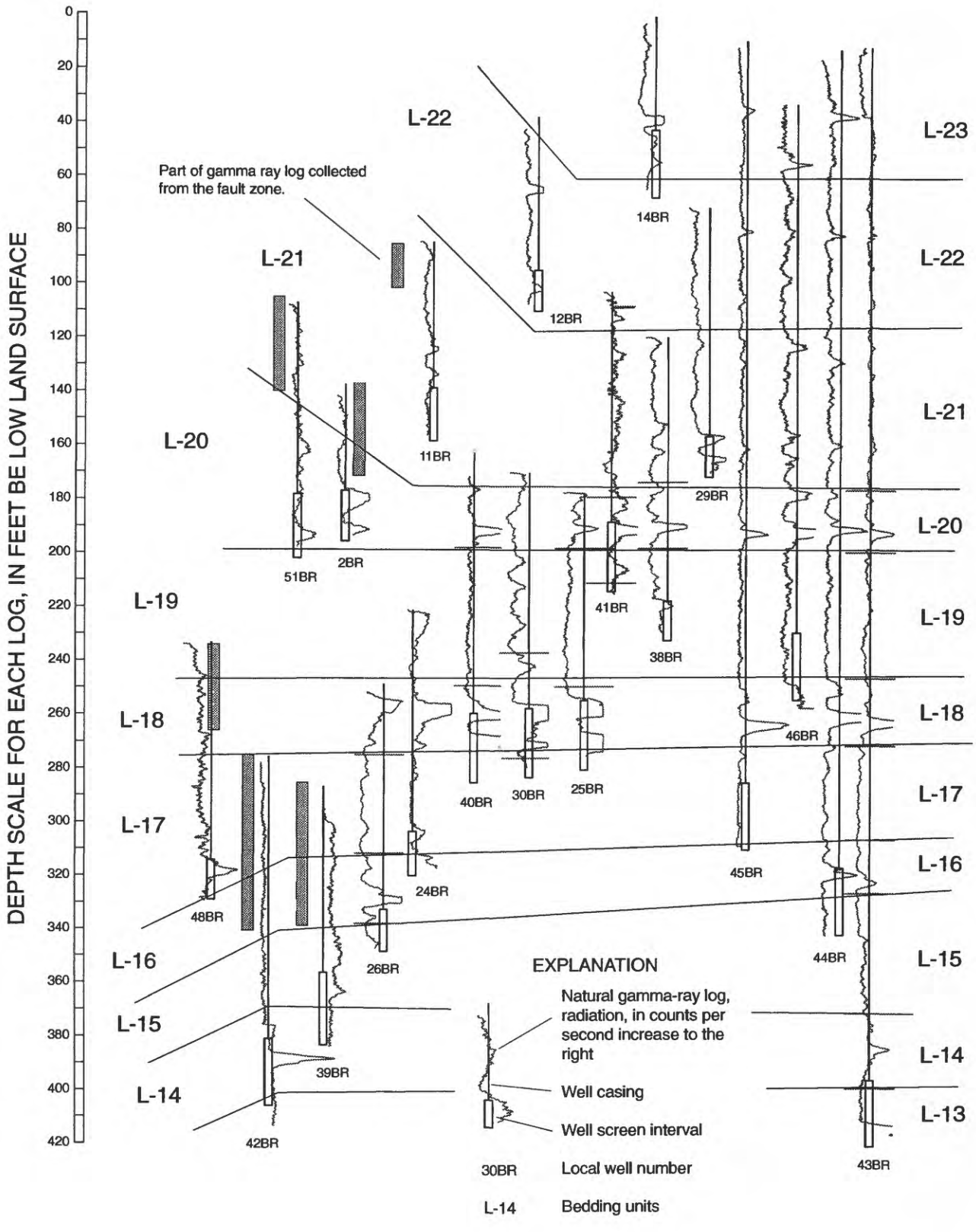

Figure 7b. Bedding units of the Lockatong Formation north of the fault, Naval Air Warfare Center, West Trenton, N.J. [Bedding units based on natural gamma-ray logs, rock type, and rock color.]

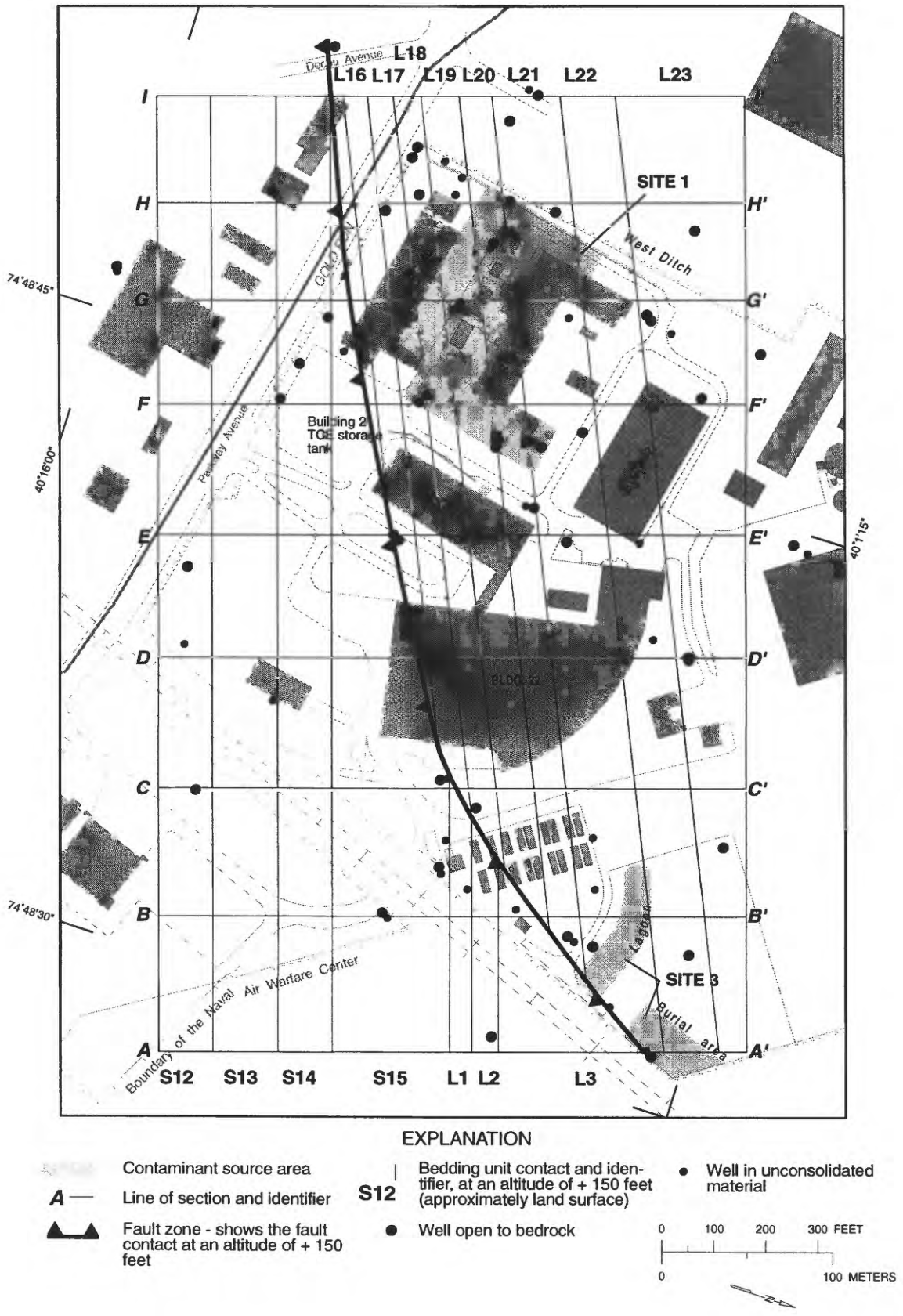

Figure 8. Bedding units and the fault trace at an altitude of + 150 feet (approximately land surface), Naval Air Warfare Center, West Trenton, N.J.

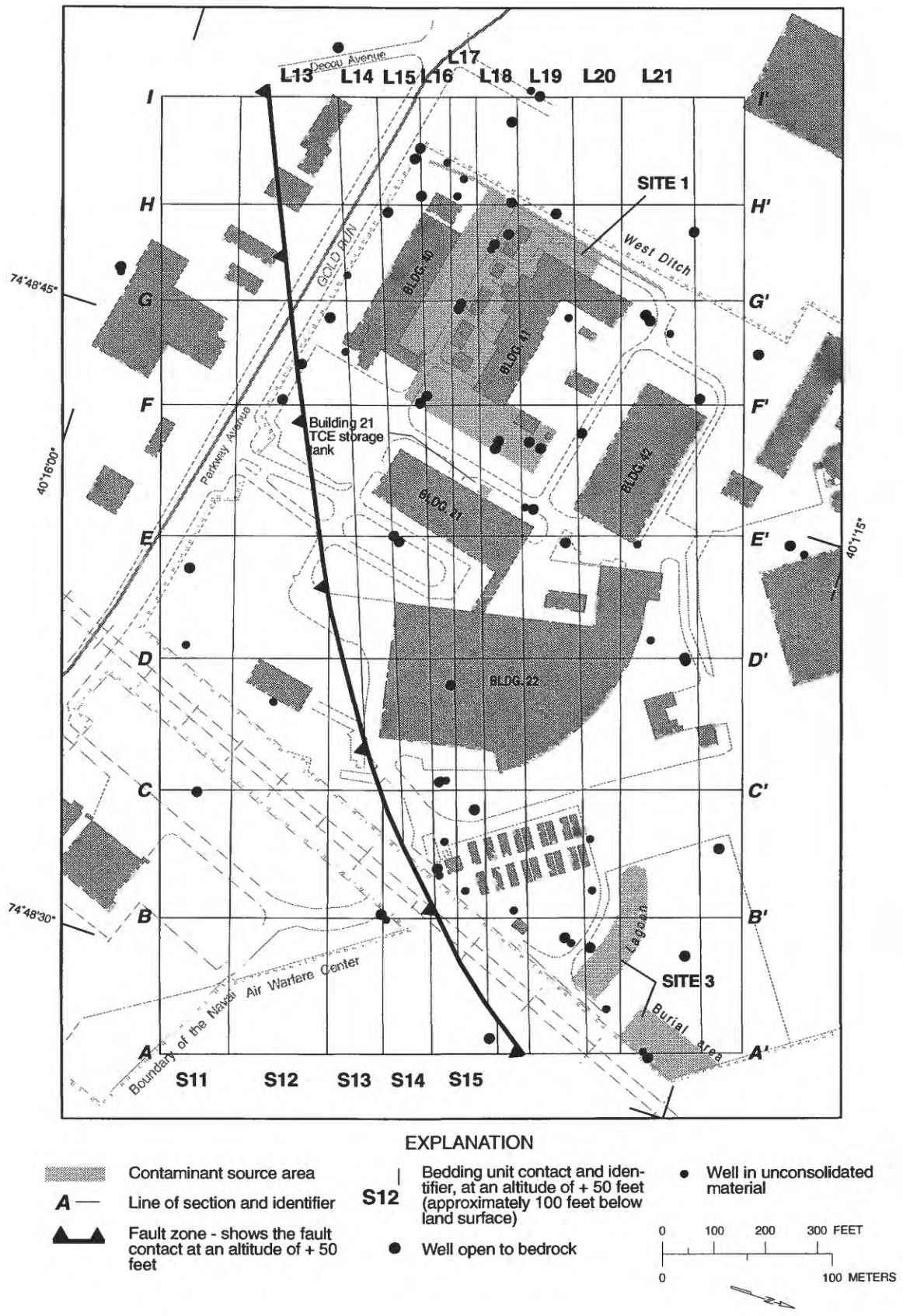

Figure 9. Bedding units and the fault trace at an altitude of + 50 feet (approximately 100 feet below land surface), Naval Air Warfare Center, West Trenton, N.J.

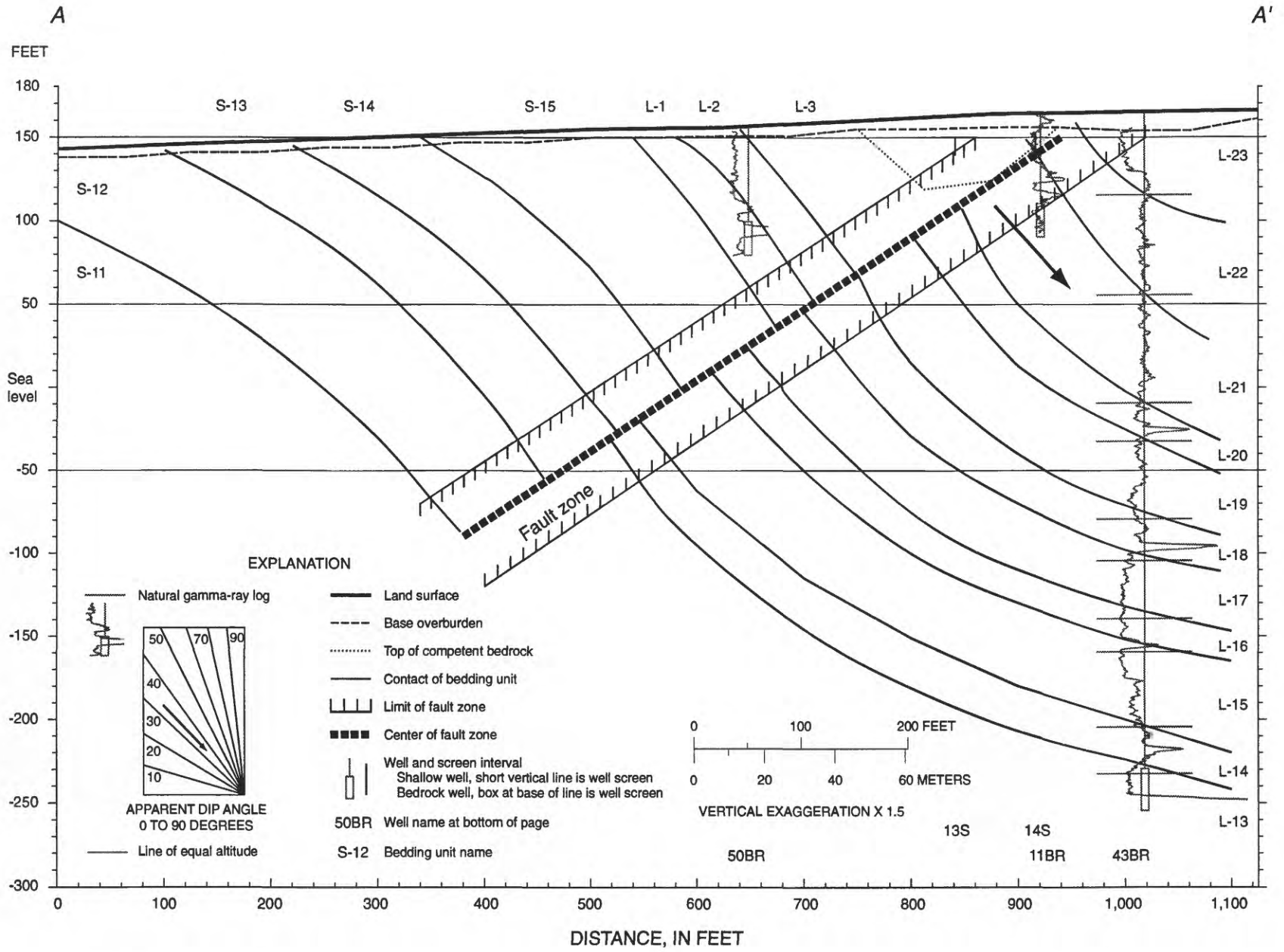

Figure 10. Section *A-A'* showing natural gamma-ray logs, dip angle from rock cores, geophysical bedding units, fault zone, and well screen placement for shallow and deep wells. Well 43BR is common to all sections for reference purposes.

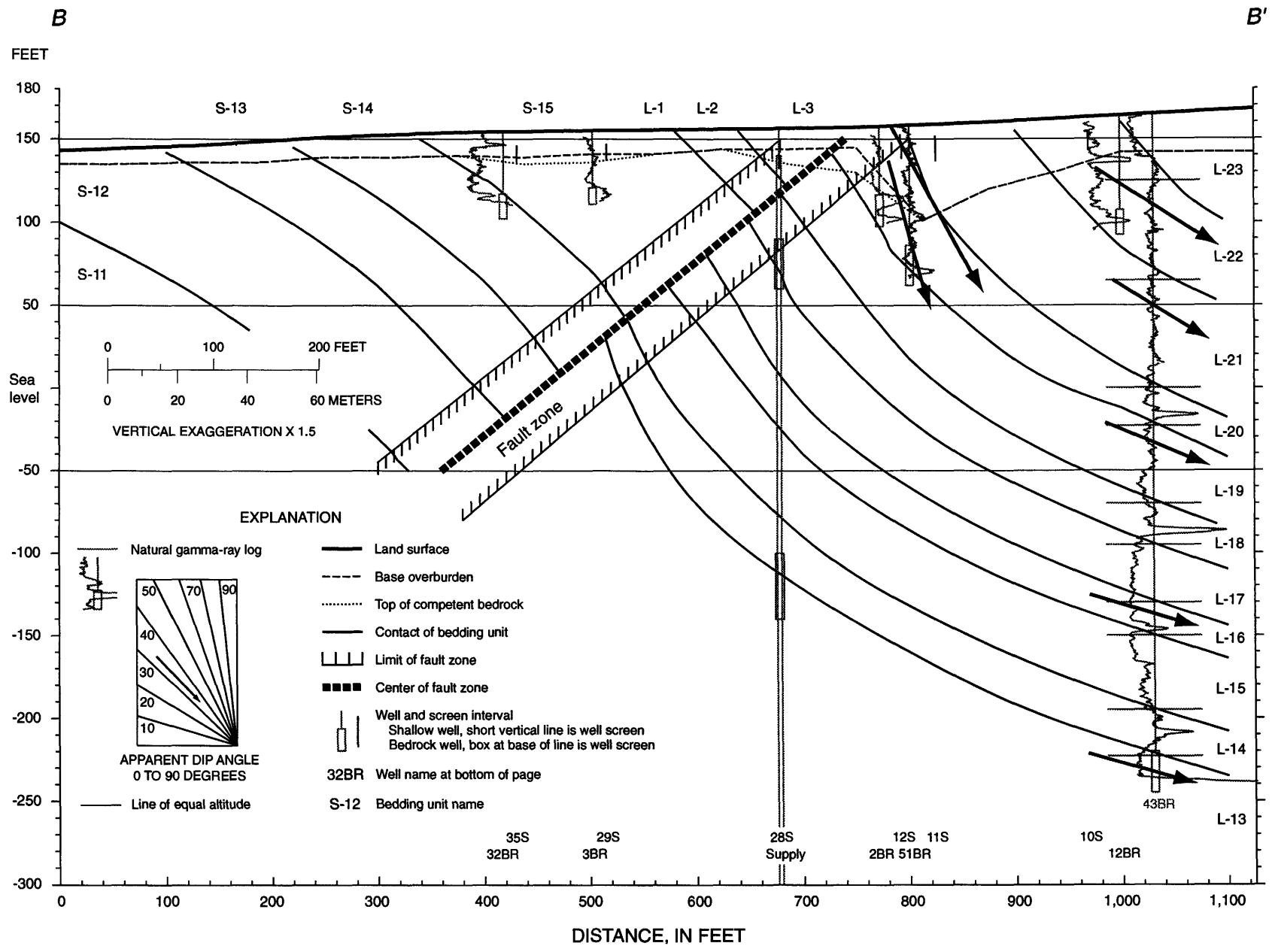

Figure 11. Section *B-B'* showing natural gamma-ray logs, dip angle from rock cores, geophysical bedding units, fault zone, and well screen placement for shallow and deep wells. Well 43BR is common to all sections for reference purposes.

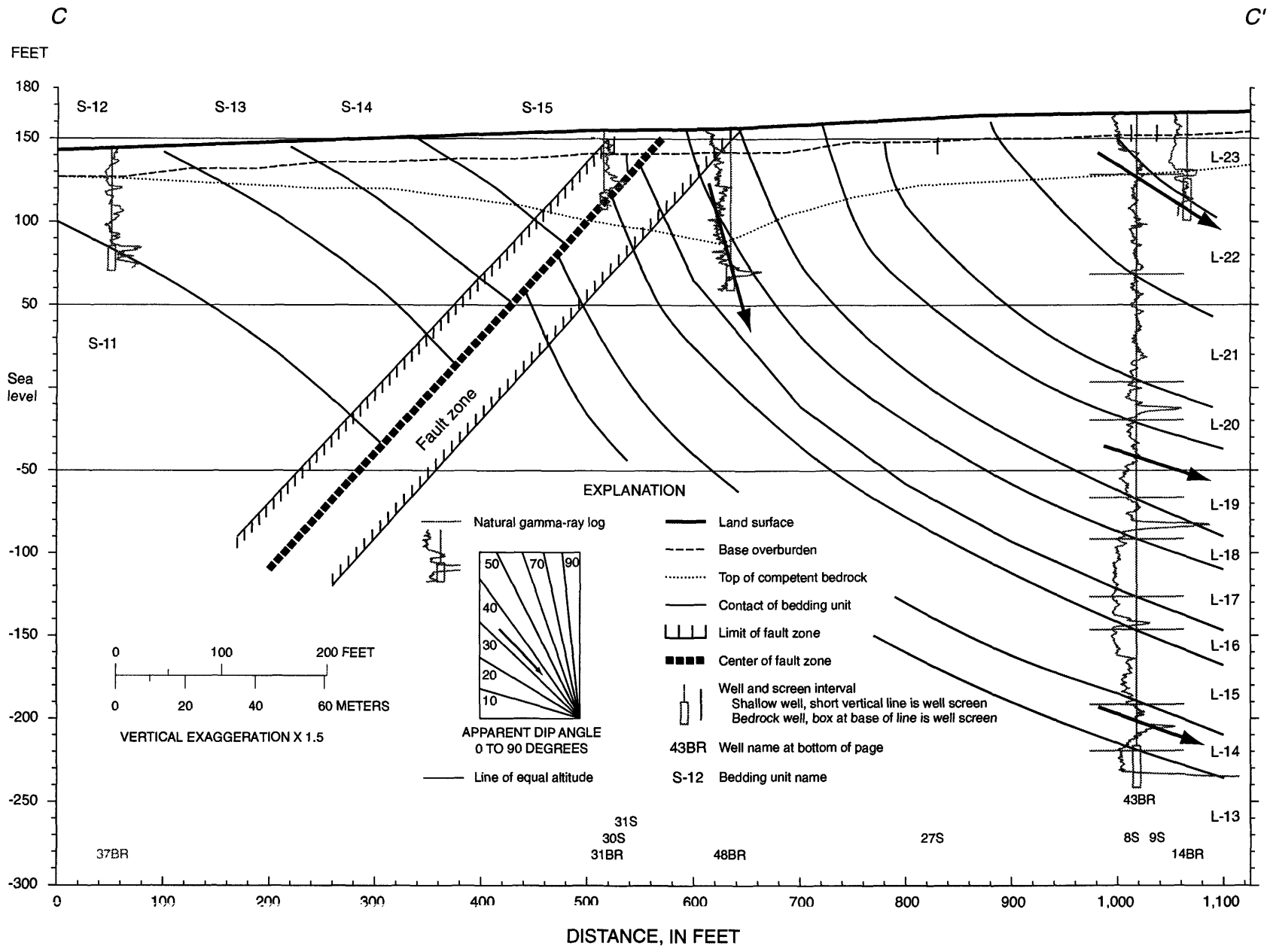

Figure 12. Section *C-C'* showing natural gamma-ray logs, dip angle from rock cores, geophysical bedding units, fault zone, and well screen placement for shallow and deep wells. Well 43BR is common to all sections for reference purposes.

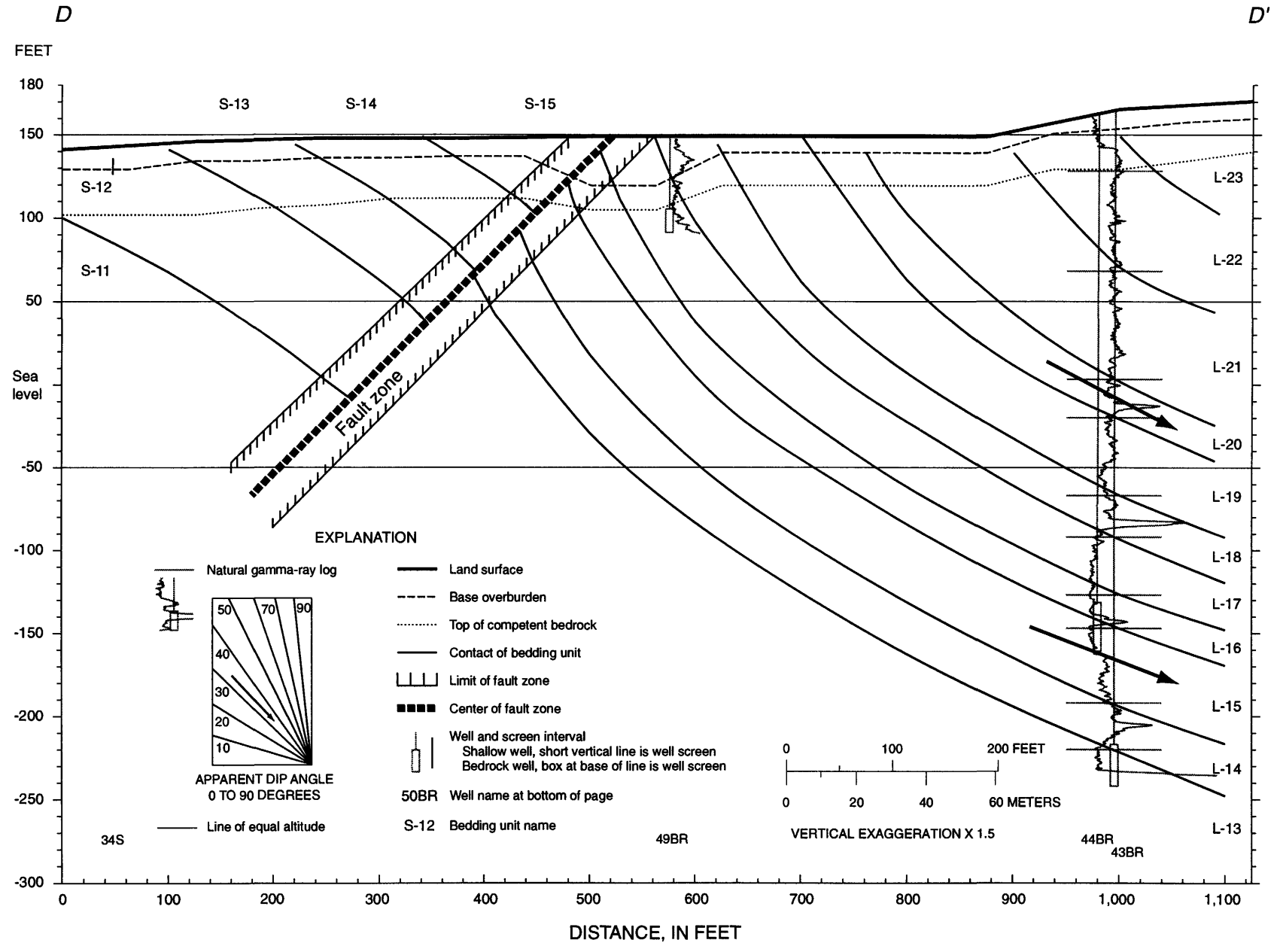

Figure 13. Section *D-D'* showing natural gamma-ray logs, dip angle from rock cores, geophysical bedding units, fault zone, and well screen placement for shallow and deep wells. Well 43BR is common to all sections for reference purposes.

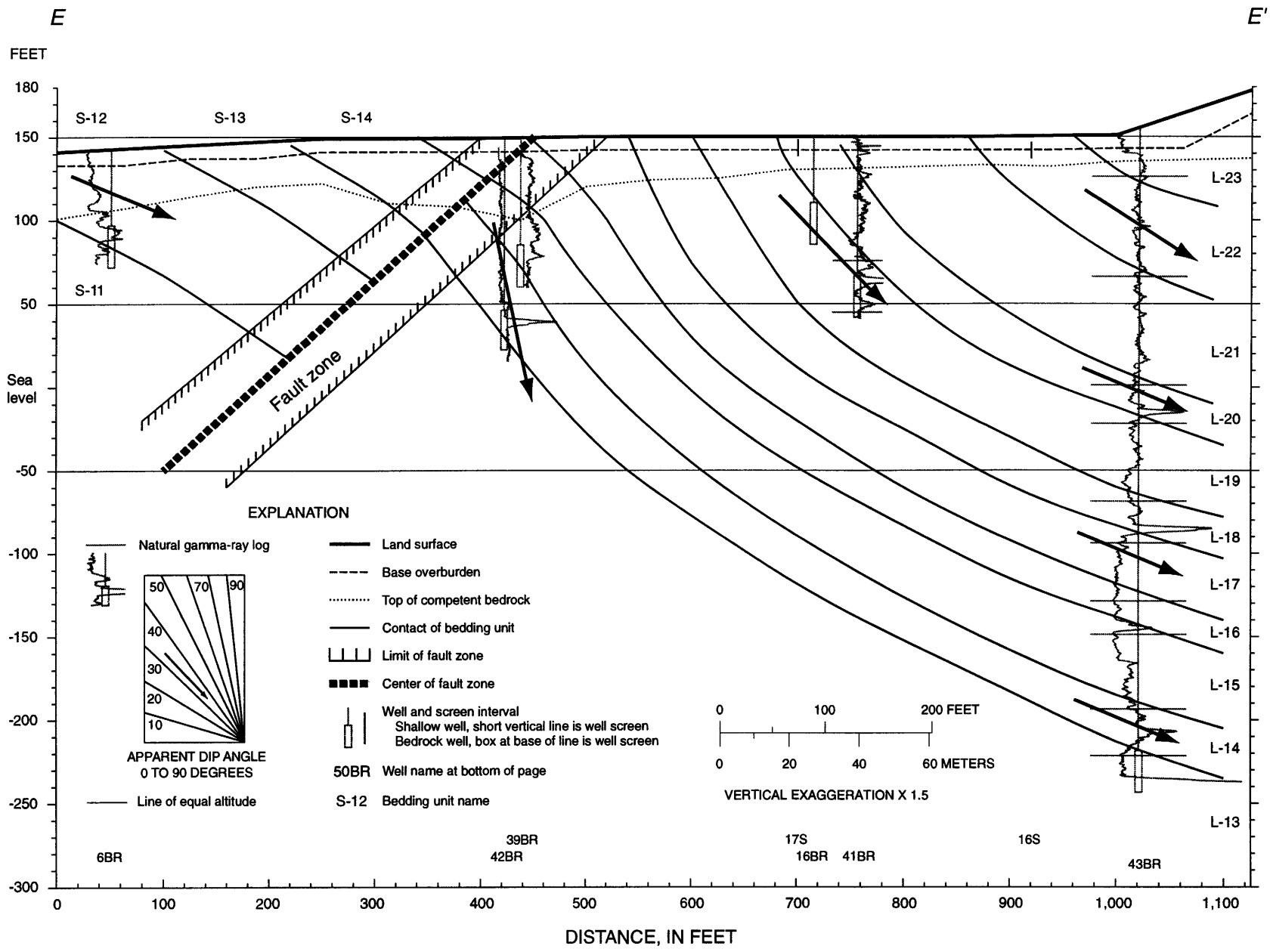

Figure 14. Section *E-E'* showing natural gamma-ray logs, dip angle from rock cores, geophysical bedding units, fault zone, and well screen placement for shallow and deep wells. Well 43BR is common to all sections for reference purposes.

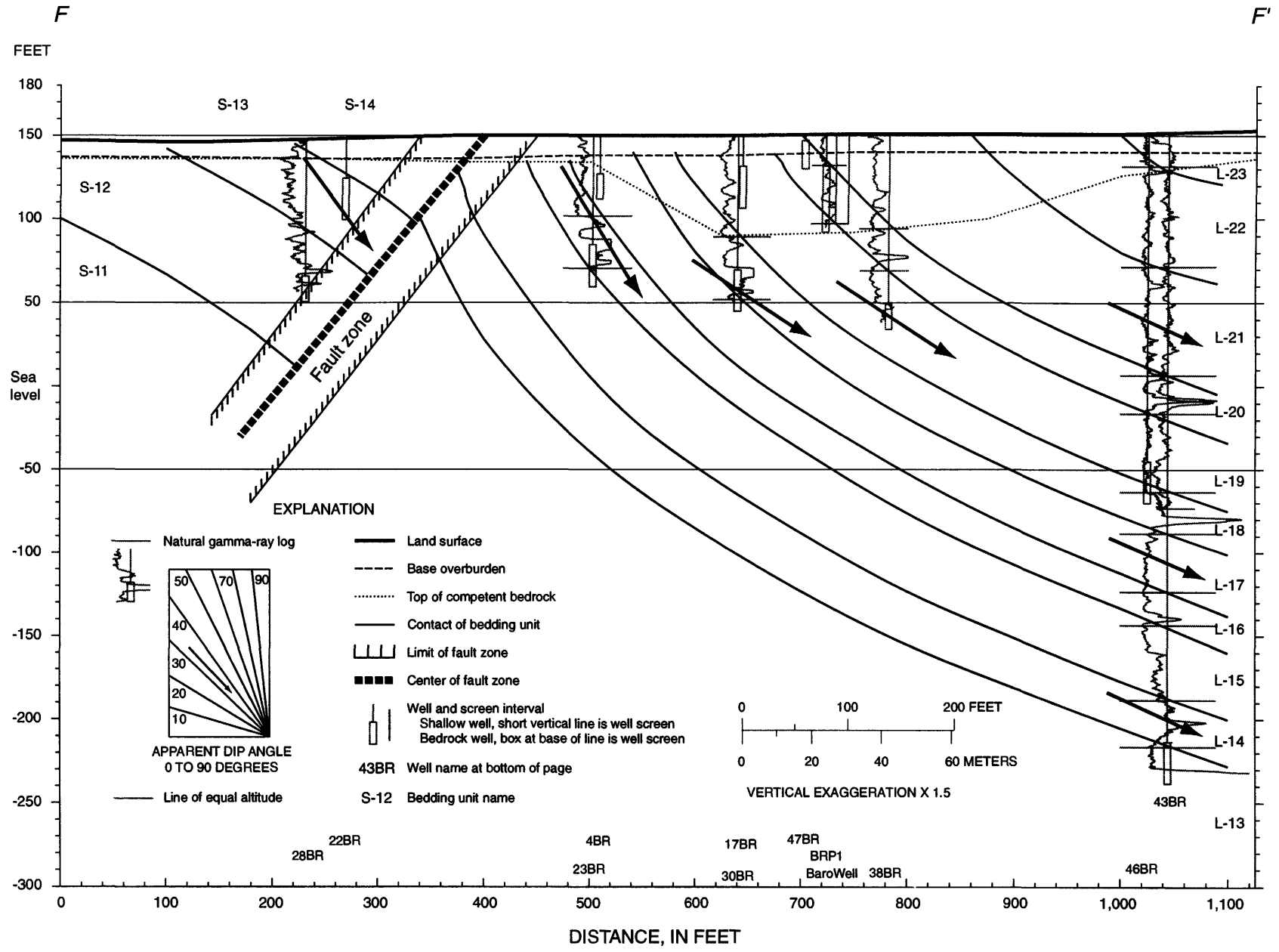

Figure 15. Section *F-F'* showing natural gamma-ray logs, dip angle from rock cores, geophysical bedding units, fault zone, and well screen placement for shallow and deep wells. Well 43BR is common to all sections for reference purposes.

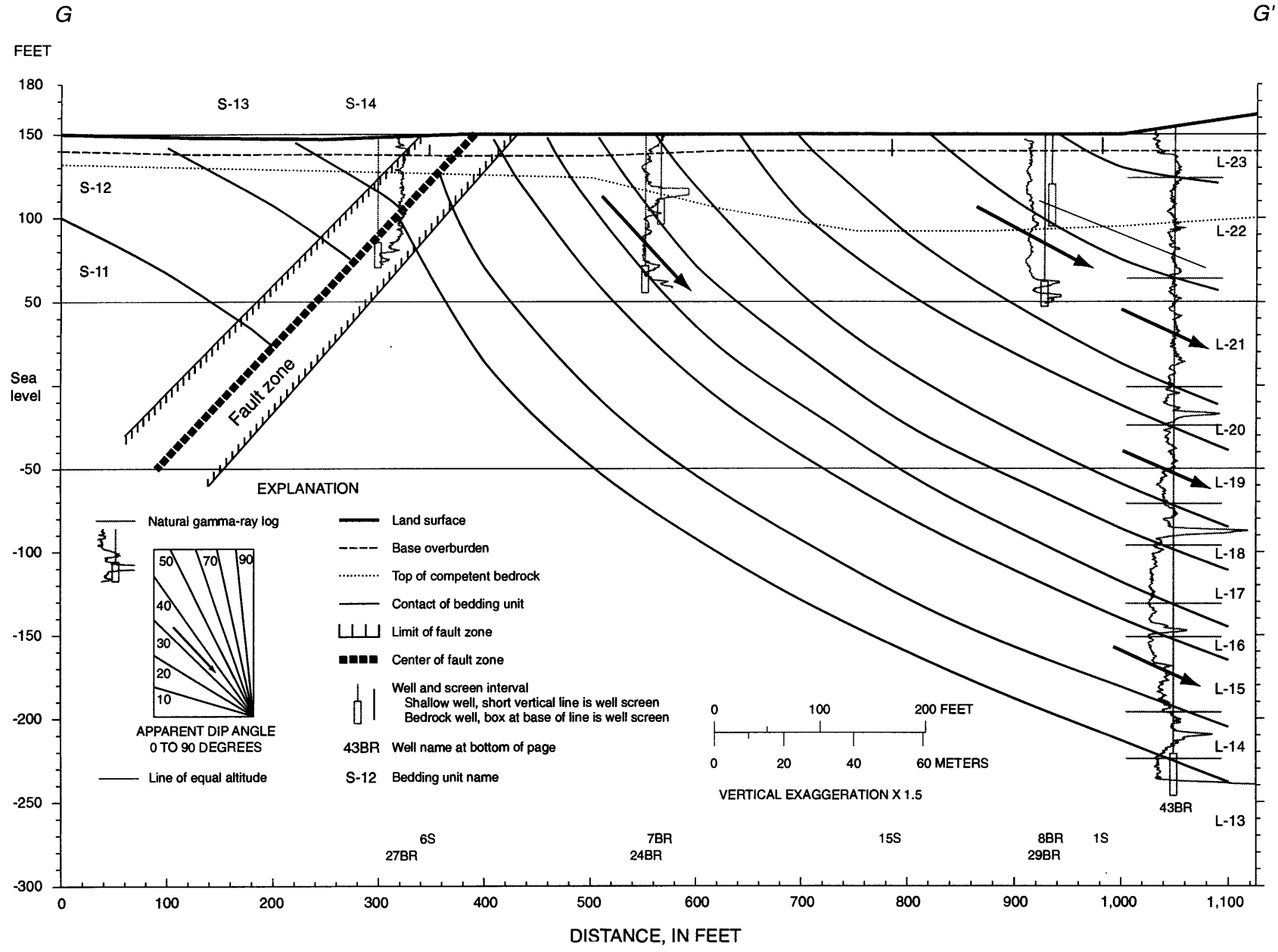

Figure 16. Section *G-G'* showing natural gamma-ray logs, dip angle from rock cores, geophysical bedding units, fault zone, and well screen placement for shallow and deep wells. Well 43BR is common to all sections for reference purposes.

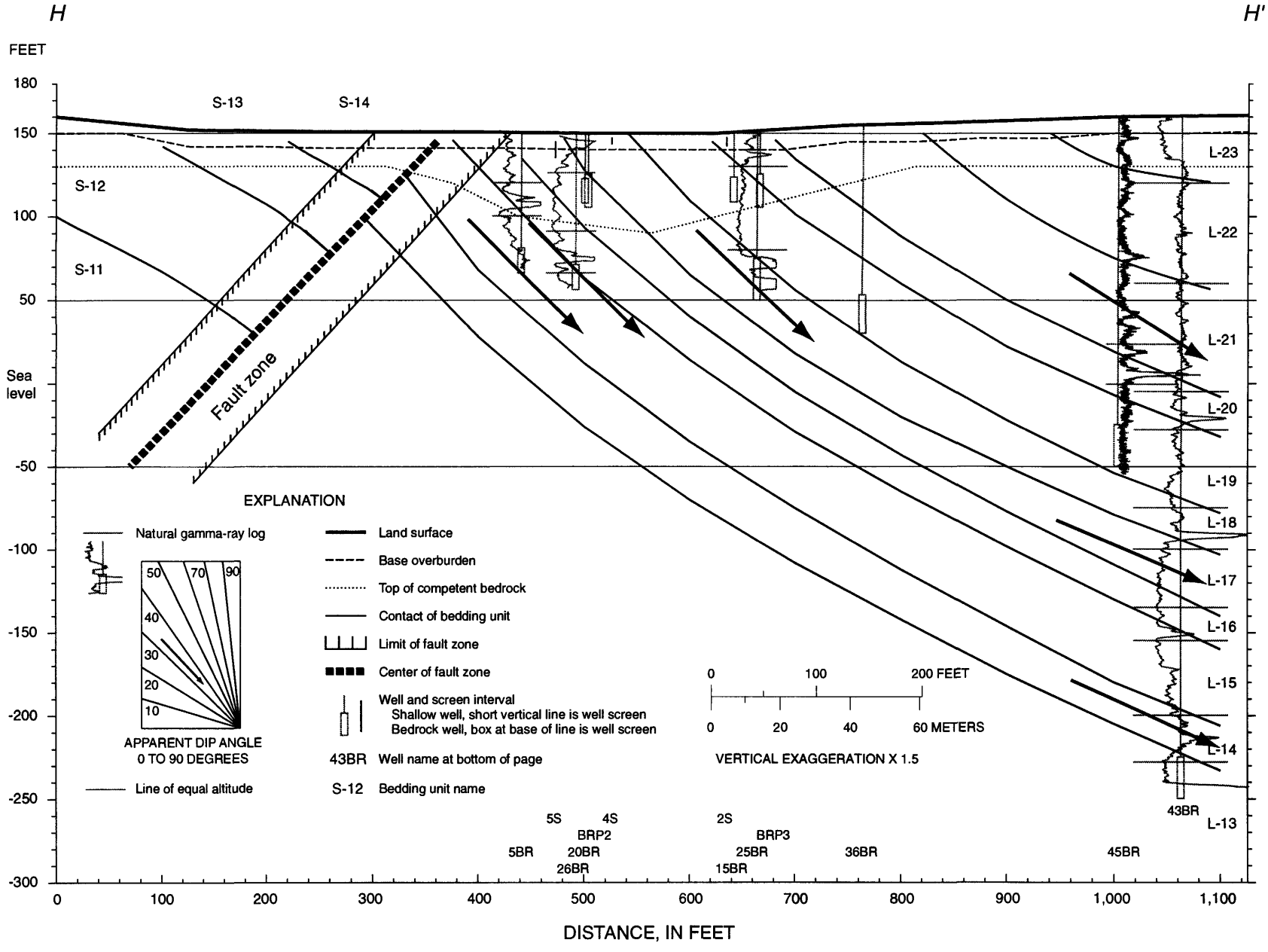

Figure 17. Section *H-H'* showing natural gamma-ray logs, dip angle from rock cores, geophysical bedding units, fault zone, and well screen placement for shallow and deep wells. Well 43BR is common to all sections for reference purposes.

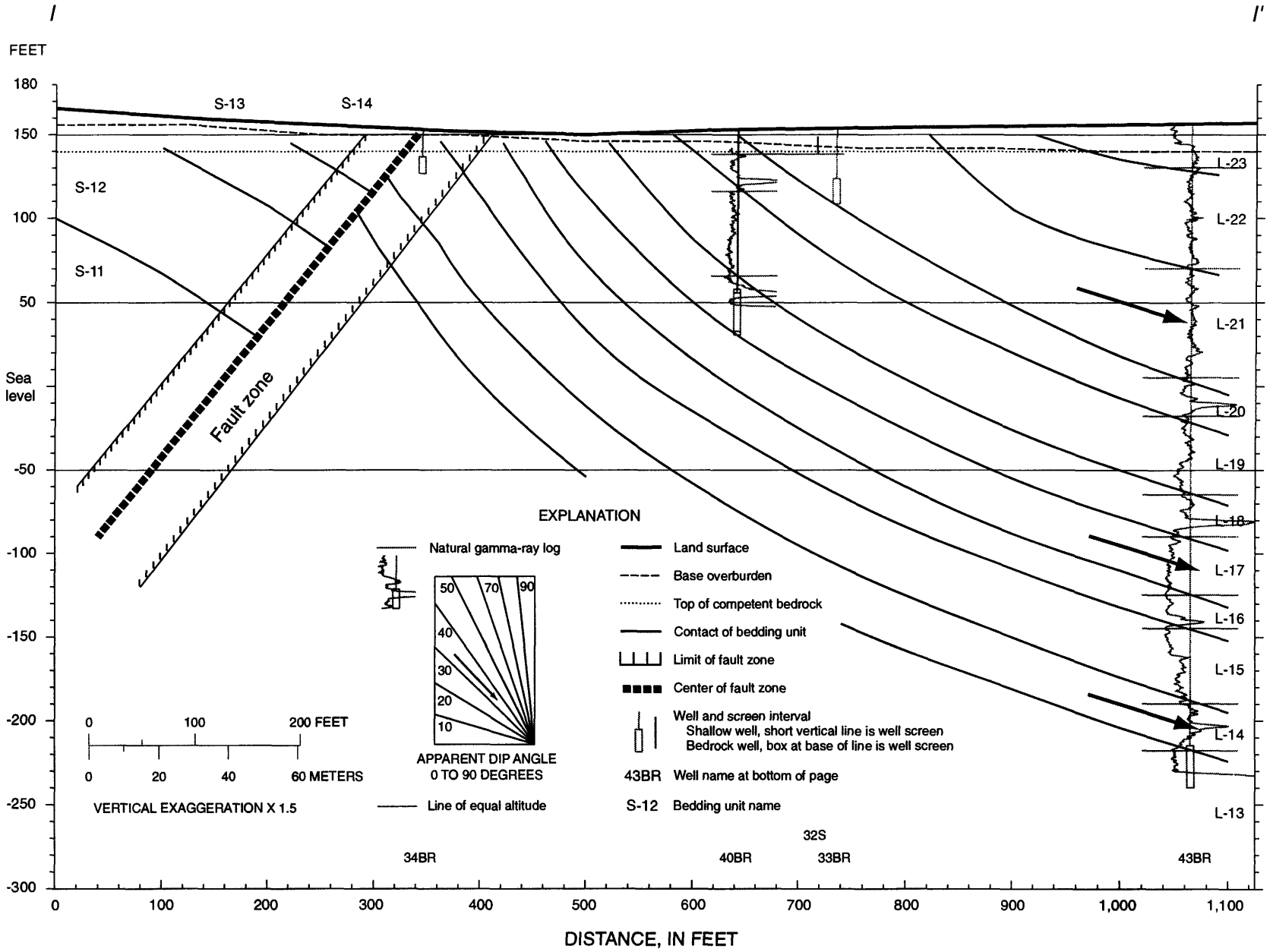

Figure 18. Section *I-I'* showing natural gamma-ray logs, dip angle from rock cores, geophysical bedding units, fault zone, and well screen placement for shallow and deep wells. Well 43BR is common to all sections for reference purposes.

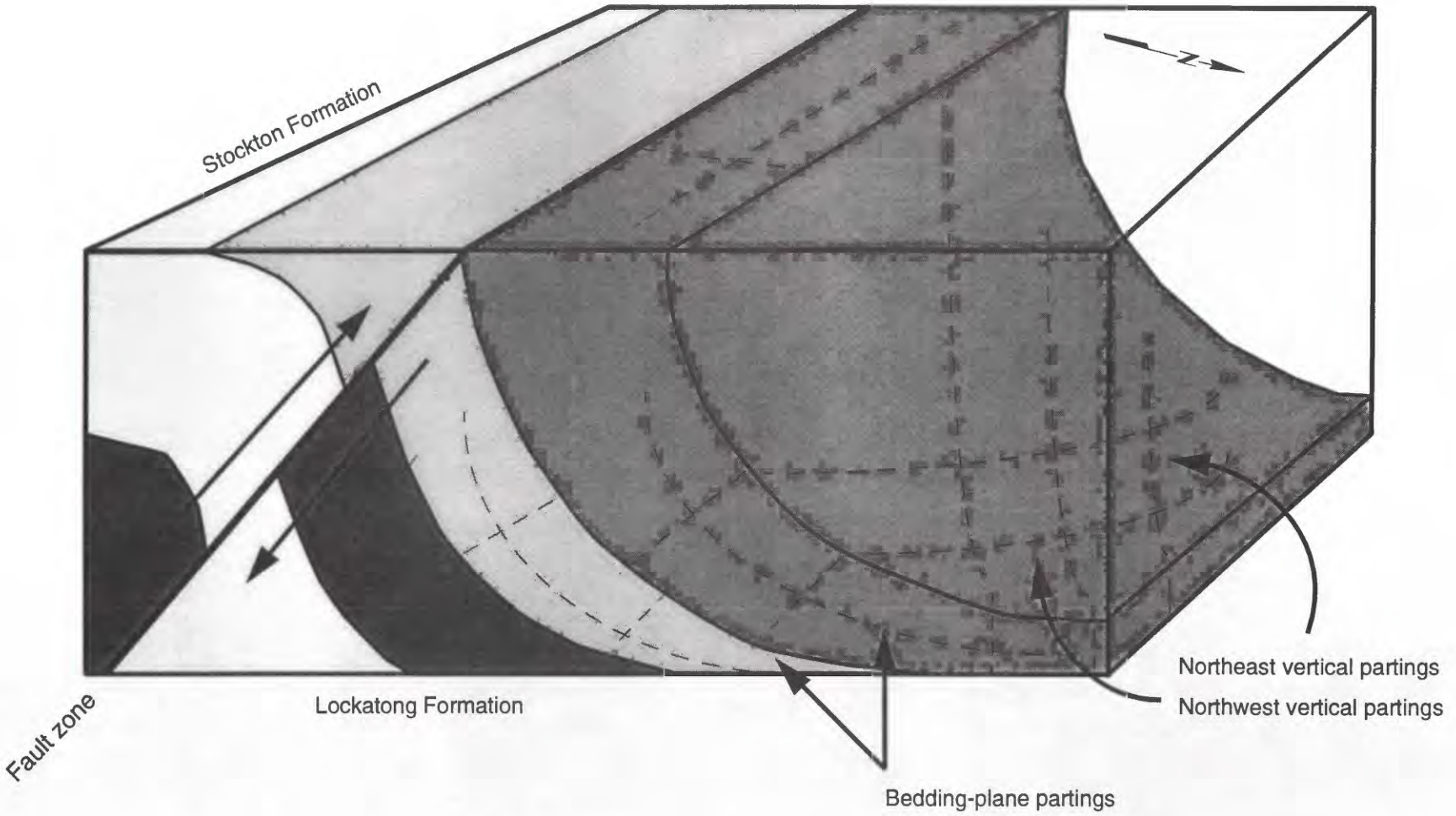

Figure 19. Simplified block diagram of study area showing diagramatic bedding units of the Stockton Formation, Lockatong Formation and the thrust fault. [Top of block represents a map view of the site, near end of block represents a sectional view and right side of the block represents a view along strike. Diagram shows the major potential flow paths via bedding-plane and vertical partings as well as the fault, which acts as a major confining unit.]

Figure 20. Rock core from well 42BR at 68 feet below land surface showing steeply dipping beds on either side of brecciated and cemented fault zone. [Right side of photograph is nearer to land surface.]

Figure 21. Rock core from well 42BR at 111 feet below land surface showing steeply dipping beds and shallow dipping fault. (Fault zone shows brecciation and cementation. Fault is nearly perpendicular to the plain of the bedding).
[Left side of photograph is nearer to land surface.]

Figure 22. Rock core from well 42BR at 127 feet below land surface showing steeply dipping beds and brecciated in the fault zone. [Left side of photograph is nearer to land surface.]

Figure 23. Rock core from well 17BR at 55 feet below land surface showing gently dipping beds and steeply dipping fault. (Fault plane is nearly perpendicular to the bedding plane. Fault zone is cemented.) [Left side of photograph is nearer to land surface.]

Figure 24. Rock core from well 51BR at 95 feet below land surface showing brecciation in fault zone. (Fault zone is cemented) [Left side of photograph is nearer to land surface.]

Figure 25. Rock core from well 42BR showing shallow dipping bedrock and well 43BR showing steeply dipping bedrock. [Left side of photograph is nearer to land surface.]

(fig. 21) shows a 3-in fault contact. Bedrock above the fault consists of light gray mudstones; bedrock below the fault zone consists of dark gray mudstone. The strike and dip of the bedrock above and below the fault is N65°E and 30° NW, and the dip angle and direction of the fault is 40° and S20°E; therefore, the fault is nearly perpendicular to the plane of the bedding. Rock core from a depth of 127 ft below land surface (fig. 22) shows a 2-in fault zone. Bedrock above and below the fault has a measured dip angle of about 70° and an dip direction of N20°W. The measured dip angle of the fault is about 30°, and the dip direction is S10°E. Again the fault plane is nearly perpendicular to the bedding.

In addition to these three examples of faulting at specific depth intervals in the core of 42BR, other examples are available. Numerous other examples of faults are found at depths of 30 to 130 ft below land surface in well 42BR. At the three depth zones noted above, the attitude of the fault is nearly perpendicular to the attitude of the bedding. Based on the data, the suite of southeast dipping faults described above form a fault zone that is about 100 ft thick.

Offset bedding, fault brecciation, and slickensides also are found in rock cores from wells 17BR (fig. 23) and 51BR (fig. 24). The core from monitoring well 17BR shows the dip of the bedding is about 25°, and the dip of the fault is nearly perpendicular to the dip of the bedding. The core from well 51BR shows a brecciated zone that is 8 to 10 in. wide. Based on these and other cores that show faulting, the fault plane is typically perpendicular to the bedding plane and the strike of the two planes is offset by about 20°.

Indirect evidence of faulting is interpreted from monitoring wells 51BR, 48BR, 22BR, 5BR, and 20BR. Typically, bedrock is fractured and pulverized in a fault zone, forming fault breccias and fault gouge. In the shallow environment, the fractured bedrock of the fault zone will chemically weather to form a thick clay zone. It was anticipated that competent bedrock would be encountered at these well sites at 10 to 20 ft below land surface; however, competent bedrock was not encountered until 40 to 65 ft below land surface, and drill cuttings from above the competent bedrock consisted of dry clay. Dry clay at a significant depth may result from weathering of the rock in a fault zone.

The fault is well located based on numerous rock cores from wells near buildings 40, 21, and 22. The fault in the Site 3 area is based on rock cores from wells 48BR and 51BR and is less well located. As a result of data from wells 48BR and 51BR, the strike direction of the fault changes from about N60°E on the west side of the NAWC to about N45°E on the east side of NAWC. The change in strike direction occurs near wells 31BR and 48BR. An alternative location of the fault in the eastern part of the NAWC is about 300 ft south of where it crosses line A (fig. 8). This interpretation assumes that the strike of the fault does not change, and therefore, the fault zone near Site 3 could be as much as 200 ft south of where it is plotted.

Analysis of static, drawdown, and stressed water levels shows that the fault zone acts as a confining unit and has a significantly lower capability to transmit water through it or within it than the bedding units. This may be because, in selected shallow areas and at depth the fault zone abruptly terminates bedding partings and vertical partings, thereby terminating the water-bearing zones. As a result of faulting and weathering, the fault zone effectively separates ground-water flow in the rocks on the north side of the fault (the Lockatong aquifer) from ground-water flow in rocks on the south side of the fault (the Stockton aquifer).

Folds

The rocks of the Lockatong Formation are folded into a synform, and rocks of the Stockton Formation are folded into an antiform (fig. 19). The general shape of the synform and antiform is based on the complementary interpretations of the natural gamma-ray anomalies and the dip angles as measured from the rock cores. The structure of the bedding based on the gamma-ray data shows a distinct synform on the north side of the fault. The bedrock dip in the core sections that were collected 200 to 300 ft from the fault is similar to the regional dip that was measured in nearby outcrops.

Along Section E-E' (fig. 14) rock cores from well 42BR show that the bedding dips from 50° to 70°, and rock cores from well 43BR show a bedding dip of about 25° (fig. 25). The dip angles from 11 rock cores collected north of the fault are used to define the synform in the Lockatong formation. The dip angle from 3 rock cores and natural gamma-ray logs from 14 wells south of the fault are used to define the antiform in the Stockton Formation. The angle of dip for the beds in rock cores from wells 28BR (fig. 15) and 6BR, and the shallowest part of well 42BR (fig. 14) were used to define the antiform in the Stockton Formation. All measured dip angles from each core are shown on the respective bedrock well in the geologic section A-A' to I-I' (figs. 10 to 18).

Bedding-Plane and Vertical Partings

In the bedding units of the Lockatong and Stockton Formation are a set of bedding-plane partings and two sets of vertical partings. The bedding-plane partings are laterally extensive and are interpreted to be the major water-bearing zones. The bedding-plane partings in the Lockatong Formation are typically planar and confined to a thin zone, whereas the bedding-plane partings of the Stockton Formation are interconnected and form a wide zone.

The vertical or near vertical partings are typically perpendicular to the bedding, although in some locations they are vertical to land surface. The major set of vertical partings has a strike of about N50°E, and the minor set has a strike of about N20°W. Vertical partings in large outcrops near the NAWC range in length from about 100 ft to more than 200 ft; however, they are limited in height. A single vertical parting typically is confined to 1 to 5 ft of bedding, although in some places, a single vertical parting may penetrate 10 ft or more of bedding. The vertical partings in the sandstone-rich units are typically widely spaced, on the order of one parting per 2 ft, whereas the vertical partings in the siltstones and mudstone are more closely space, about five partings per foot.

The three sets of partings are widespread in the bedrock, and they are the primary pathways for ground-water flow in the aquifers. A generalized block diagram of the Site 1 area shows the relative attitude of the bedding units and the fault as well as the orientation of bedding-plane partings and the two sets of vertical partings (fig. 19).

Regionally and at the NAWC, the partings become more transmissive or less transmissive as a result of chemical and physical weathering of the bedrock. Typically, strata in each bedding unit grade from a shallow zone of some weathering to a deeper zone of limited weathering. The shallow zone of some weathering is from land surface to 40 to 70 ft deep. At depths greater than about 70 ft below land surface, there is a deeper zone of limited weathering. In the shallow zone of some weathering, a high concentration of small fractures is found in addition to the bedding-plane and vertical partings, and many of the fractures are partially or completely filled by mud and silt. Because of weathering in the shallow part of each unit (1) there are more

ground-water flowpaths, (2) ground-water flow will not be as strongly controlled by the bedding partings, (3) ground water will have a tendency to flow more closely in the direction of the general ground-water-flow gradient, (4) shallow bedrock will have a higher storage capacity, and (5) the shallow parts of a bedding unit will show less drawdown than deeper parts of the same unit. Analysis of drawdown water levels from aquifer tests shows less drawdown in the shallow part of many of the bedrock units than in the deep part of the same units.

SURFACE-WATER SYSTEM

The regional surface-water system consists of the Delaware River about 2 miles west of NAWC, Gold Run and its tributaries, West Branch Shabakunk Creek and its tributaries, and an unnamed stream referred to in this report as Villa Victoria Brook, which passes through Villa Victoria School campus (fig. 6). In addition, a number of small springs are present.

Delaware River, Streams, and Springs

The Delaware River is the major river in the study area with an annual mean discharge at Trenton, N.J., of 11,660,000 ft^3/s for the period of record 1913-98. All ground-water and surface-water flow in the study area eventually discharges to the Delaware River. The headwaters for Villa Victoria Brook, Gold Run, and the West Branch Shabakunk Creek are near the NAWC, and start of flow for each stream is from springs in the Lockatong Formation. Generally each stream flows southward to cross over the fault/contact of the Lockatong and Stockton formations. Villa Victoria Brook originates in the Lockatong Formation and flows southwestward. Upon reaching the fault/contact the brook flows along the fault/contact to the Delaware River. The headwaters of Gold Run start just north of the fault/contact as springs. Water from the springs flows in a stream channel to the fault/contact. During periods of low flow, the stream loses water after it flows over the fault contact, and the channel becomes dry. The stream then reappears a few hundred feet down the channel. During periods of high flow, the channel contains flow along its whole length. The headwaters of West Branch Shabakunk Creek originate in three short tributaries, with start of flow that is north of the fault/contact. The three tributaries join at the fault/contact. There are no other tributaries to the creek in the immediate study area or over the Stockton Formation.

Three springs labeled Spring 1, Spring 2, and Spring 3 near the NAWC (fig. 6) generally flow year round. They can be dry during mid and late summer, however, when rainfall is limited and evapotranspiration is high. Spring 1 is on the west side of NAWC just north of the fault. Discharge measured in a Parshal flume ranged from 0 to about 75 gal/min. During periods of medium and low flow, discharge from the spring flows for about 100 ft, then percolates back into the aquifer. During periods of high flow, water from the spring flows to a culvert then under Parkway Avenue.

Spring 2 on the east side of the NAWC is in a forested area behind a commercial strip mall. The spring discharge point is in an area that has been filled with rocks and other debris. Farmers in the past tried to fill in the spring with rocks and other debris in an attempt to make the land more tillable. The original location of the spring may be in the wetlands about 500 feet north of where the spring is plotted in figure 6. As noted in the hydrogeologic framework section, the exact location of the fault/contact in the east part of the facility is not well known; therefore, depending on the original location of Spring 2 the fault contact could be about 500 ft south of where it was plotted in figure 6. Attempts to measure

discharge from the Spring 2 were unsuccessful. Discharge was visually estimated five times during 1987 at 0 to 0.1 ft^3/s (0 to 45 gal/min).

Spring 3, is immediately south of the circle at the Ewing Cemetery (fig. 6). The spring is believed to have originated in the cemetery because a spring is shown near there in the 1913 map (fig. 26). It is believed that water from the spring has been diverted to a culvert that carries the water to the south edge of the cemetery. Flow in the channel about 300 ft downstream from Spring 3 was measured twice. Both times flow was about 0.1 ft^3/s (about 45 gal/min). At times during the mid and late summer, there has been no flow in the channel.

West Branch of Gold Run

The West Branch of Gold Run has not been described in previous studies. As a result, it is necessary to describe it in some detail. The start of flow in the West Branch of Gold Run is Spring 1. Flow from the spring travels down a small channel through forested wetland to a culvert at the intersection of Decou Avenue and Parkway Avenue. Upon entering the culvert the stream flows underneath Parkway Avenue. Together the West Branch of Gold Run and Parkway Avenue form the southern boundary of the NAWC. Because the stream is under the street, it is not visible except in some storm grates in Parkway Avenue and at its point of exit from the culvert on the south side of Parkway Avenue, east of the General Motors employee parking lot.

A 1913 map of West Trenton (New Jersey Department of Environmental Protection, 1913) (fig. 26) shows the West Branch of Gold Run flowed southeastward through a forested wetland west of the present NAWC property to Parkway Avenue. The stream then flowed eastward for about 700 ft along the north side of Parkway Avenue. A few hundred feet west of the railroad trestle, the West Branch of Gold Run crossed under or over Parkway Avenue. The culvert or ford may have been about where the entrance gate to the NAWC is now located. Downstream from the culvert or ford, the West Branch of Gold Run flowed along the south side of Parkway Avenue under the railroad trestle to the confluence with the East Branch of Gold Run.

At present (1998), the stream still flows from Spring 1 southeastward toward Parkway Avenue, but now it enters a culvert system under Parkway Avenue. The "Plan and Profile of Parkway Avenue" maps (Mercer County Highway Department, 1942 map files) (figs. 27a and b) show the culvert system that carries the flow of the West Branch of Gold Run under Parkway Avenue. The culverts are engineered to carry the flow beneath Parkway Avenue and allow ground-water discharge to enter the culverts much the same way as the stream channel allowed ground water to enter the stream bottom. Reference location stations numbered 99 through 129 are shown on the highway maps and are used in this discussion. The stream flows into the culvert at the northwestern corner of the intersection of Parkway Avenue and Decou Avenue (station 128+50)[3]. The culvert carries flow under Parkway Avenue eastward about 2,900 ft to an exit culvert (station 100+20) east of the General Motor parking lots and west of a unused field owned by General Motors. At this location, the exit point of the culvert, the West Branch of Gold Run is visible as a permanent surface-water stream. Construction diagrams of the culvert under Parkway Avenue show that the section from the inflow culvert at Decou Avenue eastward to station 127+50 consists of 24-inch vitreous clay pipe. At station 127+50, the culvert carrying the West Branch of Gold Run joins a stormwater runoff culvert that

[3]Surveying notation to define a location that is 50 ft past station 128.

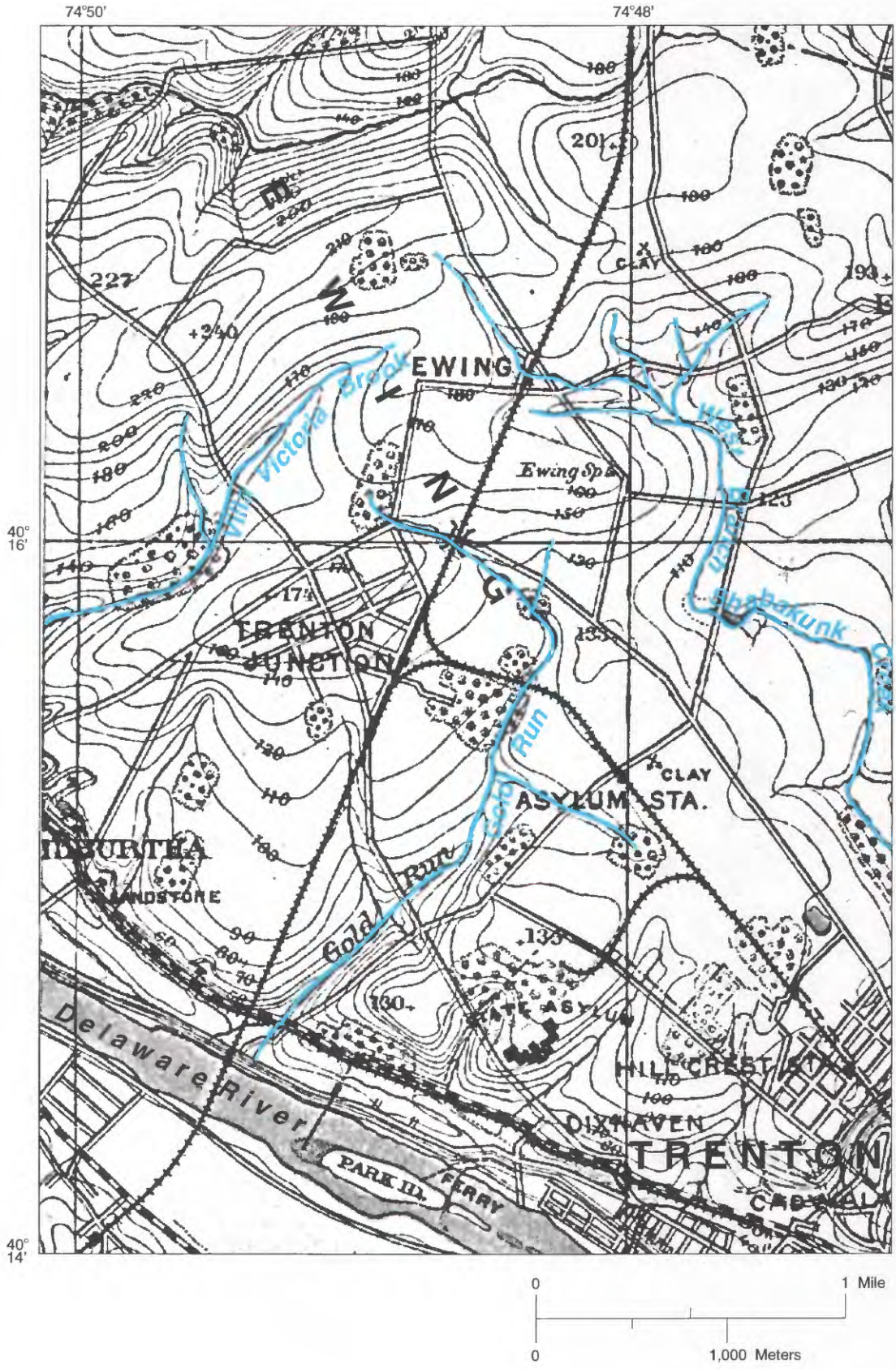

Figure 26. Map from 1913 showing the original channels of Gold Run. (From New Jersey, Geological Survey, 1913)

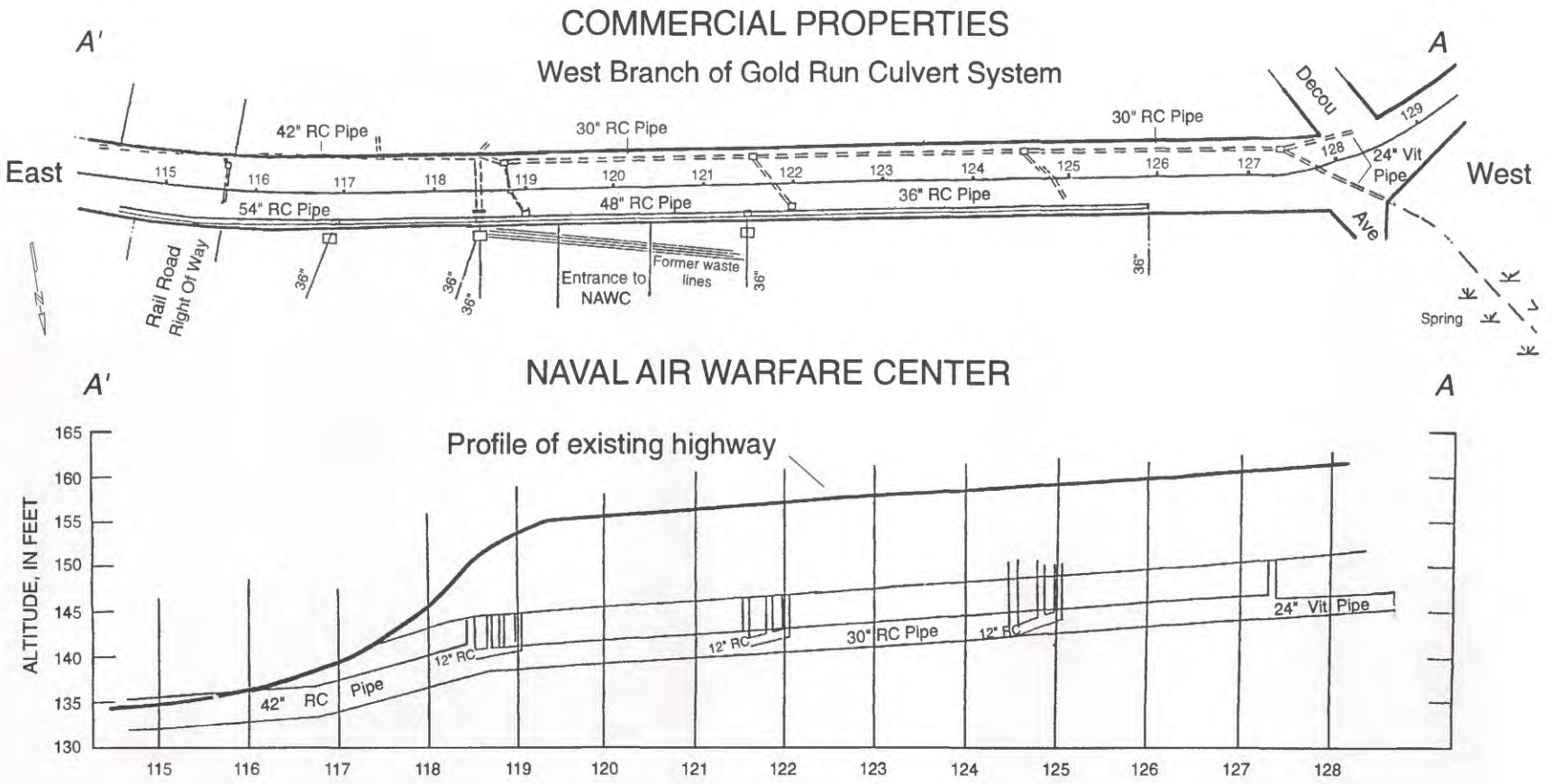

Figure 27a. The construction of the culvert underneath the south side of Parkway Avenue that acts as the channel for the West Branch of Gold Run and location of the culvert under the north side of Parkway Avenue which carries storm-water from NAWC. (Modified from Mercer County Highway, 1942, File A, Pocket 14, Folder 1 to 3)

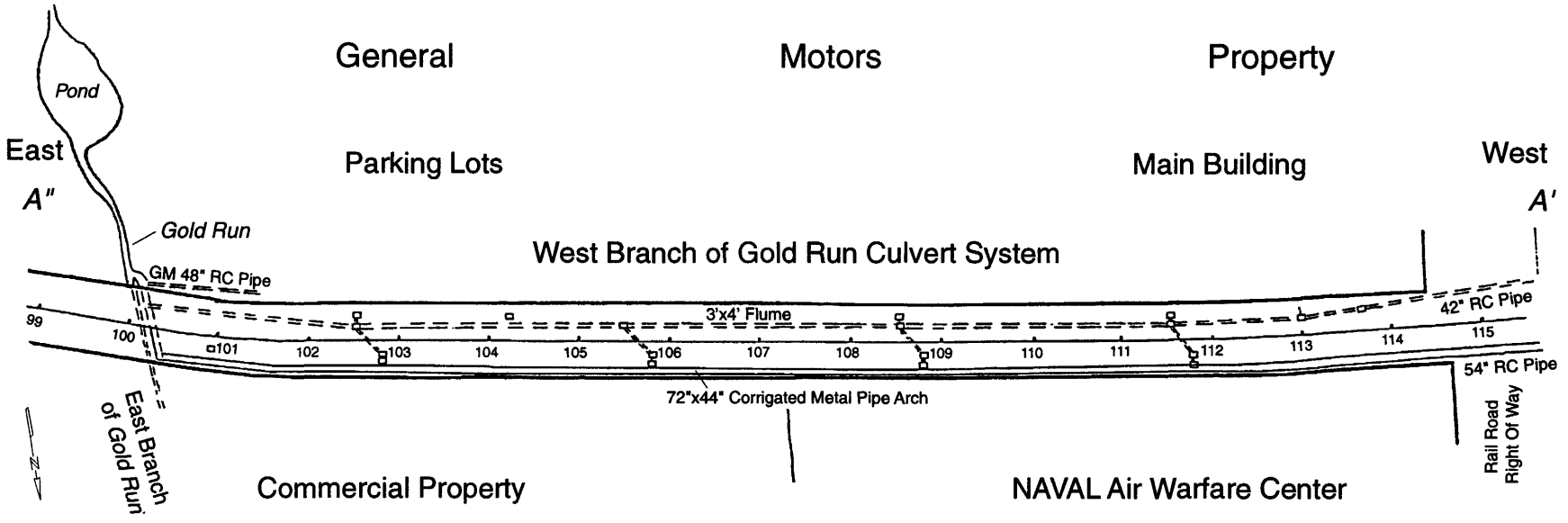

Figure 27b. The construction of the culvert underneath the south side of Parkway Avenue that acts as the channel for the West Branch of Gold Run and location of the culvert under the north side of Parkway Avenue which carries storm-water from NAWC. (Modified from Mercer County Highway, 1942, File A, Pocket 14, Folder 1 to 3)

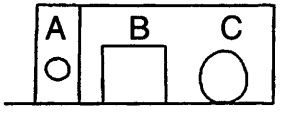

Figure 27c. The three exit culverts tthat discharge water from (A) GM parking lots, (B) West Branch of Gold Run, Parkway Avenue, and NAWC, and (C) East Banch of Gold Run

carries water under Parkway Avenue from streets west of Decou Avenue. From station 127+50 to station 118+50, the culvert is made of 30-inch reinforced concrete pipe; from station 118+50 to station 114+50, the culvert is made of 42-inch reinforced concrete; and from station 114+50 to station 100+20, the culvert is described as a 3 ft by 4 ft flume.

The vitreous clay and reinforced concrete pipe culvert in 4- to 12-ft long pieces and are laid end to end with no cement in the joints. Therefore, the joints are about 4 to 12 ft apart. Based on the construction details and road building technology, the design of the culvert allows ground water to enter and exit the culvert at each joint. The construction methods used in building this culvert allow the culvert to act similarly to the former streambed thereby allowing interaction of ground water and surface water.

The culvert where the West Branch of Gold Run emerges from beneath Parkway Avenue was visited more than 20 times during 1996-97. Flow was always observed exiting from the culvert pipe.

Three discharge culverts are visible when looking upstream to where Gold Run exits from under Parkway Avenue (fig. 27c inset). From west to east the culverts are labeled (A) GM property, (B) West Branch and the NAWC, and (C) East Branch. Culvert A (fig. 27c) is a stormwater runoff culvert from General Motors parking lots. During visits to the culvert in 1996-97, flow was seen exiting culvert A during and after heavy rainfall, but there was light or no flow from culvert A during periods of no precipitation. Culvert B (fig. 27c) carries discharge water from both of the culvert systems that are under Parkway Avenue. The culvert system under the south side of Parkway Avenue was designed to replicate the ground-water/surface-water interaction of the West Branch of Gold Run as described above. In addition, the culvert on the south side of Parkway Avenue carries stormwater run-off from Parkway Avenue and from all commercial properties, except General Motors, and from all residential properties along of Parkway Avenue from Sullivan Way to Gold Run. The culvert system under the north side of Parkway Avenue carries stormwater runoff from the NAWC. The culvert system originates on the NAWC property as a network of small culverts that discharge into one of four stormwater culverts. The four 36-inch diameter culverts discharge water to the culvert that lies under the north side of Parkway Avenue. Stormwater from NAWC property is kept separate from the West Branch of Gold Run culvert system until about 50 ft upstream from culvert B. Culvert C is the East Branch of Gold Run which carries stormwater runoff from the commercial, recreational, and wooded properties on either side of the East Branch of Gold Run.

Discharge at each exit culvert and at the main stem of Gold Run is shown in table 2. The discharge measurements were made on August 20, 1996, and September 4, 1997. Discharge on August 20, 1996, was about 1 gal/min from culvert A, about 30 gal/min from culvert B and 9.5 gal/min from culvert C. On September 4, 1997, however, culvert A and C were dry, whereas culvert B showed a discharge of about 90 gal/min. It is not certain why culvert A and C showed no flow during September 4, 1997, while culvert B was flowing nearly 10 times the rate of the previous measurement.

Precipitation data for the 3 days prior to each discharge measurement are shown in table 3. About 0.11 to 0.20 in of precipitation fell during the 48 hours prior to stream discharge measurements on September 4, 1997. The discharge resulted in a three-fold increase in discharge from the West Branch of Gold Run.

NAWC covers about 60 acres and more than 75 percent of it is covered with impermeable surfaces such as macadam, cement, or

Table 2. Individual and total discharge from three culverts at the exit of the Gold Run tributaries from under Parkway Avenue

Date	GM Pipe (A)	NAWC Pipe (B)	West Branch & East Branch (C)	Total
		[Discharge in cubic feet per second]		
8-20-96	0.0025	0.0665	0.021	0.090
9-04-97	dry	0.203	dry	0.203
		[Discharge in gallons per minute]		
8-20-96	1.122	29.85	9.42	40.39
9-04-97	dry	91.11	dry	91.11

Table 3. Precipitation at stations at Trenton State College (College of New Jersey) and Washington Crossing State Park during the day of stream gaging and the three previous days

[Precipitation, in inches]

Date	Trenton State College	Washington Crossing State Park
8-20-96	0.00	0.00
8-19-96	0.00	0.00
8-18-96	0.00	0.00
8-17-96	0.00	0.00
9-04-97	0.10	0.00
9-03-97	0.10	0.11
9-02-97	0.00	0.00
9-01-97	0.00	0.00

buildings. A rainfall of 0.1 in/d falling on an estimated 45 acres of impermeable surface would create a surface-water discharge increase of 85 gal/min in Gold Run if (1) rainfall were spread out over a full day, (2) if all rainfall discharged as overland flow to the stormwater runoff from the U.S. Navy NAWC, and (3) no precipitation evaporated or percolated into the ground.

GROUND-WATER LEVELS

This section includes static water-level data, drawdown water-level data, and stressed water-level data. Static water levels were collected during 1993-96 prior to the start up of the recovery well for the contaminated ground-water pump and treat facility. Drawdown water levels were collected during 1993-96 during each of three aquifer tests. Stressed water levels were collected at various times since the start of the pump and treat operation; however, only during August 25-27, 1997, were water-level data collected for all wells at the NAWC.

Static Water Levels

The USGS plotted and contoured the static ground-water levels in the fractured bedrock aquifer on maps and sections (figs. 28 to 38). The static water-level data presented here were collected December 4-5, 1995, prior to the start-up of the pump and treat facility.

The hydraulic gradient and ground-water flowpaths are controlled by many aspects of the hydrogeologic framework. The hydrogeologic framework includes strike, dip, and conductivities of the water-bearing zones, semi-confining zones, and fault plane/ confining unit, as well as the topography of the small valley, and location of and flow in the West Branch of Gold Run.

Hydraulic factors acting on the static water levels are the location of nearby and distant recharge areas and discharge areas for the bedding units, and the screen interval of the monitoring well. The primary recharge area for each bedding unit is the outcrop area of the bedding unit provided the outcrop area is not in a wetland. The nearest bedrock discharge area for the NAWC facility is the spring and stream channel at the head of the West Branch of Gold Run. Distant bedrock discharge areas for the site 1 and site 3 areas of NAWC include the Delaware River and Villa Victoria Brook. The water level in a particular well is primarily controlled by the water level in the outcrop area of the bedding unit that contributes water to the screen interval of the well.

The static water-levels maps show projected water-level contours on a horizontal plane at an altitude of +150 ft, which is approximately land surface (fig. 28), and at an altitude of +50 ft, which is approximately 100 ft below land surface (fig. 29). On the north side of the fault, the water-level contours indicate that the hydraulic gradient is generally southward at an altitude of 150 ft (fig. 28) and radially toward bedding unit L-15 and L-16 at an altitude of +50 ft (fig. 29). However, as discussed in the methods section, the flowpath direction may be different than the hydraulic-gradient direction. The predominate flowpath is in the water-bearing zones of each bedding unit from an area of recharge to an area of discharge (fig. 4). Therefore, the flowpath direction is westward in each bedding unit from the upland areas to spring Sp1 and the headwaters of the West Branch of Gold Run.

Static water-level contour lines in sections A-A' through I-I' (figs. 30 to 38) show that the hydraulic gradient north of the fault/contact is generally downward and southward, but along the fault/contact, the hydraulic gradient is upward and northward. Again the flowpath is predominantly within the water-bearing zones of the bedding units, and it is interpreted that the flowpath north of the fault is into the page

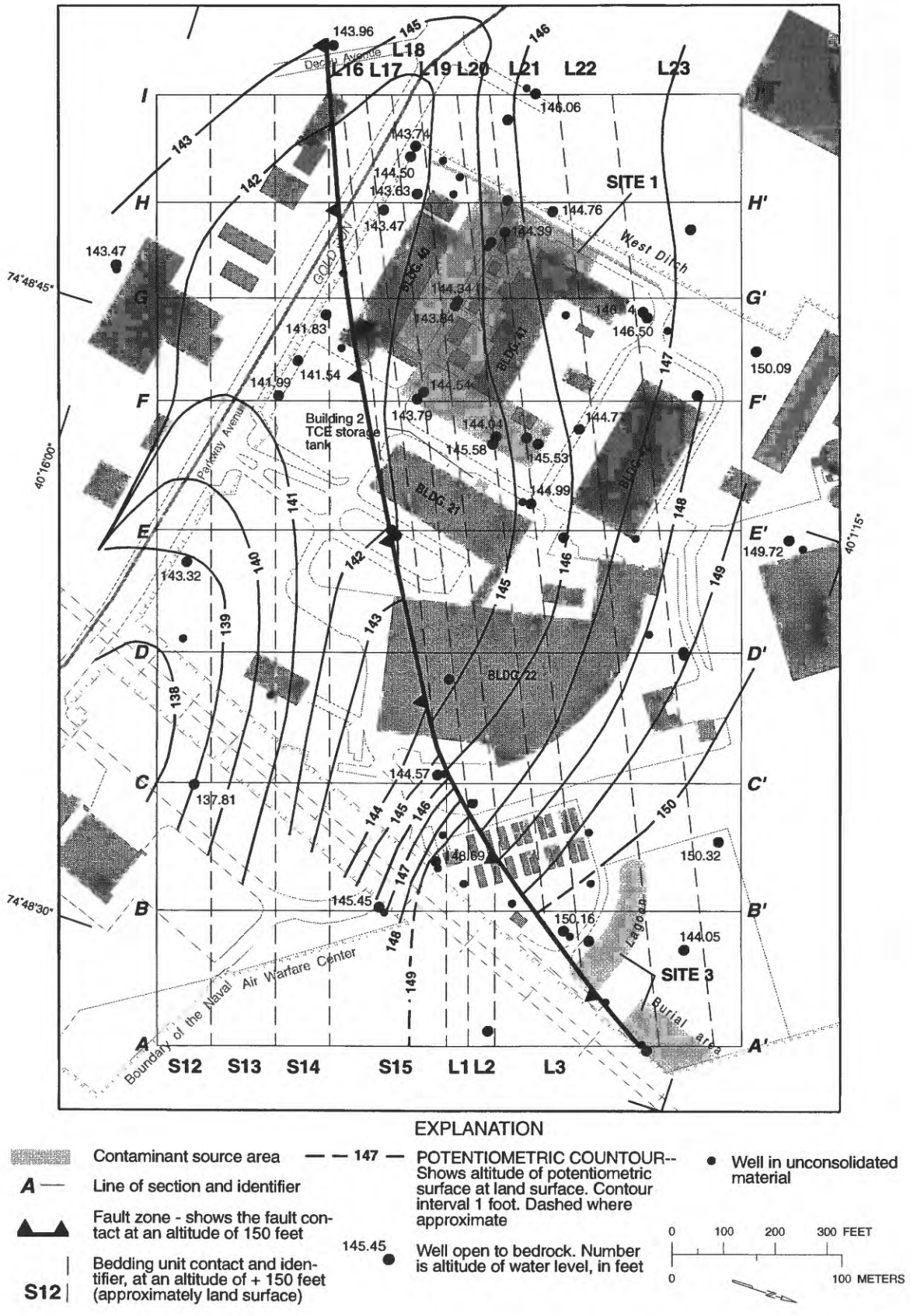

Figure 28. The static potentiometric surface at an altitude of + 150 feet, (approximately land surface) December 4, 1995, Naval Air Warfare Center, West Trenton, N.J.

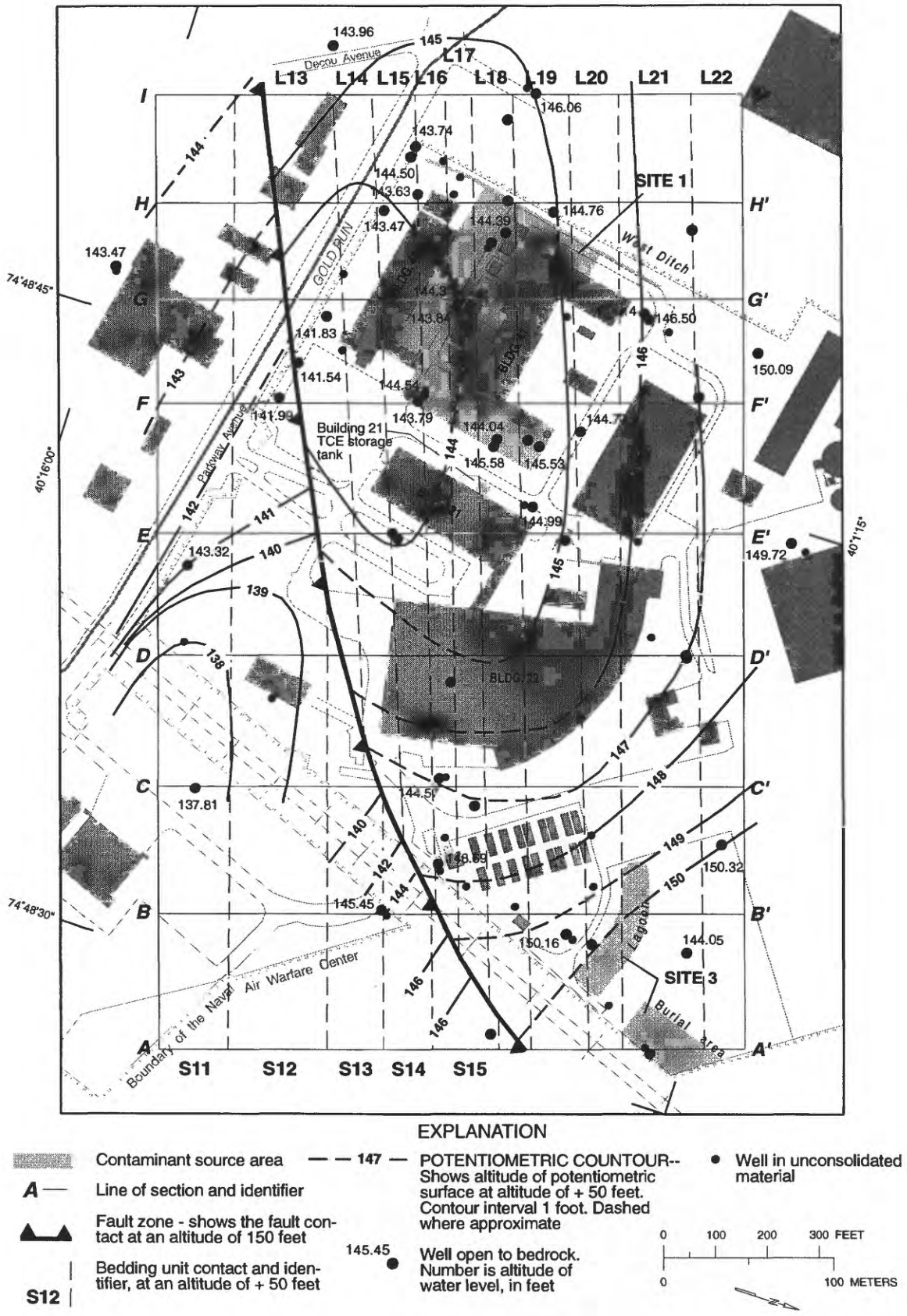

Figure 29. The static potentiometric surface at an altitude of + 50 feet, (approximately 100 feet below land surface), December 4, 1995, Naval Air Warfare Center, West Trenton, N.J.

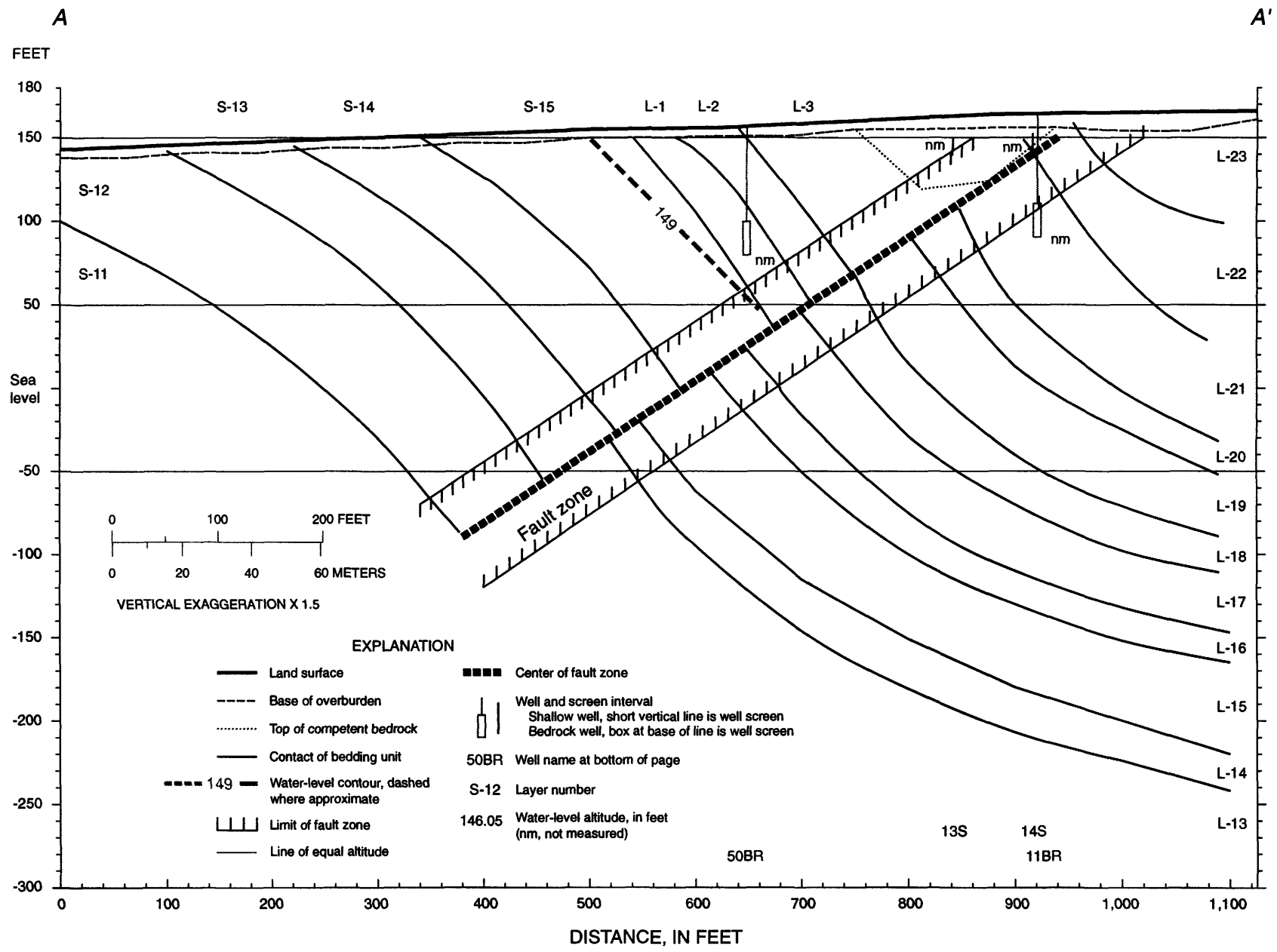

Figure 30. Section *A-A'* showing static water-level altitudes measured in bedrock wells, December 4, 1995.

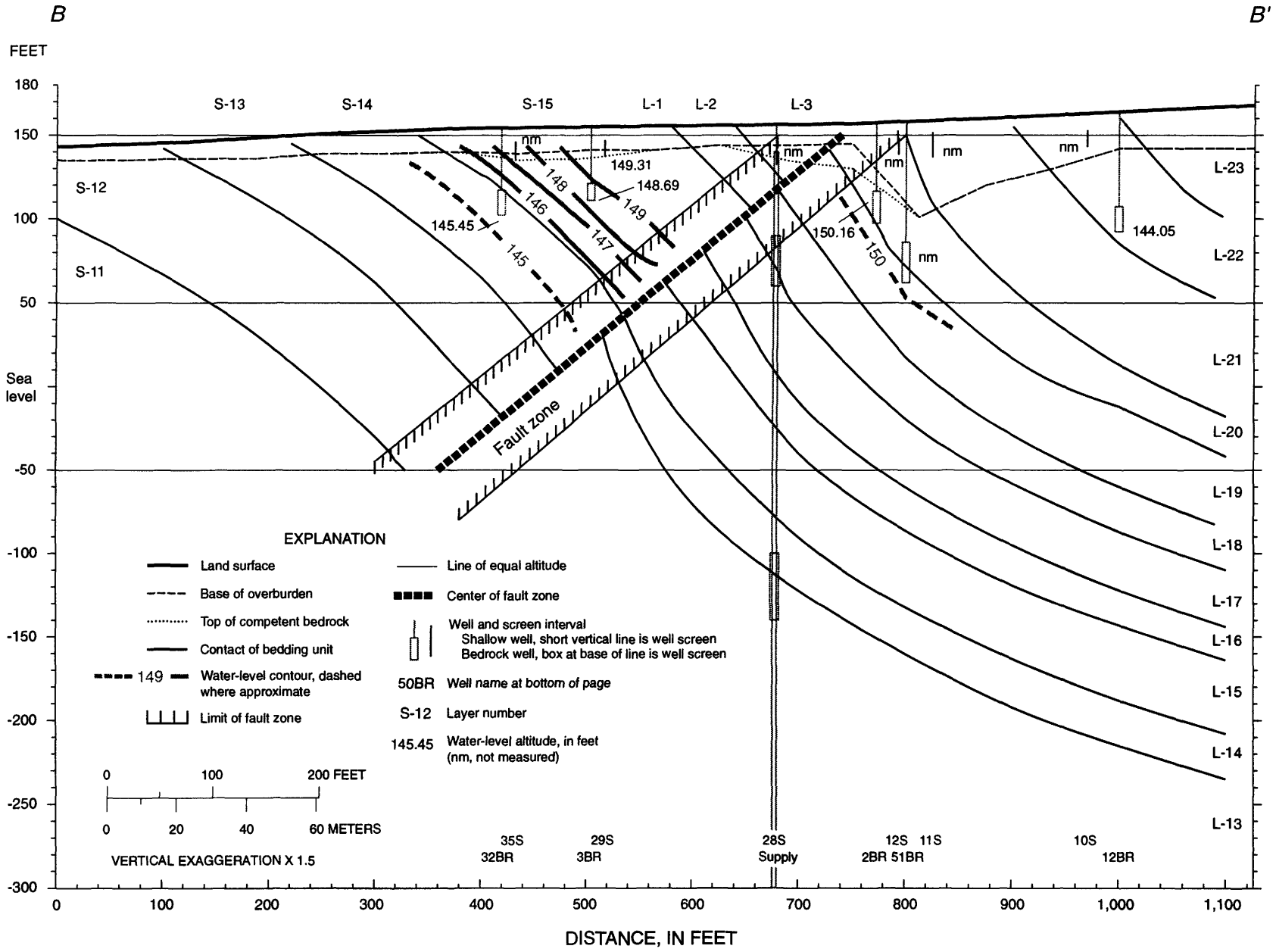

Figure 31. Section *B-B'* showing static water-level altitudes measured in bedrock wells, December 4, 1995.

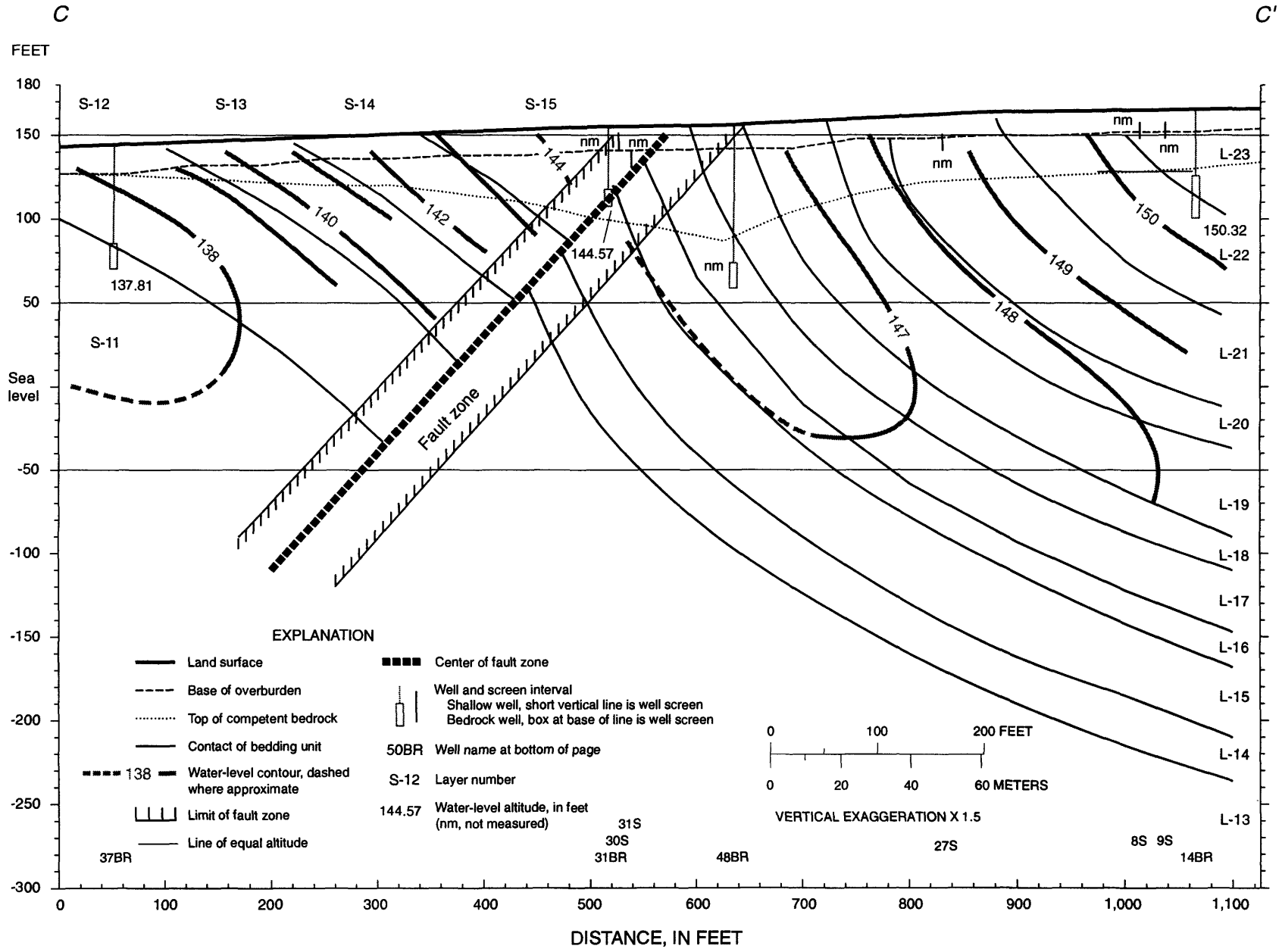

Figure 32. Section *C-C'* showing static water-level altitudes measured in bedrock wells, December 4, 1995.

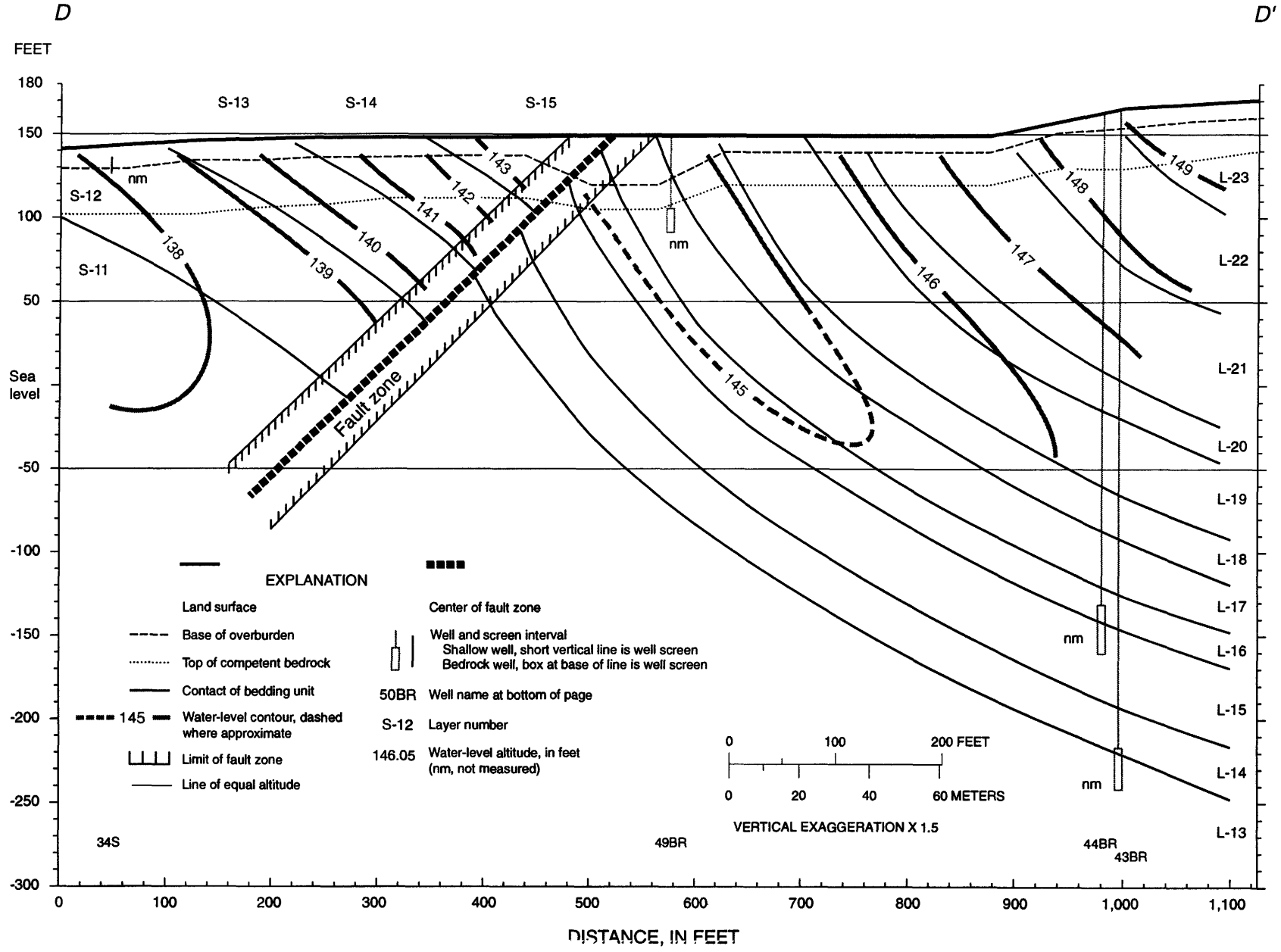

Figure 33. Section *D-D'* showing static water-level altitudes measured in bedrock wells, December 4, 1995.

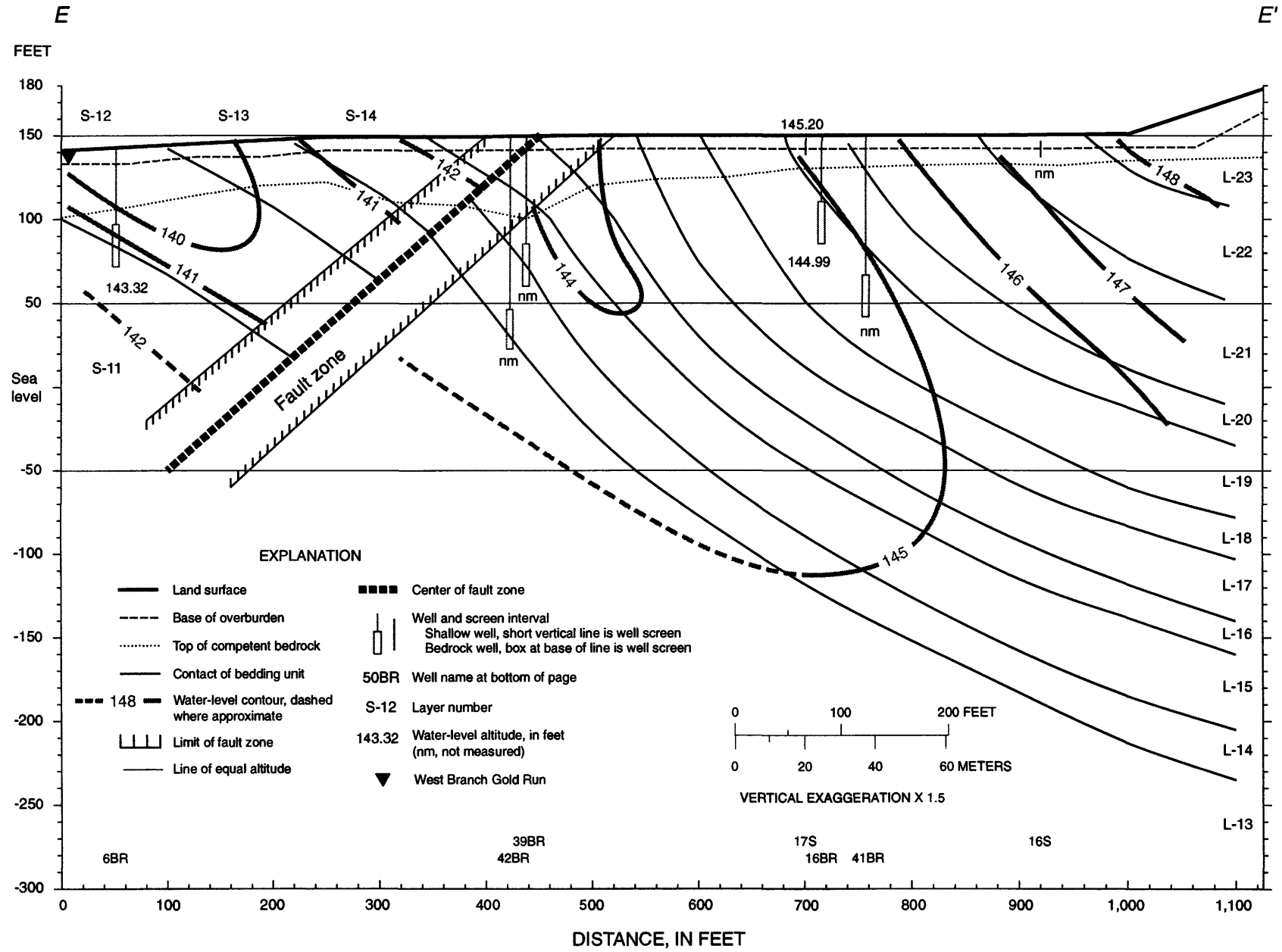

Figure 34. Section *E-E'* showing static water-level altitudes measured in bedrock wells, December 4, 1995.

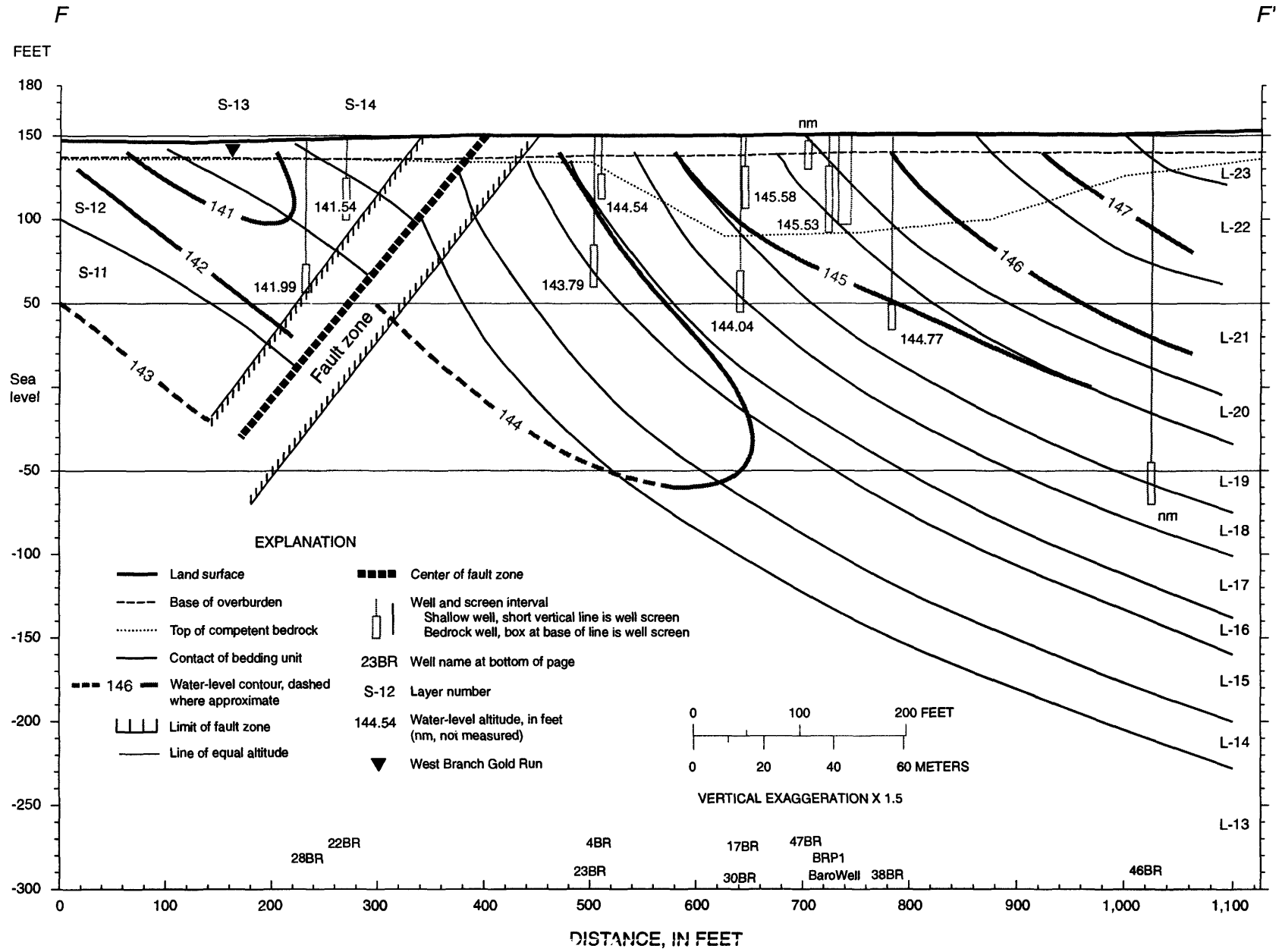

Figure 35. Section *F-F'* showing static water-level altitudes measured in bedrock wells, December 4, 1995.

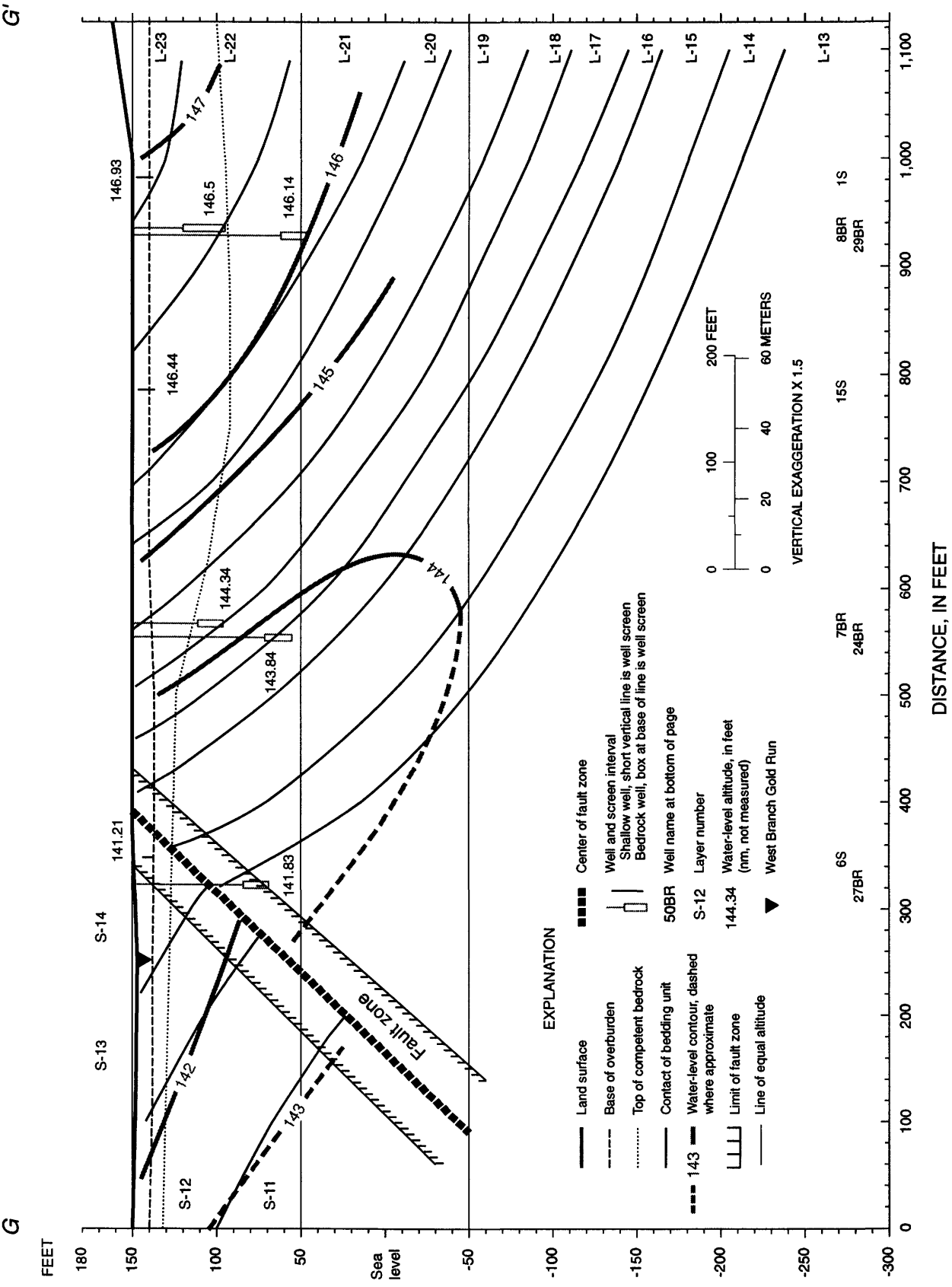

Figure 36. Section *G-G'* showing static water-level altitudes measured in bedrock wells, December 4, 1995.

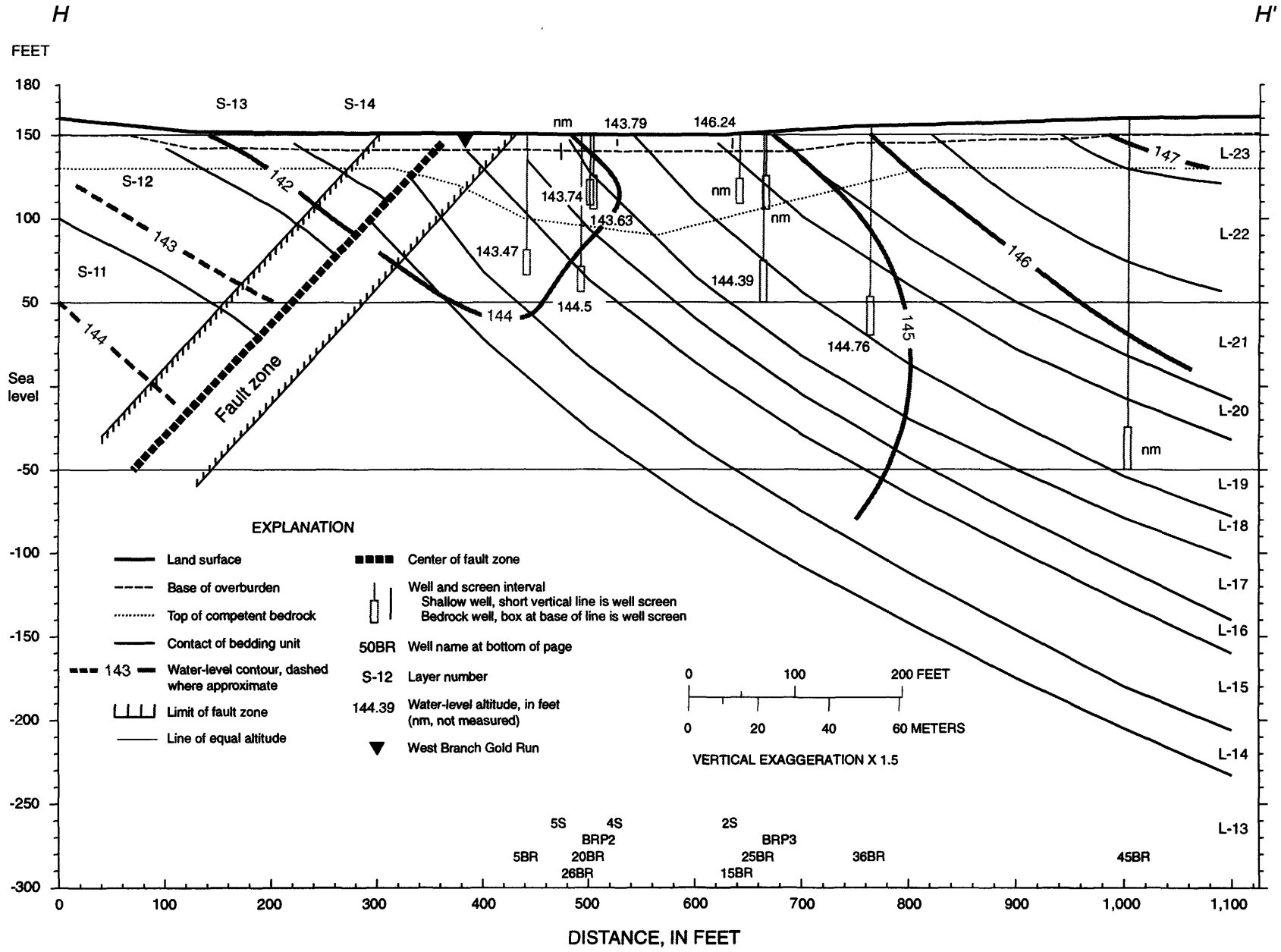

Figure 37. Section *H-H'* showing static water-level altitudes measured in bedrock wells, December 4, 1995.

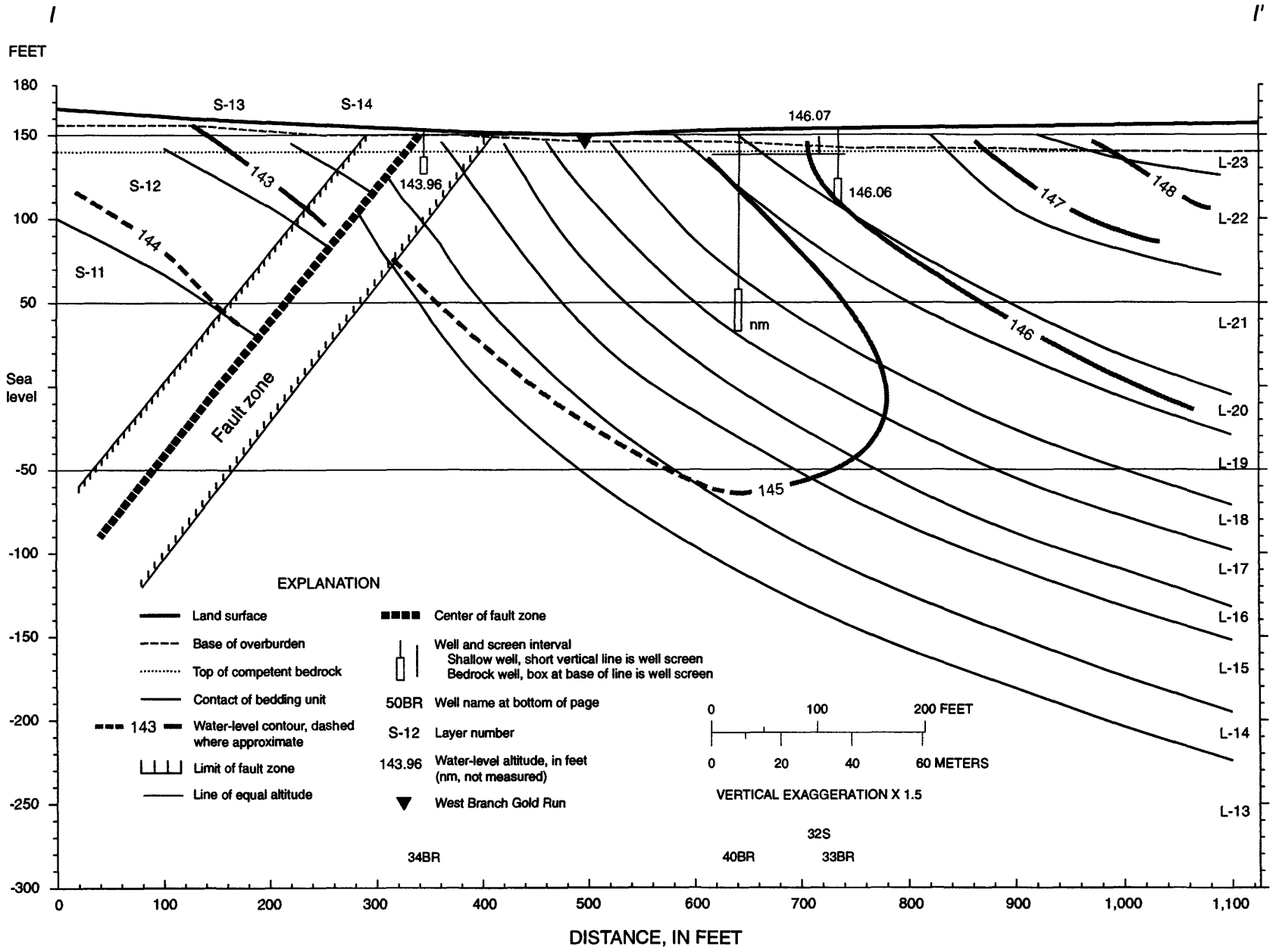

Figure 38. Section *I-I'* showing static water-level altitudes measured in bedrock wells, December 4, 1995.

or westward in each section. Well nests that show a downward hydraulic gradient include wells 7BR and 24BR (line G-G') (fig. 36), wells 8BR and 29BR (line G-G') (fig. 36), and wells 23BR and 4BR (line F-F') (fig. 35). A well nest that shows a subtle upward hydraulic gradient is wells 26BR and 5BR (line H-H') (fig. 37).

Wells in a bedding unit or in a pair of bedding units that show a westward flowpath include wells 14BR and 8BR in bedding unit L-22, wells 29BR and 33BR in bedding unit L-21, wells 2BR and 16BR in bedding units L-19 and L-20, wells 16BR and 36BR in bedding unit L-19, wells 30BR and 20BR in bedding unit L-17, and wells 23BR and 5BR in bedding units L-15 and L-16 (figs. 28 to 38).

The water-level contours at an altitude of +50 ft show an elongate potentiometric surface low on the north side of the fault that is centered on bedding units L-15 and L-16 under building 40 (fig. 29). The lowest water levels at this altitude of +50 ft and north of the fault are delineated by the 144-ft contour line. Inside the 144-ft contour line the lowest water level is below the West Branch of Gold Run. The hydraulic gradient beneath Gold Run is upward. Ground-water flowpaths in part are upward in this region with ground-water discharging to the West Branch of Gold Run. The result of this upward flow is increased discharge at Spring 1 and increased flow in the upper reaches of the West Branch of Gold Run.

The water-level contours on the south side of the fault are interpreted to show that the hydraulic gradient is upward and/or toward the West Branch of Gold Run (figs. 28-38). Well set 28BR and 22BR (line F-F') (fig. 35) shows an upward hydraulic gradient. Water levels in well 6BR (line E-E') (fig. 34) were measured more than 10 times during 1996-97. The water level was above land surface each time. Therefore, there is an upward hydraulic gradient in this area. The high water levels in well 6BR were previously attributed to a rupture in a public-supply water main near the well; however, the author interprets that the high water levels in well 6BR are a result of the elevated recharge area of bedding unit S-11. The outcrop for bedding unit S-11 is located south of the well on the hill owned by the Benevolent and Protective Order of the Elks (Elks Club). The hydraulic head created by the elevated land is causing elevated water levels in well 6BR. This feature is described in the methods section (figs. 3 and 5).

The hydraulic gradient near wells 32BR and 37BR is very steep (figs. 2, 28, and 29), and it is possible that there is a confining unit in this area. As discussed in the hydrogeologic framework, it is possible that the fault does not bend northward at well 31BR but rather it is traced to the east to a short distance south of well 50BR. The mapped location of the fault is based on evidence found in rock core from well 51BR. Further hydrogeologic investigations may be needed refine the location of the fault in the area between wells 32BR and 51BR.

Drawdown Water Levels During Aquifer Tests

Water-level data from three aquifer tests show water-level drawdowns in the pumped well and in selected wells surrounding the pumped well. Interpretation of the data show (1) that the ground-water flow under pumping conditions is predominantly within the bedding units and (2) that shallow parts of the bedding units are typically less permeable and/or contain more water in storage than the deep parts of the bedding units.

Aquifer test on Well 15BR

The first aquifer test was conducted on April 8-12, 1993. Well 15BR (line H-H') (fig. 45), which is screened in bedding unit L-19, was pumped at a rate of 25 gal/min for 72 hours. The 23 wells surrounding the pumped well were monitored for water-level draw-

downs. Maps and sections show the water-level drawdown in the 24 wells monitored during the aquifer test (figs. 39 to 46).

The results of pumping revealed two hydraulic characteristics of the bedrock aquifer. The first characteristic is that drawdown, and therefore flow, is predominantly within bedding unit L-19 while under pumping conditions. Water levels declined 2.95 and 3.87 ft in wells 36BR and 38BR respectively. It is interpreted that there is a very good connection between wells 15BR, 36BR, and 38BR via bedding partings of bedding unit L-19. Water levels declined about 1.0 to 2.31 ft in wells screened in bedding units L-18 through L-21, and water levels in wells in bedding units L-15, L-16, L-17, and L-22 declined 0.45 to 0.97 ft. Water levels in bedding units on the south side of the fault showed no water-level drawdown.

The second hydraulic characteristic of the bedrock aquifer is that the shallow part of most bedding units is less permeable and/or contains more water in storage than the deep part of the same bedding unit. The drawdown in the shallow wells is less than drawdown in wells that are in the deeper part of the same bedding unit. For example, drawdown in deep bedrock wells 36BR and 38BR is 2.95 and 3.57 ft, respectively, whereas drawdown in shallow bedrock wells 16BR and 17BR is 1.52 and 1.12 ft, respectively. All four wells are screened in bedding unit L-19.

Two maps show drawdown for the Lockatong aquifer and one map shows drawdown for bedding unit L-19. The first map shows drawdown at an altitude of + 150 ft, which is about land surface (fig. 39), and the second map shows drawdown at an altitude of + 50 ft, which is about 100 ft below land surface (fig. 40). Both maps show that the center of the elongate cone of depression stayed within bedding unit L-19. The drawdown maps show that drawdown along the strike of the bedding is about four times greater than the drawdown perpendicular to the bedding plane. The hydraulic gradient is about four times greater along strike than it is perpendicular to the strike direction or a ratio of 4:1, thus the Lockatong aquifer in this region is quite anisotropic.

The third map shows drawdown in the plane of bedding unit L-19 based on water-level drawdown values from 7 wells (fig. 41). The map shows that drawdown in the down dip direction is about half of drawdown along the strike direction. Therefore, individual bedding units are more isotropic with a ratio of about 2:1 than the Lockatong aquifer when taken as a whole with a ratio of 4:1.

In summary, the Lockatong aquifer is interpreted to have an anisotropic hydraulic conductivity based on the shape of the contours in drawdown maps. However, individual bedding unit L-19 or water-bearing zones in the bedding units have a nearly isotropic hydraulic conductivity. In addition, based on water level drawdown data, more water is available in storage in the shallow part than in the deep part of each bedding unit. The high fracture density in the shallow part of the bedding units accounts for the higher storage capacity. The shallow part of each bedding unit is less permeable than the deep part of the same bedding unit because more of the rock has weathered to a clay in the shallow part than in the deep part of the same aquifer. As a result of the higher storage and less permeability in the shallow pats of the bedding unit, the areal extent of the cone of depression is less in the shallow part of the bedding units than in the deep part of the same bedding unit.

Aquifer test on Well BRP1

A second aquifer test was conducted on August 9-12, 1995. Well BRP1, screened in bedding units L-19 and L-20, was pumped at a rate of 25 gal/min for 48 hours while eight wells surrounding the pumped well were monitored for water-level drawdown.

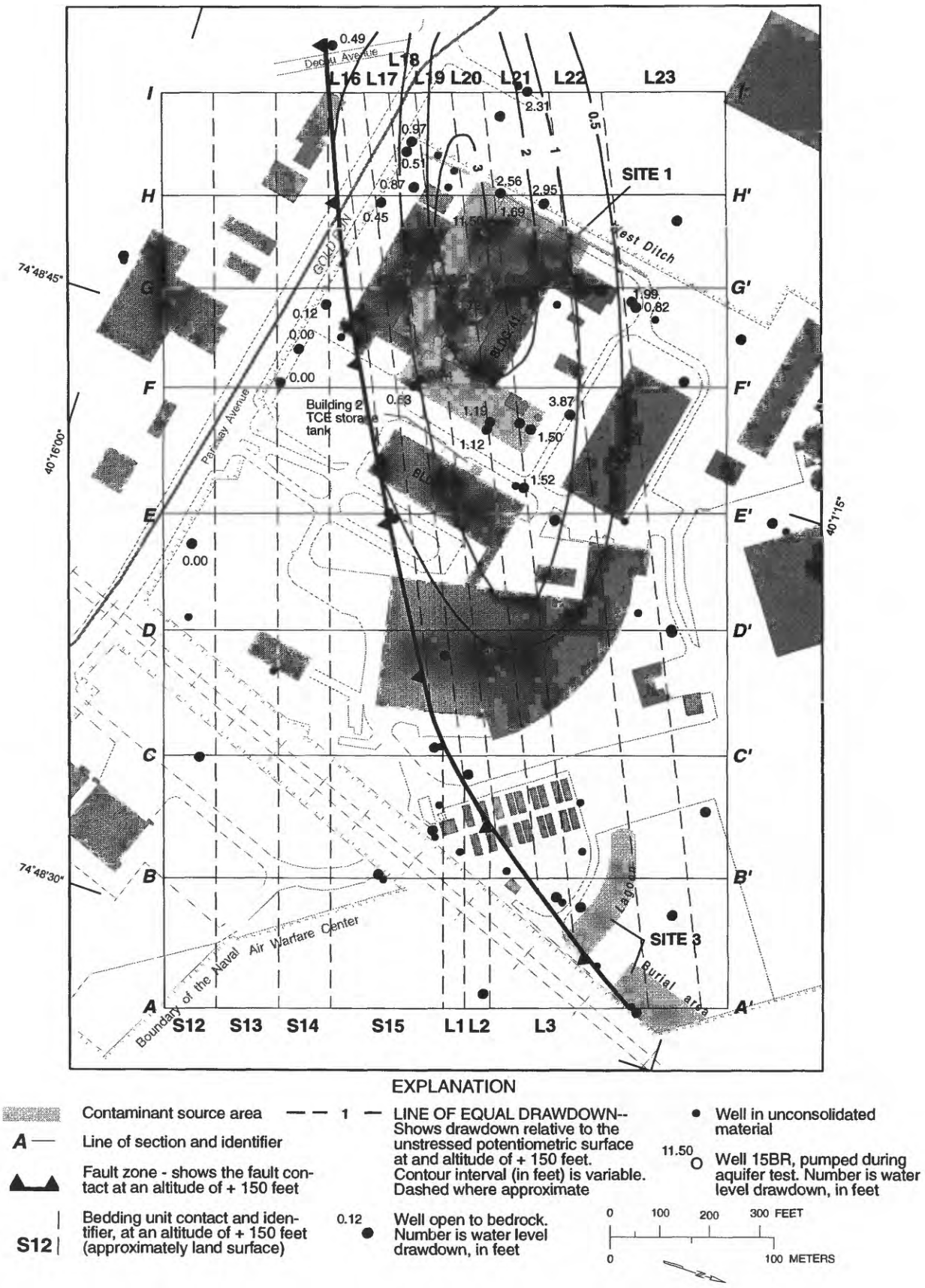

Figure 39. Drawdown during the aquifer test with well 15BR pumping, shown at an altitude of + 150 feet (approximately land surface), Naval Air Warfare Center, West Trenton, N.J.

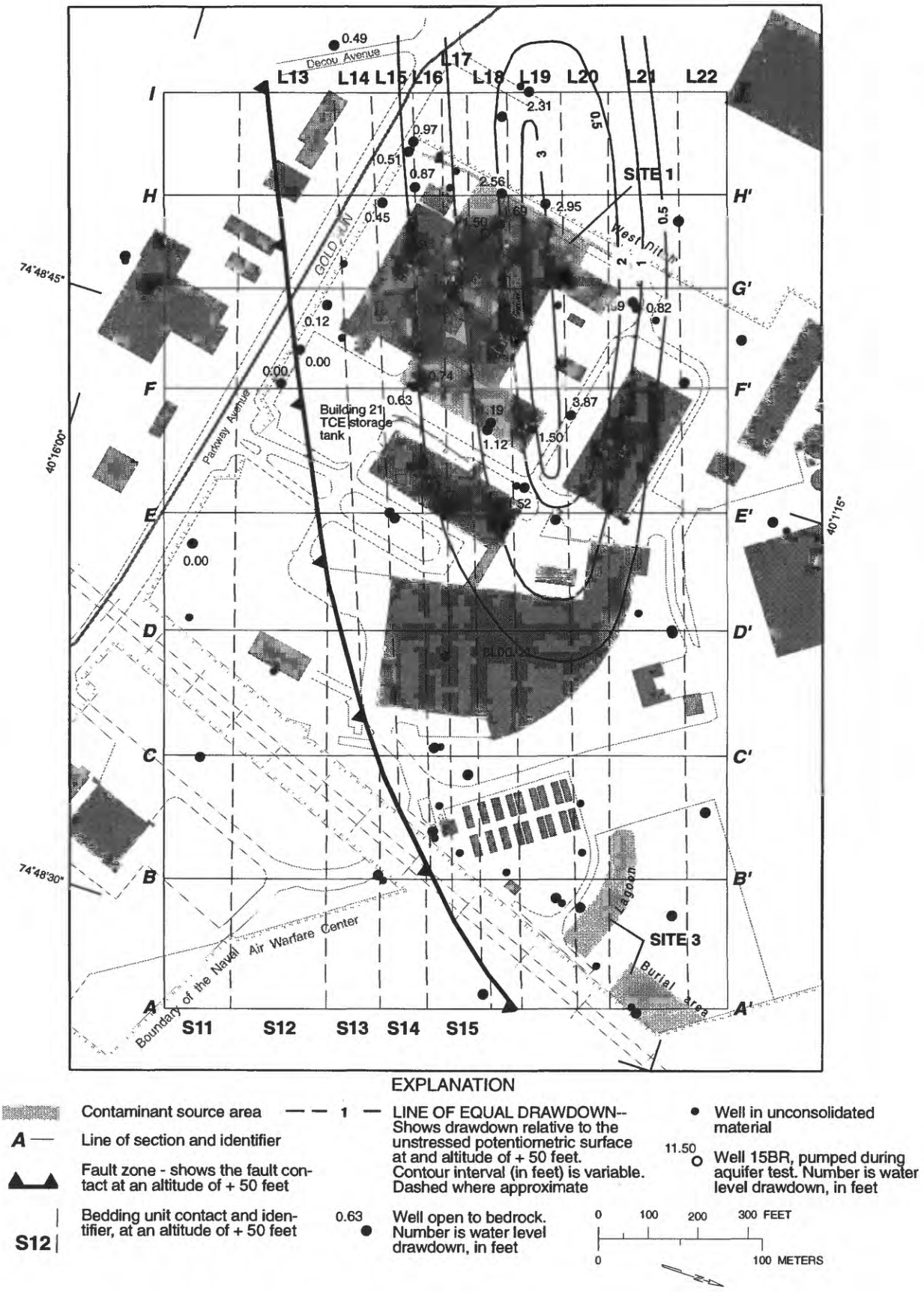

Figure 40. Drawdown during the aquifer test with well 15BR pumping, shown at an altitude of + 50 feet (approximately 100 feet below land surface), Naval Air Warfare Center, West Trenton, N.J.

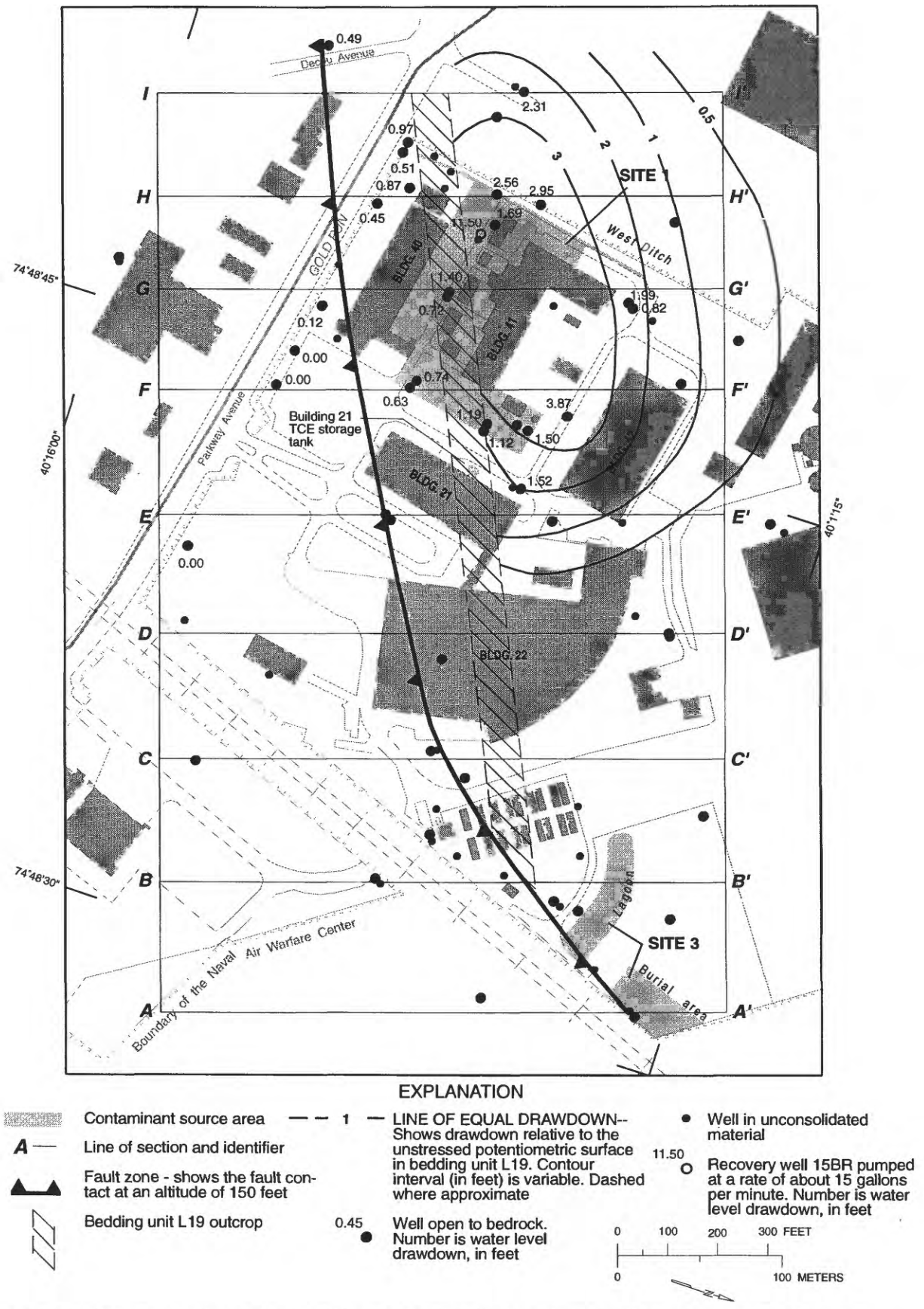

EXPLANATION

- Contaminant source area
- A — Line of section and identifier
- Fault zone - shows the fault contact at an altitude of 150 feet
- Bedding unit L19 outcrop
- — — 1 — LINE OF EQUAL DRAWDOWN--Shows drawdown relative to the unstressed potentiometric surface in bedding unit L19. Contour interval (in feet) is variable. Dashed where approximate
- 0.45 ● Well open to bedrock. Number is water level drawdown, in feet
- ● Well in unconsolidated material
- 11.50 ○ Recovery well 15BR pumped at a rate of about 15 gallons per minute. Number is water level drawdown, in feet

0 100 200 300 FEET
0 100 METERS

Figure 41. Drawdown in bedding unit L19 during the aquifer test with well 15BR pumping, Naval Air Warfare Center, West Trenton, N.J.

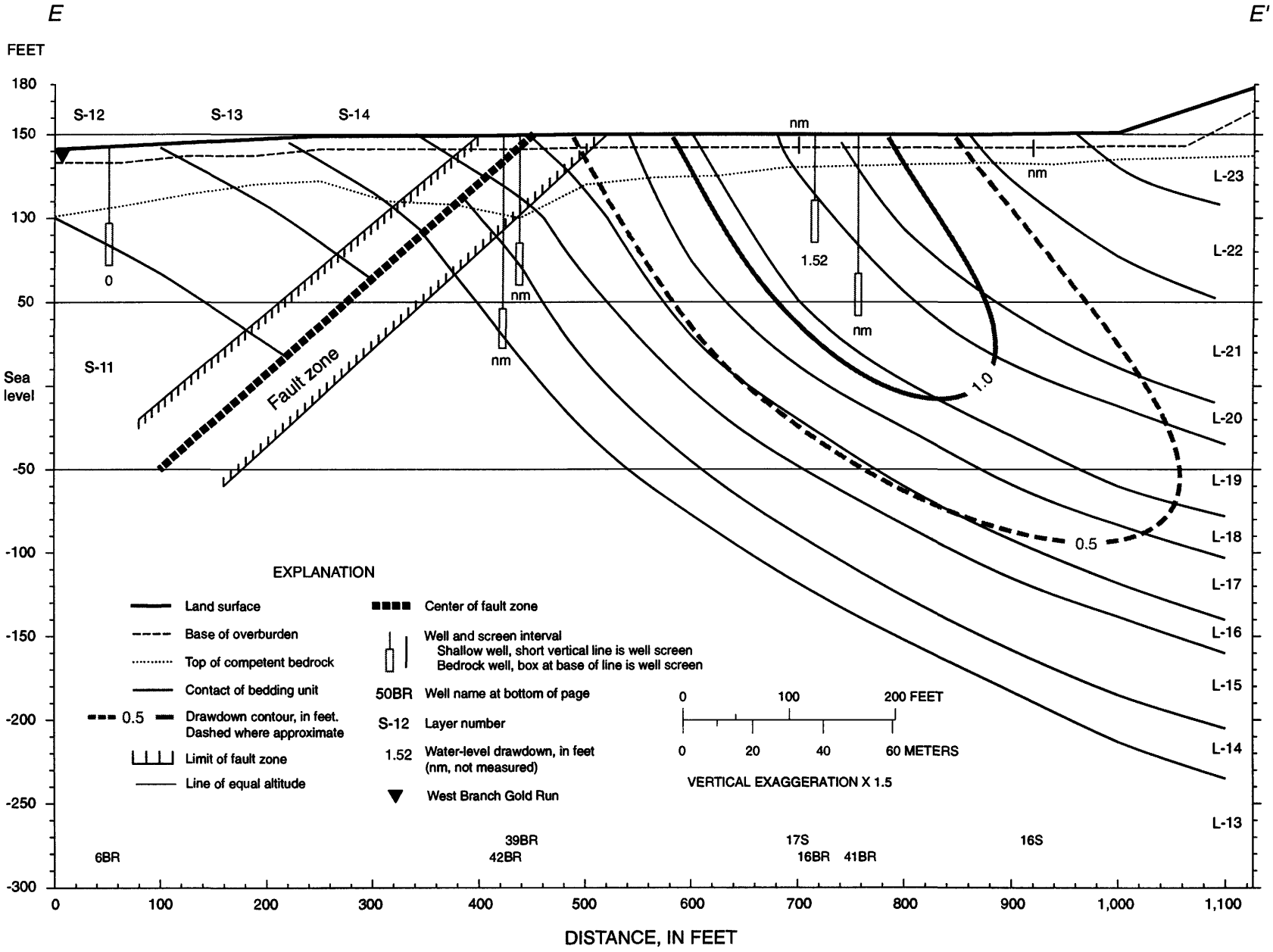

Figure 42. Water-level drawdowns measured in wells along section *E-E'* during the aquifer test while pumping well 15BR.

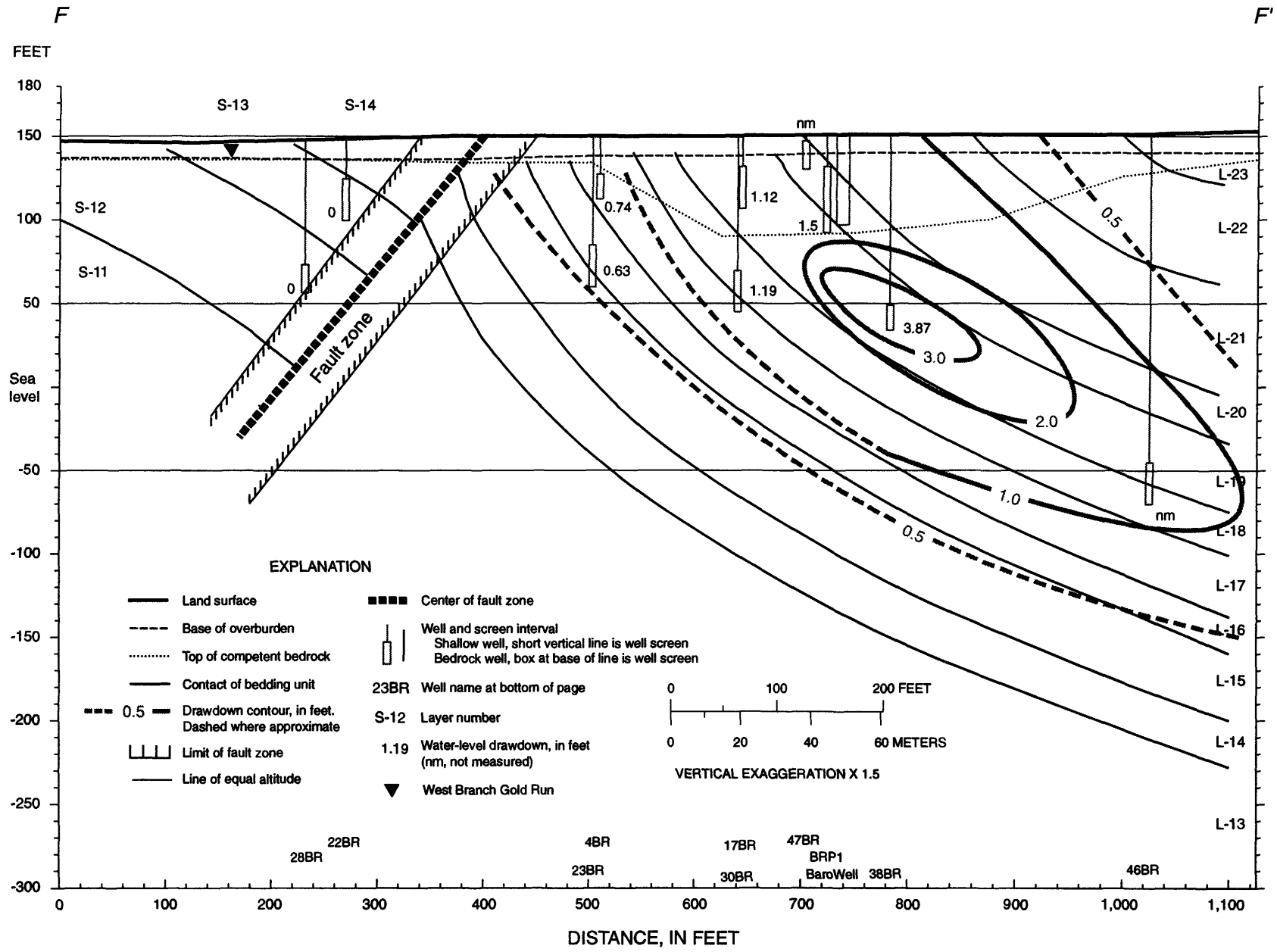

Figure 43. Water-level drawdowns measured in wells along section *F-F'* during the aquifer test while pumping well 15BR.

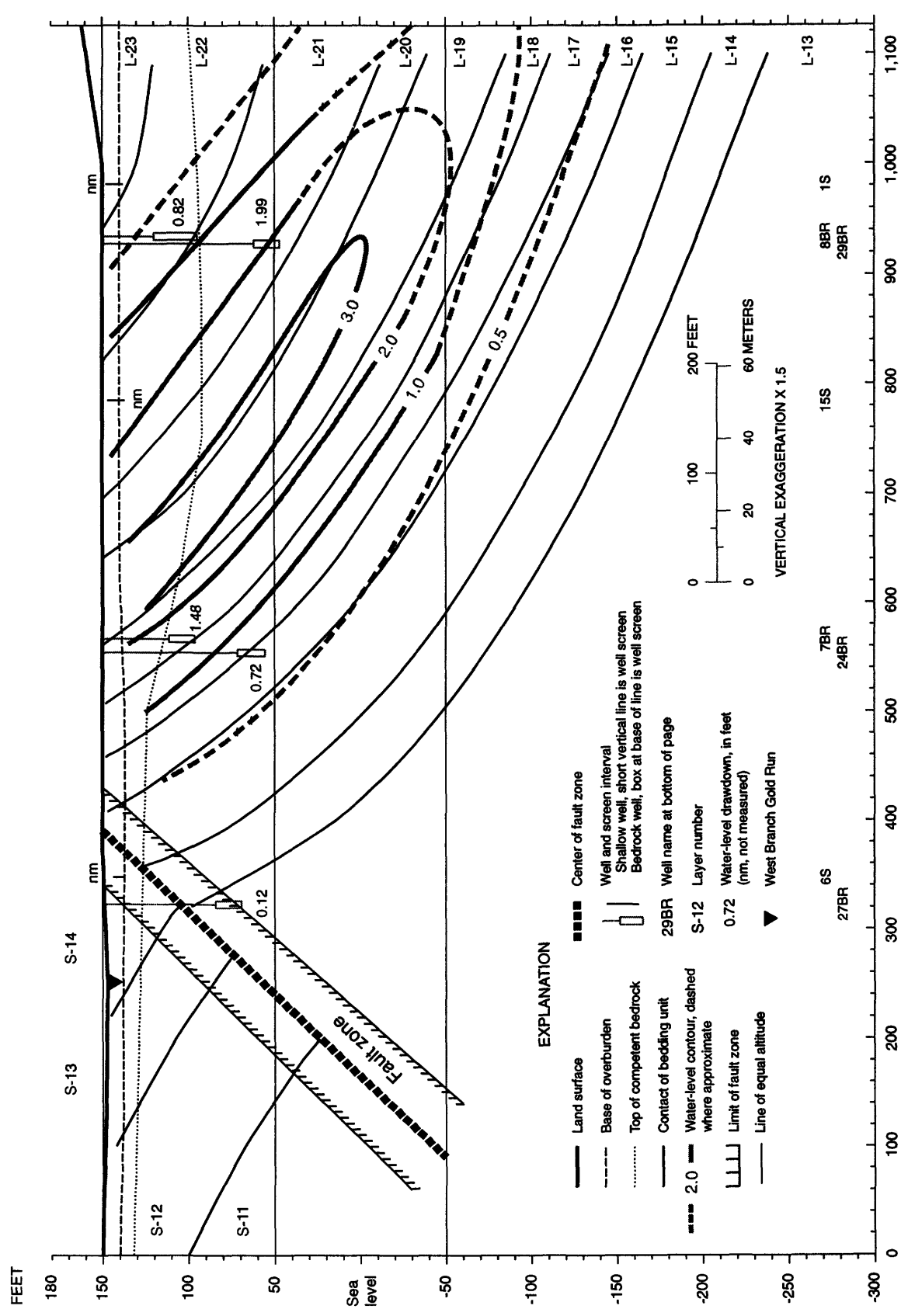

Figure 44. Water-level drawdowns measured in wells along section *G-G'* during the aquifer test while pumping well 15BR.

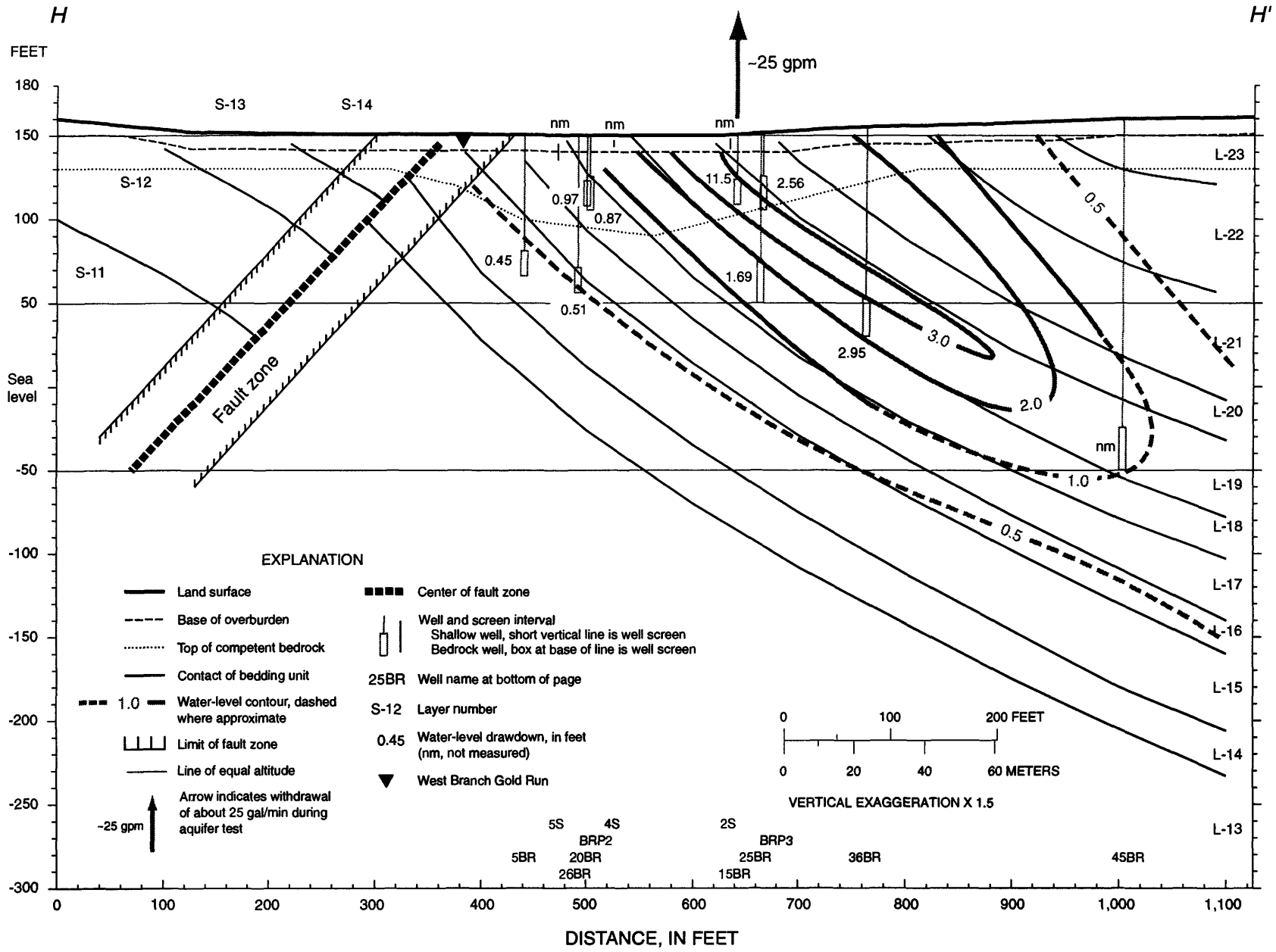

Figure 45. Water-level drawdowns measured in wells along section *H-H'* during the aquifer test while pumping well 15BR.

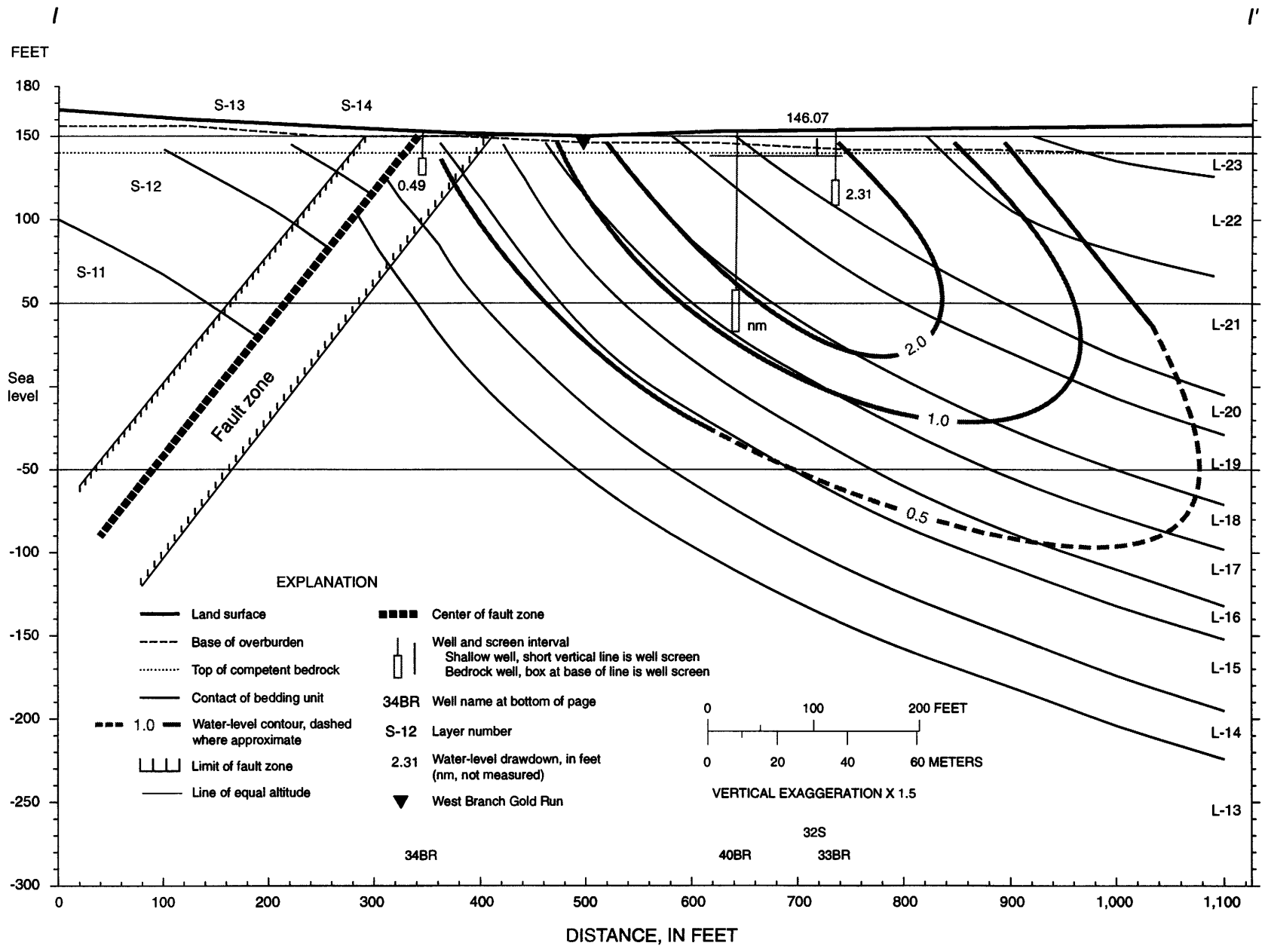

Figure 46. Water-level drawdowns measured in wells along section *I-I'* during the aquifer test while pumping well 15BR.

Drawdown sections and maps (figs. 47 to 51) show the drawdown in the nine wells that were monitored during the aquifer test.

Well BRP1, the pumped well, is located about 40 ft east of the "Barometric well" (line F-F') (fig. 50). The Barometric well is not actually a well but rather an underground tank that is 12 ft in diameter and about 50 ft deep. The Barometric well was used as part of the work effort at the NAWC. It was installed in 1958 by drilling and blasting a hole in the bedrock that was 25 to 30 ft in diameter and about 60 ft deep. During the installation of well 38BR, the driller and site geologist noted air being released from the ground surrounding the Barometric well. The method of installation of the Barometric well and the subsequent release of air during drilling of well 38BR indicate that the bedrock near the Barometric well is highly fractured due to the blasting. In addition, it is likely that blasting fractured the rock where well BRP1 is located.

The results of the aquifer test show that well 16BR screened in bedding unit L-19 and well 29BR screened in bedding unit L-21 have drawdowns of 1.83 and 1.82 ft respectively. These drawdowns are the largest of the nine wells that were measured. Well 16BR is about 130 ft and well 29BR is about 340 ft from the pumped well; however, well 16BR is screened about 50 ft below land surface, and well 29BR is screened about 90 ft below land surface. Although the drawdowns are nearly equal in the two wells, there is less relative drawdown in well 16BR than in well 29BR because it is shallower, in spite of it being closer to and in the same bedding unit as well BRP1. As a result, (a) more water is stored in the shallow part of the aquifer, (b) the shallow part of the aquifer is less permeable, and/or (c) a confining unit is present between the water-bearing zone of the pumped well and well 16BR.

Wells screened in bedding units below L-19 had drawdowns of 0.15 to 0.4 ft, and the well in bedding units above L-22 had a drawdown of 0.91 ft. Water levels were not measured south of the fault, so the effect of drawdown in that area is not known.

The drawdown map at an altitude of + 150 ft (about land surface) (fig. 47) and at an altitude of +50 ft (about 100 ft below land surface) (fig. 48) shows that drawdown along strike is about four times greater than it is perpendicular to the strike of the bedding. Therefore, the Lockatong aquifer has an anisotropy ratio of 4:1 at land surface and at a depth of 100 ft. There are insufficient data to draw the drawdown within any bedding unit or set of bedding units. Bedding units L-20 and L-21 have an isotropy ratio that is close to 1:1 to a depth of at least 200 ft below land surface because there was a 1.82 ft of drawdown in well 29BR, which is screened in the same bedding unit as the pumped well.

Aquifer test on Well 5BR

A third aquifer test was conducted on August 15-17, 1995. Well 5BR, screened in bedding units L-15 (line H-H') (fig. 56) was pumped at a rate of 25 gal/min for 42 hours. Twelve surrounding wells were monitored for water levels. Drawdown sections and maps show the drawdown in the 13 wells monitored during the aquifer test (figs. 52 to 57).

The results of the aquifer test show that wells 26BR, 24BR, and 23BR, screened in bedding units L-15 and L-16, had the largest drawdowns ranging from 7.05 to 2.03 ft. Wells 4BR and 20BR, screened in bedding unit L-17, showed water-level declines of 1.09 and 0.91 ft, respectively. Water levels declined 0.73 ft in well 7BR located in the shallow part of bedding unit L-18, and water levels did not respond in well 15BR located in the deeper part of bedding unit L-18. Water levels in the fault zone showed a decline of 0.27 ft; however, slug test data for well 27BR (Donald Rice, U.S. Geological Survey, written commun., 1997) show that the well has an

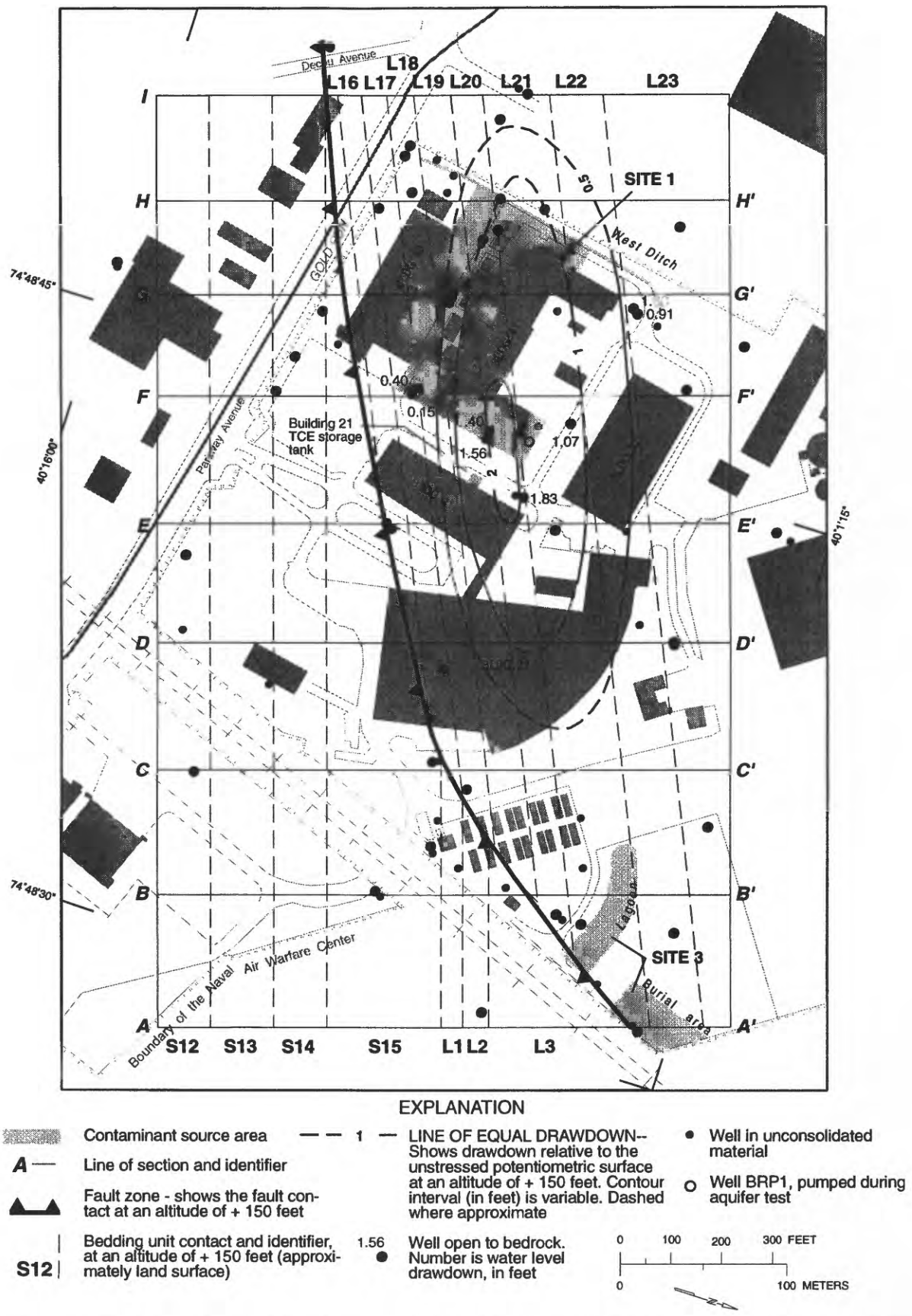

Figure 47. Drawdown during the aquifer test with well BRP1 pumping, shown at an altitude of + 150 feet (approximately land surface), Naval Air Warfare Center, West Trenton, N.J.

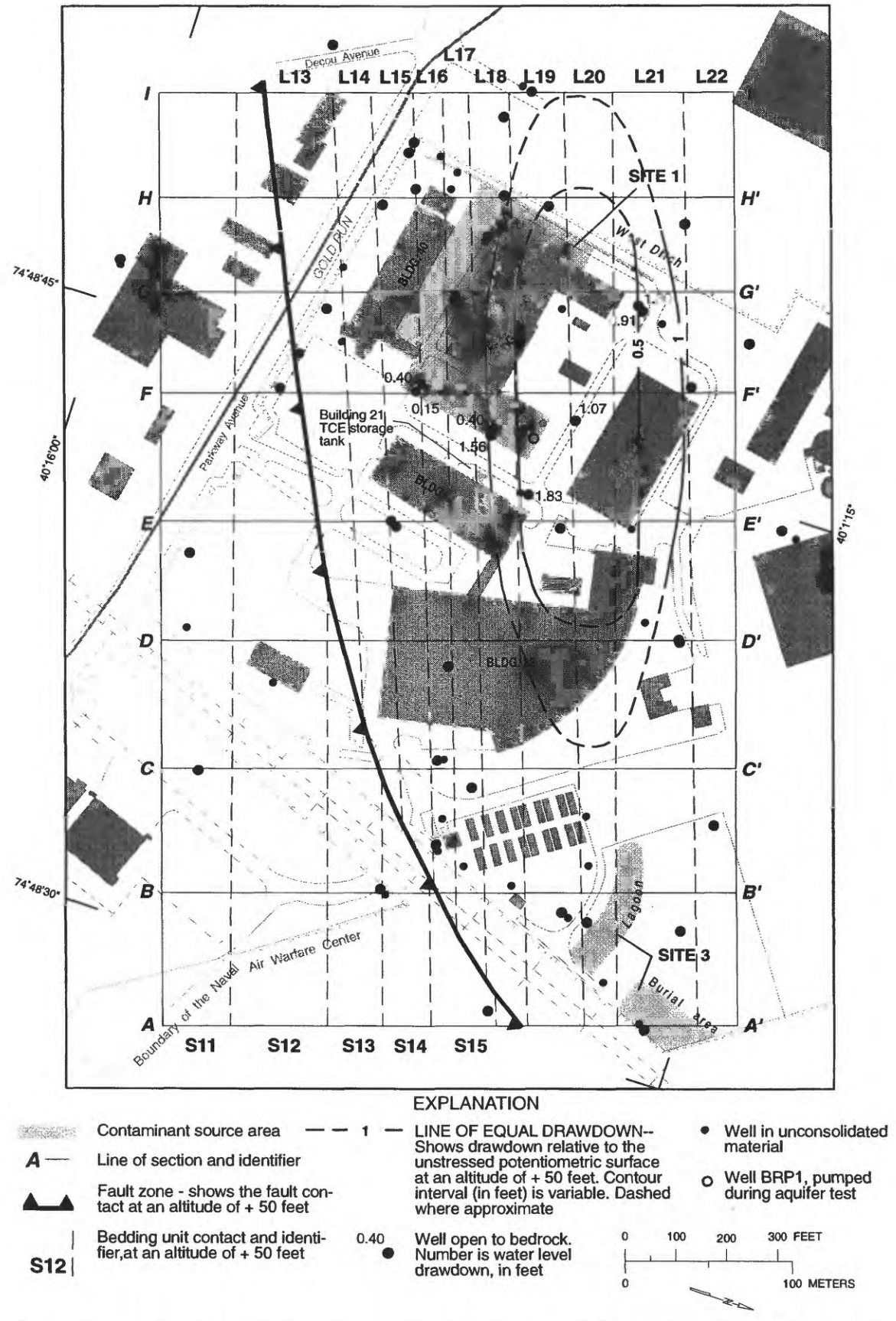

Figure 48. Drawdown during the aquifer test with well BRP1 pumping, shown at an altitude of + 50 feet (approximately 100 feet below land surface), Naval Air Warfare Center, West Trenton, N.J.

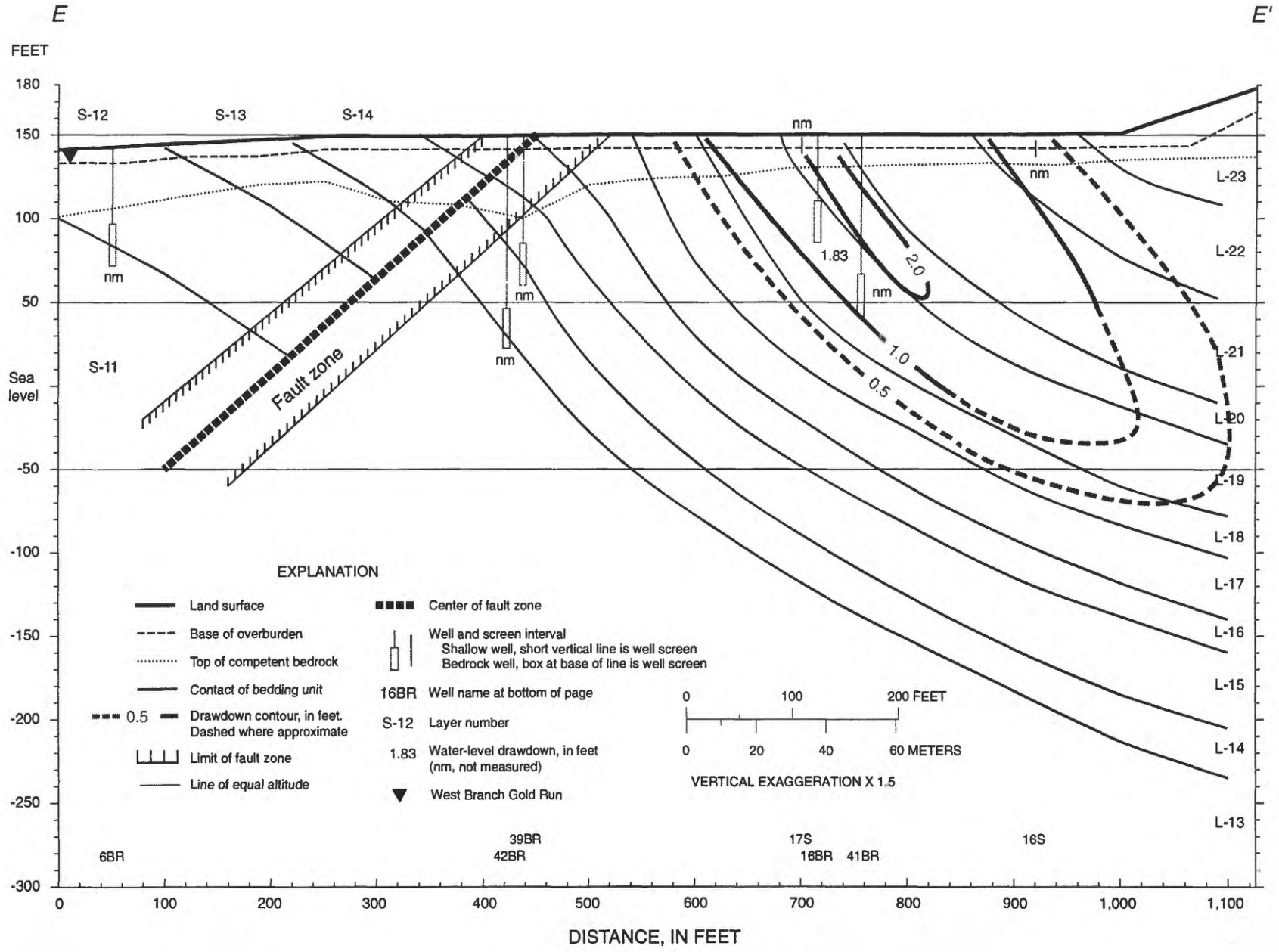

Figure 49. Water-level drawdowns measured in wells along section *E-E'* during the aquifer test while pumping well BRP1.

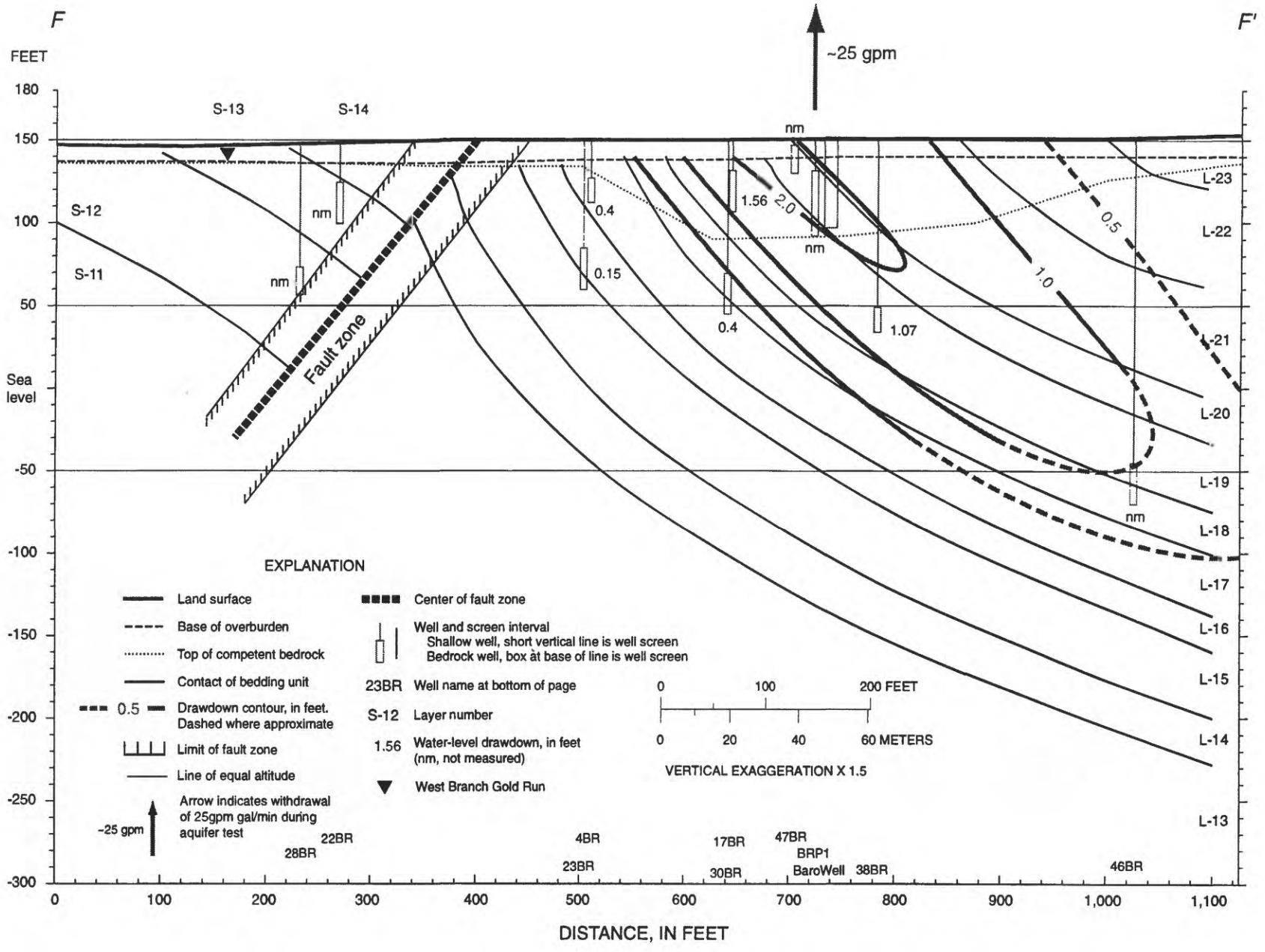

Figure 50. Water-level drawdowns measured in wells along section *F-F'* during the aquifer test while pumping well BRP1.

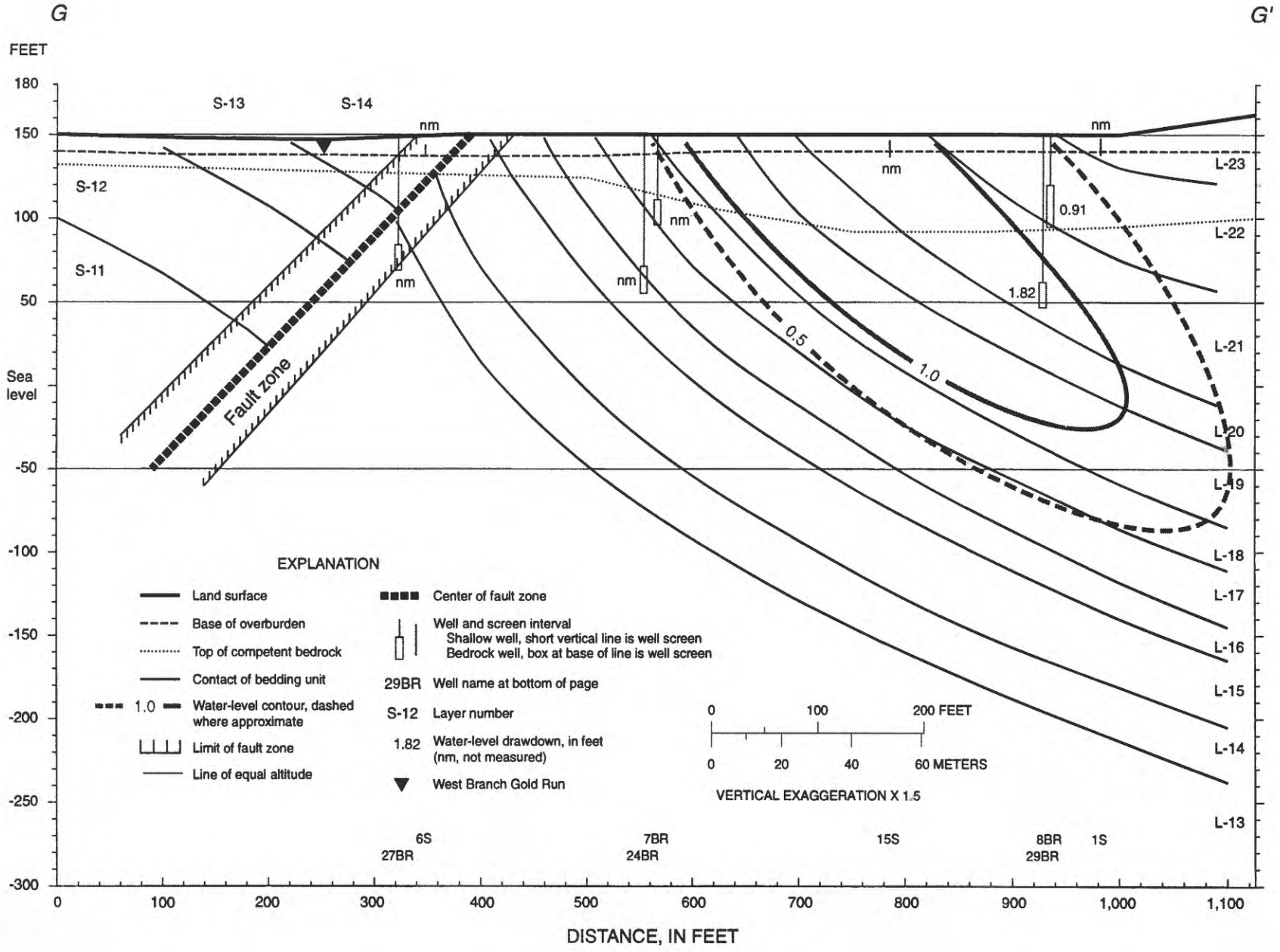

Figure 51. Water-level drawdowns measured in wells along section *G-G'* during the aquifer test while pumping well BRP1.

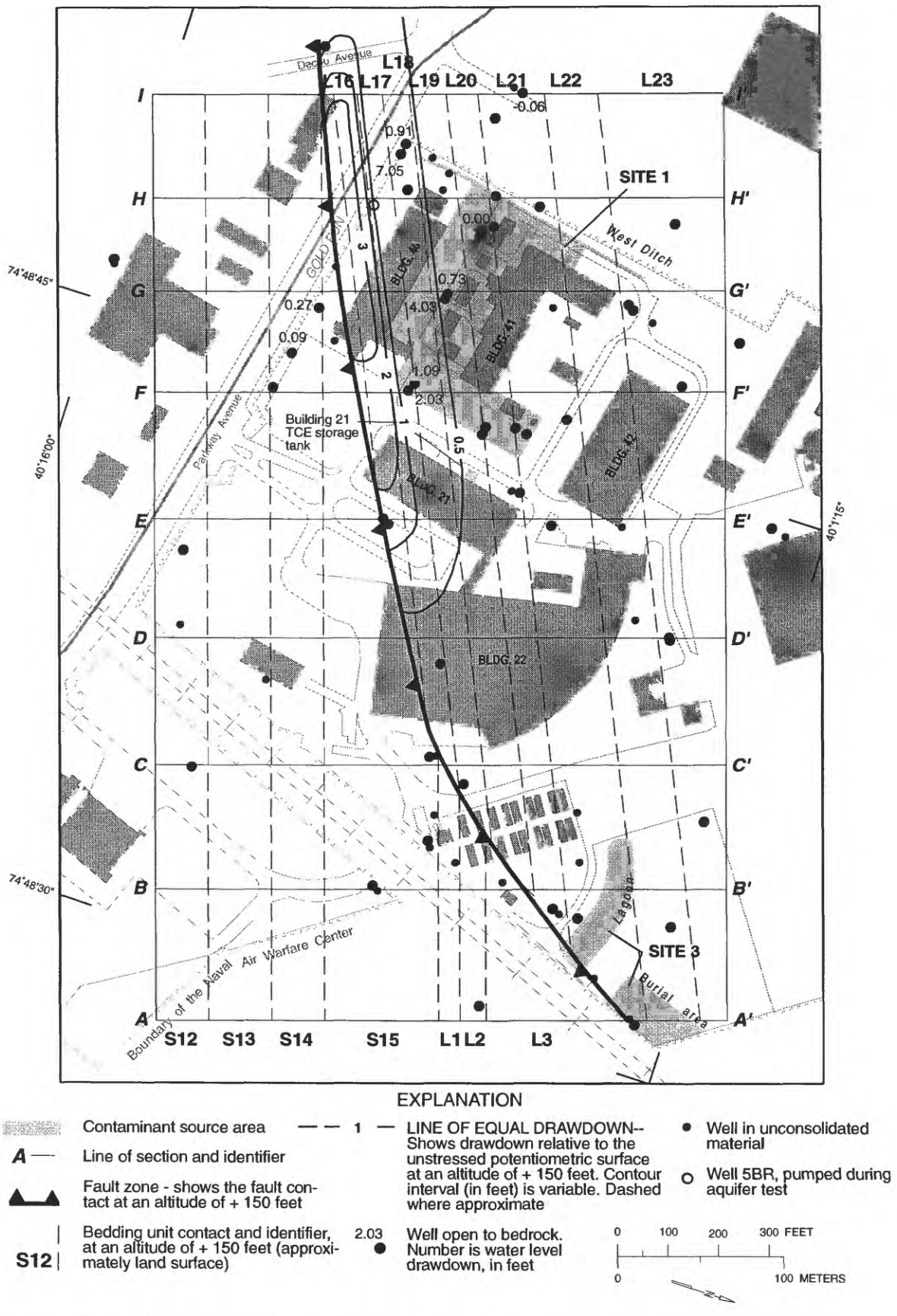

Figure 52. Drawdown during the aquifer test with well 5BR pumping, shown at an altitude of + 150 feet (approximately land surface), Naval Air Warfare Center, West Trenton, N.J.

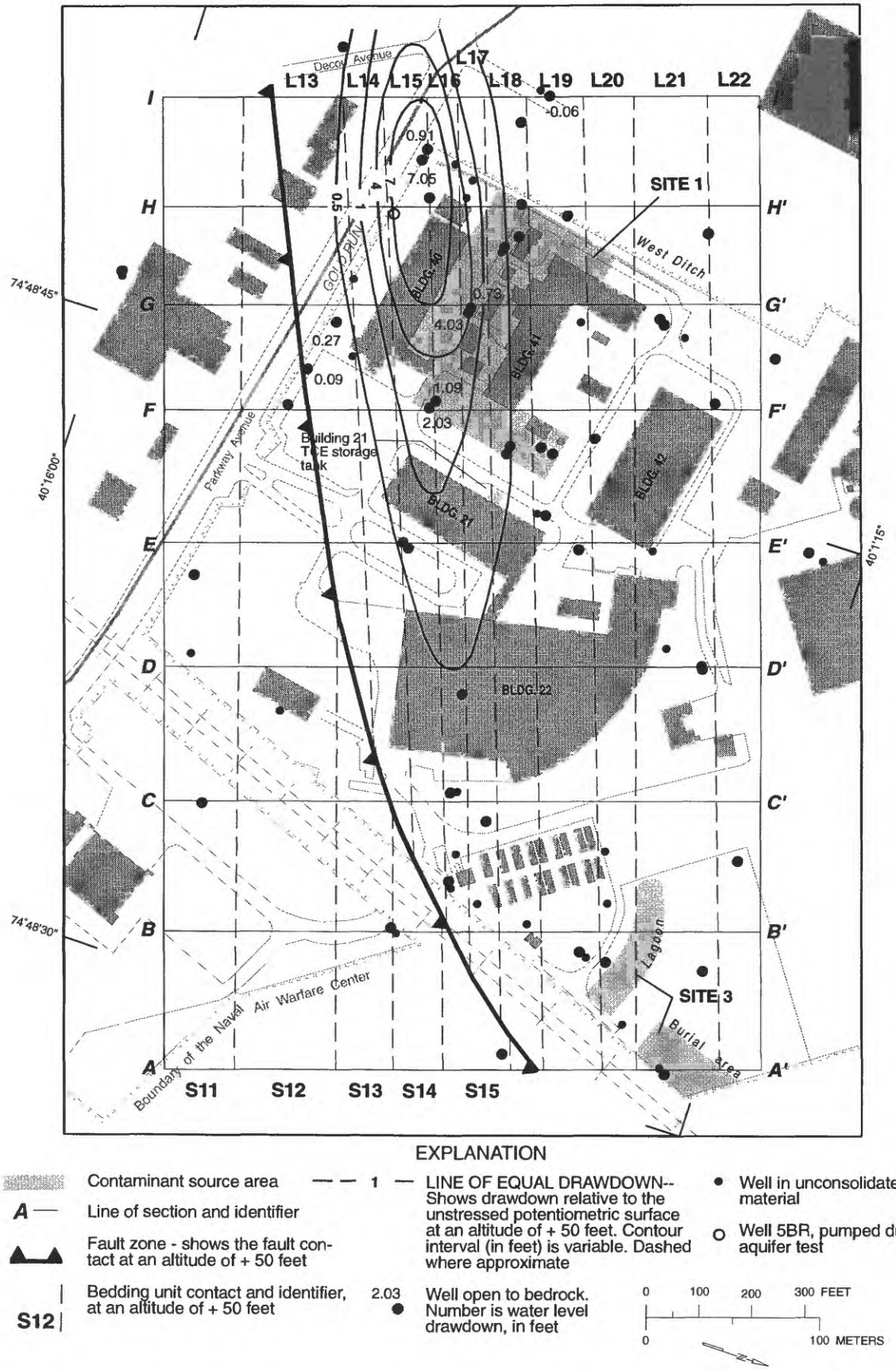

Figure 53. Drawdown during the aquifer test with well 5BR pumping, shown at an altitude of + 50 feet (approximately 100 feet below land surface), Naval Air Warfare Center, West Trenton, N.J.

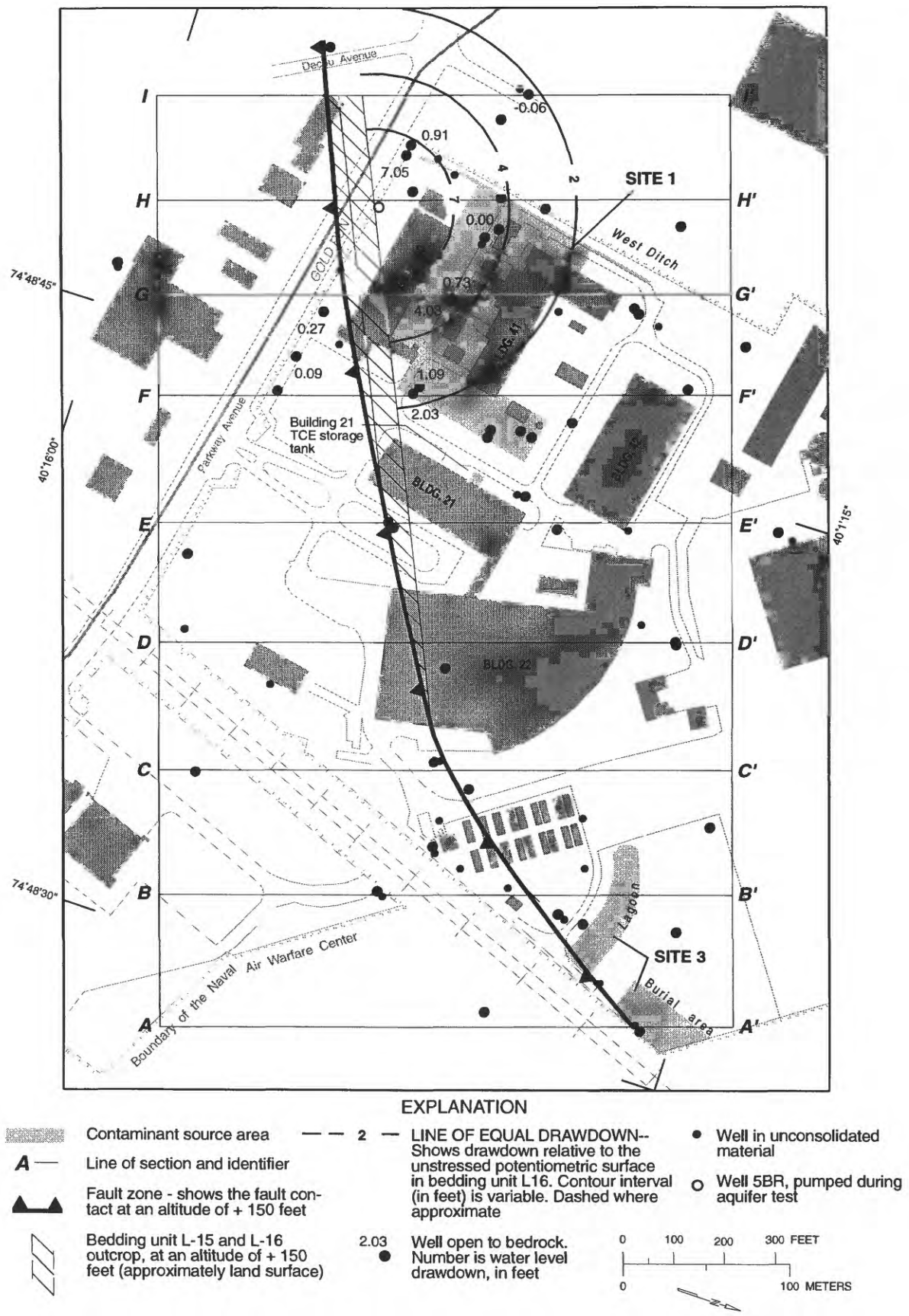

Figure 54. Drawdown in bedding unit L15 and L16 during the aquifer test with well 5BR pumping, Naval Air Warfare Center, West Trenton, N.J.

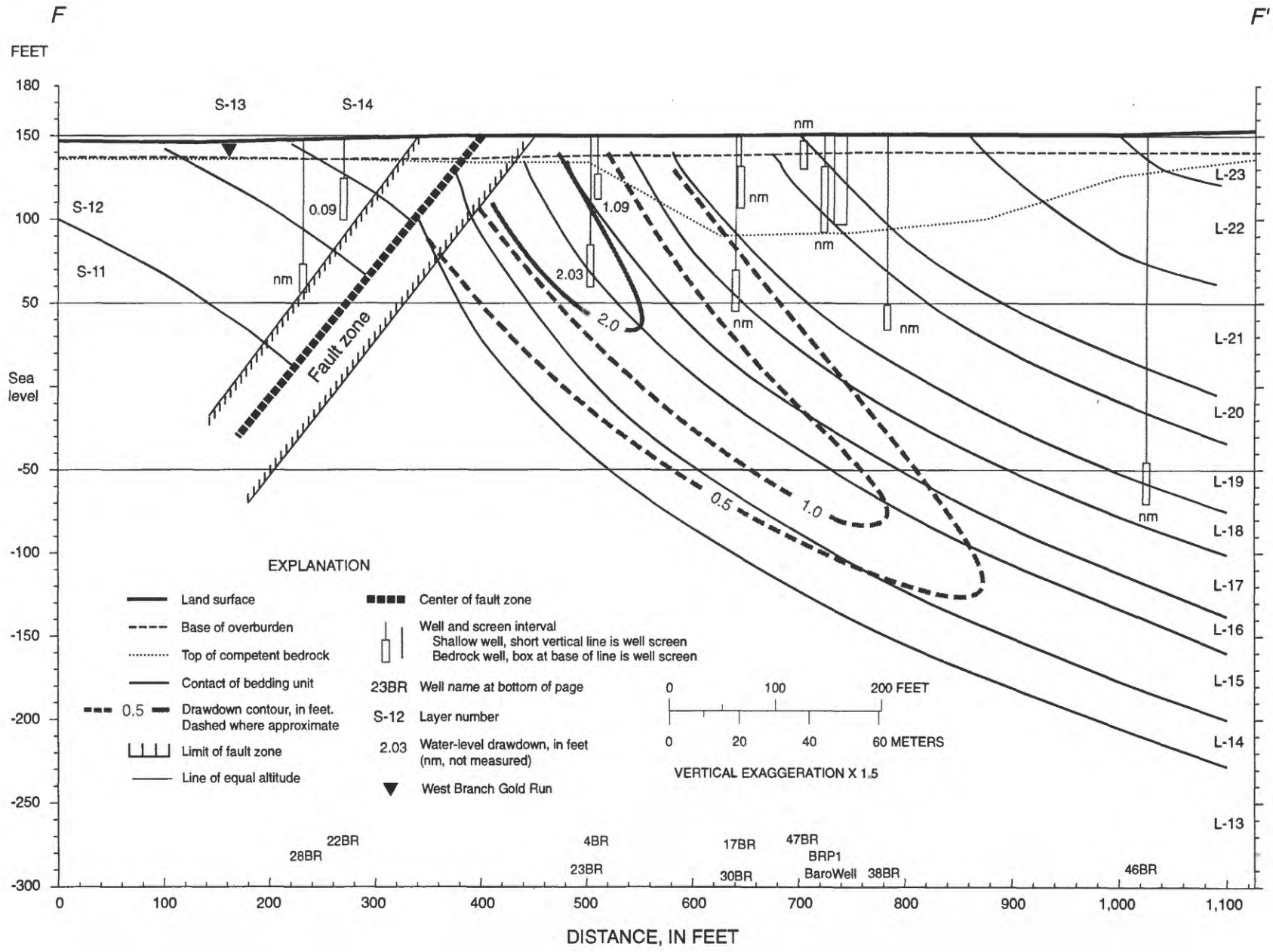

Figure 55. Water-level drawdowns measured in wells along section *F-F'* during the aquifer test while pumping well 5BR.

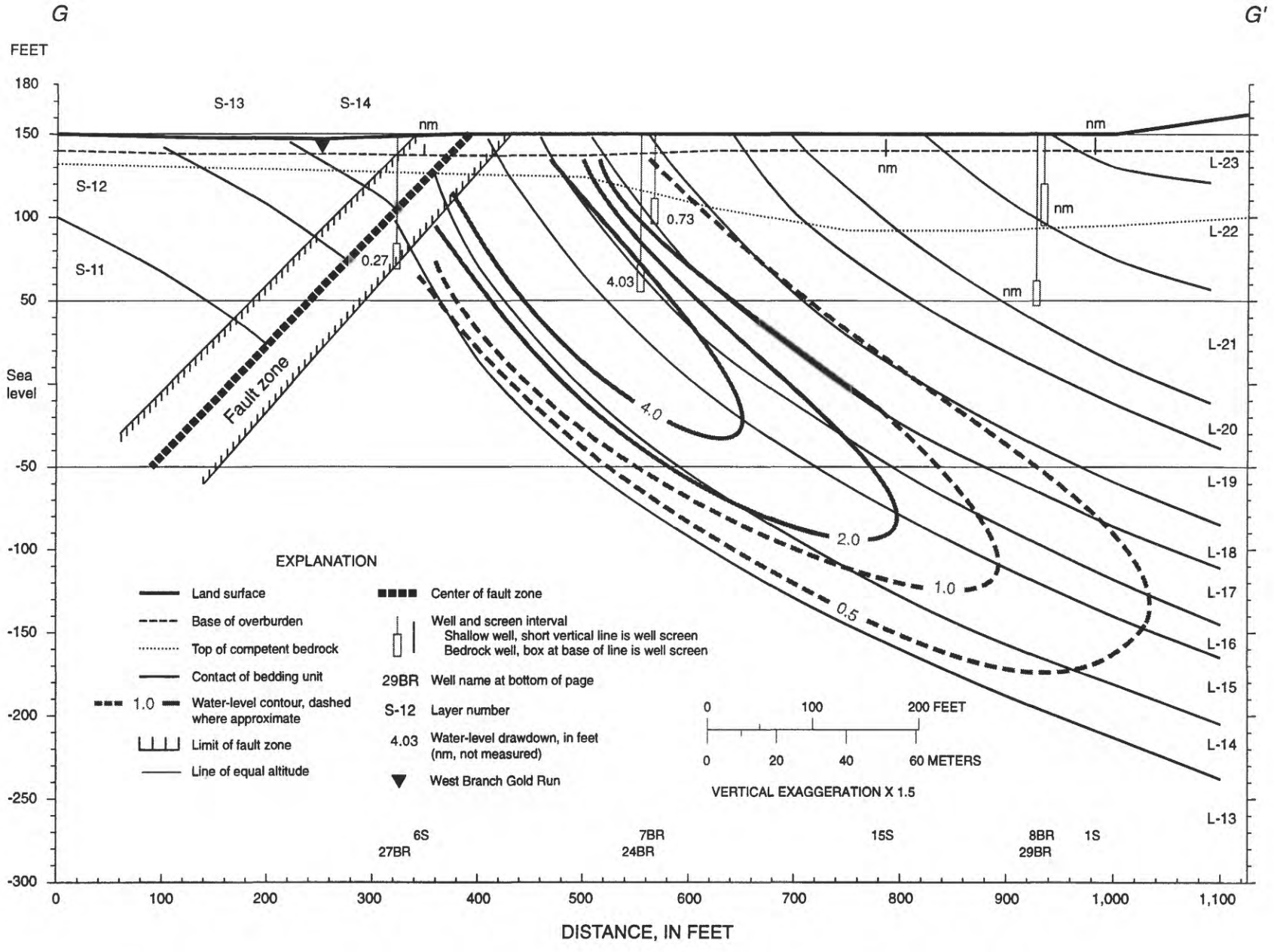

Figure 56. Water-level drawdowns measured in wells along section *G-G'* during the aquifer test while pumping well 15BR.

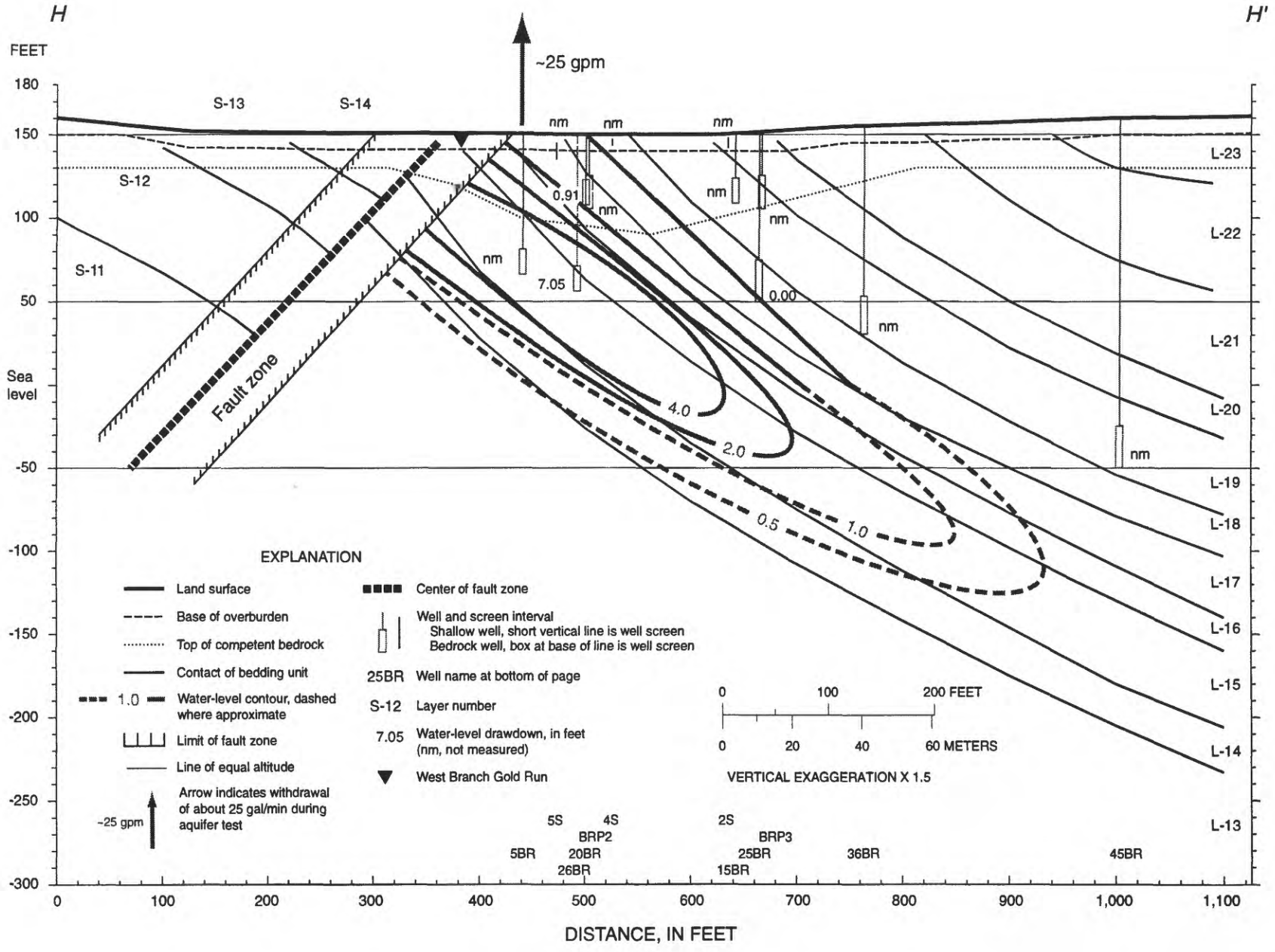

Figure 57. Water-level drawdowns measured in wells along section *H-H'* during the aquifer test while pumping well 5BR.

exceptionally low hydraulic conductivity; therefore, it should not respond to pumping. Because there was no drawdown in well 25BR, the water levels in wells screened above bedding unit L-18 did not respond to the pumping test.

The water level declined 0.09 ft in well 22BR, but this decline in water level in the Stockton aquifer is not necessarily the result of the aquifer test. Water levels in well 34BR increased 0.06 ft during the aquifer test, but the increase is interpreted to be the result of an unknown factor other than the aquifer test.

Drawdown maps (figs. 52 and 53) show that the center of the zone of greatest drawdown stayed in bedding units L-15 and L-16. The drawdown along strike and at an altitude of + 150 ft (about land surface) is about 10 times greater than the drawdown perpendicular to the strike of the bedding. Therefore, the anisotropy ratio is 10:1 for the shallow part of the Lockatong aquifer near well 5BR. In contrast, the drawdown along strike and at an altitude of + 50 ft (about 100 ft below land surface) is about 4 times greater than the drawdown perpendicular to the strike of the bedding. Therefore, the anisotropy ratio is 4:1 for the deeper part of the Lockatong aquifer. The drawdown map for bedding units L-15 and L-16 is based on values from three wells (fig. 54). Drawdown along strike is shown to be nearly identical to drawdown that is down dip. As a result, bedding units L-15 and L-16 are nearly isotropic with a ratio of about 1:1. The 10:1 ratio of anisotropy for the shallow bedrock near well 5BR is a result of the relatively steep bedrock dip, about 65° to 70°, and the proximity of the pumped well to the fault zone. At a depth of about 100 ft the bedrock dip is shallower, about 40°, and the fault zone is farther away.

Summary of Aquifer Test Data Analyzed for Drawdown

The three aquifer tests show that the Lockatong aquifer is anisotropic and that the dip of the bedrock controls the anisotropy of the aquifer. The greater the dip, the greater the anisotropy of the aquifer. However, individual water-bearing zones are more isotropic than the aquifer to a depth of about 200 ft below land surface.

In addition, more water is available in storage in the shallow parts of each bedding unit because of a high fracture density and/or because the bedding units are less permeable in the shallow parts. Therefore, the areal extent of the cone of depression is less in the shallow part of the bedding units than in the deep part of the bedding units.

Stressed Water Levels During Operation of the Recovery Well

Stressed water levels were measured in all wells at the NAWC during August 25-27, 1997, during the operation of the recovery well for the pump and treat facility. The water-level maps and sections show the cone of depression in conjunction with the hydraulic gradient of the region (figs. 58 to 68). Well 15BR, the recovery well screened in bedding unit L-19, was pumped at a rate of about 15 to 18 gal/min. The pump was operated for 3 months or more prior to water-level measurements.

The cone of depression created by the pumped well extends from bedding units L-17 to L-21. At land surface, the cone of depression extends from the West Branch of Gold Run to the east end of Building 41 (fig. 58). The water-level mound that lies inside the 144-ft contour east of the cone of depression is an area of unstressed water levels similar to water levels measured in 1995 (fig. 28). This mound shows that drawdown is limited in bedding units L-17 and L-18 in this area as a result of pumping of well 15BR.

The cone of depression at an altitude of +50 ft (about 100 ft below land surface) remains centered in bedding units L-17 to

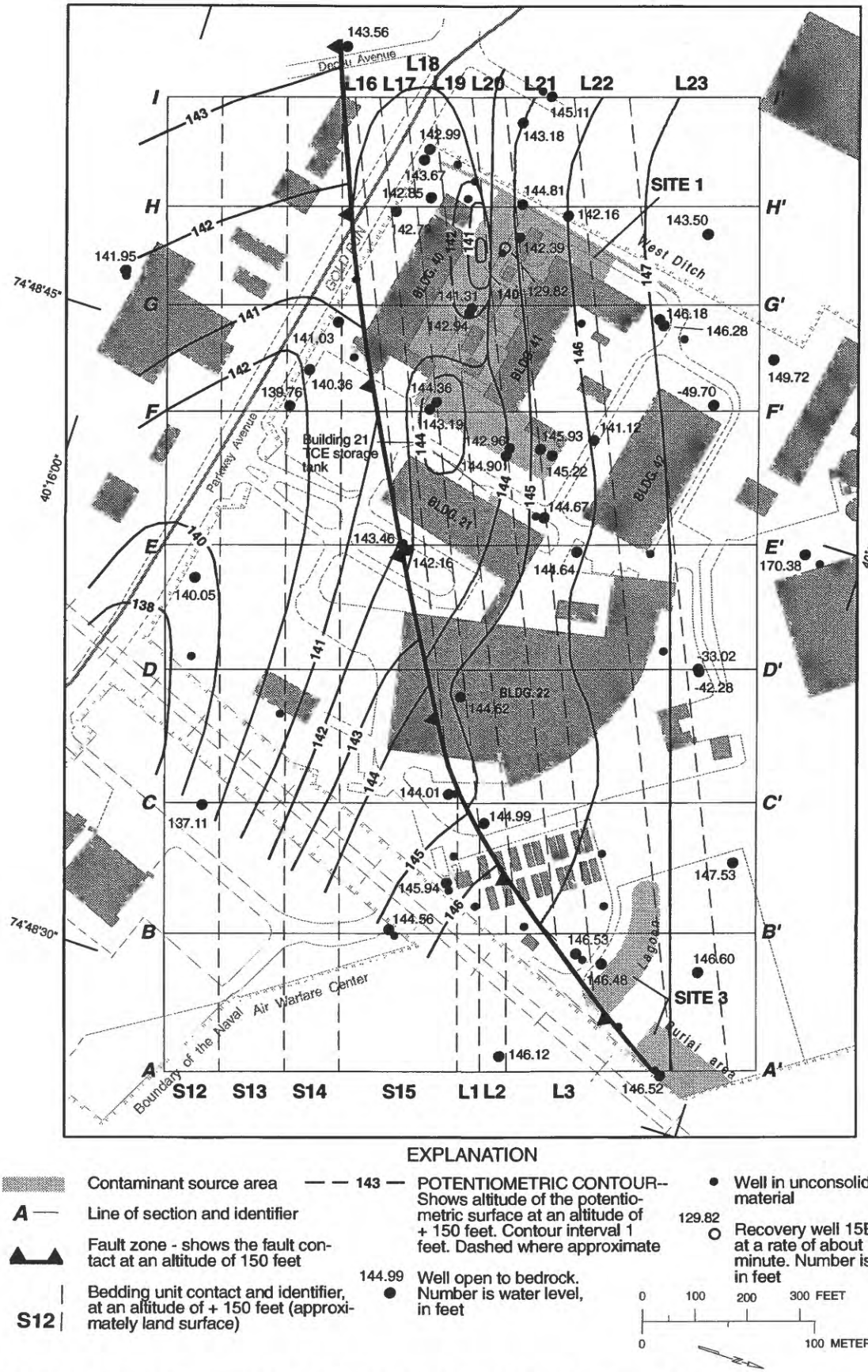

Figure 58. The stressed potentiometric surface in August 1997 shown at an altitude of 150 feet (approximately land surface), Naval Air Warfare Center, West Trenton, N.J.

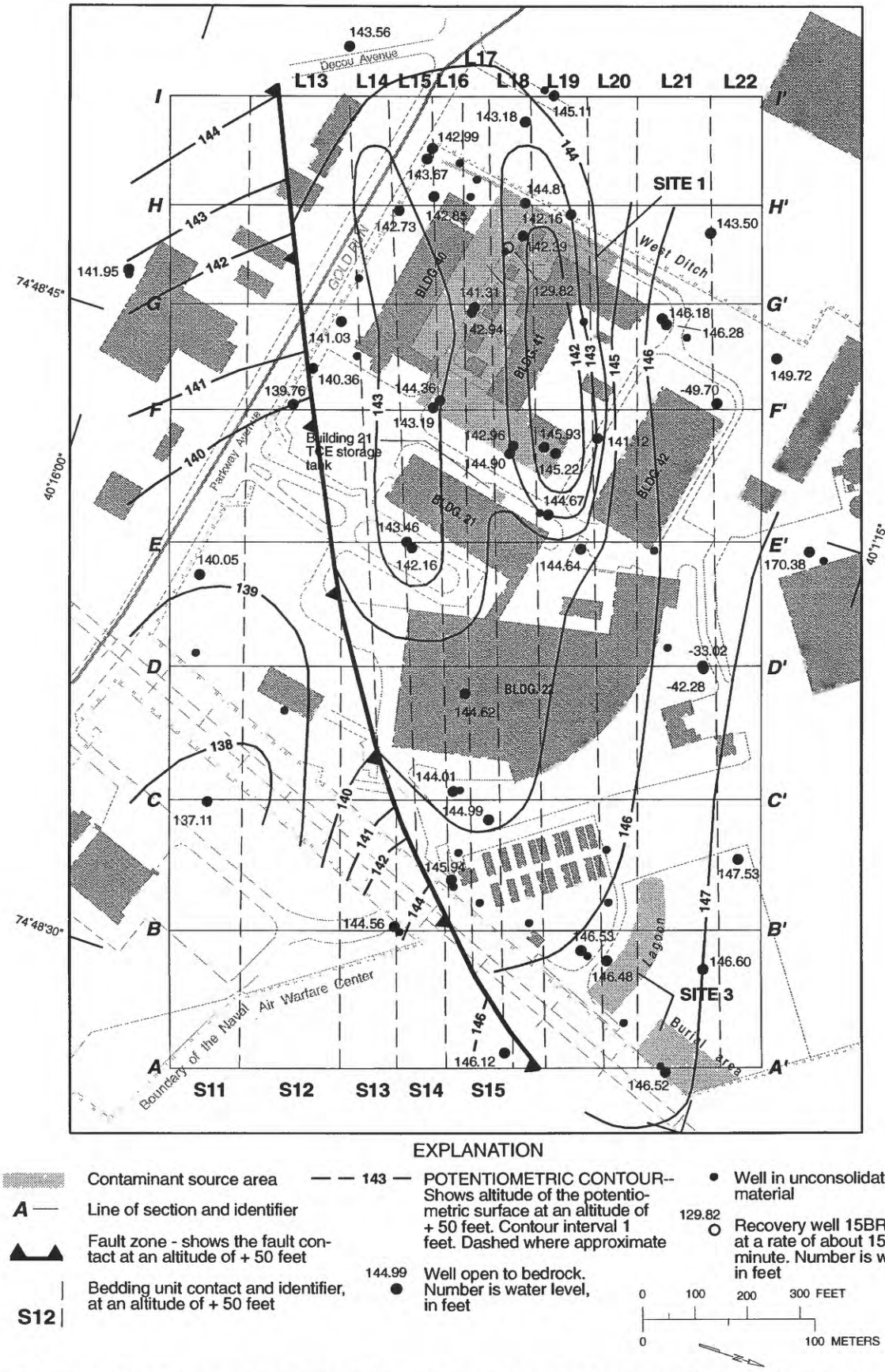

Figure 59. The stressed potentiometric surface in August 1997 shown at an altitude of + 50 feet (approximately 100 feet below land surface), Naval Air Warfare Center, West Trenton, N.J.

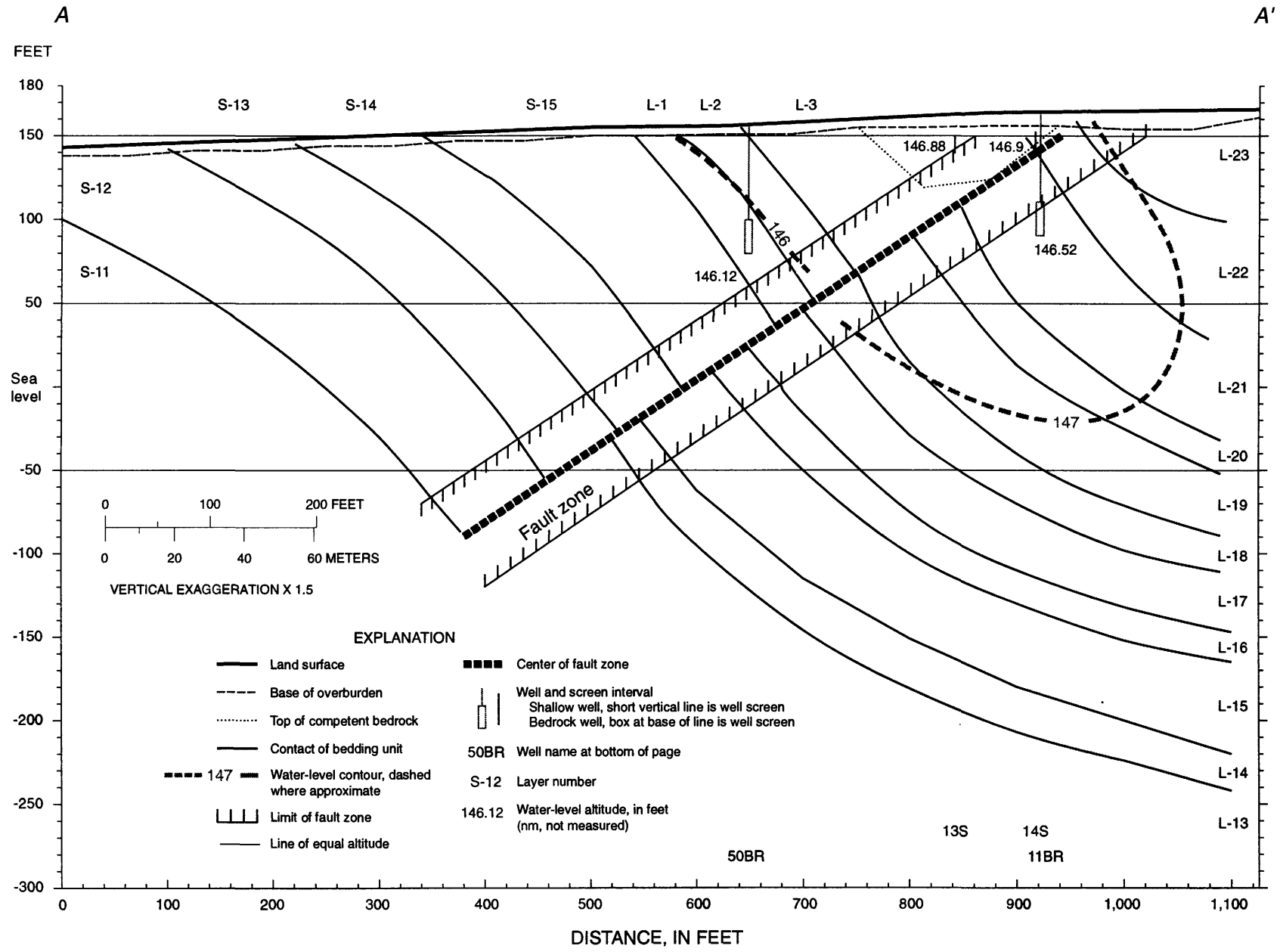

Figure 60. Stressed water-level altitude measured in wells along section *A-A'* during operation of the recovery well 15BR, August 25-27, 1997.

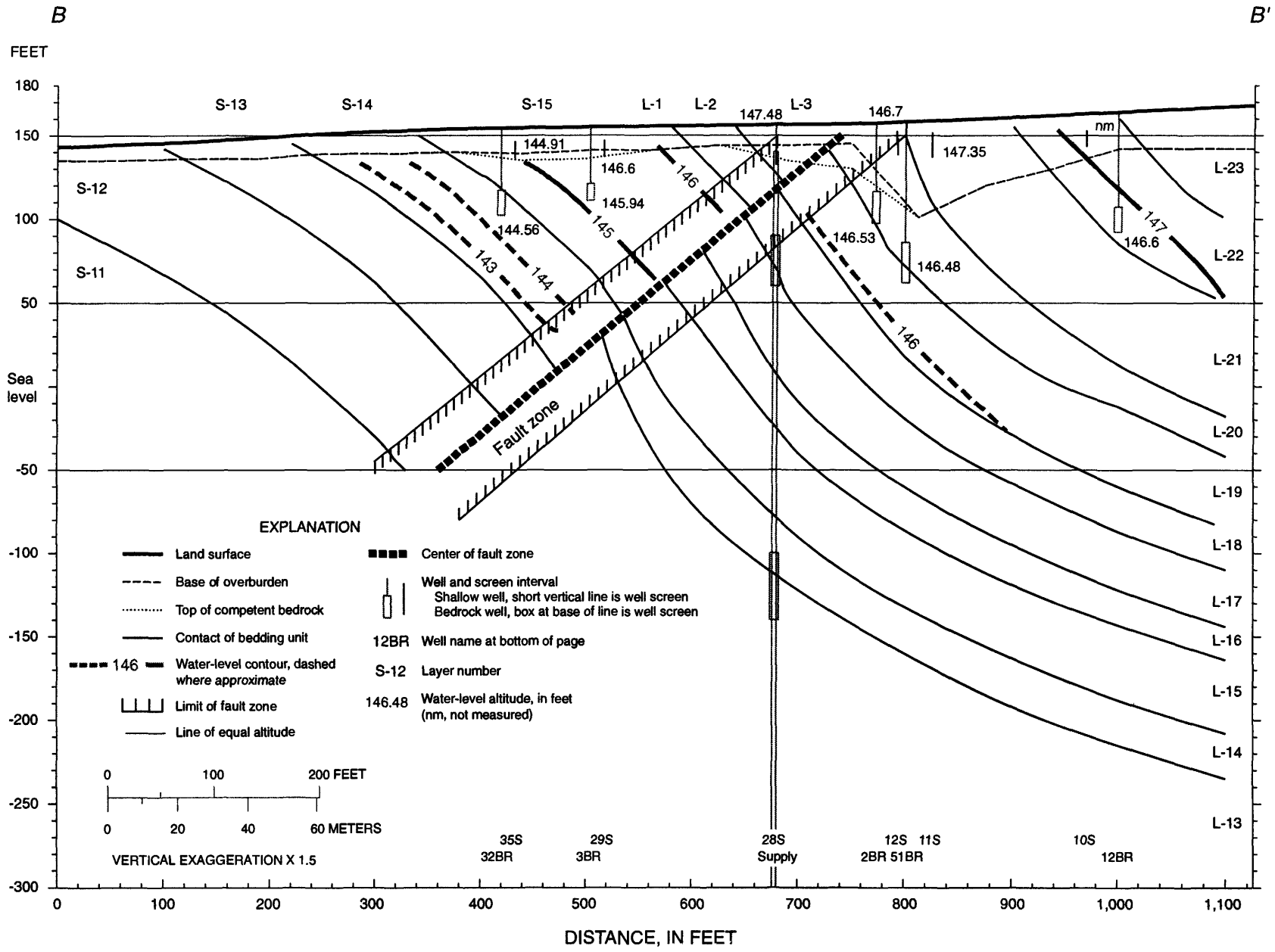

Figure 61. Stressed water-level altitude measured in wells along section *B-B'* during operation of the recovery well 15BR, August 25-27, 1997.

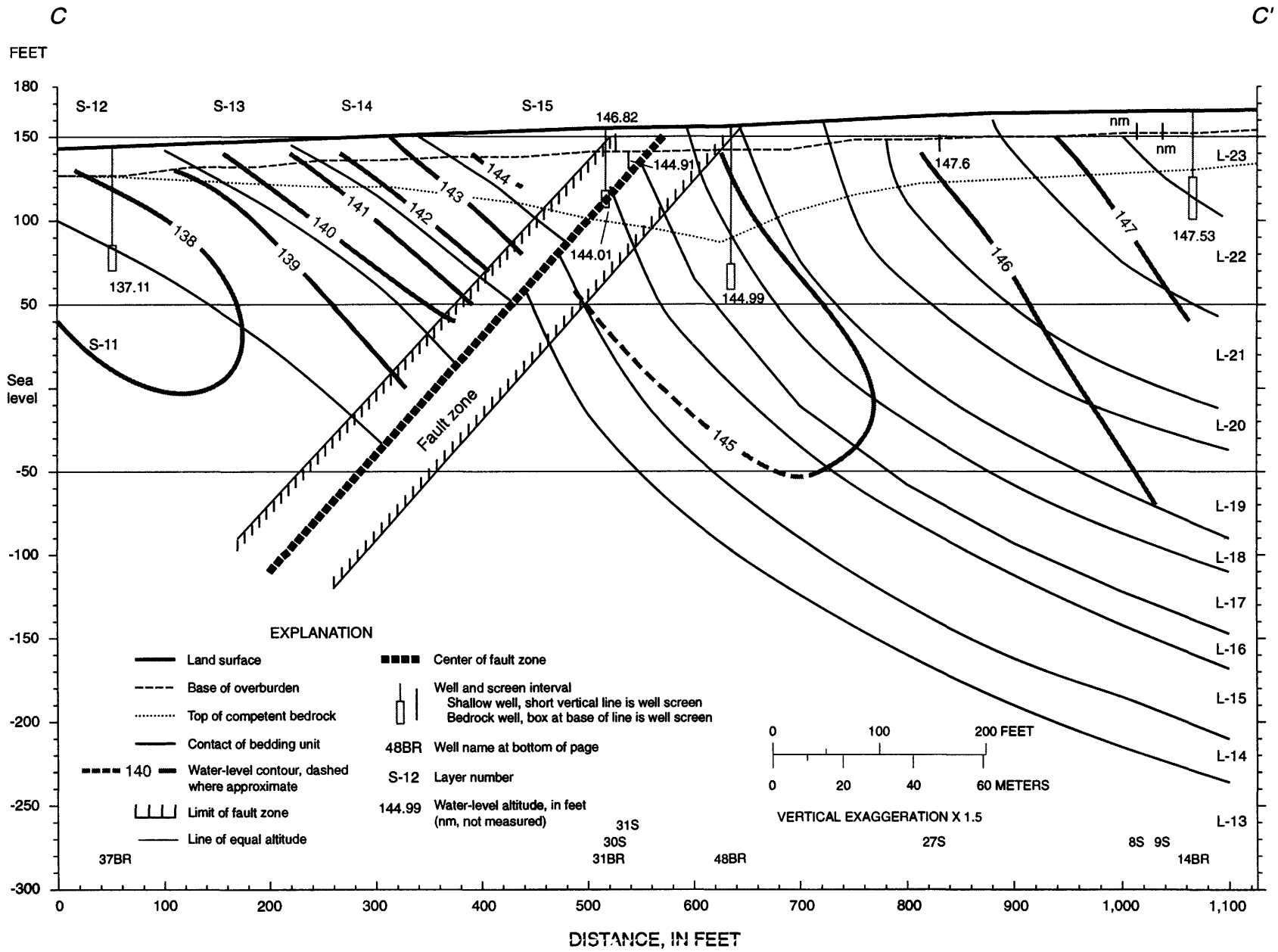

Figure 62. Stressed water-level altitude measured in wells along section *C-C'* during operation of the recovery well 15BR, August 25-27, 1997.

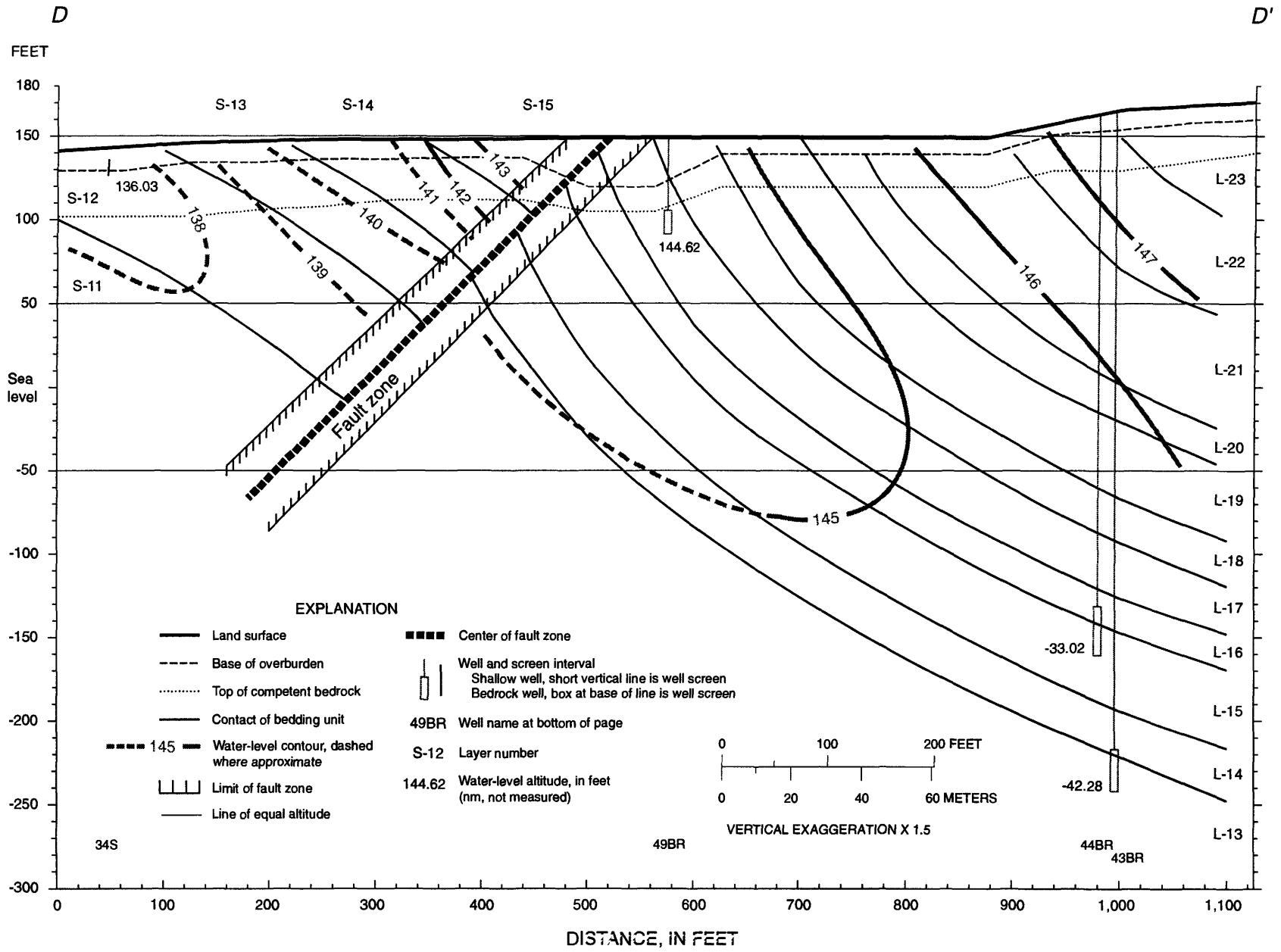

Figure 63. Stressed water-level altitude measured in wells along section *D-D'* during operation of the recovery well 15BR, August 25-27, 1997.

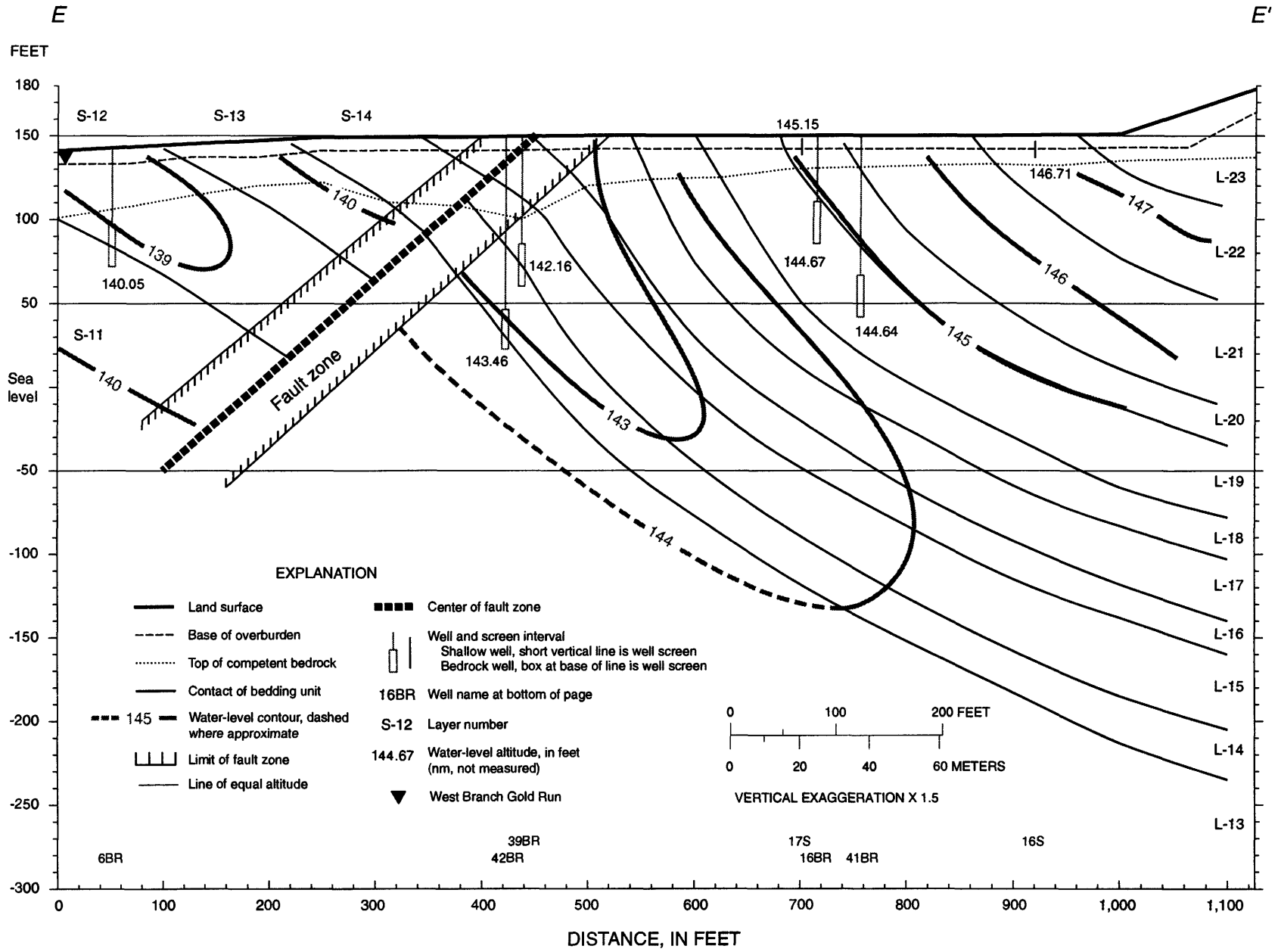

Figure 64. Stressed water-level altitude measured in wells along section *E-E'* during operation of the recovery well 15BR, August 25-27, 1997.

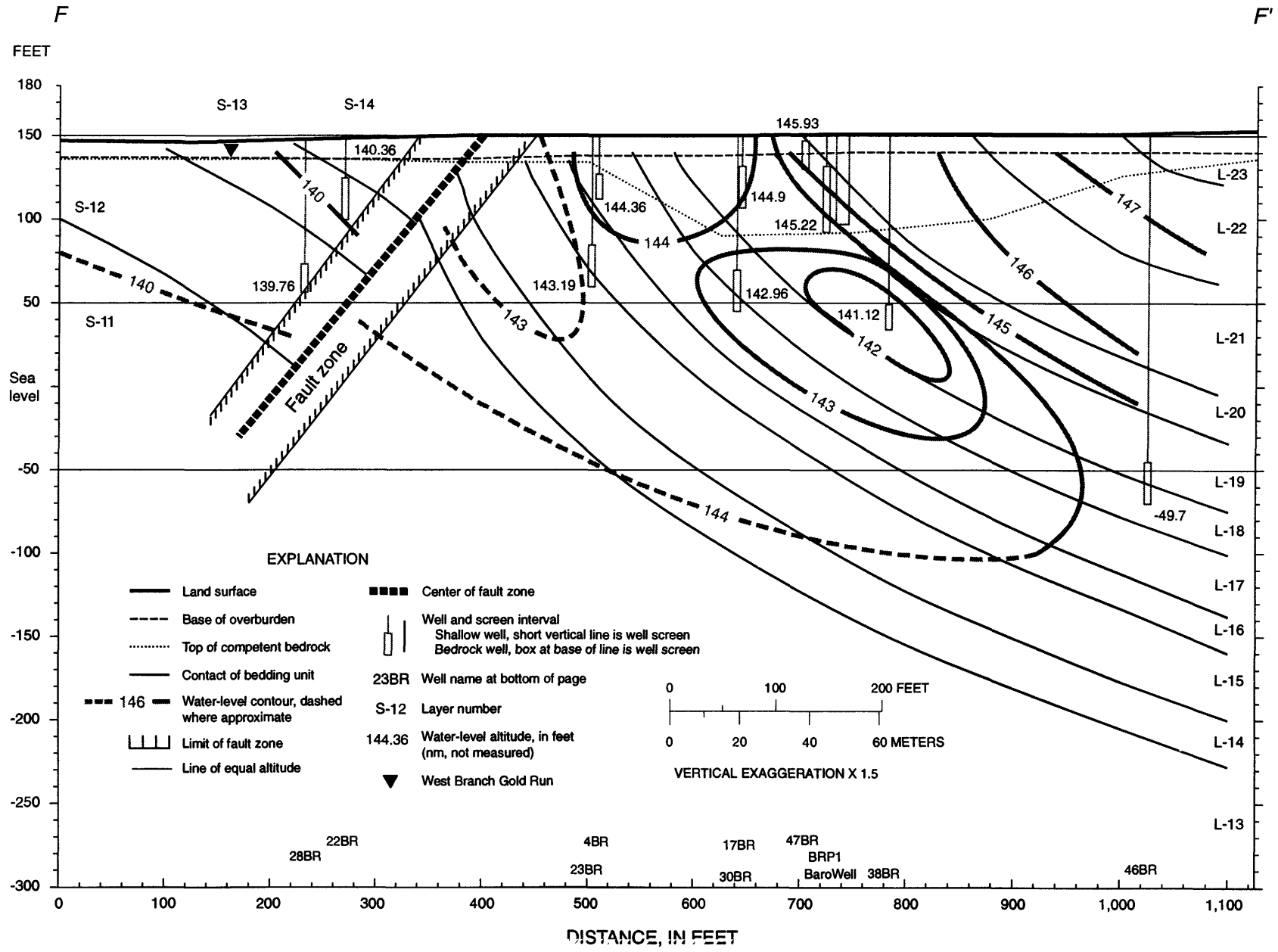

Figure 65. Stressed water-level altitude measured in wells along section *F-F'* during operation of the recovery well 15BR, August 25-27, 1997.

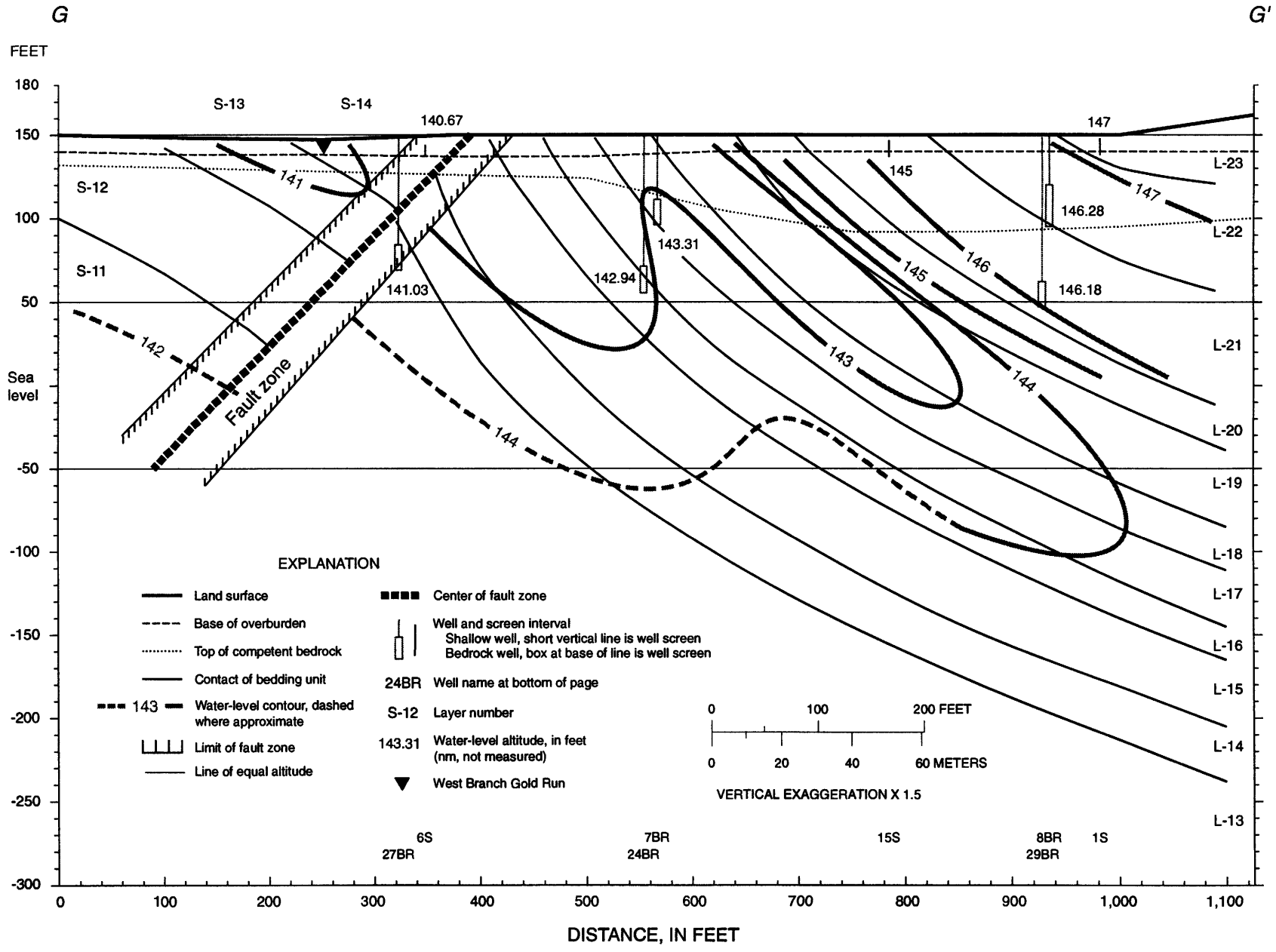

Figure 66. Stressed water-level altitude measured in wells along section *G-G'* during operation of the recovery well 15BR, August 25-27, 1997.

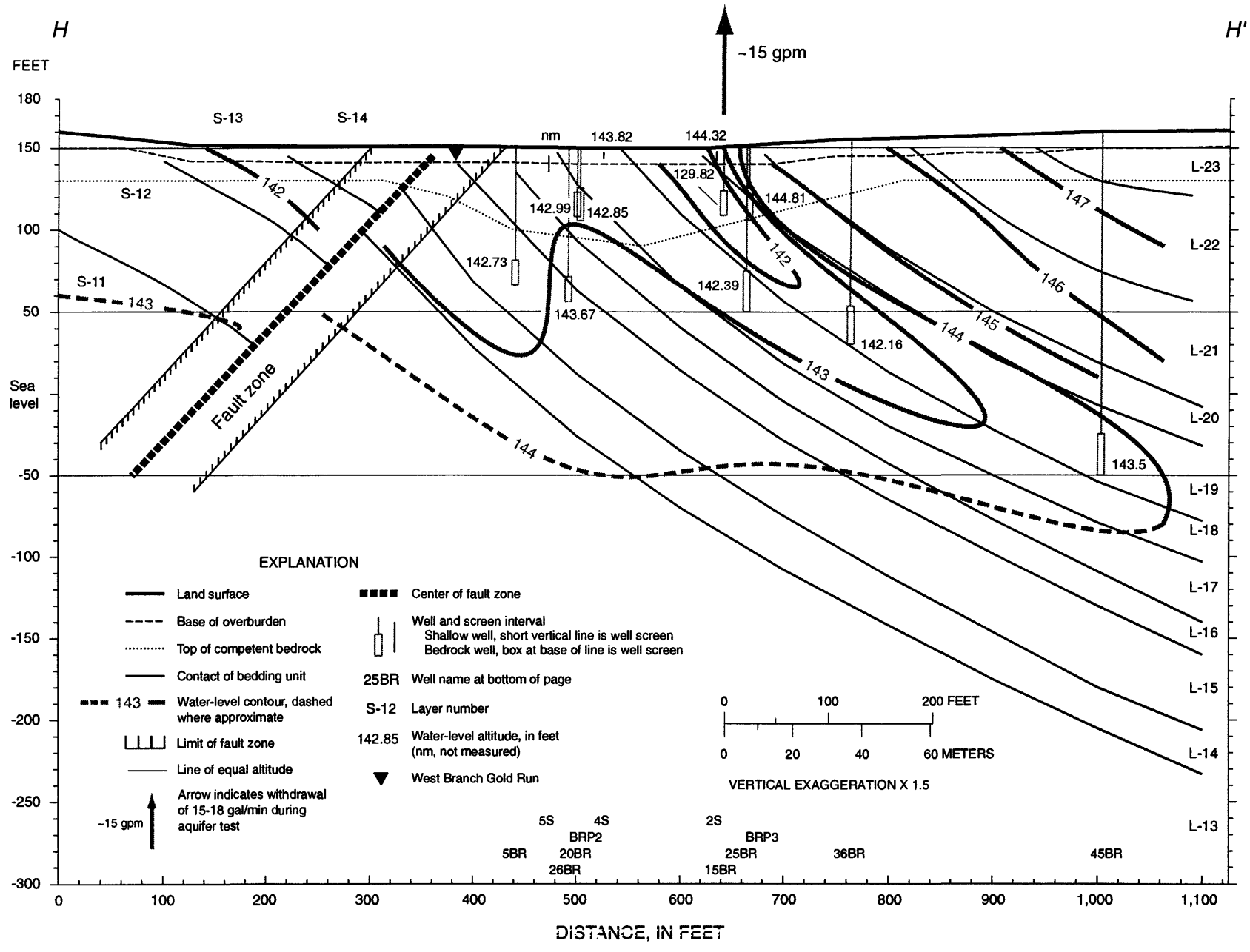

Figure 67. Stressed water-level altitude measured in wells along section *H-H'* during operation of the recovery well 15BR, August 25-27, 1997.

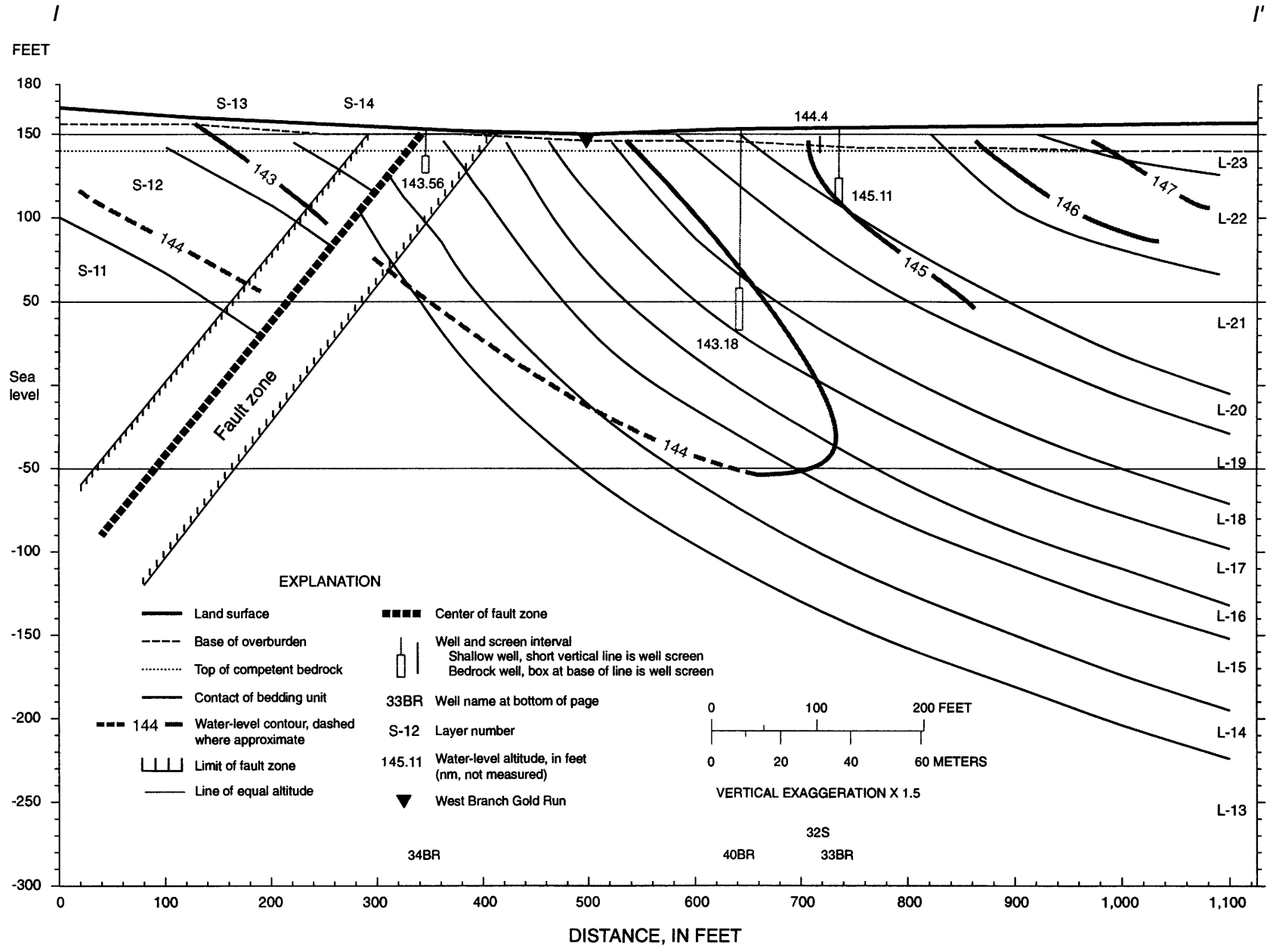

Figure 68. Stressed water-level altitude measured in wells along section *I-I'* during operation of the recovery well 15BR, August 25-27, 1997.

L-21. It extends westward to the West Branch of Gold Run and eastward about 200 ft further to well 41BR (fig. 59). The fact that the cone does not expand further west beyond the West Branch of Gold Run indicates that sufficient water is supplied by the West Branch of Gold Run to supply the stressed system from that direction. The fact that the cone of depression expands farther eastward indicates that water must come from areas along the zone of greatest hydraulic conductivity. The closed 143-ft contour south of the cone of depression and centered on bedding unit L-15 (fig. 59) is a subtle modification of water levels as measured under static conditions (fig. 29).

In section E-E', (fig. 64) the hydraulic gradient is upward from well 42BR to 39BR as shown in figure 5. Water levels in well 6BR are above land surface and the hydraulic gradient is toward the West Branch of Gold Run. In section F-F' (fig. 65) the contours show the hydraulic gradient is toward bedding unit L-19; this indicates that flow is affected by the cone of depression created by pumping well 15BR. The water-level altitude in well 46BR is -49.7 ft or about 150 ft below land surface. Water levels did not recover in the 3 months after completion of drilling, development, and sampling of the well. As a result, the hydraulic conductivity of bedding units L-18 and L-19 is very low at this depth. The water level in well 38BR is the lowest of all wells in the cone of depression, with the exception of the pumped well. There is a very direct contact between wells 15BR and 38BR. Water levels in wells 23BR and 4BR show a downward hydraulic gradient, which indicate that the ground-water flow in this area is not toward the cone of depression caused by pumping, but rather is toward the natural hydraulic low in bedding unit L-15 caused by ground-water discharge westward to the West Branch of Gold Run. Water levels in wells 22BR and 28BR show southeastward and upward flow to the West Branch of Gold Run.

Section G-G' (fig. 66) shows that the hydraulic gradient in bedding units L-22 and L-21 is downward as determined from water levels in wells 8BR and 29BR. The hydraulic gradient in bedding units L-19 is shown to be updip because of water-level data shown in sections F-F' and H-H'. The hydraulic gradient is interpreted to be downward in bedding units L-16 to L-18 based on water levels in wells 7BR and 24BR. Flow in bedding unit L-15 is interpreted to be westward (into the page) as discussed earlier. In section H-H' (fig. 67), the hydraulic gradient in bedding units L-17 to L-22 is towards the cone of depression, which is centered on well 15BR and in bedding unit L-19. Water levels in wells 45BR, 36BR, and 15BR are 143.50, 142.16, and 129.83 ft, respectively. This indicates an updip hydraulic gradient in bedding unit L-19. Water levels in wells 20BR, 26BR, and 5BR show a hydraulic gradient toward bedding unit L-15 and updip flow direction in bedding unit L-15.

Water level in wells 43BR and 44BR (line D-D') (fig. 63) did not recover after drilling, development, and water-quality sampling. The lack of recovery in bedding units L-13 to L-16 is either because (a) there is no outcrop of bedding units L-13 to L-16, or (b) the aquifer has a very low hydraulic conductivity at depths of 300 ft below land surface and deeper. Bedding units L-13 to L-16 do not crop out along Section D-D' or in upgradient areas east and northeast of the wells. As a result, the only source of water is from vertical fractures. Because the predominant flowpath is along the bedding-plane partings and there are no bedding-plane partings that crop out to supply water from land surface in this area, there is poor recovery of water levels in these two wells. An alternative reason for low water levels is that the bedding-plane and vertical partings in the Lockatong Formation have all but closed because of the high overburden pressures at depths of 300 ft. Therefore, the hydraulic conductivity of the Lockatong

aquifer is near zero at depth of 300 ft and greater. In all likelihood the lack of recovery in these two wells is a combination of the two reasons.

The hydraulic gradients on the south side of the fault are toward the West Branch of Gold Run. This indicates that the West Branch of Gold Run is still an active stream and it behaves as a hydraulic divide. It is interpreted that shallow ground water on the base between the West Branch of Gold Run and the fault/ contact will discharge to the West Branch of Gold Run and will not cross underneath the stream.

In summary, the cone of depression caused by pumping well 15BR predominantly lowers water levels in bedding unit L-19. However, the drawdown only extends from the West Branch of Gold Run about 500 ft west of well 15BR to well 41BR about 500 ft east of well 15BR. Pumping acts, to a lesser extent, to lower water levels in bedding units L-17, L-18, and L-20 to L-23. The recovery well may intercept contamination from other bedding units; however, the recovery well also may lower water levels in some wells but not change the hydraulic gradient or the flowpaths and therefore not capture the contamination. From a conservative viewpoint, contamination is being removed from the immediate vicinity of the recovery well especially in bedding units L-17 to L-20 but the pumping well may not be recovering water from other areas. Contamination in areas outside the capture zone of the pumped well will not be captured; however, contamination south of the cone of depression created by well 15BR will follow the natural flow gradient and may discharge to the West Branch of Gold Run.

WATER QUALITY

Water-quality samples have been collected on selected dates from the bedrock and over burden wells at the Naval Air Warfare Center since the first monitoring wells were installed in 1990. Water-quality data, including values of TCE, cis-DCE, and VC, were published in reports by International Technology Corporation, (July, 1994, table 4-1A and 4-1B), EA Engineering, Science, and Technology, Inc., (February, 1996, table 4-1; August, 1997, table 1).

Some wells were sampled many times, whereas other wells were sampled only once. TCE, cis-DCE and VC are discussed in that order, and their concentrations are shown in figures. Sections A, B, and C, which cross the Site 3 area are discussed first, followed by sections D and E between Sites 1 and 3. The two scenarios for Site 1, which is crossed by sections F, G, and H, are discussed, and finally section I, which is west of Site 1, is discussed.

Trichloroethylene (TCE)

The two source areas for TCE contamination at the NAWC were first identified by International Technology Corporation (July 1994), as Site 1 and Site 3 (fig. 2). Site 1 is the brine-handling area and consists of the TCE storage and handling facilities between buildings 40 and 41, the network of above-ground TCE pipelines, waste lines that lead to the barometric well, and the West Ditch where TCE-laden wastewater was disposed. Site 3 consists of a former wastewater lagoon and sludge disposal area. These areas are shown in the map view (figs. 69 to 71) and in the sections as lines at land surface (figs. 72, 73, and 77 to 80). In addition to the two areas identified above, a third source may exist. Building 21, a metal-working facility and a nearby TCE underground storage tank may be a site where TCE was used and stored during routine operations.

Because TCE was used at the NAWC for about 40 years, it is probable that some of it has been released aerially. There may be an

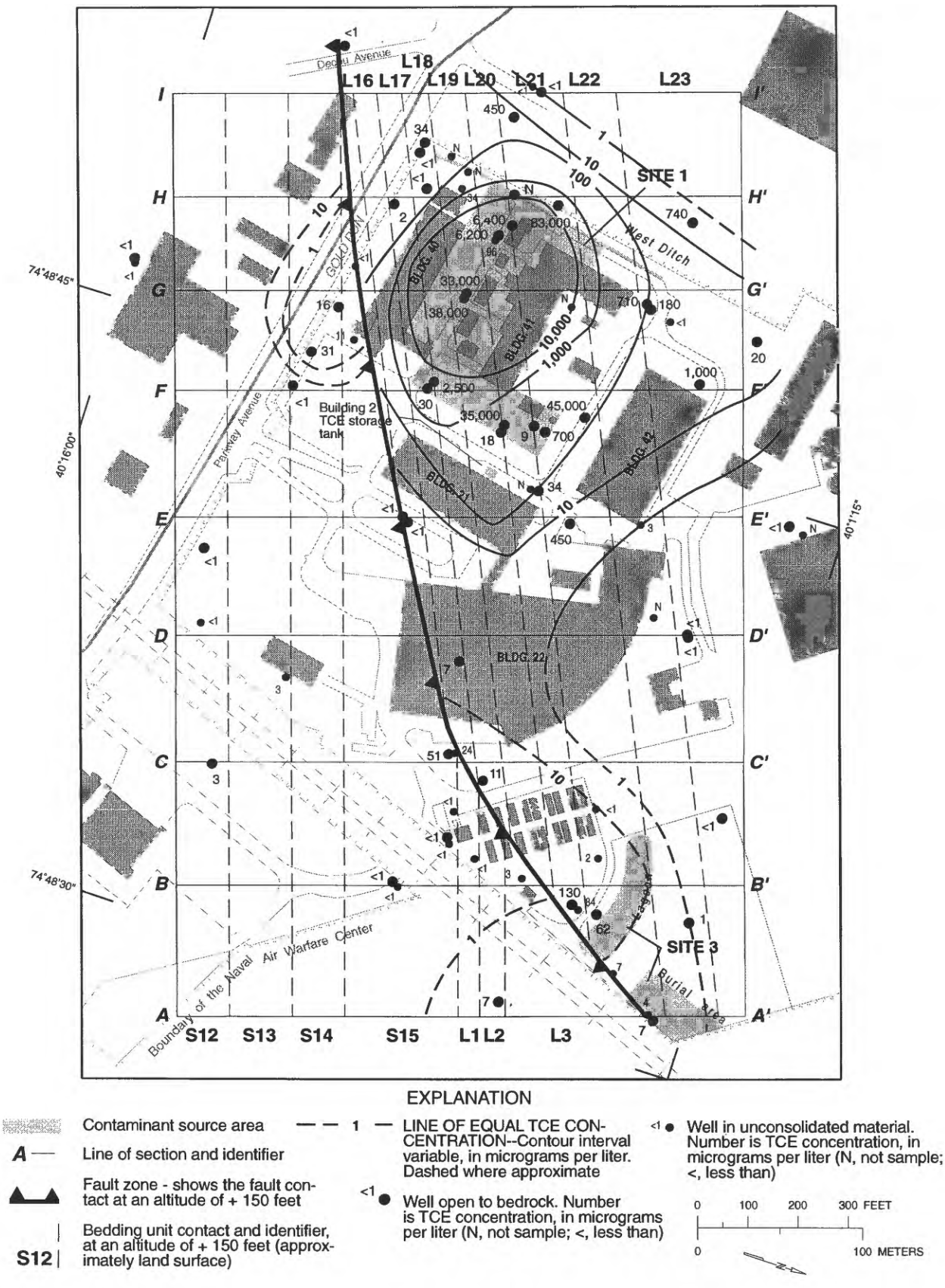

Figure 69. TCE concentrations, in micrograms per liter, in water samples from bedrock and shallow wells, June 1997, and contours for top of bedrock (an altitude of + 150 feet and approximately land surface), scenario 1 and 2, Naval Air Warfare Center, West Trenton, N.J.

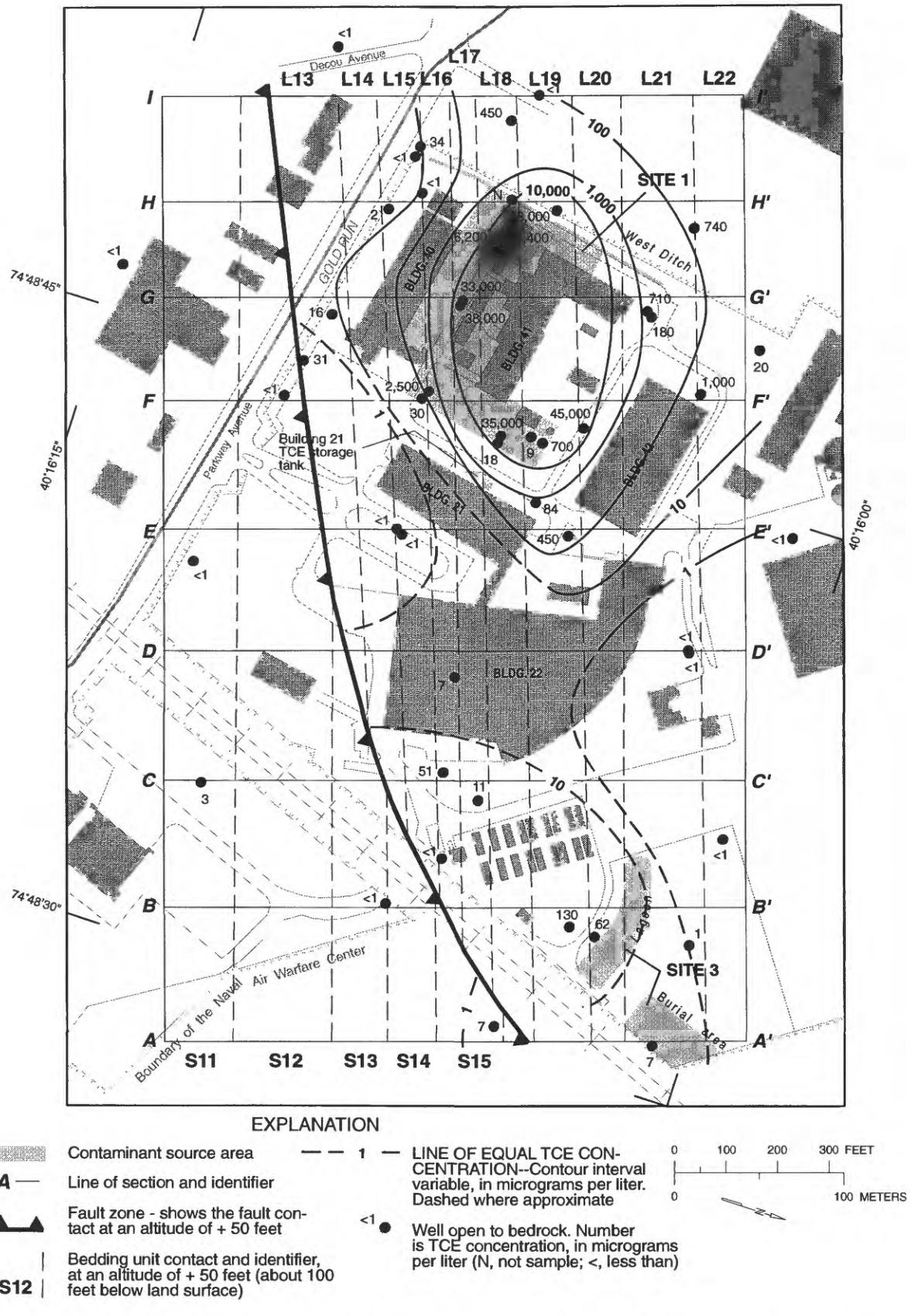

Figure 70. TCE concentrations, in micrograms per liter, in water samples from bedrock and shallow wells, June 1997, and contours for an altitude of + 50 feet (about 100 feet below land surface), scenario 1 and 2, Naval Air Warfare Center, West Trenton, N.J.

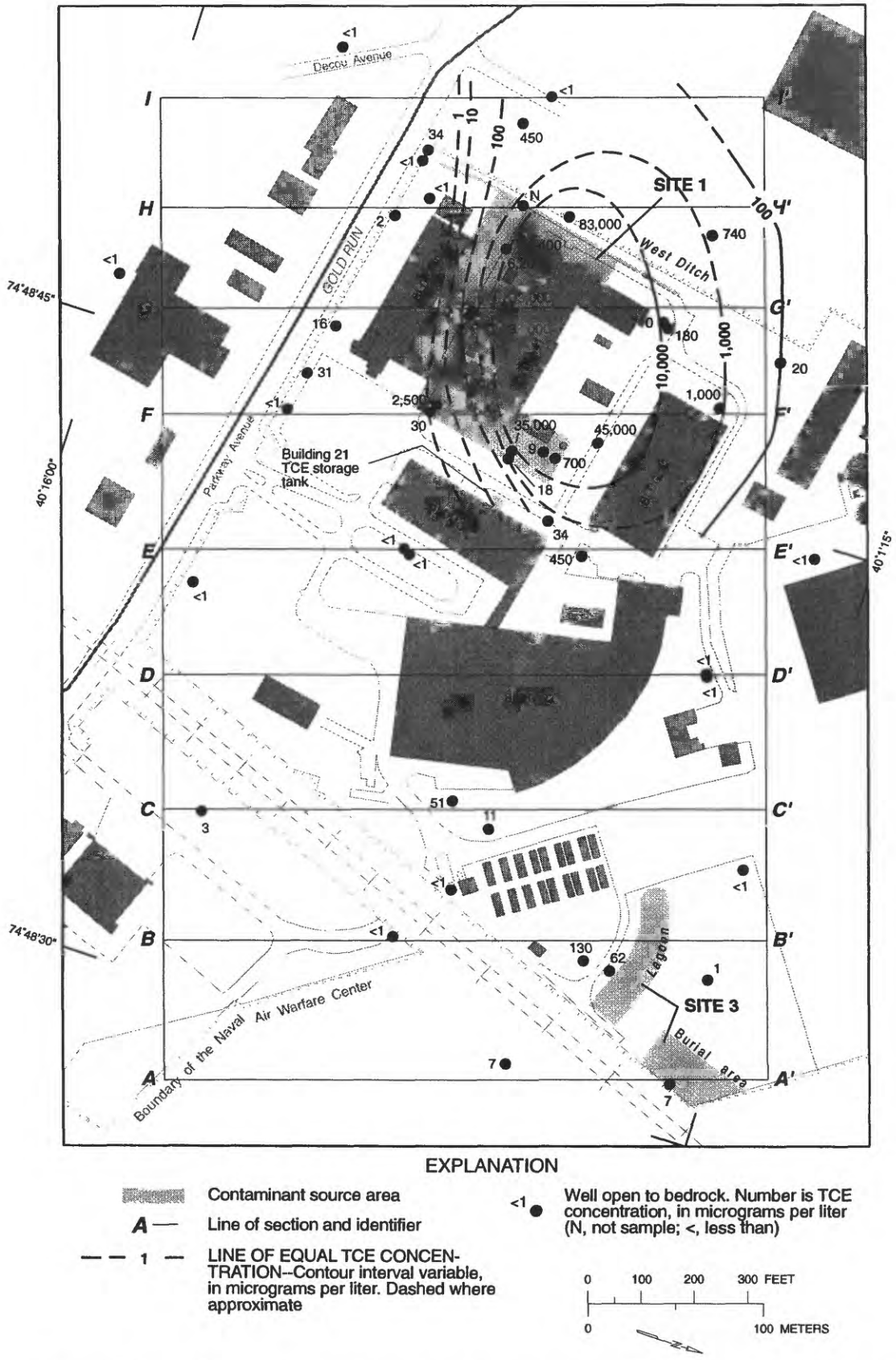

Figure 71a. TCE concentrations, in micrograms per liter, in water samples from bedrock wells, June 1997, and contours for an altitude of - 50 feet (about 200 feet below land surface), scenario 1, Naval Air Warfare Center, West Trenton, N.J.

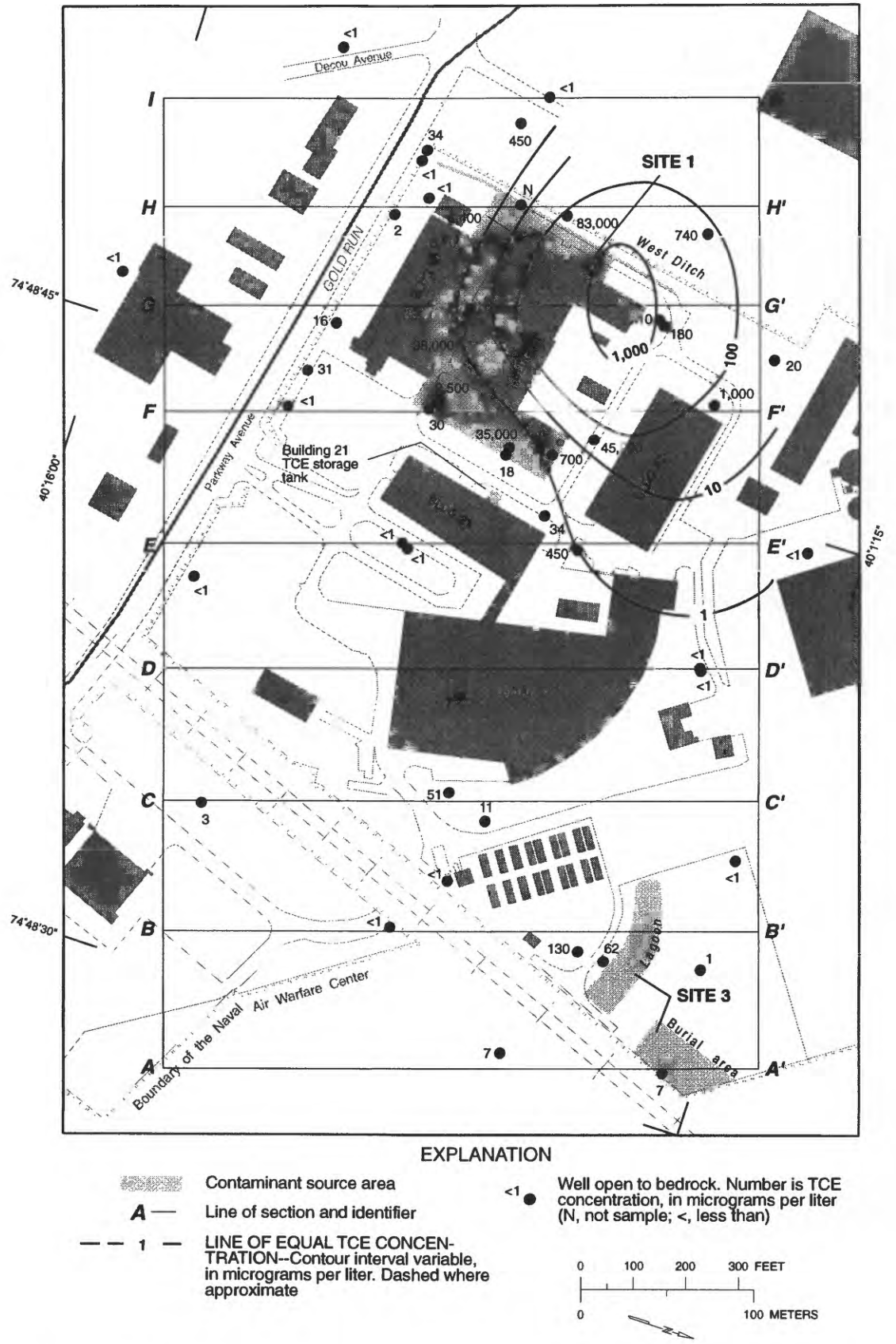

Figure 71b. TCE concentrations, in micrograms per liter, in water samples from bedrock wells, June 1997, and contours for an altitude of - 50 feet (about 200 feet below land surface), scenario 2, Naval Air Warfare Center, West Trenton, N.J.

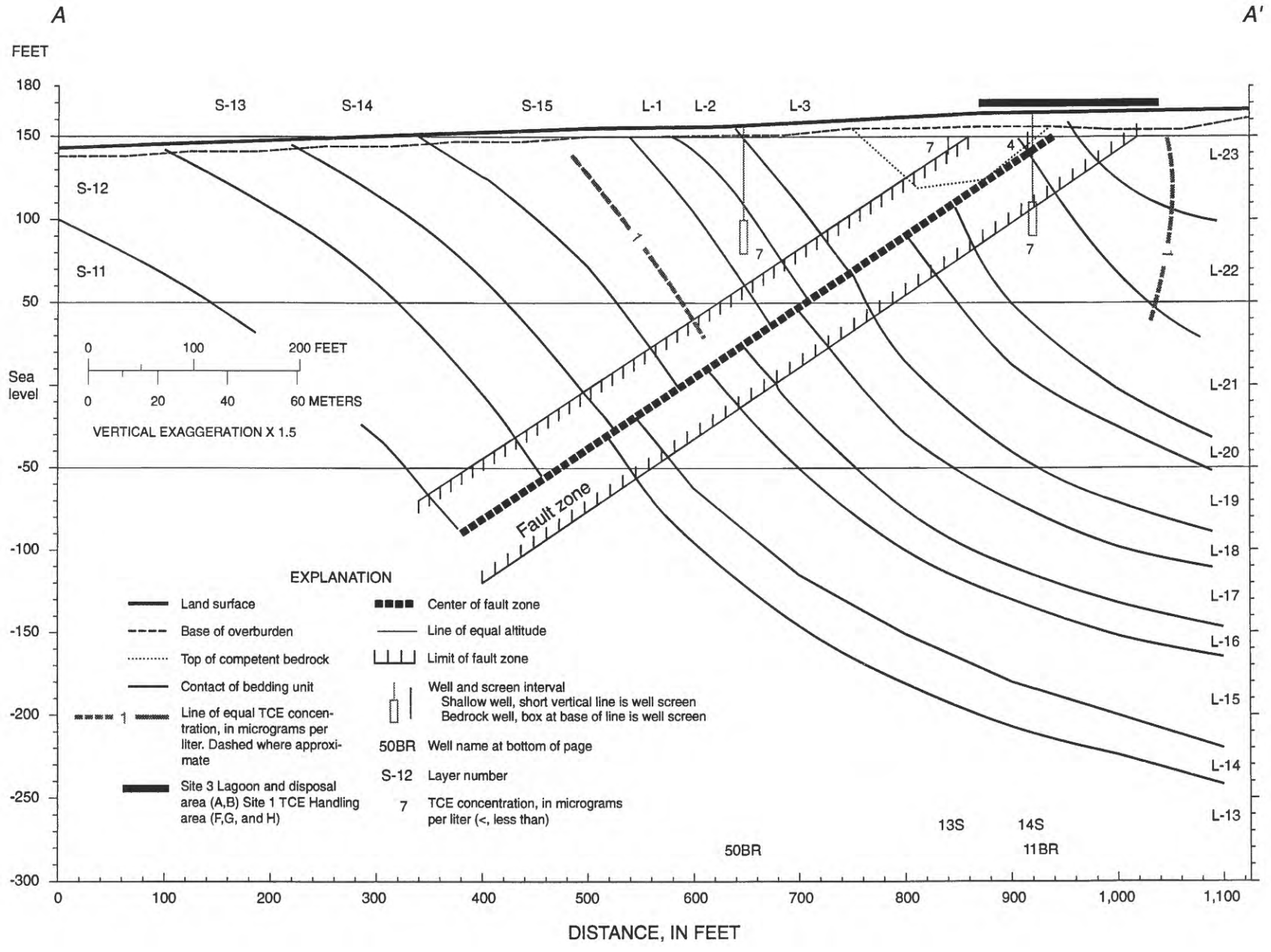

Figure 72. Section *A-A'* showing TCE concentrations in water samples from bedrock and overburden wells, June 1997.

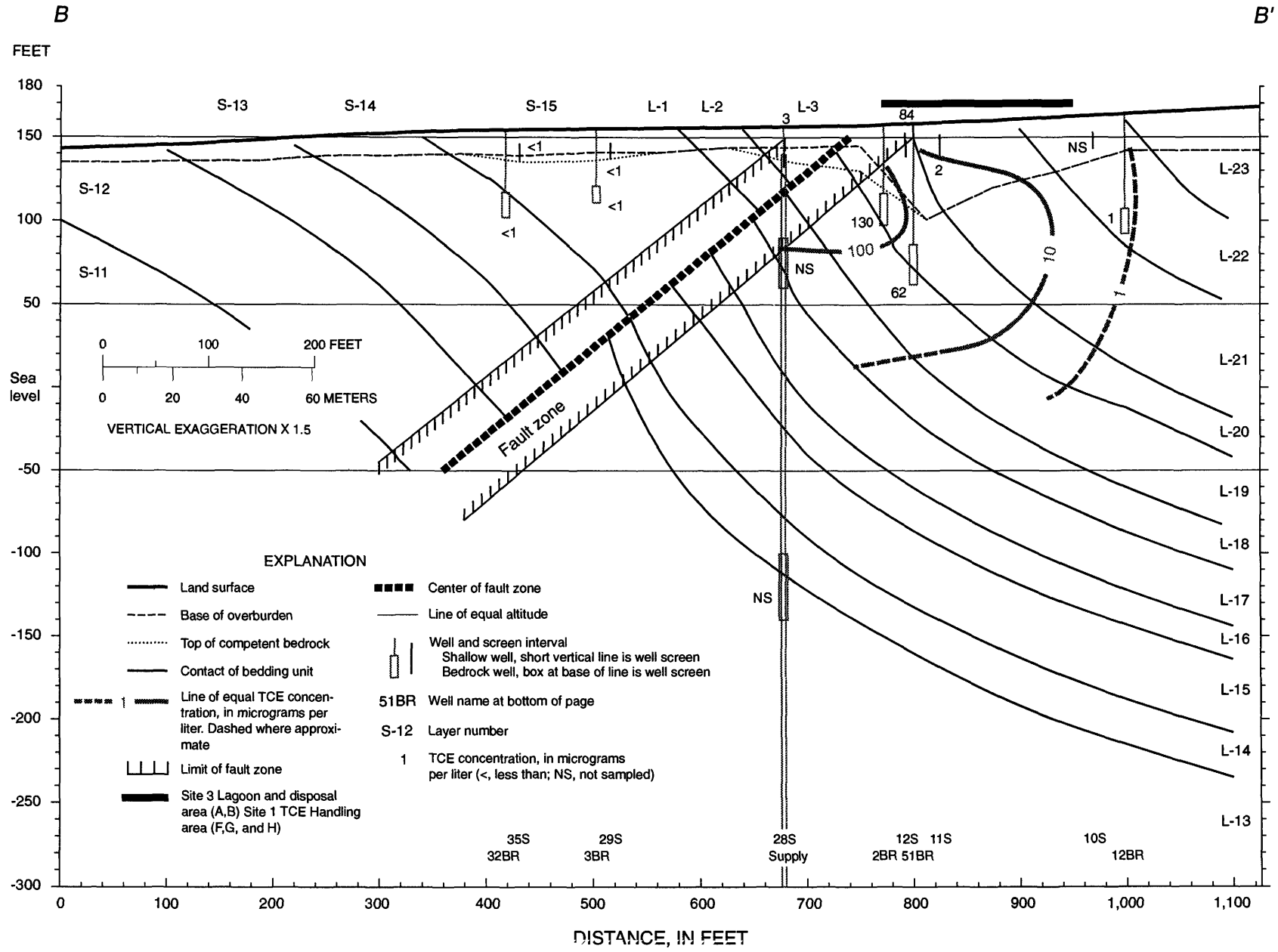

Figure 73. Section *B-B'* showing TCE concentrations in water samples from bedrock wells, June 1997.

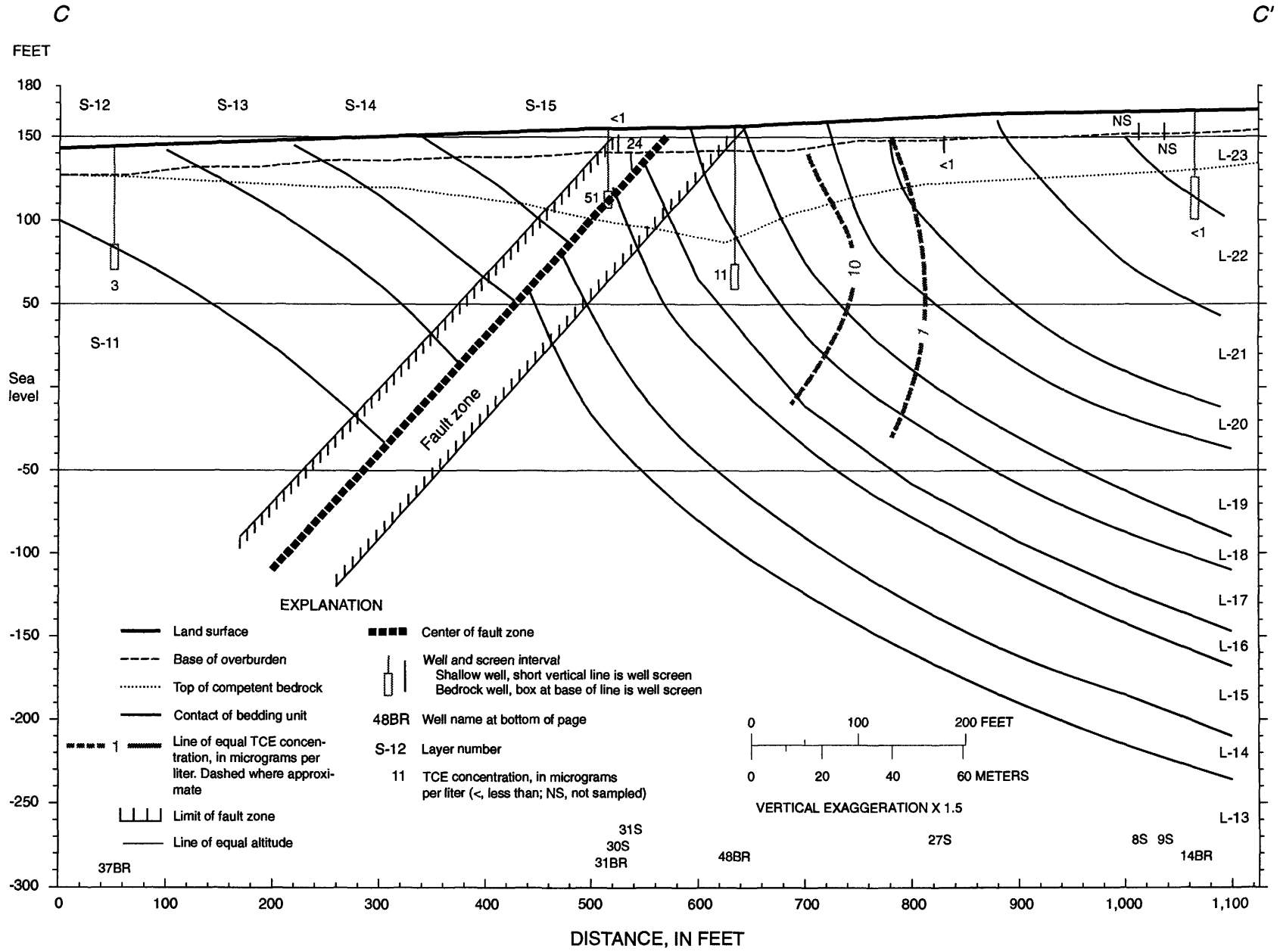

Figure 74. Section *C-C'* showing TCE concentrations in water samples from bedrock wells, June 1997.

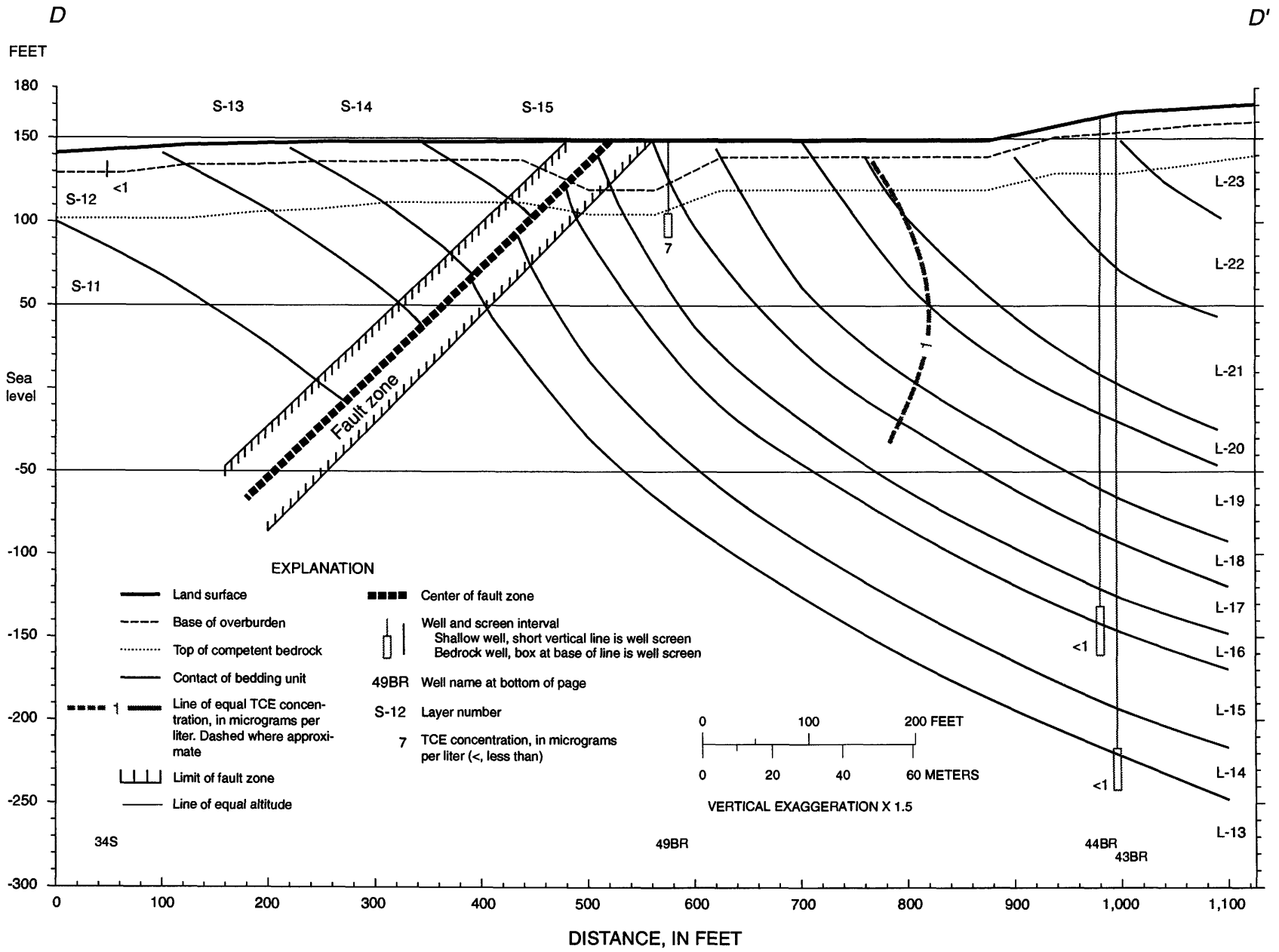

Figure 75. Section *D-D'* showing TCE concentrations in water samples from bedrock wells, June 1997.

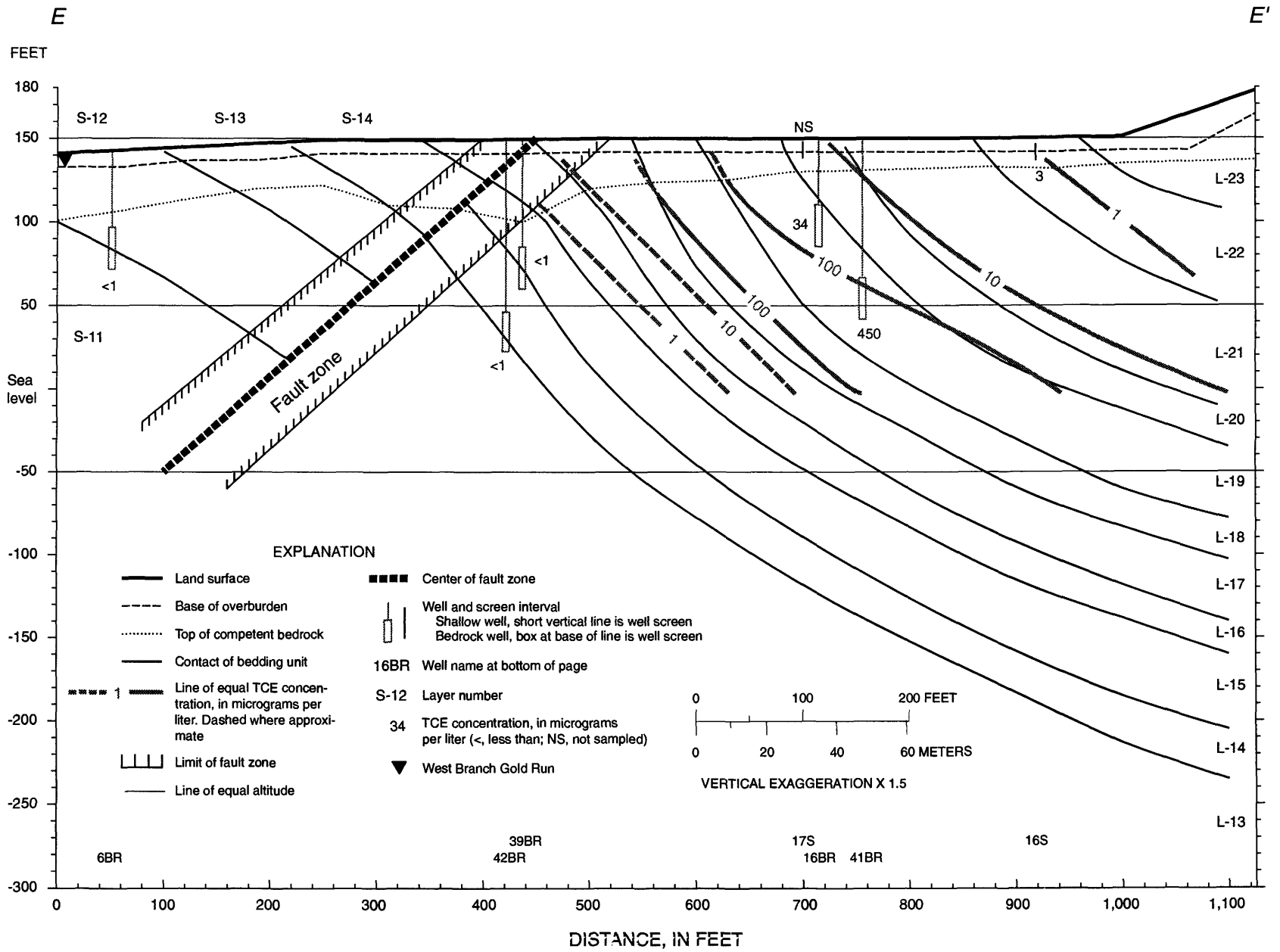

Figure 76a. Section *E-E'* showing TCE concentrations in water samples from bedrock wells, June 1997, for Scenario 1.

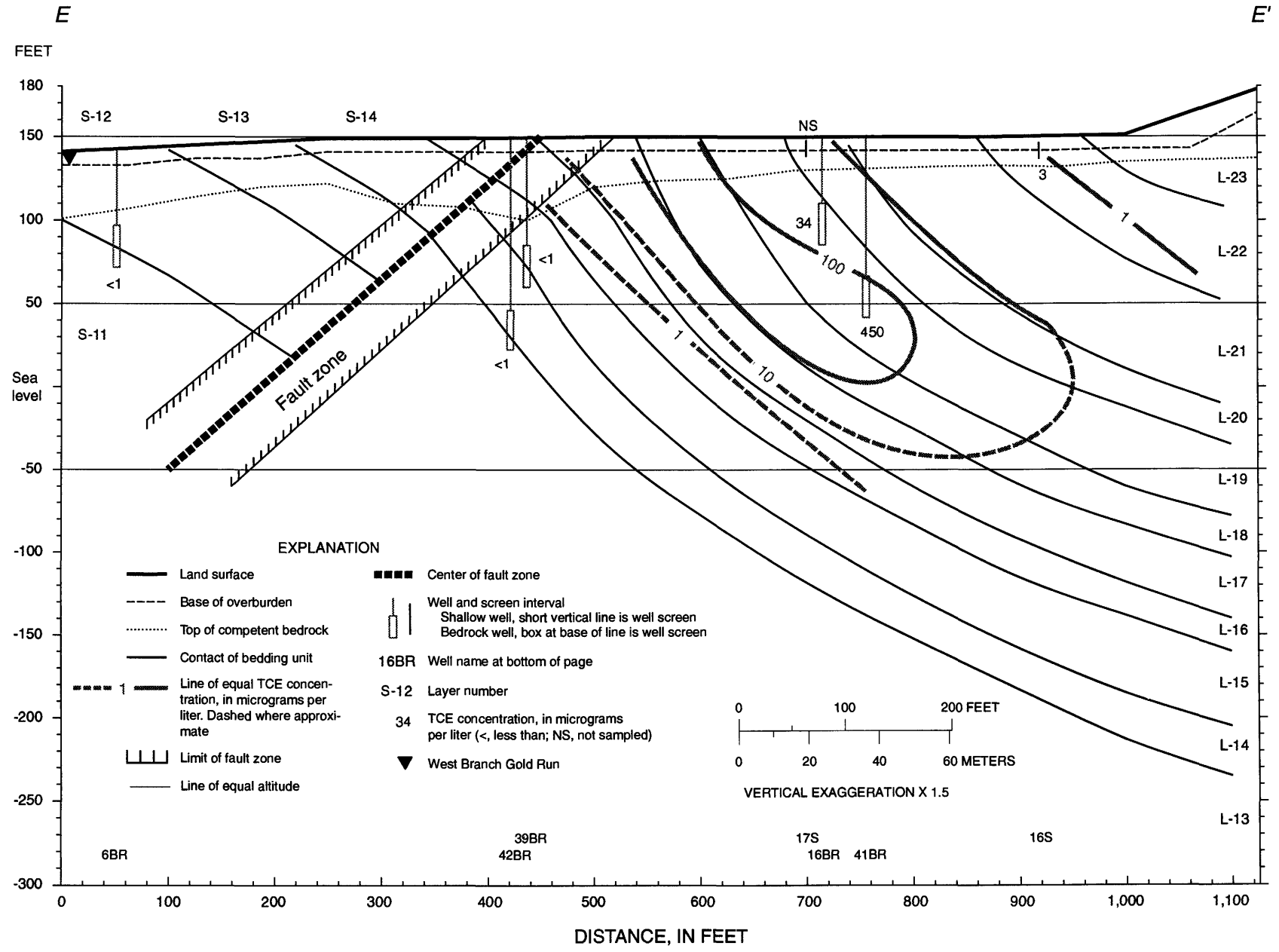

Figure 76b. Section *E-E'* showing TCE concentrations in water samples from bedrock wells, June 1997, for Scenario 2.

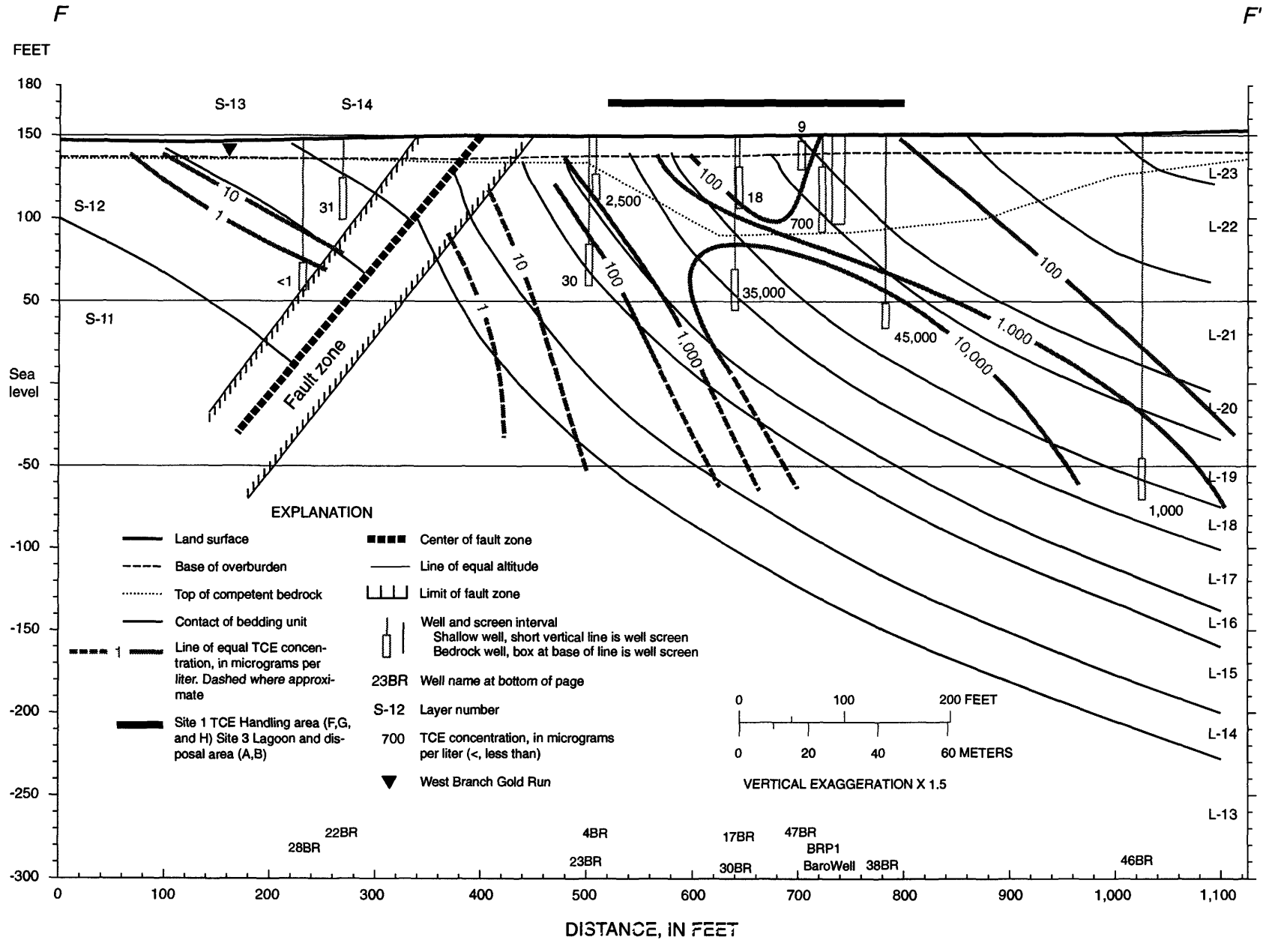

Figure 77a. Section *F-F'* showing TCE concentrations in water samples from bedrock wells, June 1997, for Scenario 1.

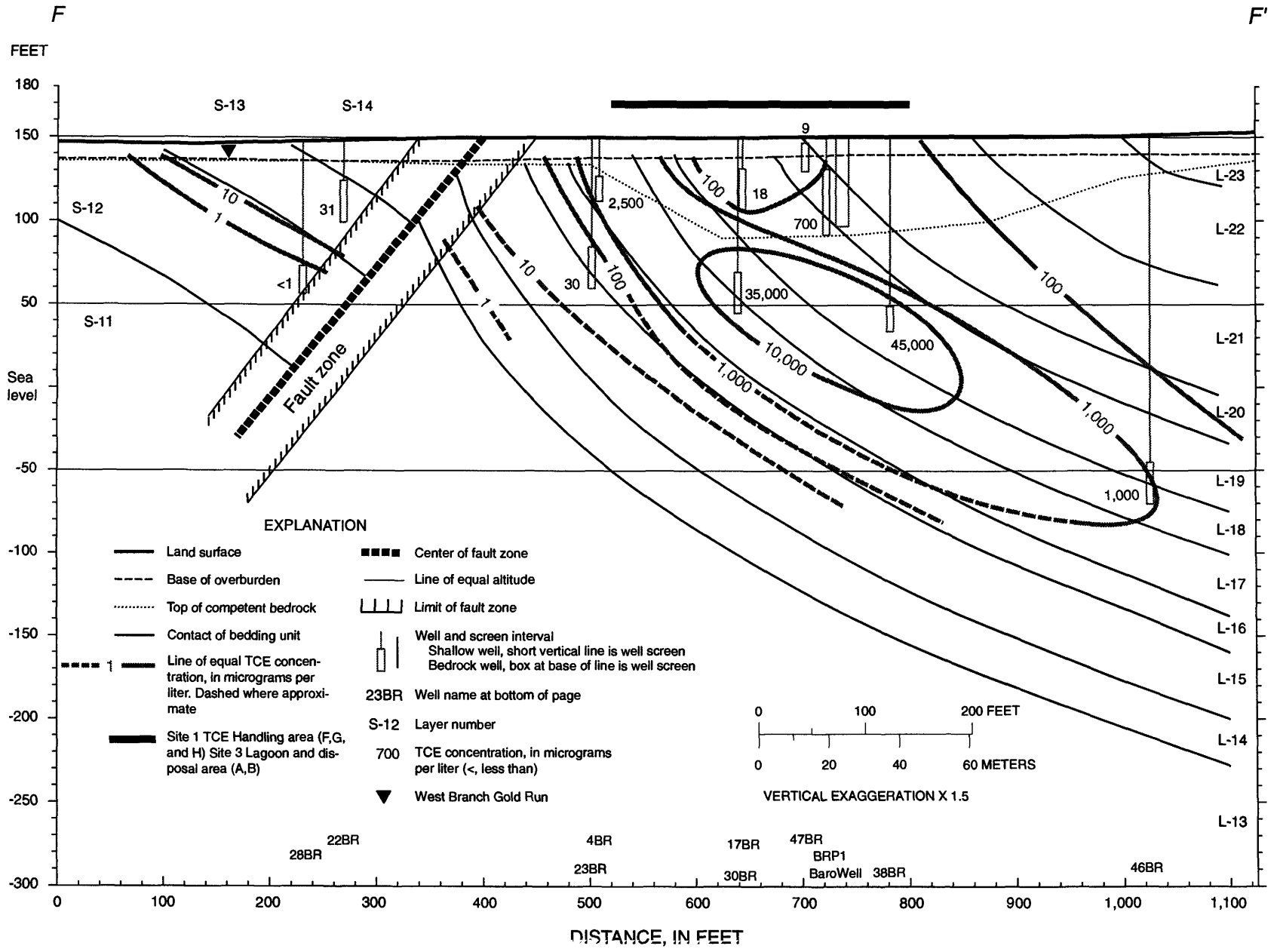

Figure 77b. Section *F-F'* showing TCE concentrations in water samples from bedrock wells, June 1997, for Scenario 2.

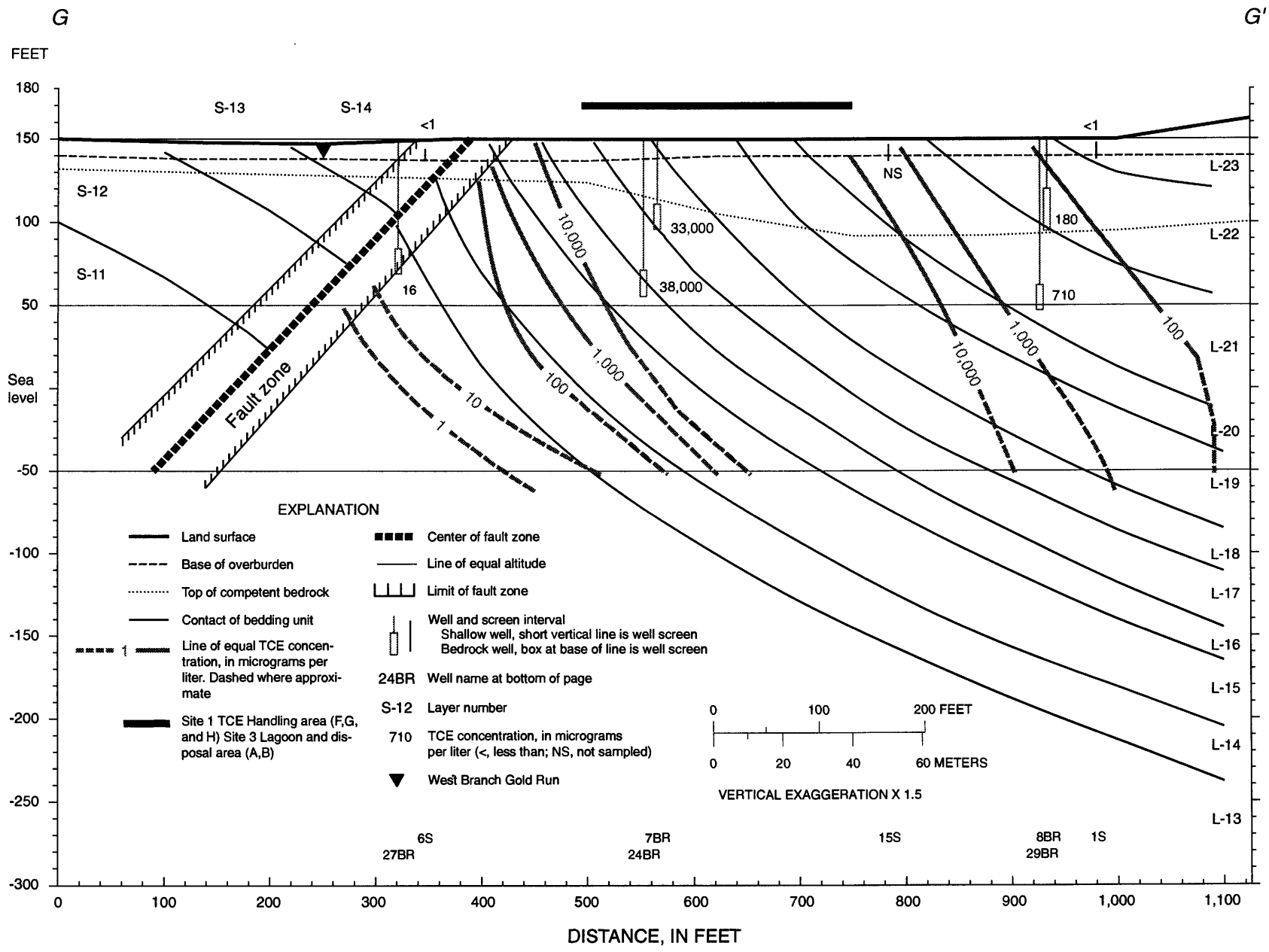

Figure 78a. Section *G-G'* showing TCE concentrations in water samples from bedrock wells, June 1997, for Scenario 1.

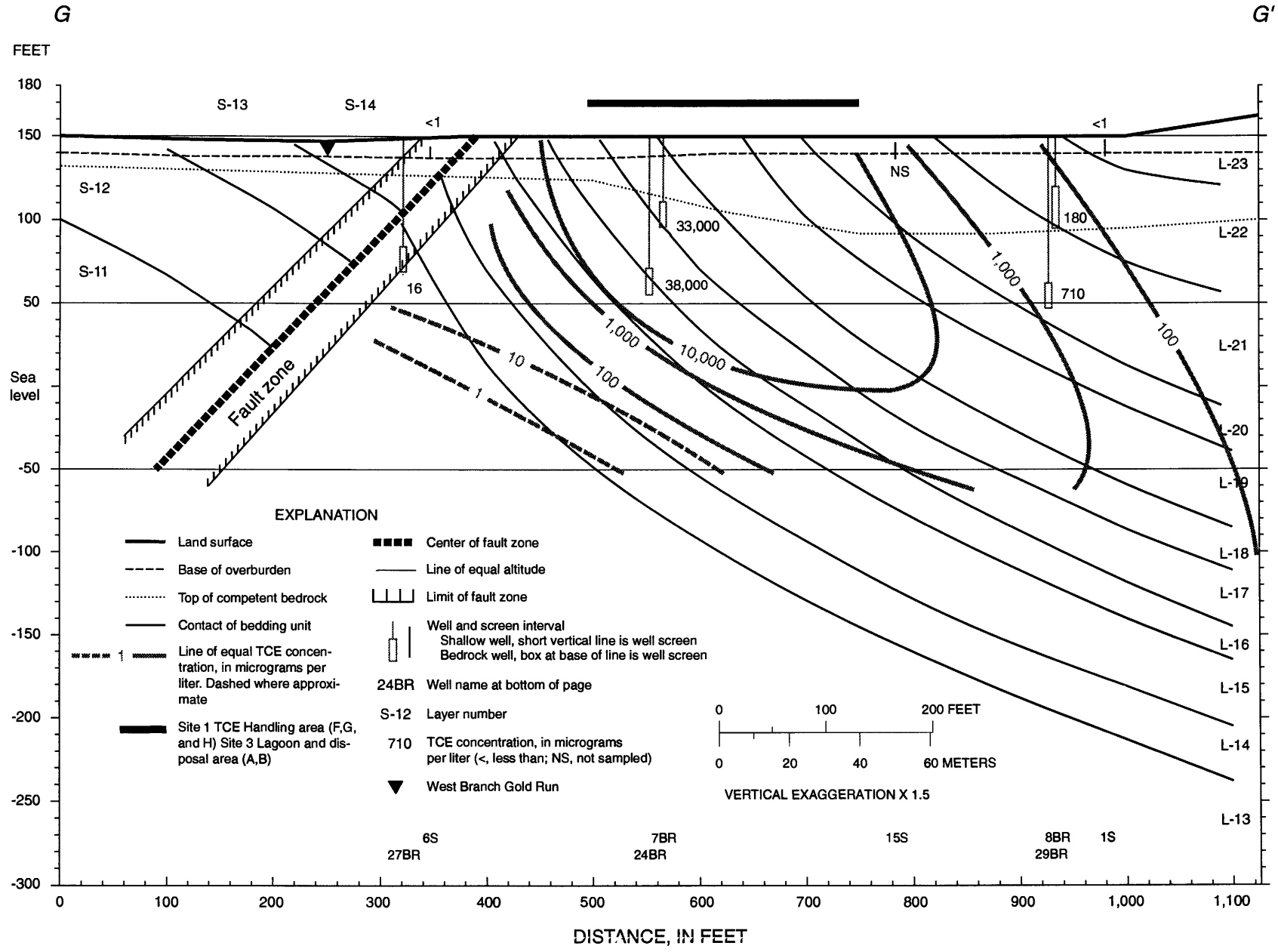

Figure 78b. Section *G-G'* showing TCE concentrations in water samples from bedrock wells, June 1997, for Scenario 2.

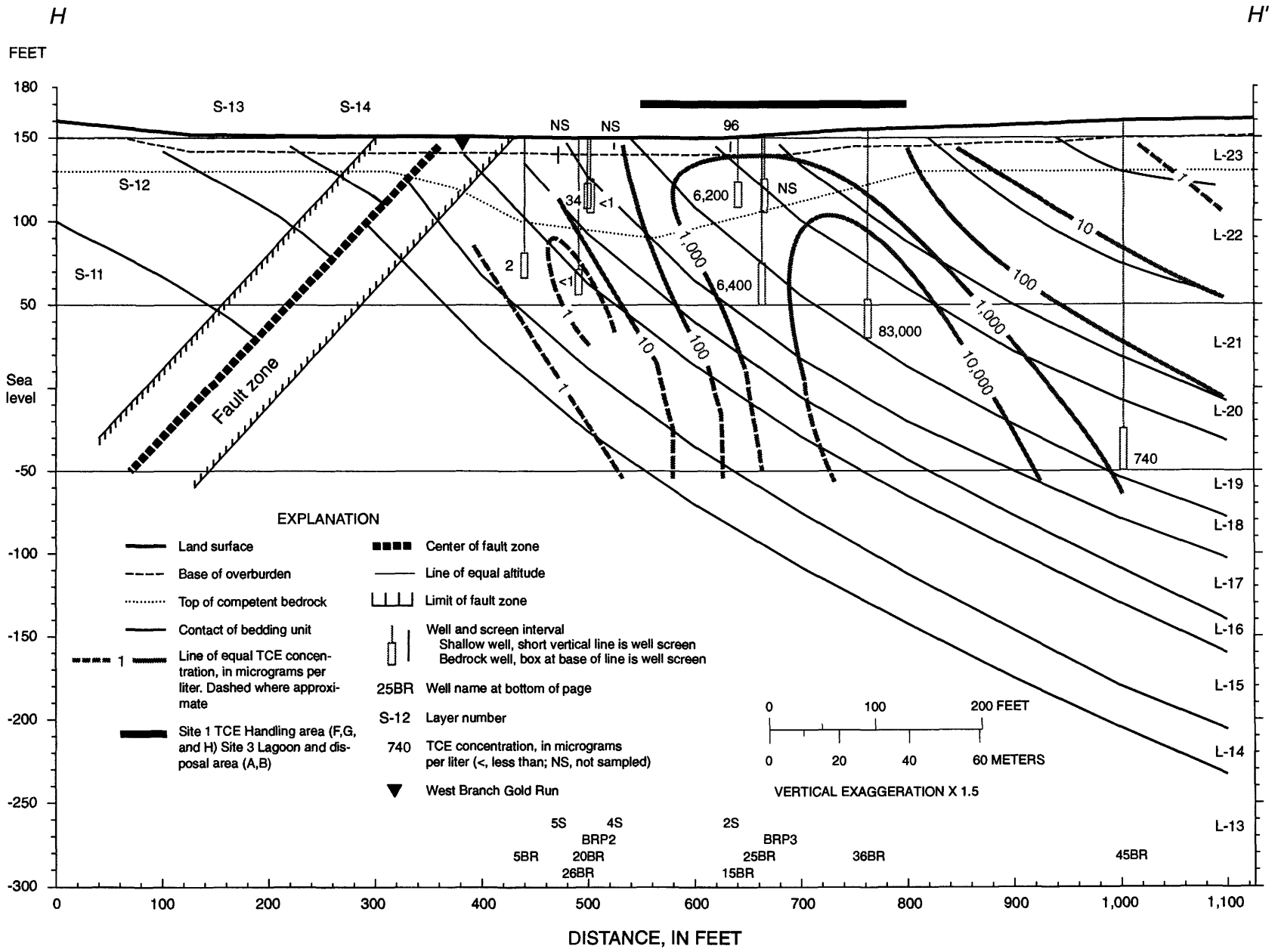

Figure 79a. Section *H-H'* showing TCE concentrations in water samples from bedrock wells, June 1997, for Scenario 1.

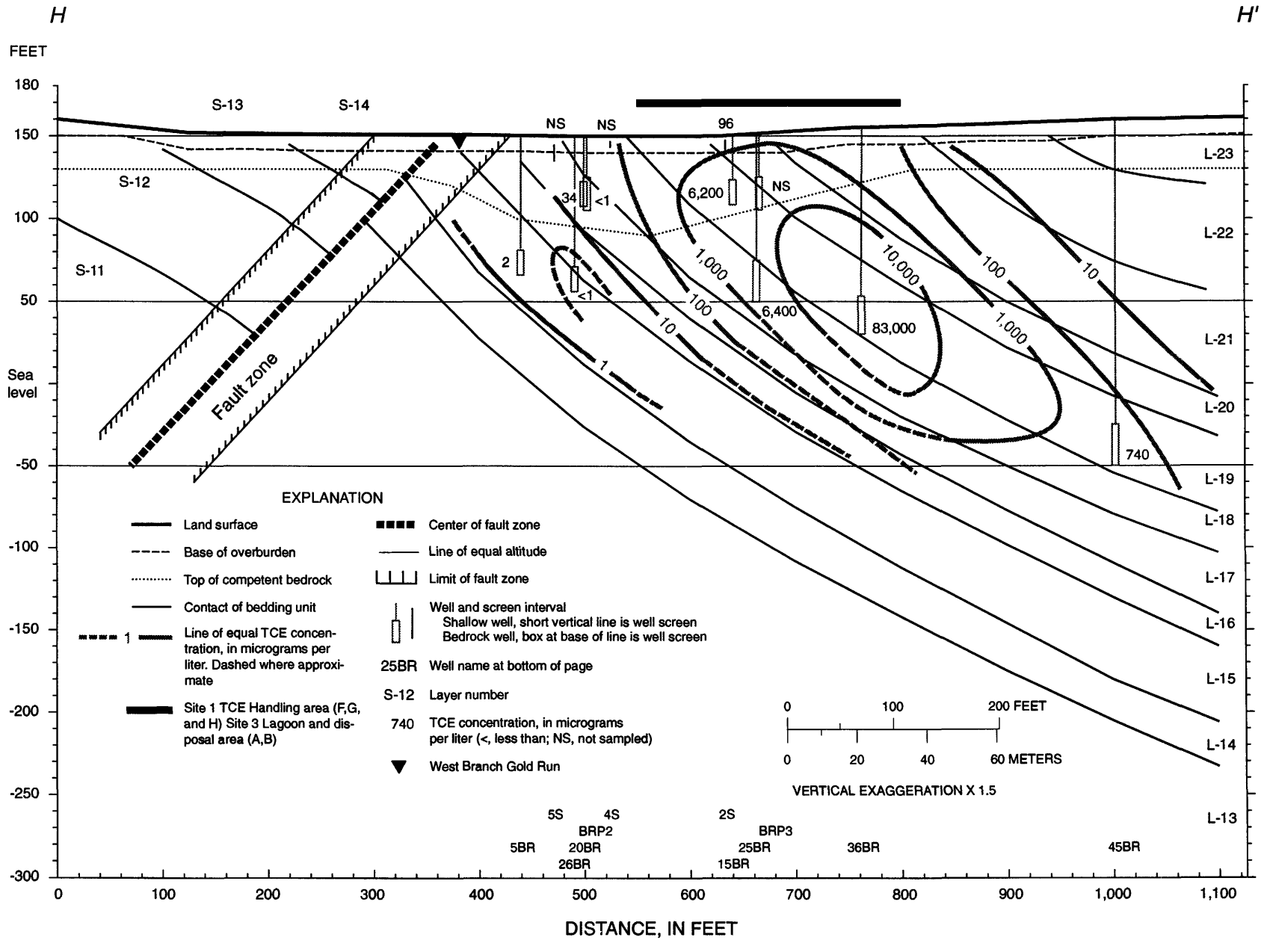

Figure 79b. Section *H-H'* showing TCE concentrations in water samples from bedrock wells, June 1997, for Scenario 2.

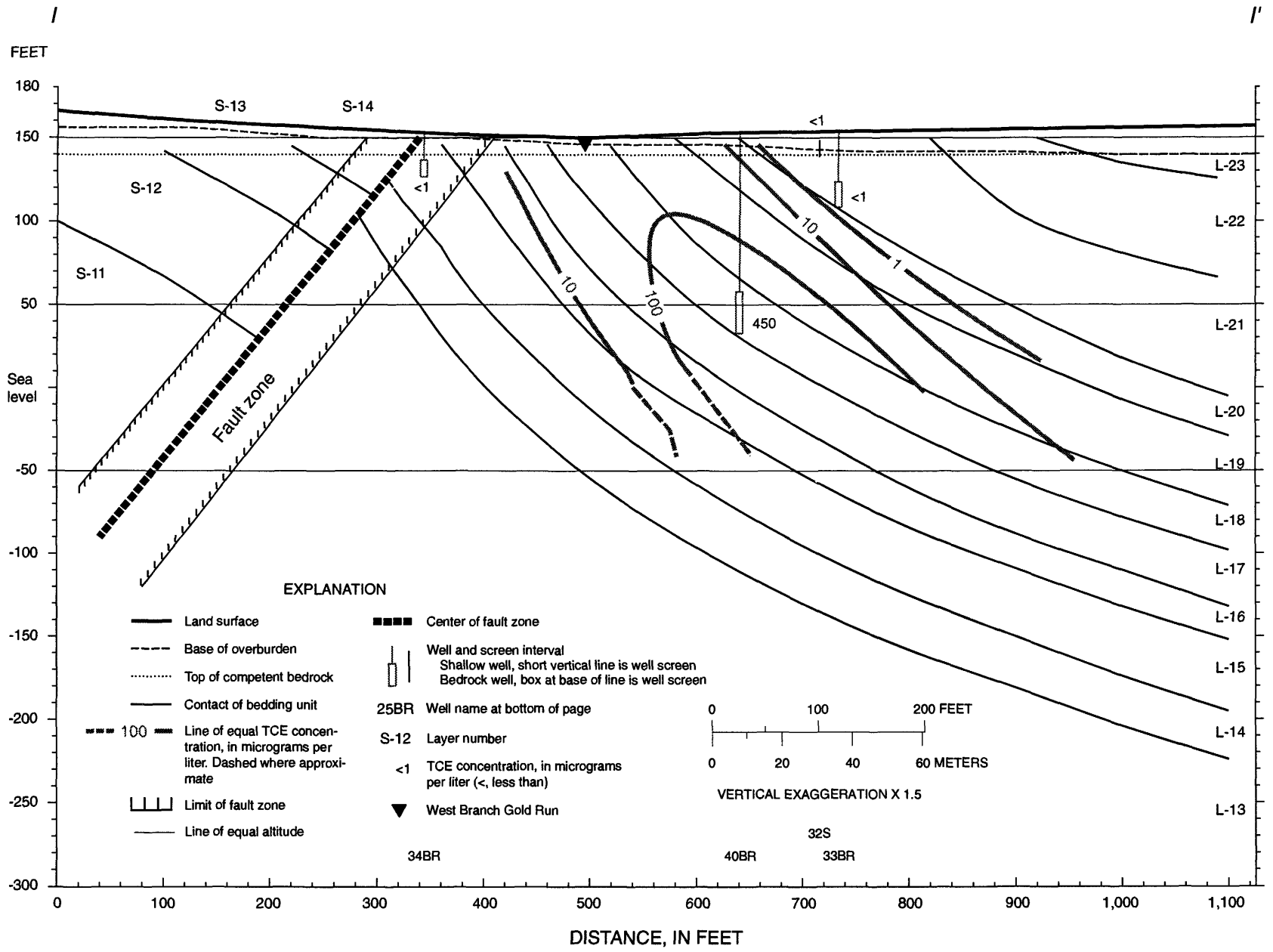

Figure 80a. Section *I-I'* showing TCE concentrations in water samples from bedrock wells, June 1997, for Scenario 1.

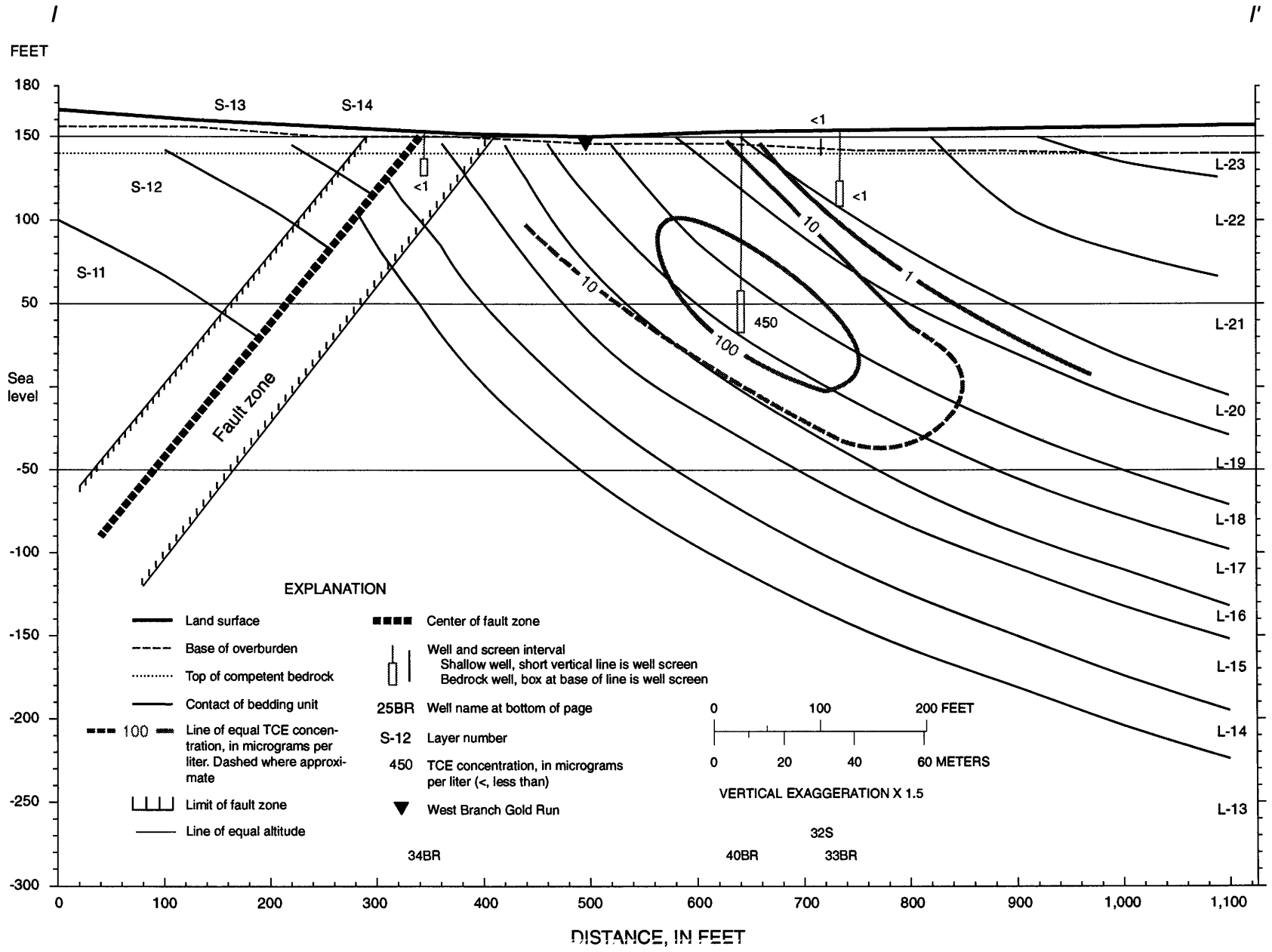

Figure 80b. Section *I-I'* showing TCE concentrations in water samples from bedrock wells, June 1997, for Scenario 2.

extensive zone around the NAWC where sediments and ground water show background concentrations of TCE that range from 1 to 10 µg/L. In selected areas away from Site 1, Site 3, and building 21, TCE may be present in ground water as a result of an isolated spill or other single event.

TCE contamination in the aquifer can be in two forms: pure TCE, also known as dense non-aqueous phase liquid (DNAPL) TCE, and dissolved TCE, which is TCE in solution in ground water. In this report, the two phases of TCE will be referred to as DNAPL TCE and dissolved TCE.

DNAPL TCE was never recovered in water samples from monitoring wells at NAWC. The principle mechanism for conversion of DNAPL TCE to dissolved TCE is dissolution in ground water. Dissolved TCE was recovered in water samples from 36 of the 48 bedrock wells that were sampled during June 1997 in the study area. At most wells, the concentration of dissolved TCE has decreased over time. The decrease is a result of biodegradation, abiotic degradation, dispersion, adsorption, dilution, and evaporation. Collectively, actions that decrease the concentration of TCE in ground water are referred to as natural attenuation.

There are two possible scenarios for DNAPL TCE contamination in the Site 1 area. The first scenario is that DNAPL TCE sank into the aquifer to depths greater than 250 ft below land surface and is currently at those depths. The second scenario is that DNAPL TCE sank into the aquifer but dissolved and degraded when it reached a depth of 100 ft below land surface. In scenario 2, no DNAPL TCE is present at depths greater than 100 ft. It is uncertain which scenario is correct in the Site 1 area; therefore, both scenarios are discussed in detail. In the Site 3 area, only dissolved TCE was deposited at land surface; therefore, there can be no DNAPL TCE at depth.

Site 3: Lagoon and Sludge Disposal Area

Prior to the mid-1980's, dissolved TCE was deposited into the Site 3 lagoon (fig. 69), where it evaporated or infiltrated to the water table. During June 1997, 11 bedrock wells shown on sections A, B, and C were sampled for TCE (figs. 72, 73, and 74). Well 2BR had a TCE concentration of 130 µg/L in 1997, whereas during 1992-93, the TCE concentration was 320, 230, and 110 µg/L. Well 11BR had a TCE concentration of 7 µg/L in 1997, but had TCE concentrations of <1 to 16 µg/L during 1992-93. These data indicate that the TCE concentration is decreasing with time in the Site 3 area. The TCE concentration in well 51BR was 62 µg/L, but it was sampled only during June 1997. Well 31BR was sampled in 1993 and 1997 with a concentration of 23 and 51 µg/L, respectively. It is unclear why TCE concentrations increased in well 31BR. Well 14BR shows undetected levels of TCE, and well 48BR was sampled only once with a TCE concentration of 11 µg/L in 1997.

Ground-water flow in the Site 3 area is along strike and to the west-southwest. The shape of the TCE plume and the decrease in TCE concentrations downgradient indicates that the plume is moving from the lagoon source area along the north side of the fault towards the west-southwest along with the ground water. The lagoon and the sludge disposal area may straddle the fault. It is possible that some dissolved TCE may have flowed to the south side of the fault. TCE concentrations of 7 µg/L in well 50BR and 3 µg/L in well 37BR may be associated with contamination from the Site 3 area.

During the early 1990's, the sludge disposal area was excavated and deemed remediated by the N.J. Department of Environmental Protection. Therefore, it is no longer considered to be a source of TCE contamination. (Donna Gaffigan, N.J. Department of Environmental Protection, oral commun. 1997).

Area Between Site 3 and Site 1

Sections D and E cross the area between Sites 3 and 1. TCE was reportedly used for metal-cleaning purposes in building 21, and site construction plans show a buried TCE storage tank west of the building 21 (fig. 69). Concentrations of TCE were 7 µg/L in well 49BR and 450 µg/L in well 42BR, but those wells were sampled only once. Concentrations of TCE were 34 µg/L in water samples from well 16BR and are much lower than the 190, 250 and 87 µg/L reported during 1992-93 (International Technology Corporation, (July 1994, table 4-1A and 4-1B). The relatively low TCE concentrations in wells 49BR, 16BR, and 42BR may indicate that the wells are on the eastern flank of the Site 1 contamination plume, or it may reflect contamination as a result of metal cleaning in building 21 and possible underground storage of TCE.

TCE was undetected in wells 6BR, 13BR, 39BR, and 42BR in 1997. TCE was not detected in 1993 in wells 6BR and 13BR (International Technology Corporation, (July 1994, table 4-1A and 4-1B). Wells 39BR and 42BR were sampled only once.

Site 1: Brine-Handling Area

DNAPL TCE spilled or leaked onto the ground and dissolved TCE flowed into ditches at Site 1. The TCE infiltrated downward to below the water table resulting in DNAPL and dissolved TCE contamination. To evaluate the extent of possible DNAPL and dissolved TCE at Site 1, water samples from bedrock monitoring wells were collected and analyzed during June 1997. Concentrations of TCE are plotted in map view (figs. 69 to 71) and in section view (figs. 77 to 79) for the two scenarios.

Scenario 1 assumes that DNAPL TCE exists from land surface to a depth greater than 200 ft below land surface. Scenario 2 assumes that DNAPL TCE does not exist at depths greater than 100 ft below land surface. For both scenarios, the map view for TCE concentrations at land surface (fig. 69) and at 100 ft below land surface (fig. 70) are essentially identical. However, the interpretation of TCE concentrations at a depth of 200 ft below land surface for scenario 1 (fig. 71a) is significantly higher than the interpretation for scenario 2 (fig. 71b). Correspondingly, the interpretation for the section view F, G, and H for Scenario 1 (figs. 77a, 78a, and 79a) and Scenario 2 (figs. 77b, 78b, and 79b) are nearly identical to a depth of 100 ft below land surface but are significantly higher at depths greater than 100 ft below land surface. Figures 77a, 78a, and 79a show open contours at depths greater that 100 ft below land surface and potential DNAPL TCE in a zone between the 10,000-µg/L contours at depth greater than 200 ft below land surface.

Scenario 1: DNAPL TCE at depths greater than 250 feet

DNAPL TCE from land surface sank into the bedrock aquifer below Site 1 and moved downward driven by gravity and density differences. The DNAPL TCE flowpaths were in the more permeable shallow-dipping water-bearing zones and near vertical partings. In the water-bearing zones, the DNAPL TCE flowed in the downdip direction of N20°W. In places where the DNAPL TCE intercepted a vertical parting, it would flow vertically downward. Thus, the DNAPL TCE would ultimately flow downward and northwestward. The only thing that would stop the flow of DNAPL TCE was the closure of fractures with depth. Most fractures are closed at a depth of 500 ft below land surface, and more likely, most are closed by 300 ft below land surface.

DNAPL TCE flow direction was essentially unaffected by the regional hydraulic gradient and the ground-water-flow direction.The result of Scenario 1 is a plume that contains significant amounts of DNAPL TCE

at a depth of 200 to 300 ft below land surface in bedding units L-15 to L-19 and about 100 ft north of the Site 1 surficial source area. The DNAPL TCE plume in Scenario 1 exists inside the 10,000-µg/L contour lines (figs. 71a and 77a, 78a, and 79a).

As stated earlier, DNAPL TCE has not been found in any well at the NAWC. The saturation limit of TCE in water is 1,100,000 µg/L. Results of laboratory and field tests at other contamination sites have shown that ground-water samples that contain TCE concentrations in excess of 22,000 µg/L, which is 2 percent of the saturation limit, may indicate that DNAPL TCE is near the sampling site (Chappell, 1993). Based on these data, the following five wells may have DNAPL TCE near the screen interval: wells 30BR and 38BR, Section F (fig. 77a); wells 7BR and 24BR, Section G (fig. 78a); and well 36BR, Section H (fig. 79a). Collectively, these wells are screened in bedding units L-16 to L-19. Presently, there are no wells with screens directly below the wells 30BR, 38BR, 24BR, and 36BR and in bedding units L-15 to L-17. In summary, it is interpreted that DNAPL TCE may be present in fractures and partings below these wells.

Dissolved TCE was detected in 21 of 23 bedrock wells that were sampled north of the fault along sections F, G, and H (figs. 77a, 78a, and 79a). TCE concentrations in these 21 bedrock wells ranged from 18 to 83,000 µg/L. TCE was detected in one of three bedrock wells south of the fault in the Site 1 area.

Wells 45BR and 46BR were installed in 1997 to determine how far north the dissolved TCE plume moved in bedding units L-18 and L-19. TCE concentrations in wells 45BR and 46BR were 960 and 1,000 µg/L respectively in 1997. These concentrations indicate that dissolved TCE has moved north of wells 45BR and 46BR in bedding units L-18 and L-19 and also indicate that DNAPL TCE has not moved north of these wells. Drilling additional wells into bedding units L-16 to L-19 north of well 45BR and 46BR may be considered if it is decided to map the precise location of the northern limit of the dissolved TCE plume.

Wells 40BR and 45BR were installed to determine how far west the dissolved TCE plume moved in bedding units L-18 and L-19. Concentrations in wells 40BR and 45BR were 450 and 910 µg/L, respectively in 1997. These values indicate that dissolved TCE but not DNAPL TCE has moved west of these wells in these bedding units. Drilling additional wells into bedding units L-16 to L-19 west of wells 40BR and 45BR may be considered to determine the concentration of TCE and the effect of ground-water levels near the head-waters of the West Branch of Gold Run.

The southern extent of the TCE plume is limited by the fault. A TCE concentration of 31 µg/L measured in a water sample from well 22BR is the only site with TCE on the south side of the fault in the Site 1 area. The TCE concentrations from well 22BR were 18 to 85 µg/L during 12 sampling events in 1995 and 10 to 16 µg/L during 4 sampling events in 1992-93. Well 22BR is within 20 ft west of a storm sewer outfall box. It is plausible that TCE contamination in this well is related to the TCE contamination in or around the storm sewer line. Wells 28BR and 35BR, also south of the fault in the Site 1 area, have produced water with undetected levels of TCE. Well 28BR was sampled twice in 1995 and showed undetected and 12 µg/L TCE concentrations. Well 35BR was sampled 12 times during 1995 and showed undetected TCE concentrations during 8 sampling events, estimated 2 to 3 µg/L during 3 sampling events, and 45 µg/L during 1 sampling event. It is interpreted that the concentration of 45 µg/L is a result of cross contamination while sampling the well.

Wells 41BR, 42BR, and 39BR were drilled in 1997 to determine the eastern extent of the TCE plume in bedding units L-19 and L-13 to L-14. TCE concentration in well 41BR

was 450 µg/L, and TCE was undetected in the other two wells. Water-quality data from well 41BR indicate that dissolved TCE has moved either from Site 1 in an eastward direction within bedding unit L-19 to this site or more likely from building 21 northward and downward in bedding unit L-19. Drilling additional wells into bedding units L-16 to L-19 east of well 41BR may be considered to further delineate the extent of the plume but that may not be possible because of existing buildings and service lines.

Scenario 2: No DNAPL TCE at depths greater than 100 feet

DNAPL TCE from land surface sank in to the bedrock aquifer below Site 1 and moved downward and northward much like that described in Scenario 1. The DNAPL TCE degraded, dissolved, adsorbed, and dispersed in the uppermost 100 ft of overburden and bedrock. As a result of this scenario DNAPL TCE did not move into the deeper part of the bedrock aquifer. The configuration of the contour lines at land surface and 100 feet below land surface are identical for Scenarios 1 and 2 (figs. 69 and 70). At a depth of 200 ft below land surface, the contour lines for Scenario 2 (fig. 71b) are much lower values than for Scenario 1. Sections F, G, and H show closed contours for depths greater than 100 ft below land surface for scenario 2 (figs. 77b, 78b, and 79b), whereas the sections show open contours for scenario 1 (figs. 77a, 78a, and 79a). Scenario 2 indicates that the maximum concentrations of TCE are located in the uppermost 100 ft of the bedding units L-16 to L-19.

Area West of Site 1

TCE concentrations in bedrock wells along section I west of Site 1 range from undetected to 450 µg/L. Ground-water-flow direction at the Site 1 area is westward. Dissolved TCE may have moved with the ground-water flow, and therefore, TCE concentrations may be high in bedding units L-15 to L-19 as shown along section I. However, the TCE concentration may have declined significantly as a result of natural attenuation and is at very low or undetected concentrations west of Site 1 contamination plume.

cis-1,2-Dichloroethylene (cis-DCE)

The U.S. Navy did not use cis-DCE as part of the routine operation at the NAWC. Therefore, in all likelihood, all cis-DCE in the aquifer results from biodegradation of dissolved TCE in reducing environments and abiotic degradation of dissolved TCE in oxidizing environments. cis-DCE concentrations are shown in maps and sections (figs. 81 to 92). Thirty-one of the 48 bedrock wells sampled during June 1997 show cis-DCE concentration above the detection limit of 1 µg/L. Five bedrock wells show cis-DCE concentrations that range from 11,000 to 52,000 µg/L, 4 wells show cis-DCE concentrations that range from 1,900 to 7,200 µg/L, 6 wells show cis-DCE concentrations that range from 120 to 800 µg/L, 16 wells show concentrations that range from 1 to 99 µg/L, and 17 wells show no detectable cis-DCE.

Site 3: Lagoon and Sludge Disposal Area

Water samples from bedrock wells in the Site 3 area showed cis-DCE concentrations that range from undetected to 33 µg/L during 1997. The higher concentrations were directly under the lagoon and the former sludge disposal area. Well 11BR showed cis-DCE concentrations of 26 µg/L (fig. 85), and wells 2BR and 51BR showed concentrations of 33 and 29 µg/L, respectively (fig. 84). Concentrations in well 11BR were 120 to 15 µg/L during 1992-93 and 16 to 26 µg/L in 1995. Concentrations in well 2BR were 18 to 45 µg/L in 1993. Well 5BR was sampled only once. Because ground-water flow in the Site 3 area is

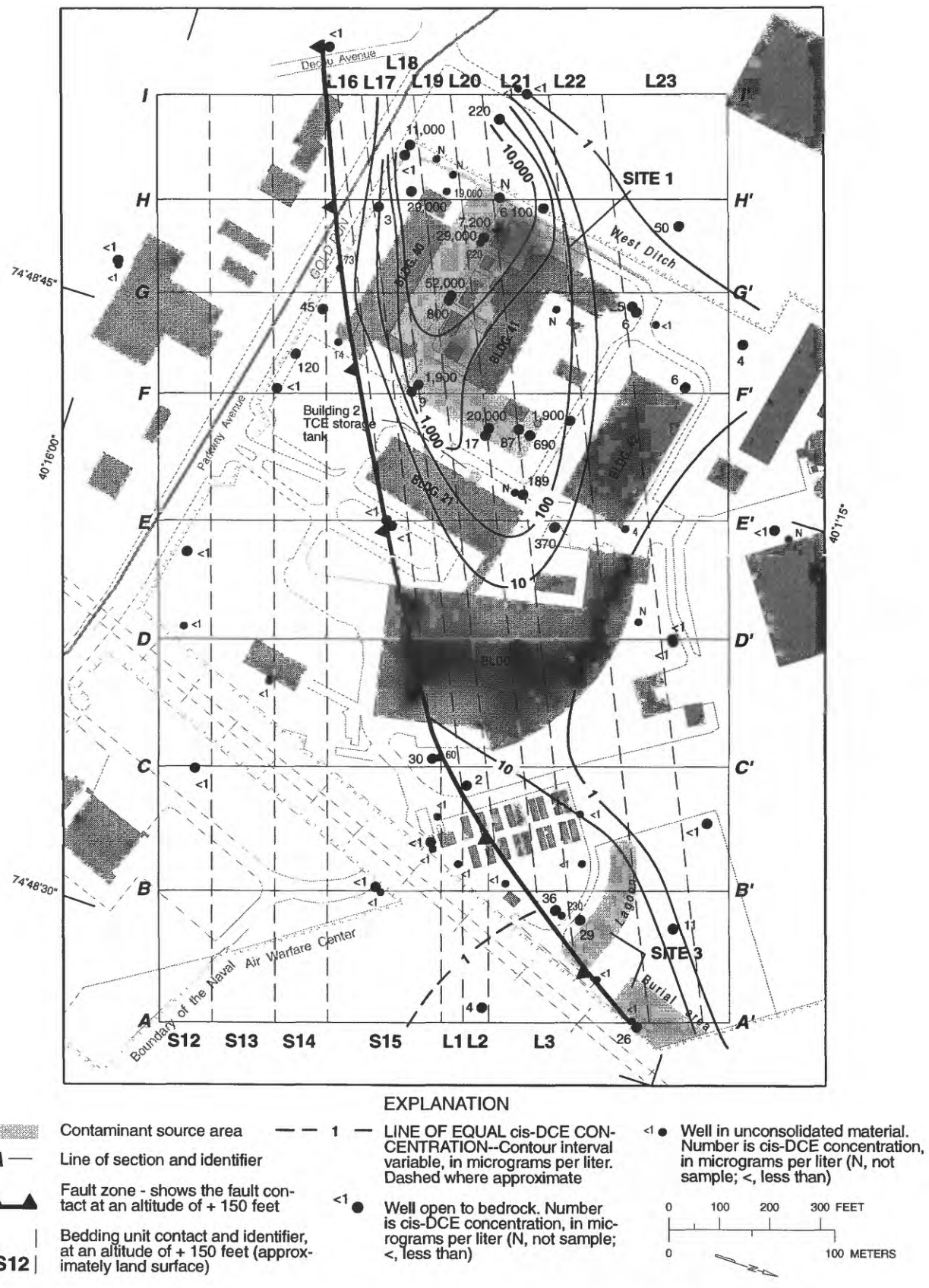

Figure 81. cis-DCE concentrations, in micrograms per liter, in water samples from bedrock and shallow wells, June 1997, and contours for top of bedrock (an altitude of + 150 feet and approximately land surface), Naval Air Warfare Center, West Trenton, N.J.

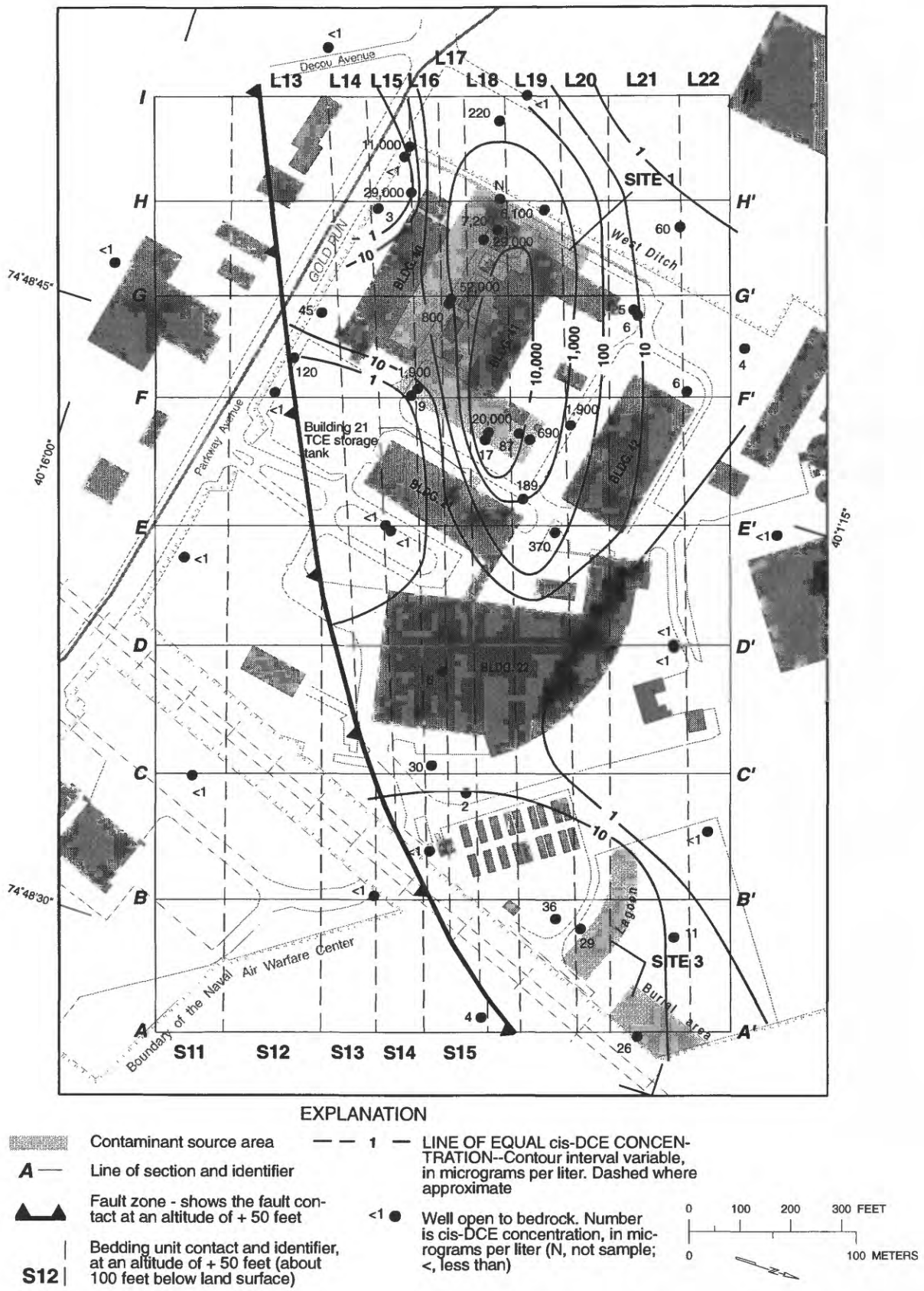

Figure 82. cis-DCE concentrations, in micrograms per liter, in water samples from bedrock, June 1997, and contours for an altitude of + 50 feet (about 100 feet below land surface), Naval Air Warfare Center, West Trenton, N.J.

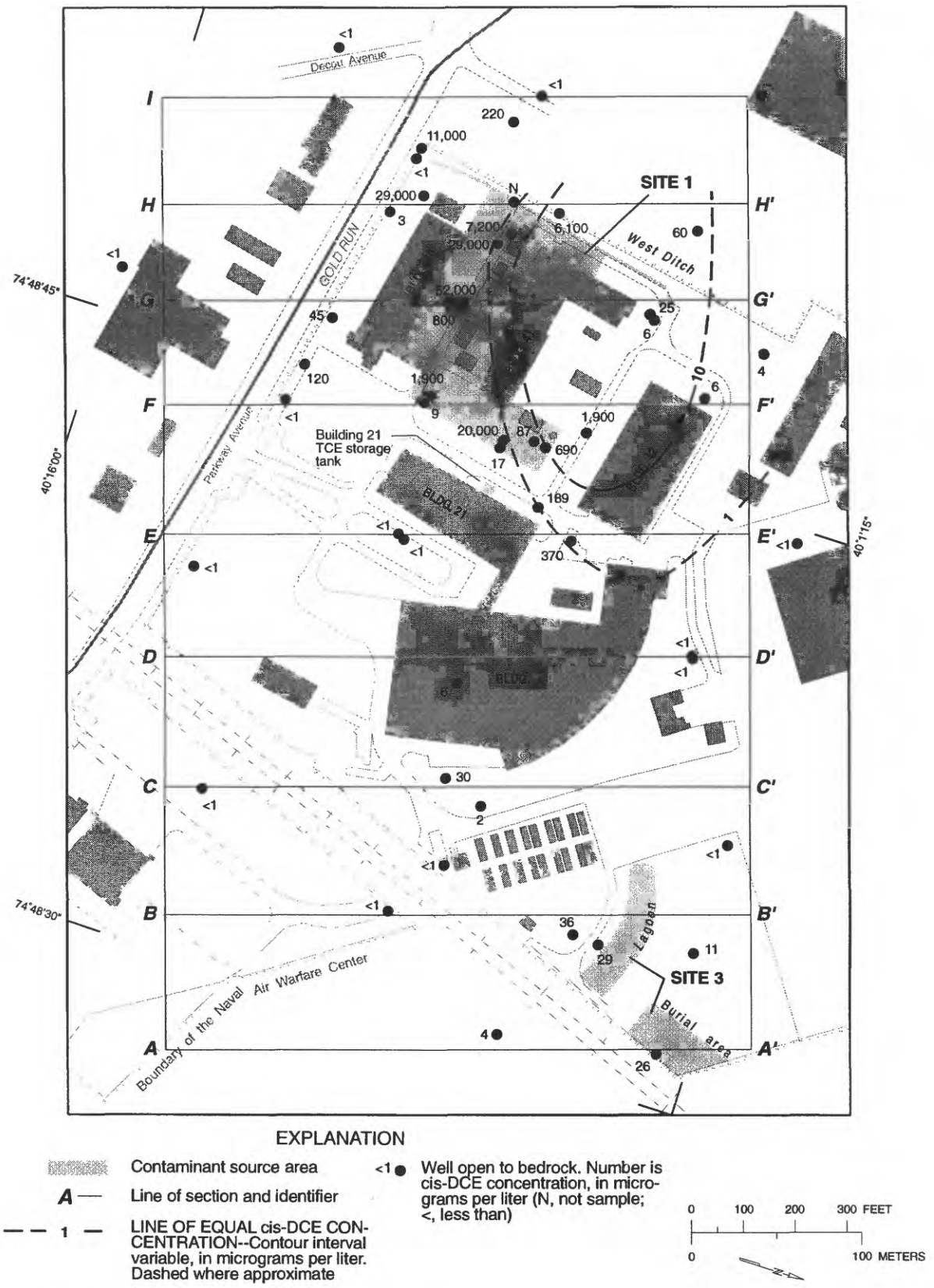

Figure 83. cis-DCE concentrations, in micrograms per liter, in water samples from bedrock wells, June 1997, and contours for an altitude of - 50 feet (about 200 feet below land surface), Naval Air Warfare Center, West Trenton, N.J.

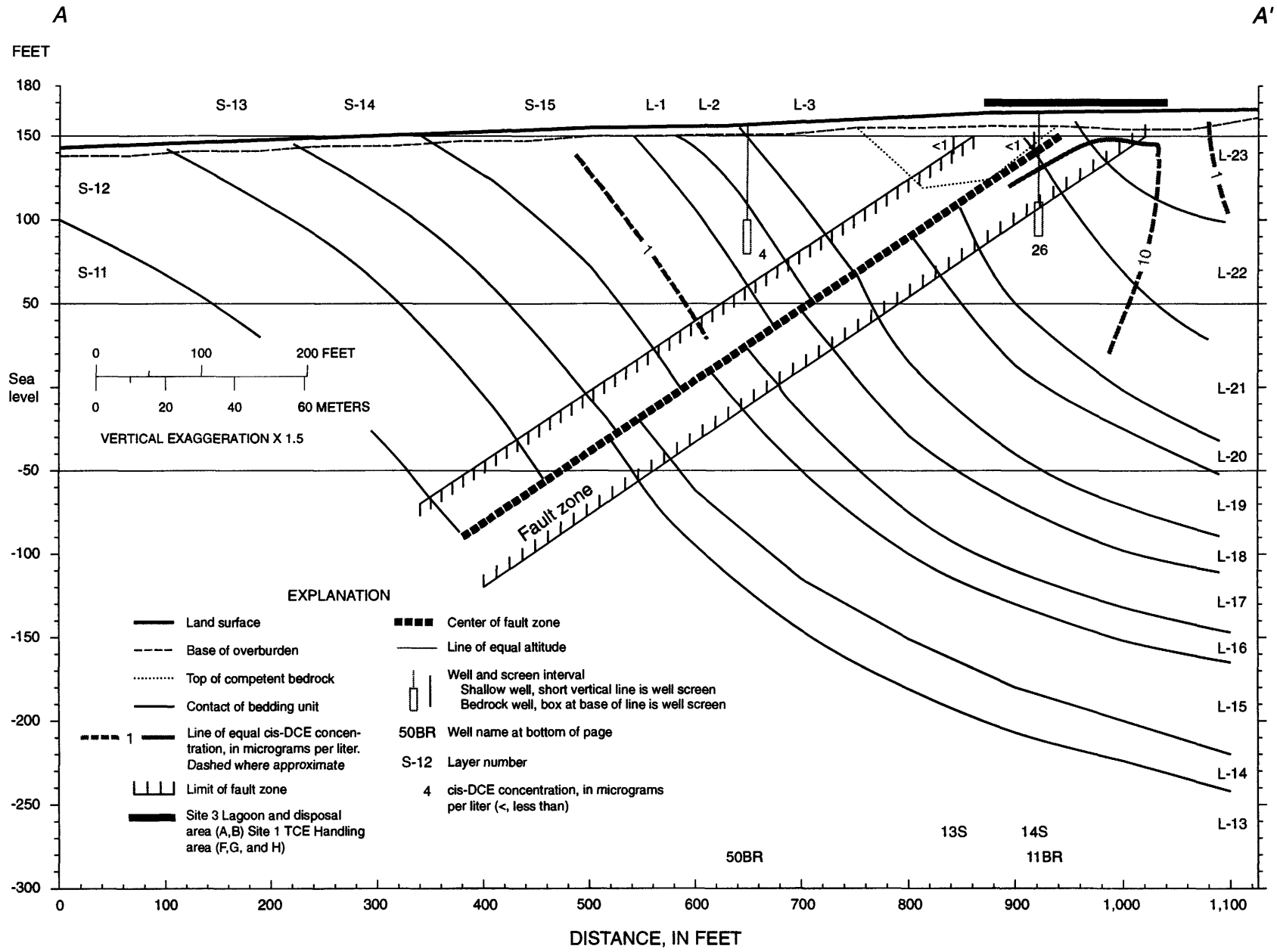

Figure 84. Section *A-A'* showing cis-DCE concentrations in water samples from bedrock and overburden wells, June 1997.

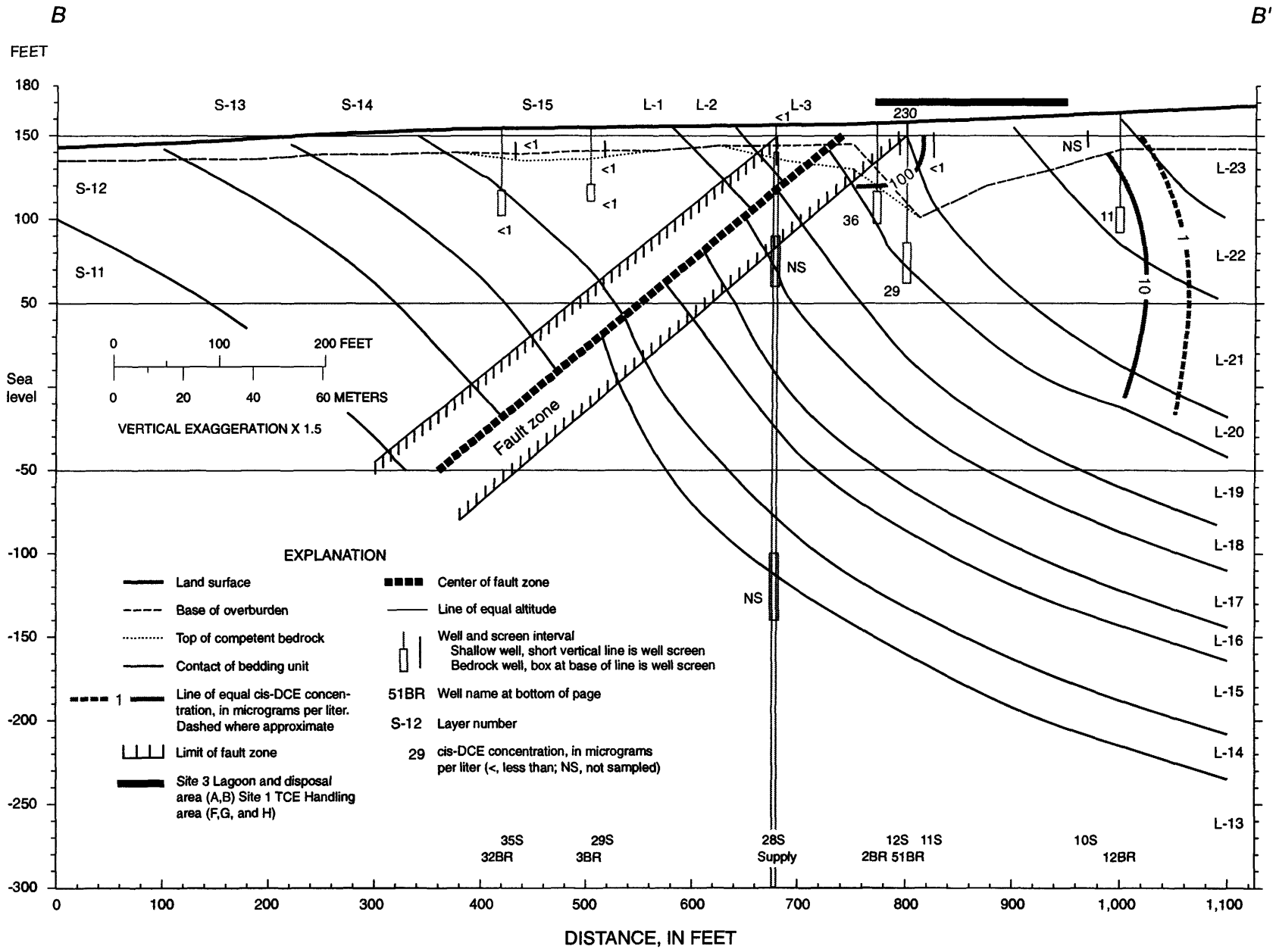

Figure 85. Section *B-B'* showing cis-DCE concentrations in water samples from bedrock wells, June 1997.

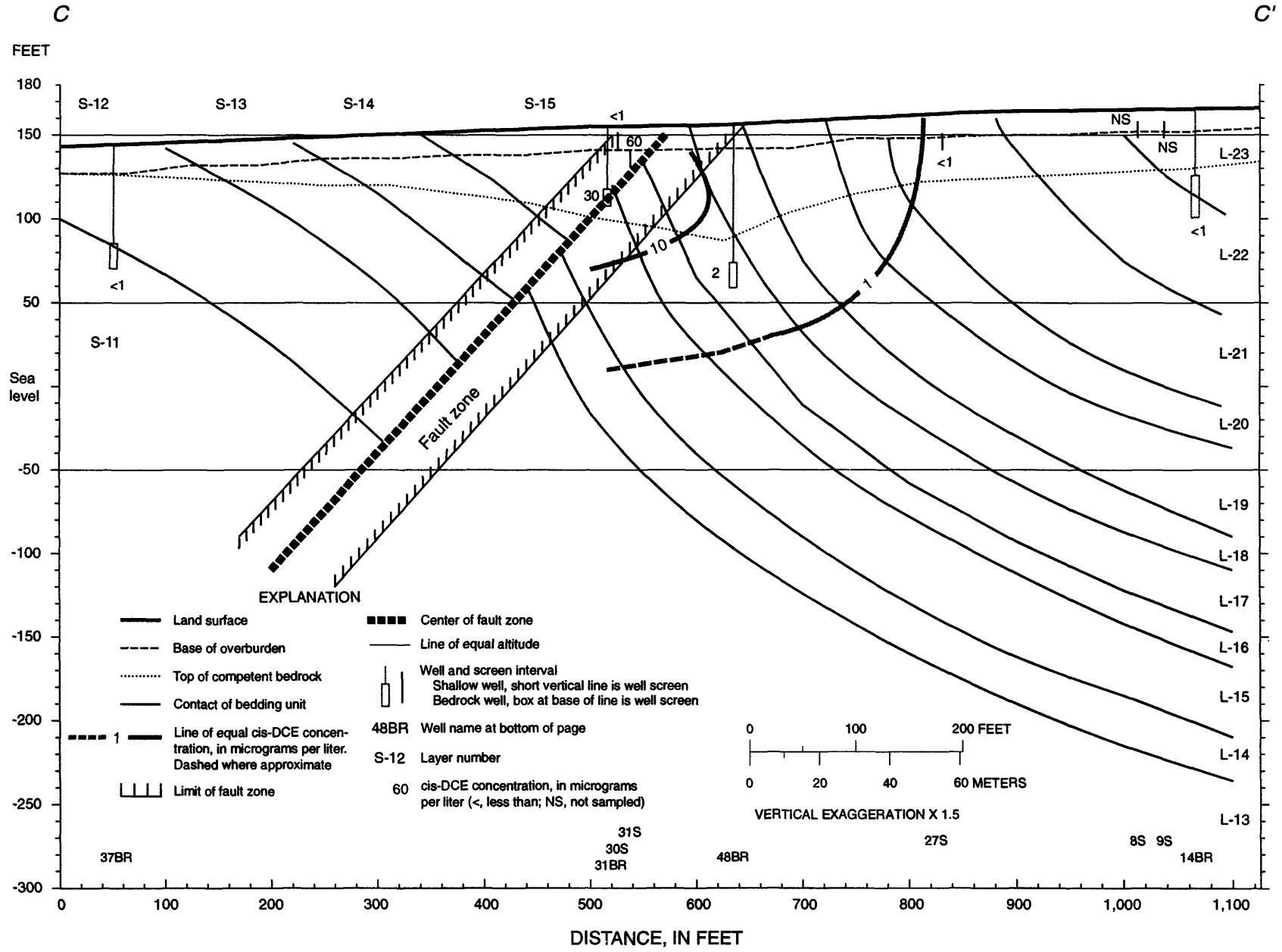

Figure 86. Section *C-C'* showing cis-DCE concentrations in water samples from bedrock wells, June 1997.

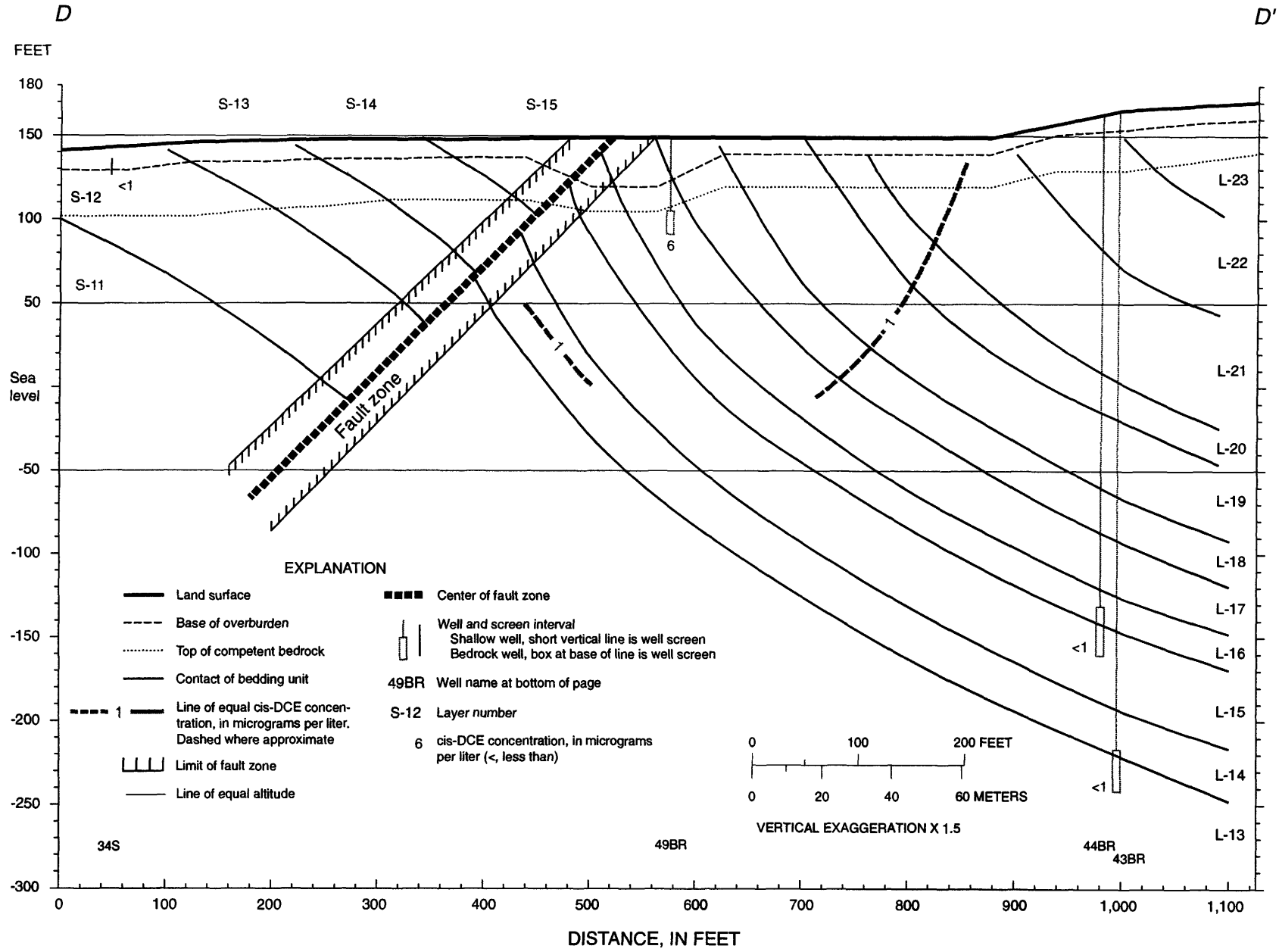

Figure 87. Section *D-D'* showing cis-DCE concentrations in water samples from bedrock wells, June 1997.

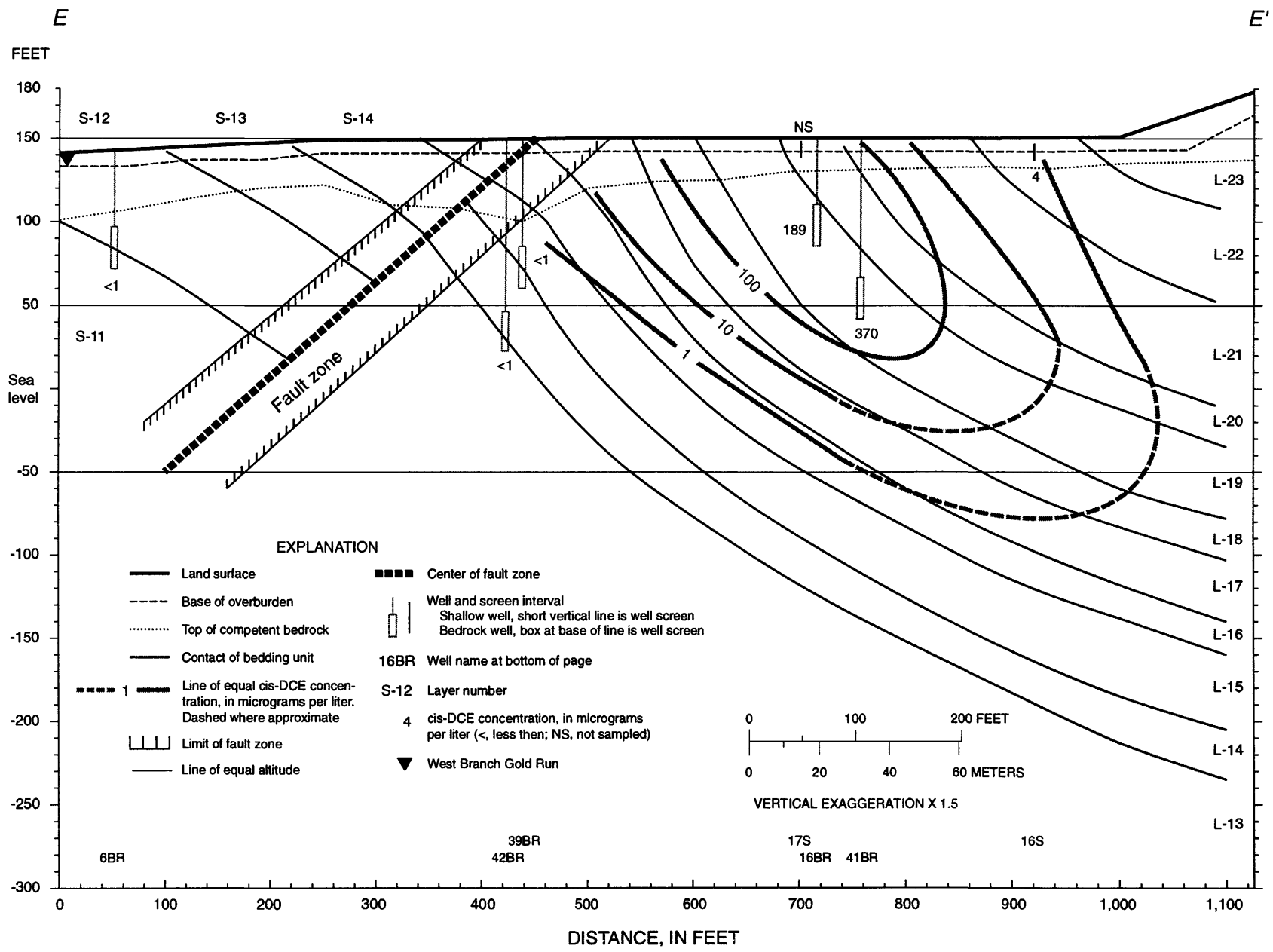

Figure 88. Section *E-E'* showing cis-DCE concentrations in water samples from bedrock wells, June 1997.

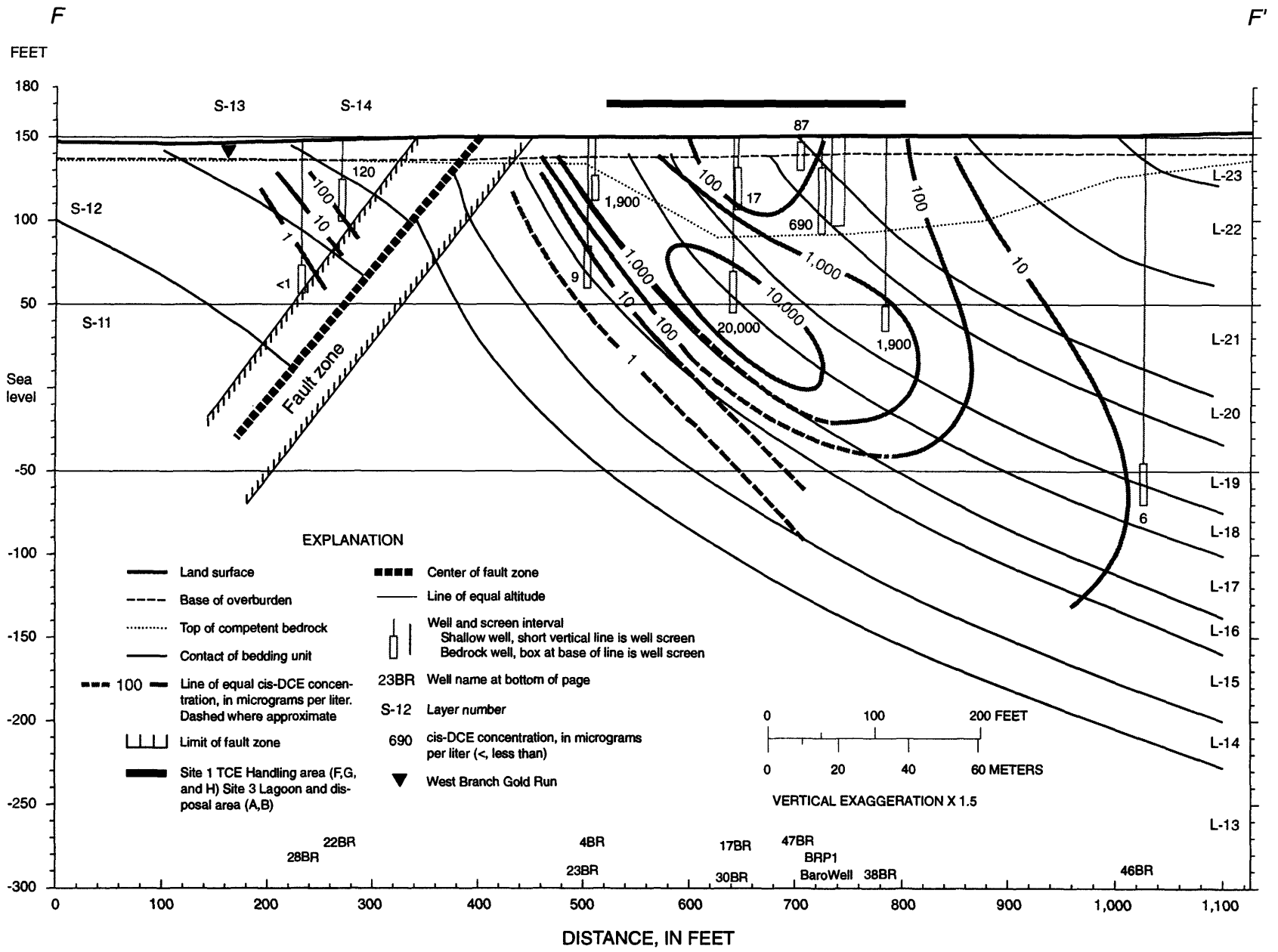

Figure 89. Section *F-F'* showing cis-DCE concentrations in water samples from bedrock wells, June 1997.

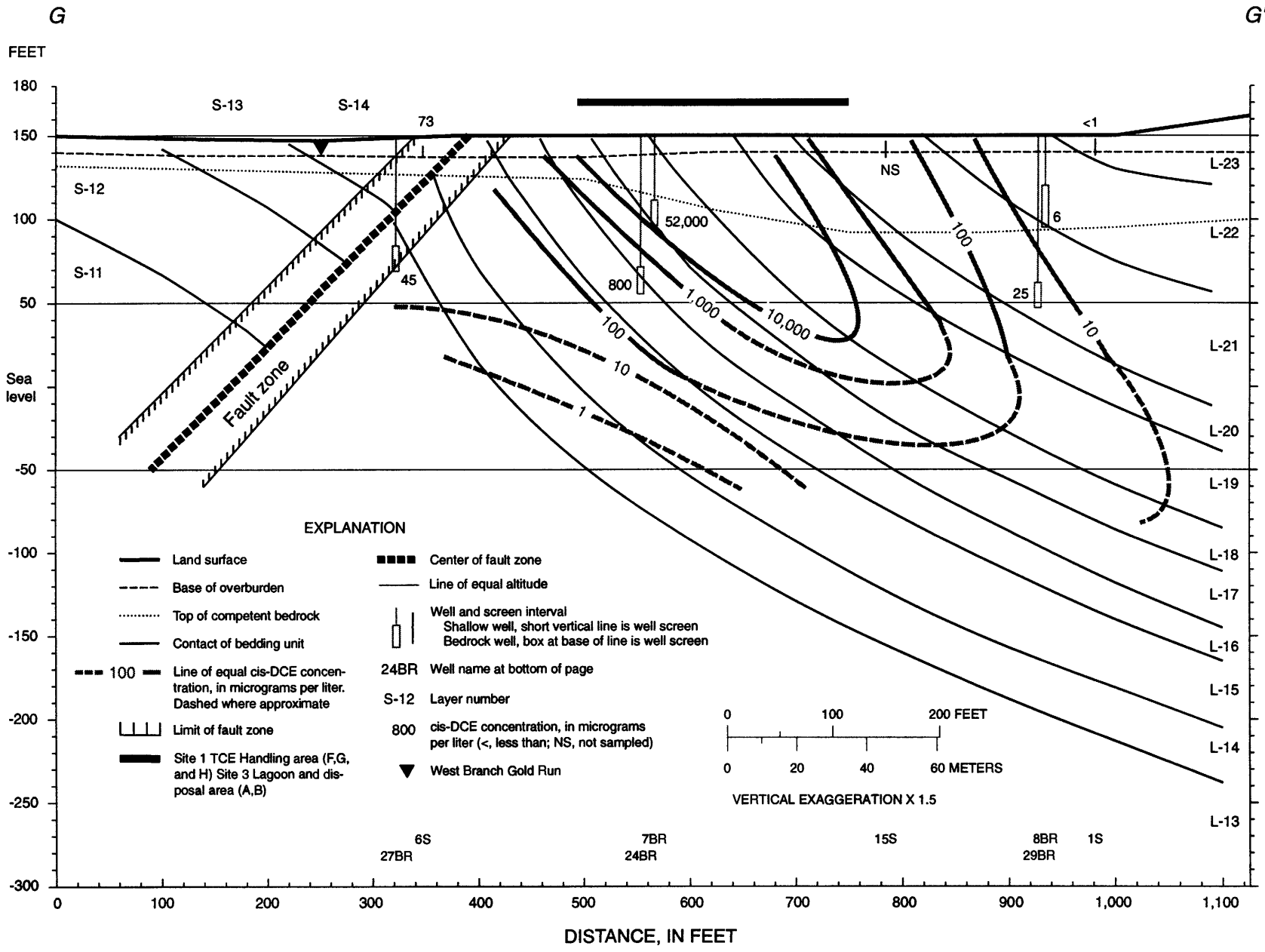

Figure 90. Section *G-G'* showing cis-DCE concentrations in water samples from bedrock wells, June 1997.

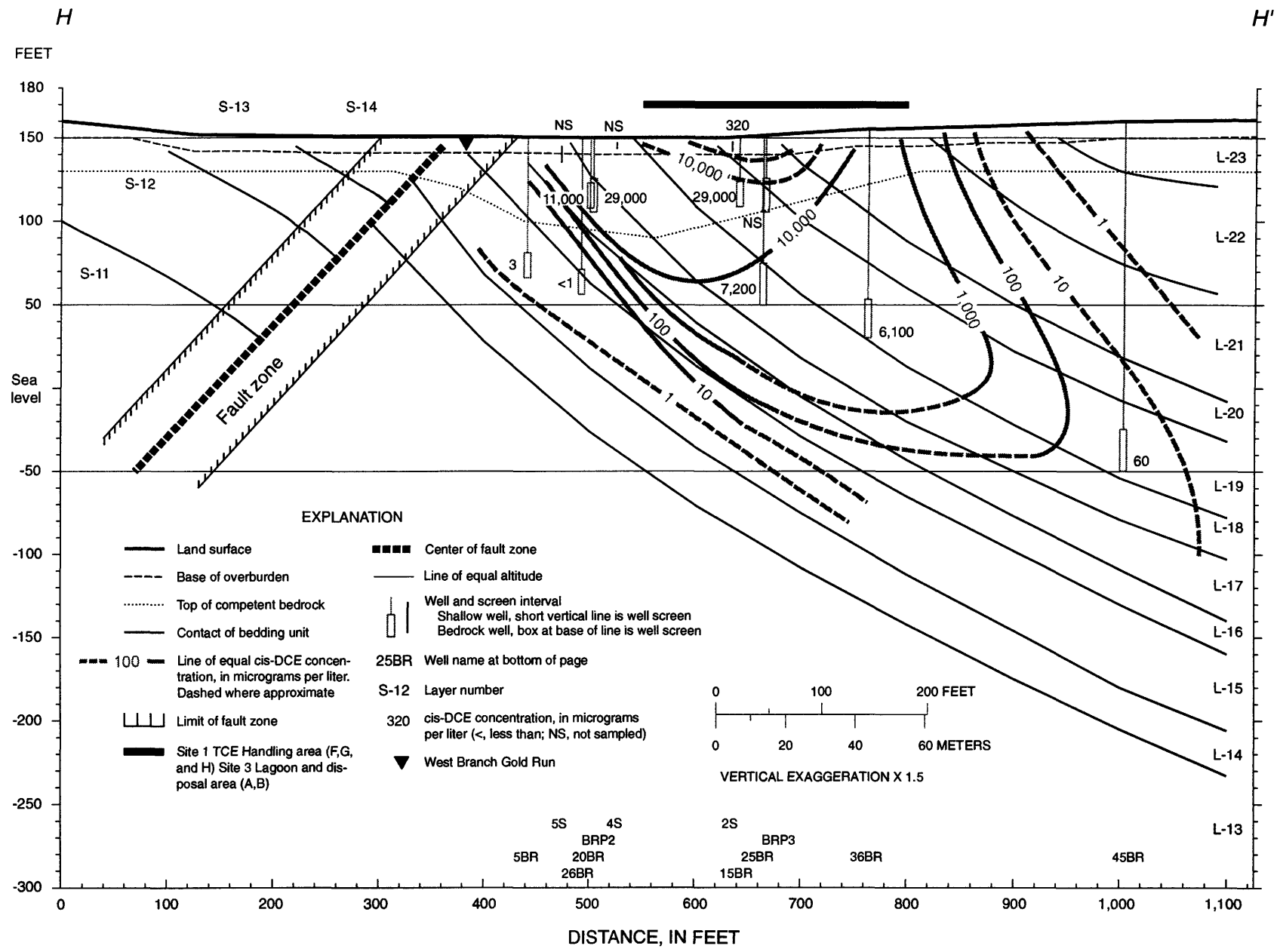

Figure 91. Section *H-H'* showing cis-DCE concentrations in water samples from bedrock wells, June 1997.

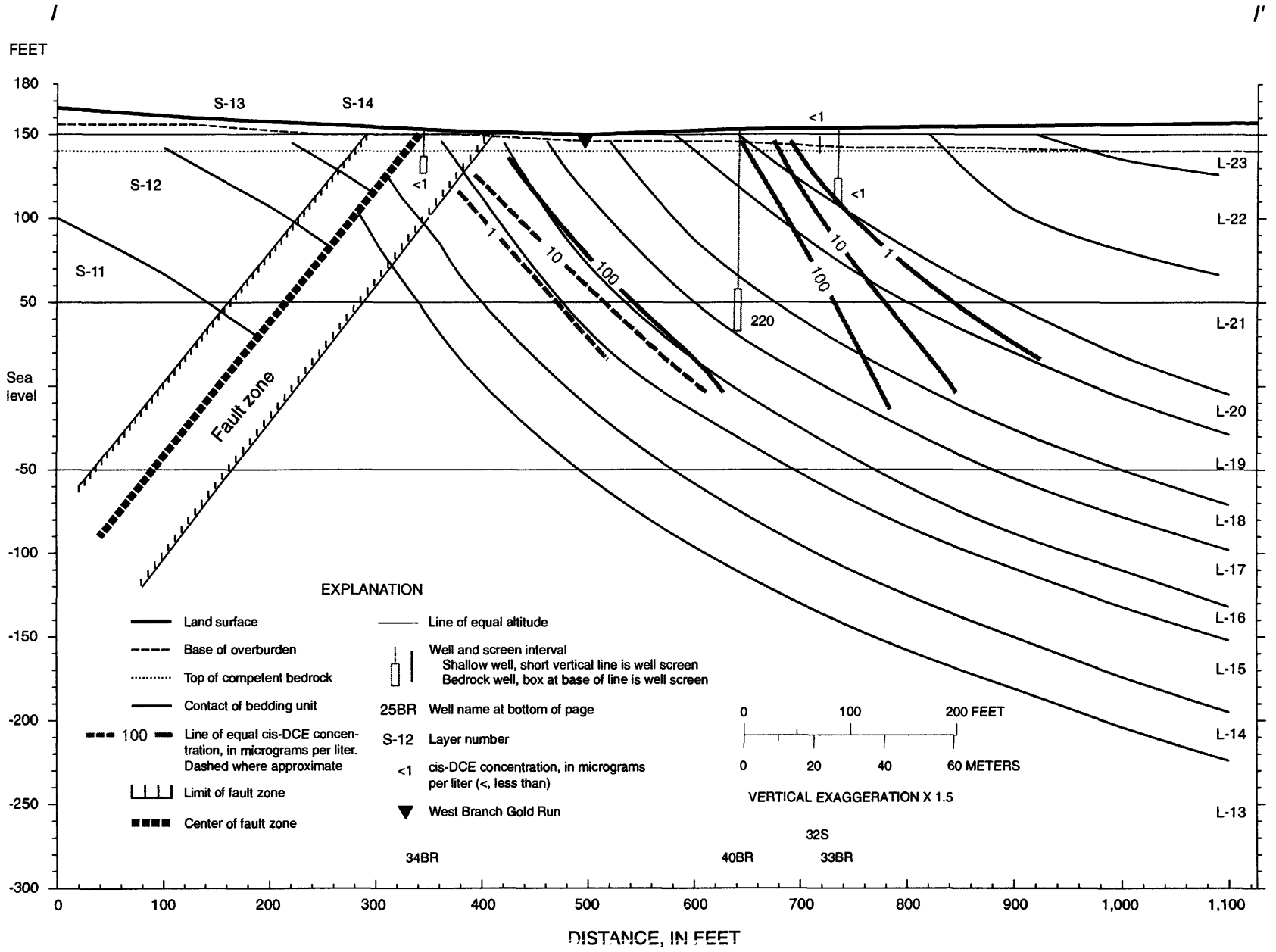

Figure 92. Section *I-I'* showing cis-DCE concentrations in water samples from bedrock wells, June 1997.

from east to west along the north side of the fault, well 31BR is downgradient from the lagoon and it shows a cis-DCE concentration of 30 µg/L. cis-DCE concentration in well 31BR was 8 µg/L in 1993.

Area between Site 3 and Site 1

Concentration of cis-DCE in wells 16BR and 41BR in the area between site 3 and site 1 (section D and E) were 189 and 330 µg/L, respectively, in 1997. cis-DCE concentrations in well 16BR were 97 to 250 µg/L in three sampling events during 1993. These cis-DCE concentrations may indicate a relatively high degradation of TCE in bedding unit L-19.

Site 1: Brine-Handling Area

Concentrations of cis-DCE in the Site 1 area ranged from <10 to 52,000 µg/L. Water samples from five wells show cis-DCE concentrations greater than 11,000 µg/L and samples from four wells showed cis-DCE concentrations that range from 1,900 to 7,200 µg/L in 1997. These concentrations of cis-DCE indicate that TCE is biodegrading. The center of the cis-DCE plume as defined by the 10,000-µg/L contour line at land surface (fig. 81) has migrated from the Site 1 source area (fig. 2) about 200 ft southwestward. Ground water in the upper 100 ft of the Lockatong aquifer is believed to discharge into the West Branch of Gold Run north of the fault. Therefore, the cis-DCE contamination dissolved in the ground water also discharges into the stream.

Three wells south of the fault in the Site 1 area were sampled in 1997 for cis-DCE. Wells 35BR and 28BR showed <1 to 2 µg/L of cis-DCE during 1992-93, 1995, and 1997. Water samples from well 22BR showed cis-DCE concentrations of 132 µg/L in 1997 and concentrations of 10 to 16 µg/L in 1995. It is interpreted that the TCE at the site of well 22BR is being degraded to cis-DCE.

Area West of Site 1

There are insufficient data along Section I or in areas to the west of section I to confirm movement of TCE or cis-DCE onto the west side of the West Branch of Gold Run. Ground-water-flow direction and the movement of the cis-DCE plume is indicated by the southwestward shift of the center of the cis-DCE plume. Ground water moves much more slowly at depths greater than 100 ft below land surface than at land surface, and TCE biodegrades more slowly at depths greater than 100 ft below land surface than nearer to land surface. As a result, there is not much apparent movement of the center of the DC plume at 100 feet below land surface (fig. 82) when compared with TCE at the same depth (fig. 70). At a depth of 200 ft below land surface, the cis-DCE concentrations were less than 10 µg/L. Therefore, there is little TCE degradation to cis-DCE occurring at this depth.

Vinyl chloride (VC)

The U.S. Navy did not use VC as part of the routine operation at the NAWC. Therefore, in all likelihood, all VC in ground water is a product of biodegradation of cis-DCE in reducing environments and abiotic degradation in oxidizing environments. VC concentrations are shown in maps and sections (figs. 93 to 104). In 1997, water samples from 16 of the 48 bedrock wells contained VC concentrations greater than the detection limit. Water from well 20BR showed VC concentrations of 21,000 µg/L and wells 15BR, 26BR, and 7BR showed VC concentrations that range from 3,700 to 9,200 µg/L. Each of these four wells are screened within 50 ft of land surface; therefore, the conditions for degradation of cis-DCE to VC are interpreted to be most favorable at shallow depths at the NAWC. Five wells had VC concentrations from 10 to 1,000 µg/L, 7 wells had VC concentrations from 1 to 10 µg/L, and VC was undetected in 32 wells.

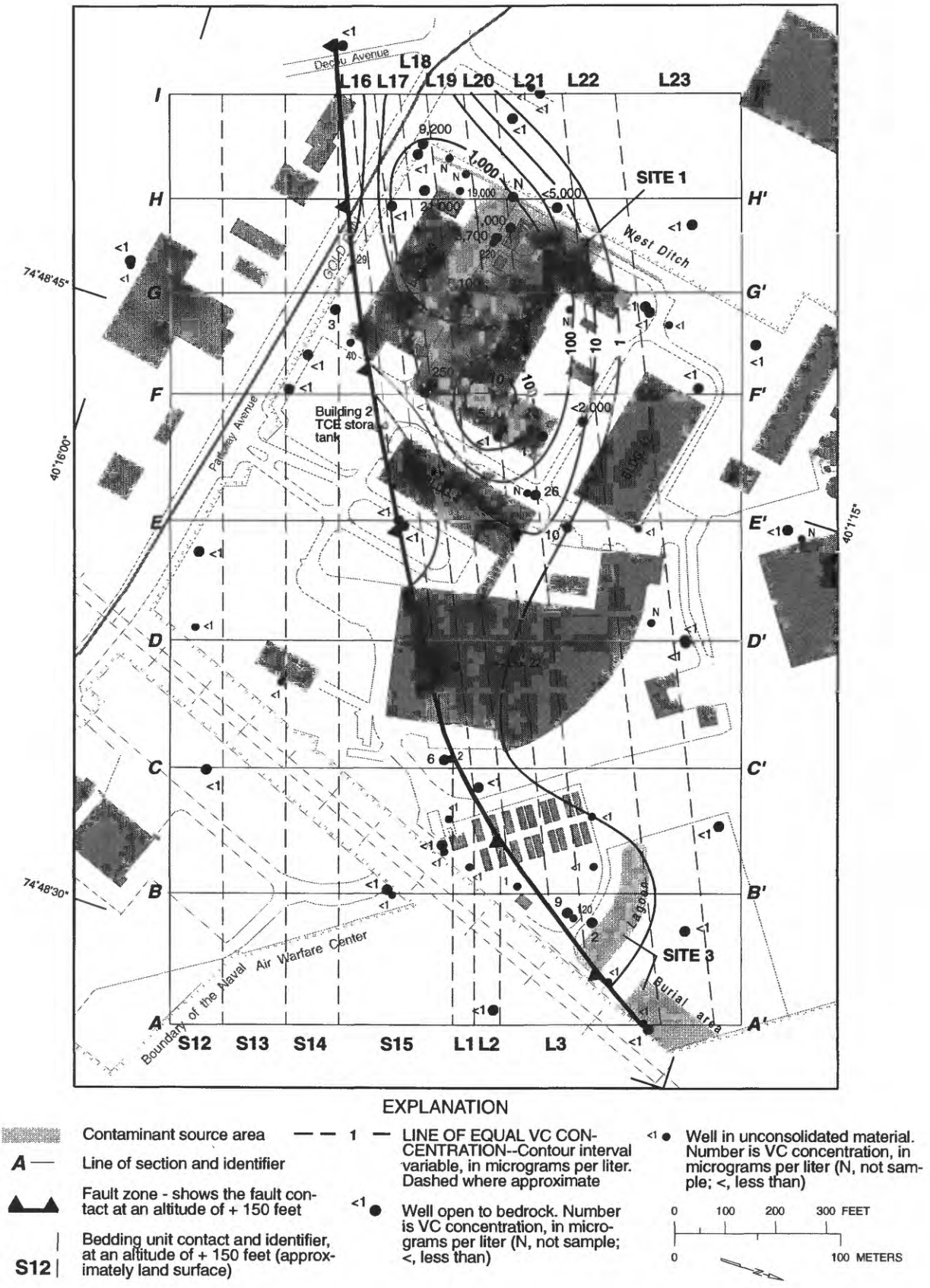

Figure 93. VC concentrations, in micrograms per liter, in water samples from bedrock and shallow wells, June 1997, and contours for top of bedrock (an altitude of + 150 feet and approximately land surface), Naval Air Warfare Center, West Trenton, N.J.

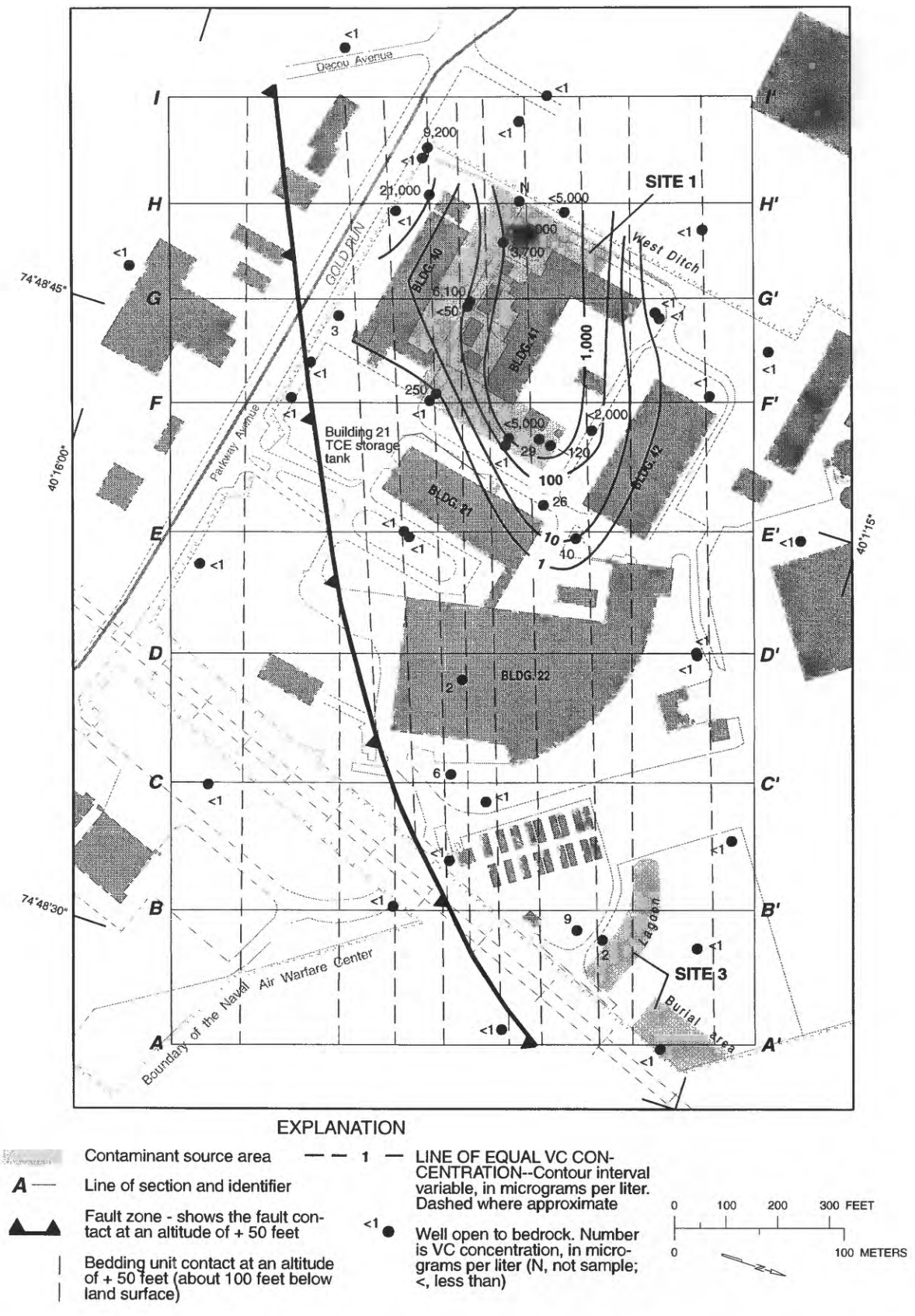

Figure 94. VC concentrations, in micrograms per liter, in water samples from bedrock, June 1997, and contours for an altitude of + 50 feet (about 100 feet below land surface), Naval Air Warfare Center, West Trenton, N.J.

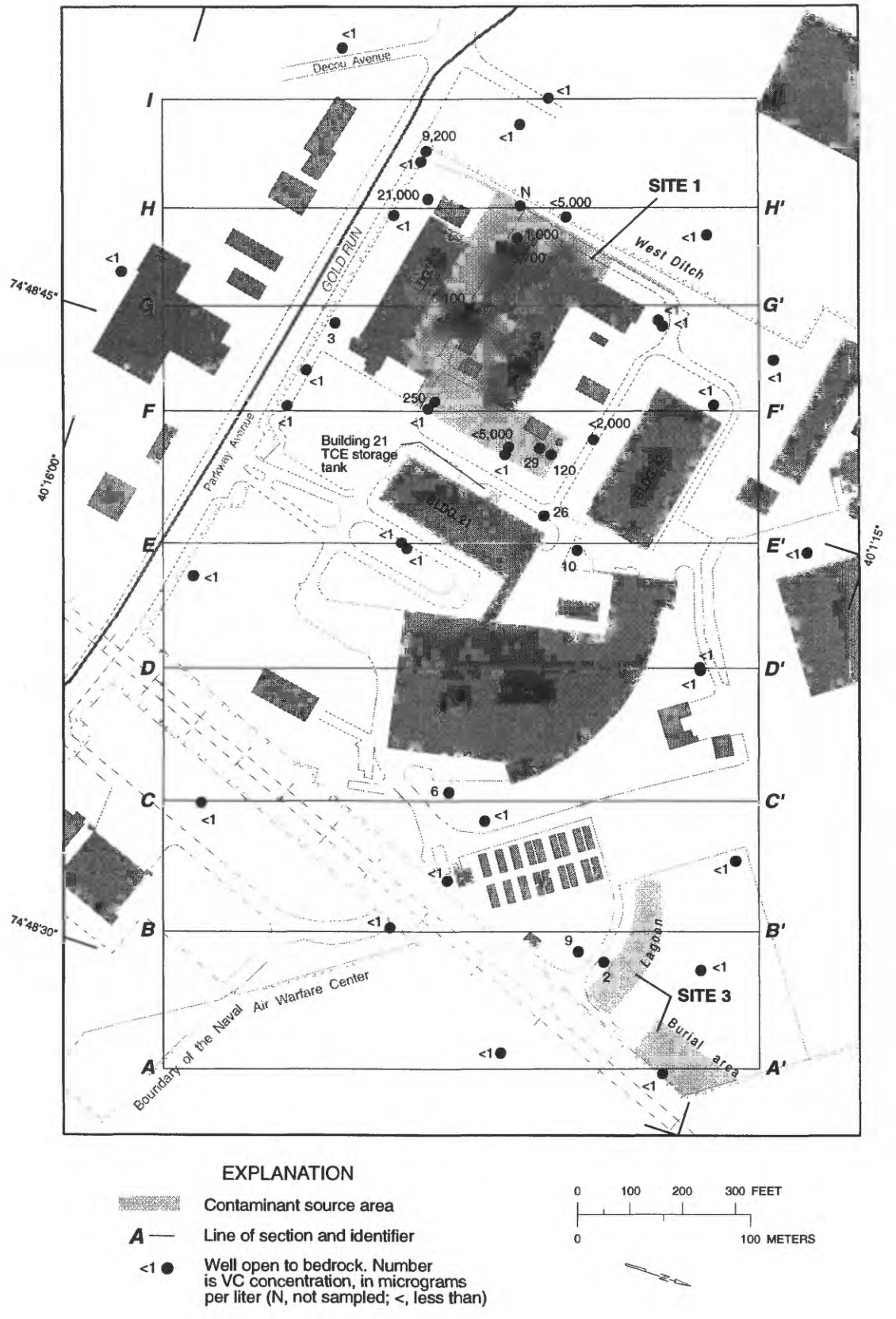

Figure 95. VC concentrations, in micrograms per liter, in water samples from bedrock wells, June 1997, and contours for an altitude of - 50 feet (about 200 feet below land surface), Naval Air Warfare Center, West Trenton, N.J.

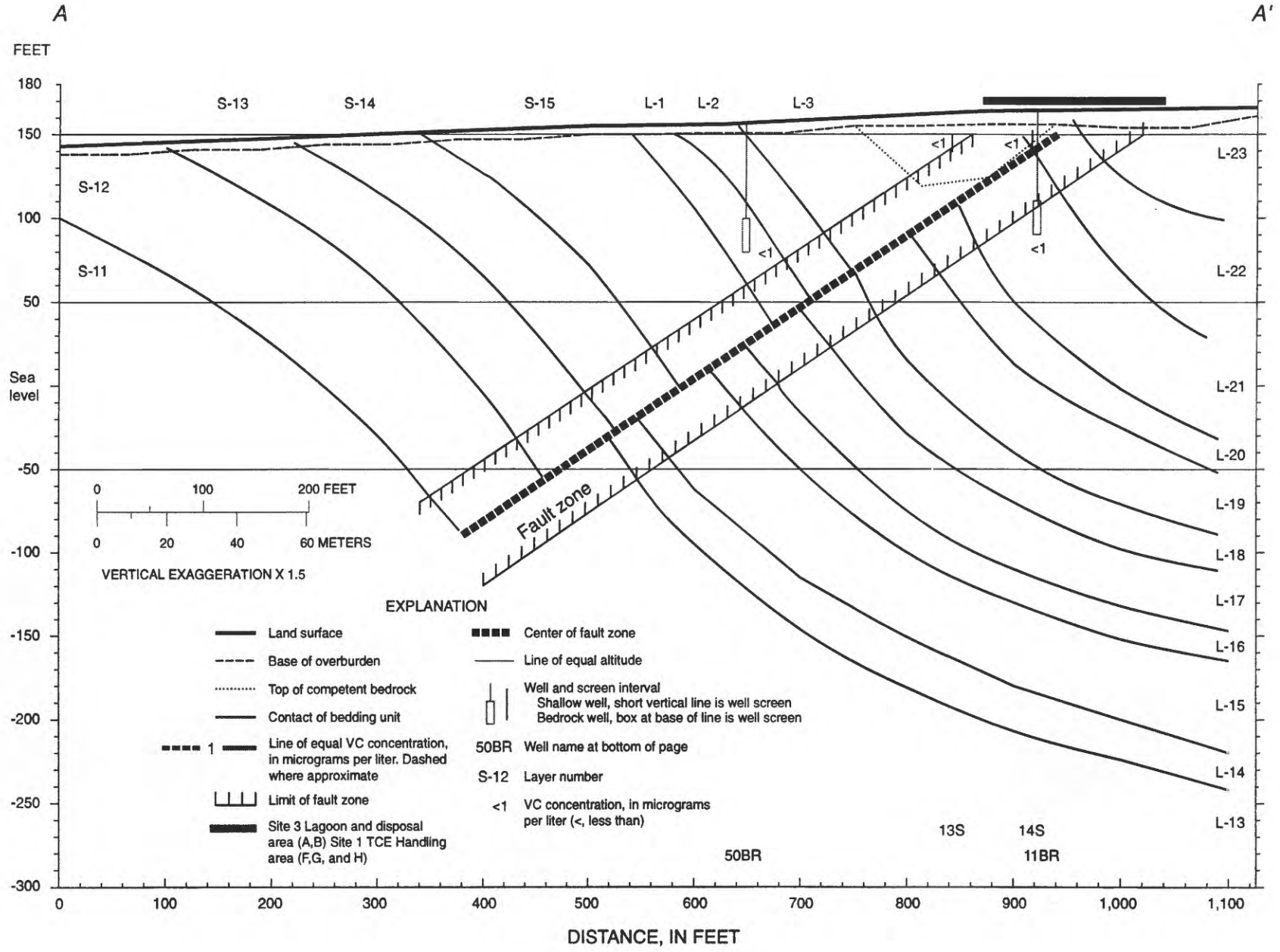

Figure 96. Section *A-A'* showing VC concentrations in water samples from bedrock and overburden wells, June 1997.

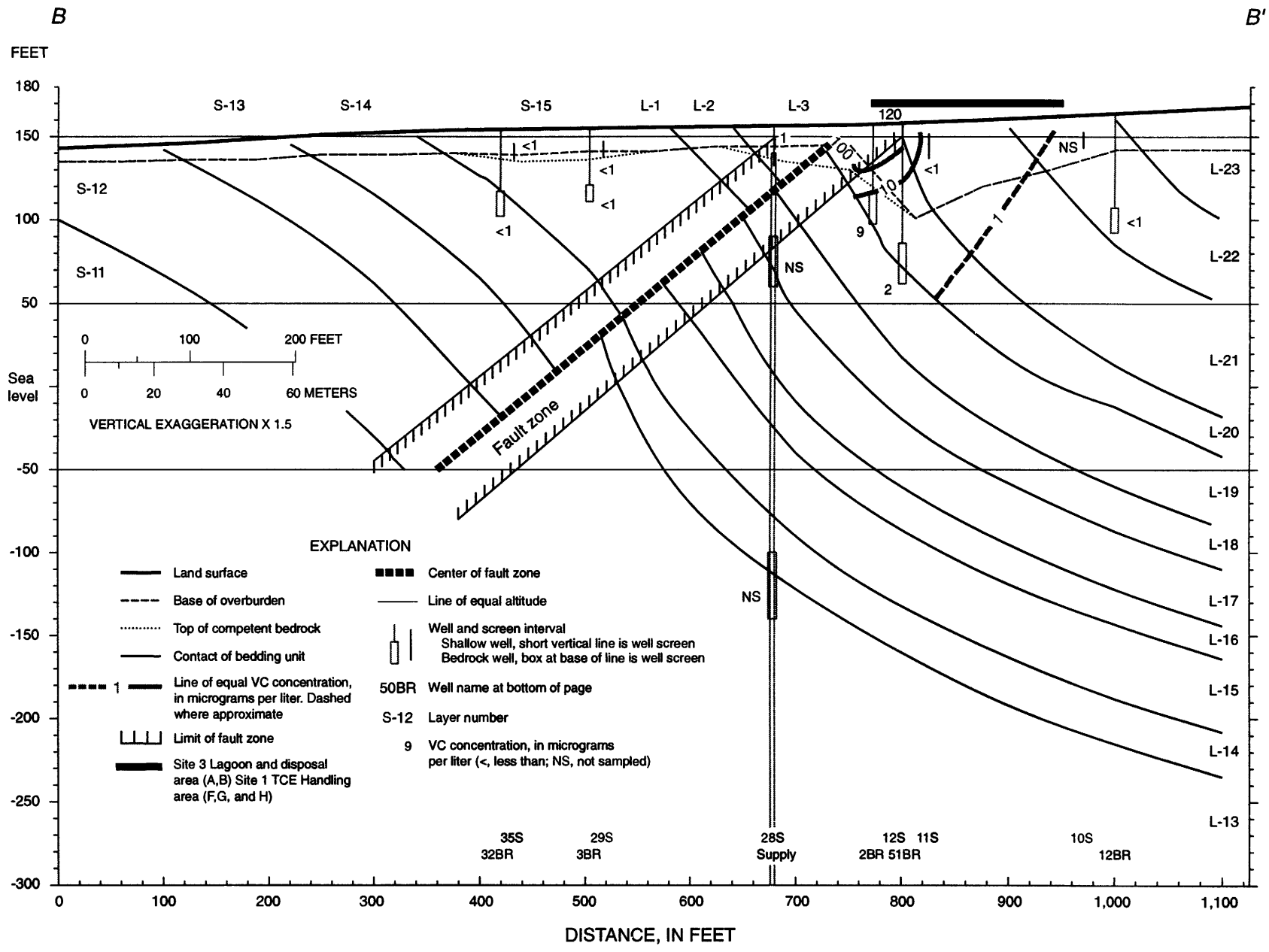

Figure 97. Section *B-B'* showing VC concentrations in water samples from bedrock wells, June 1997.

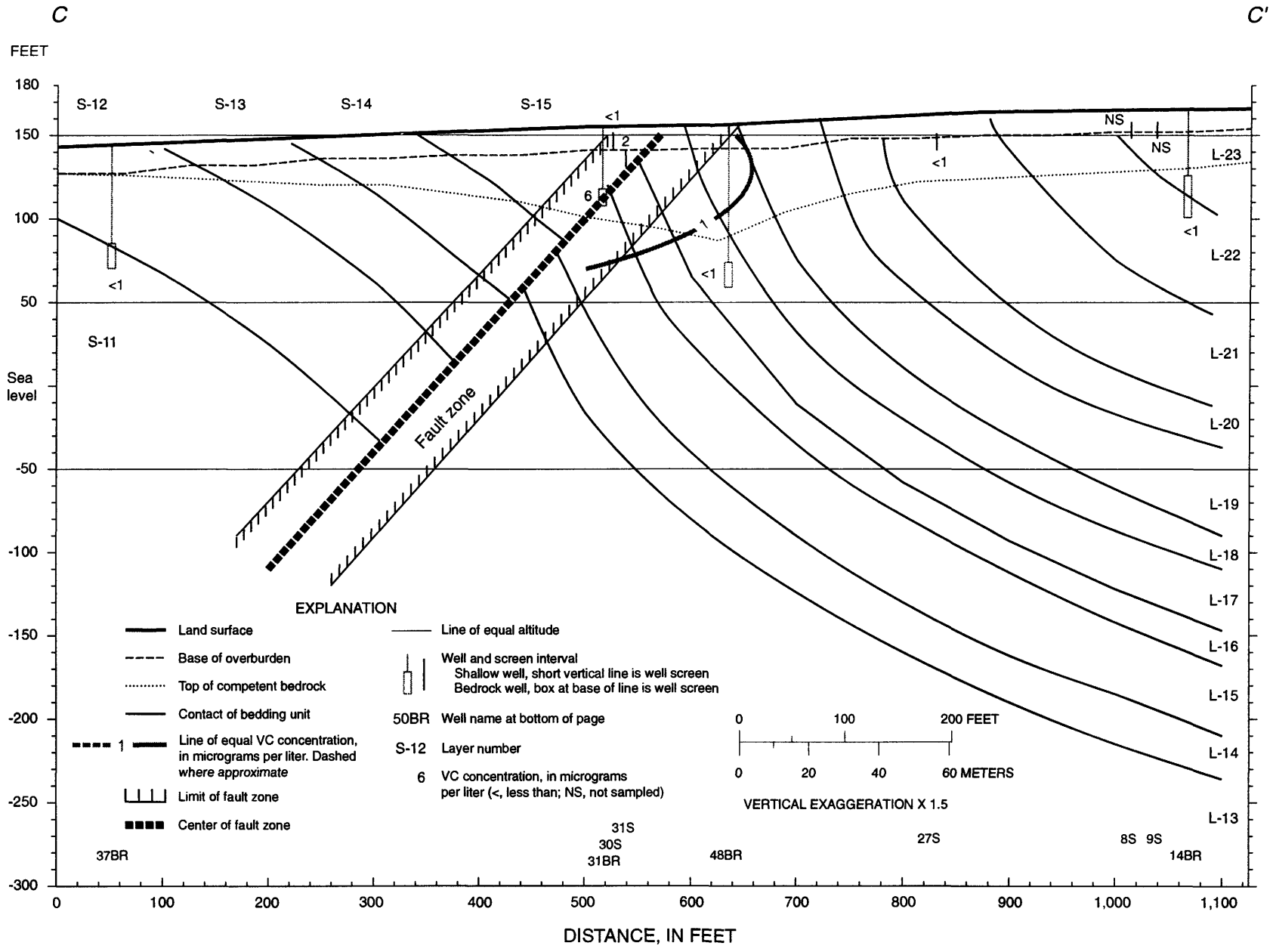

Figure 98. Section *C-C'* showing VC concentrations in water samples from bedrock wells, June 1997.

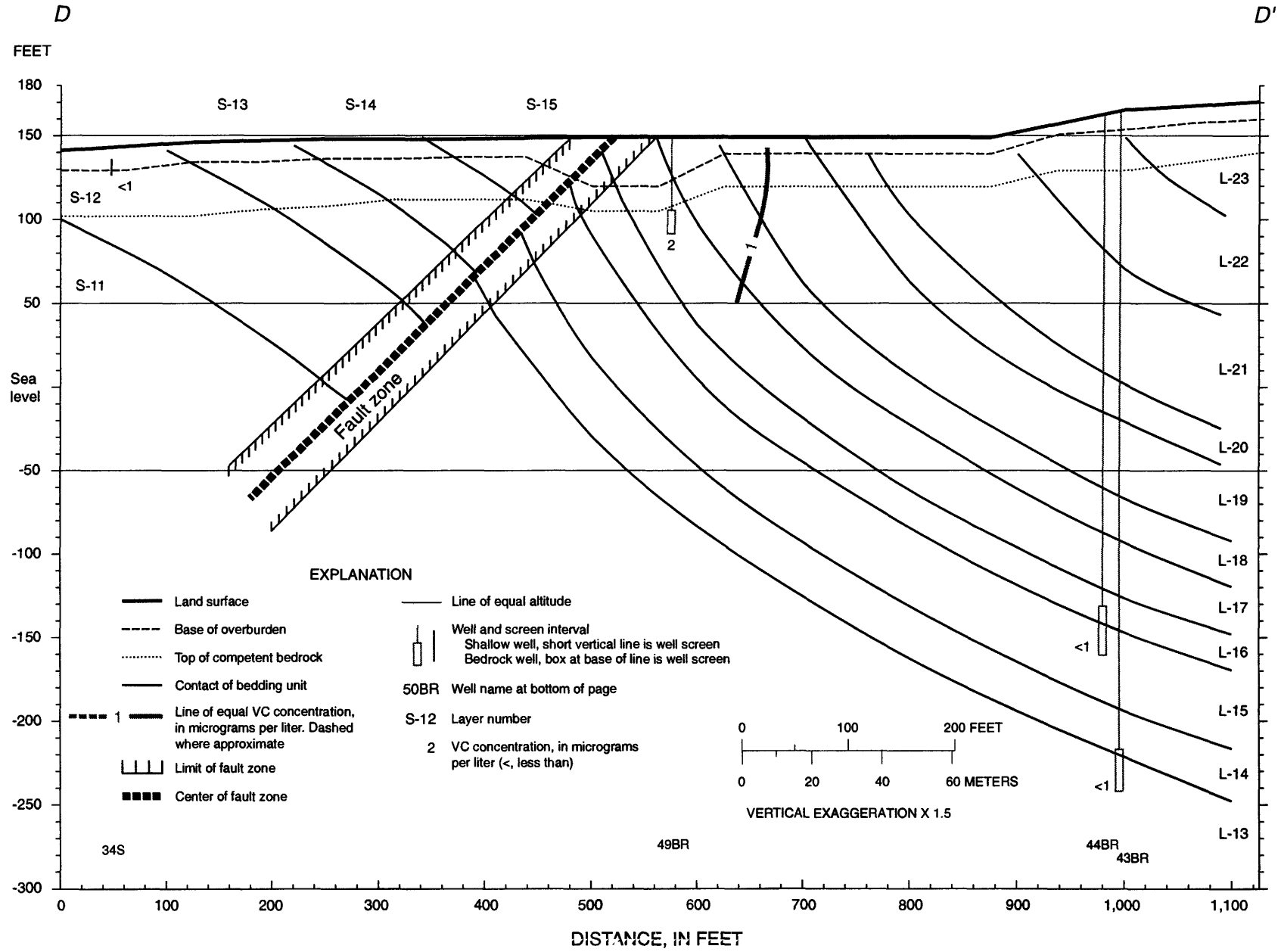

Figure 99. Section *D-D'* showing VC concentrations in water samples from bedrock wells, June 1997.

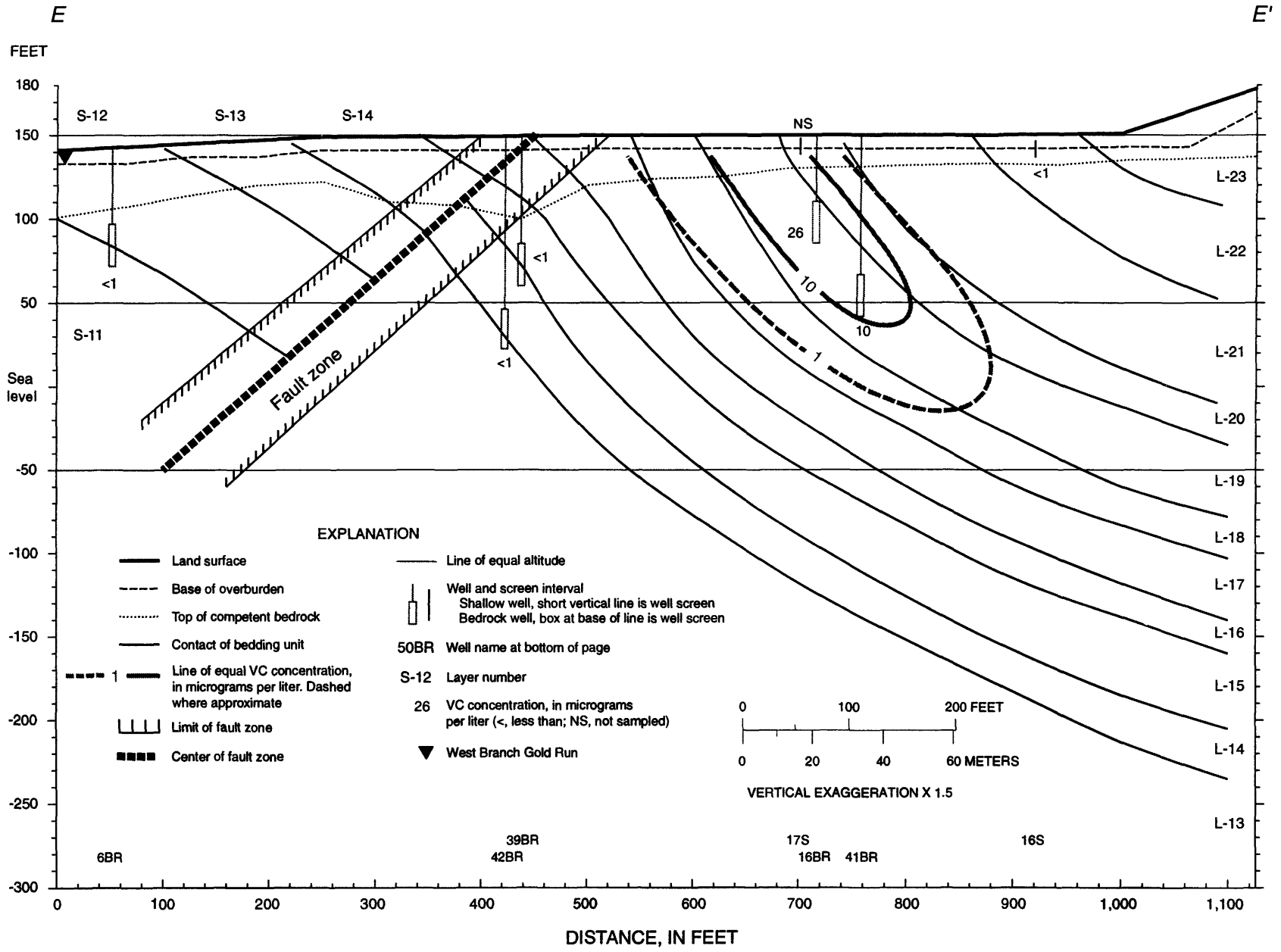

Figure 100. Section *E-E'* showing VC concentrations in water samples from bedrock wells, June 1997.

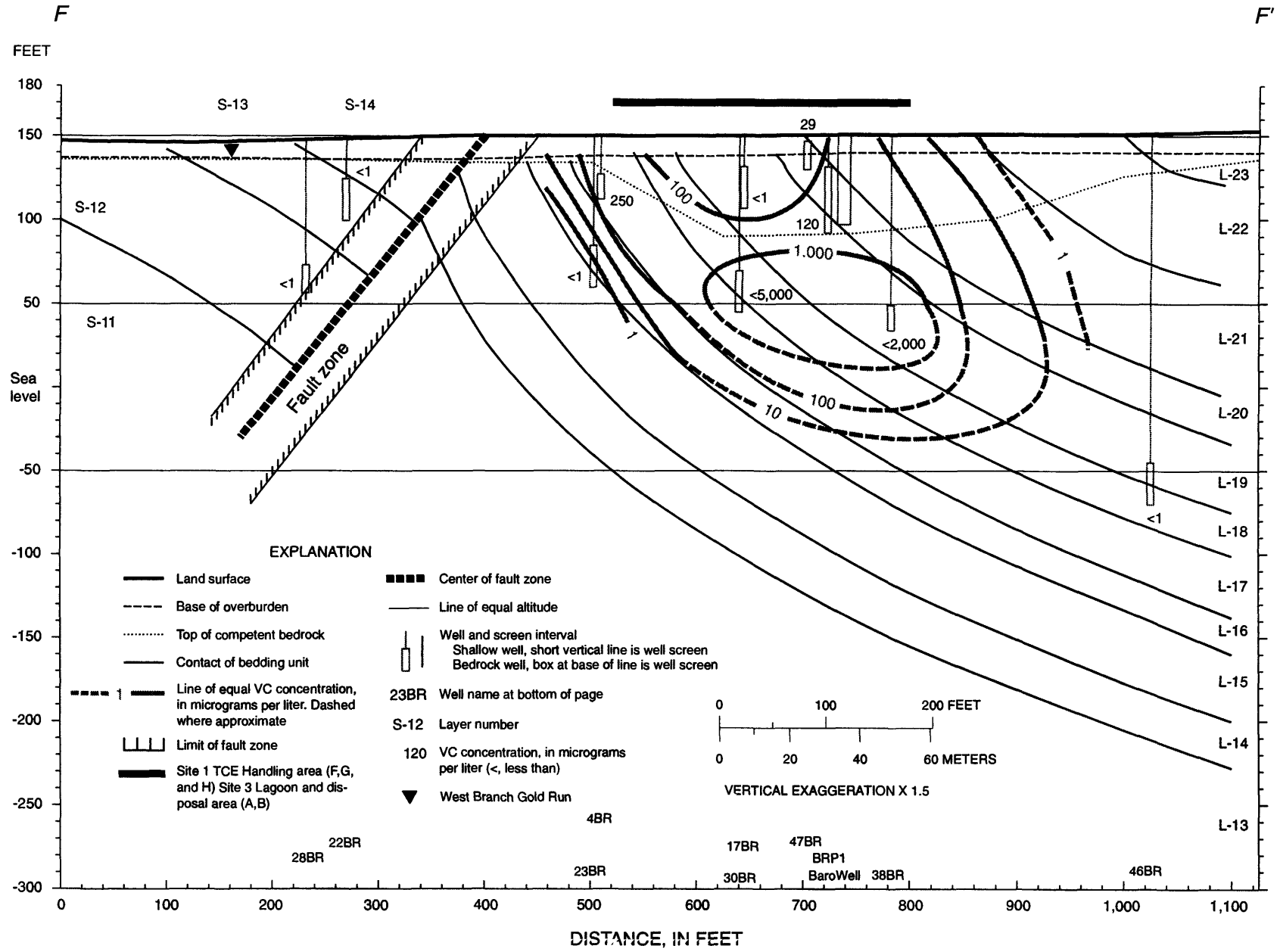

Figure 101. Section *F-F'* showing VC concentrations in water samples from bedrock wells, June 1997.

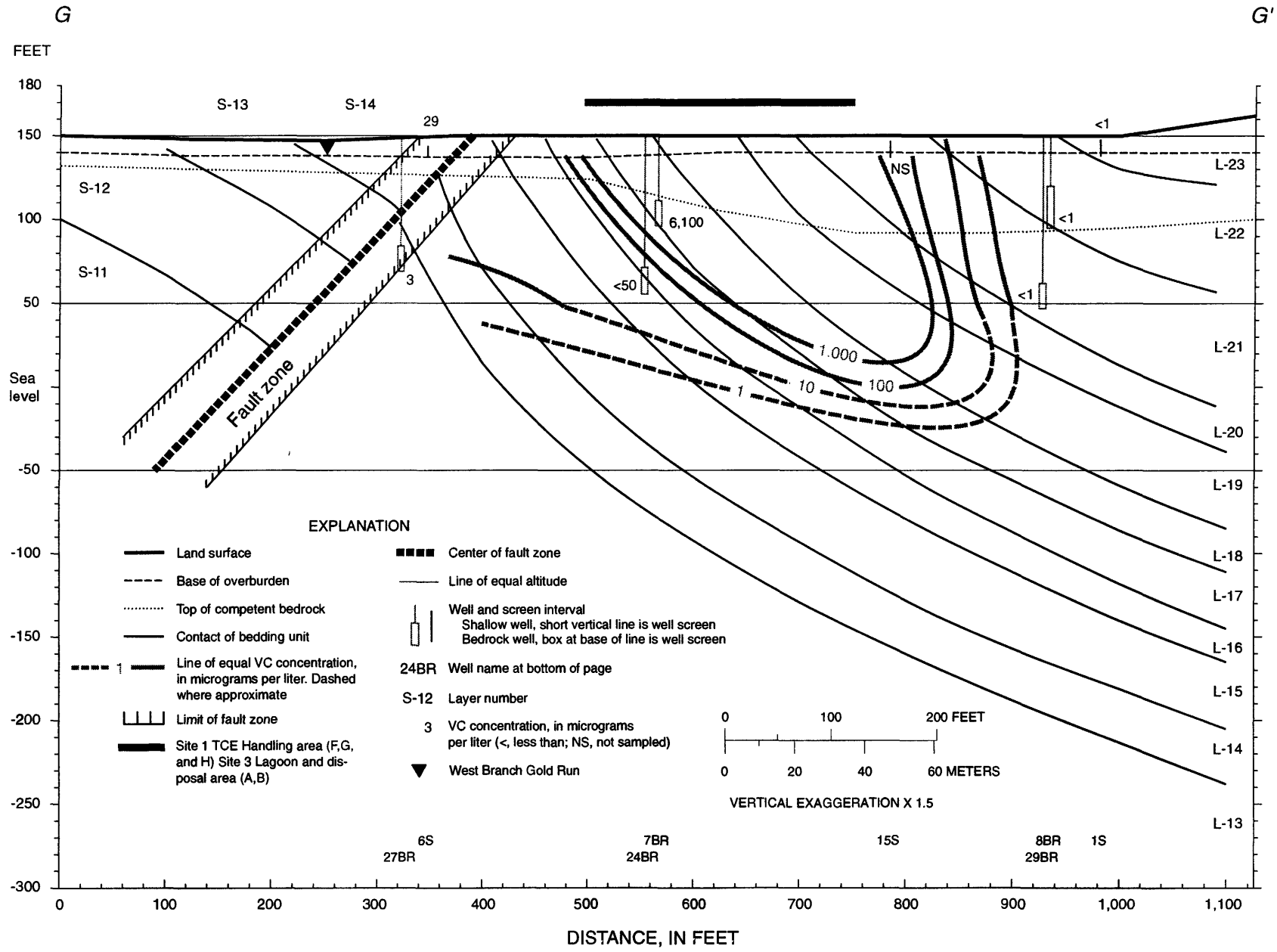

Figure 102. Section *G-G'* showing VC concentrations in water samples from bedrock wells, June 1997.

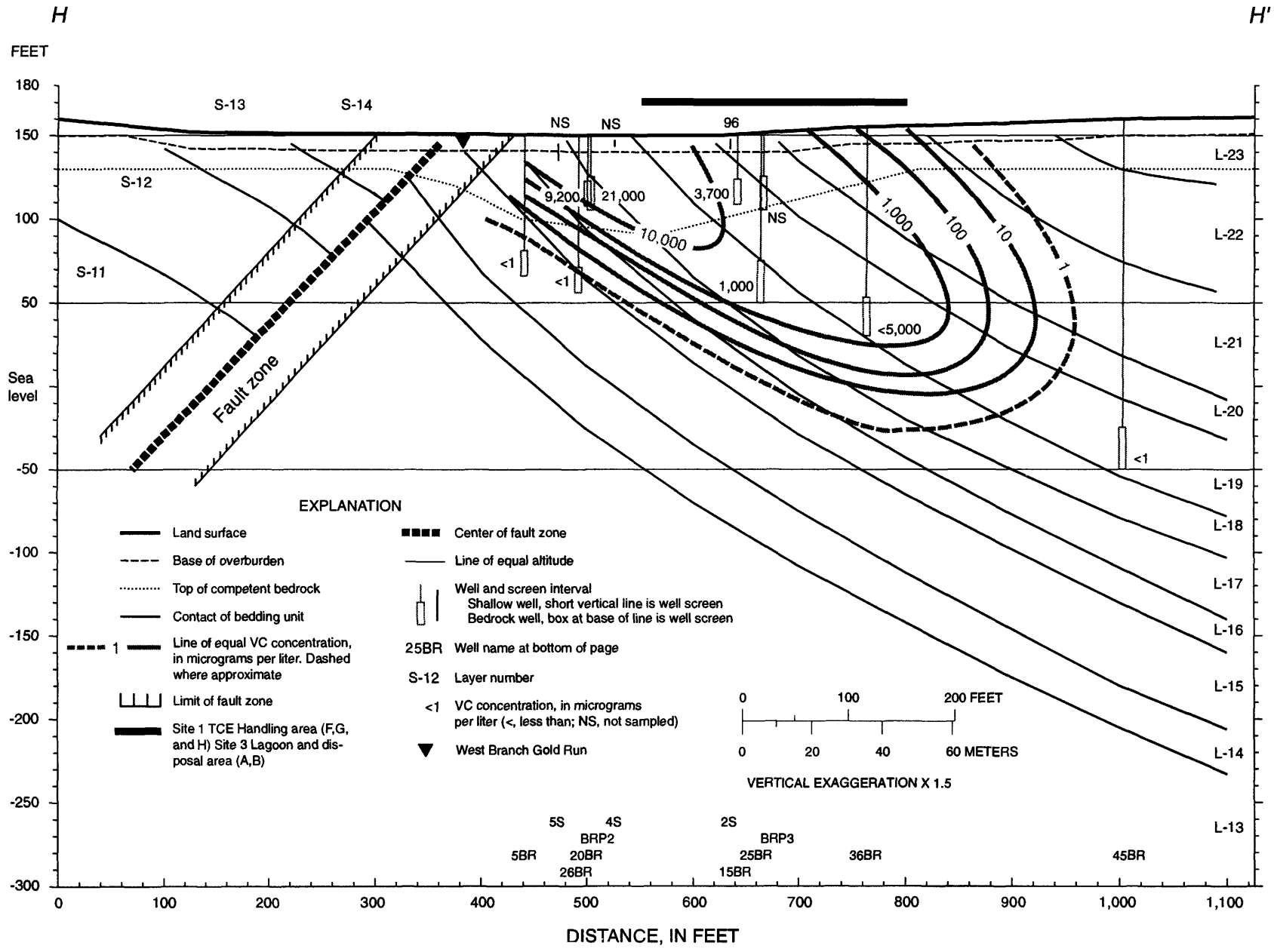

Figure 103. Section *H-H'* showing VC concentrations in water samples from bedrock wells, June 1997.

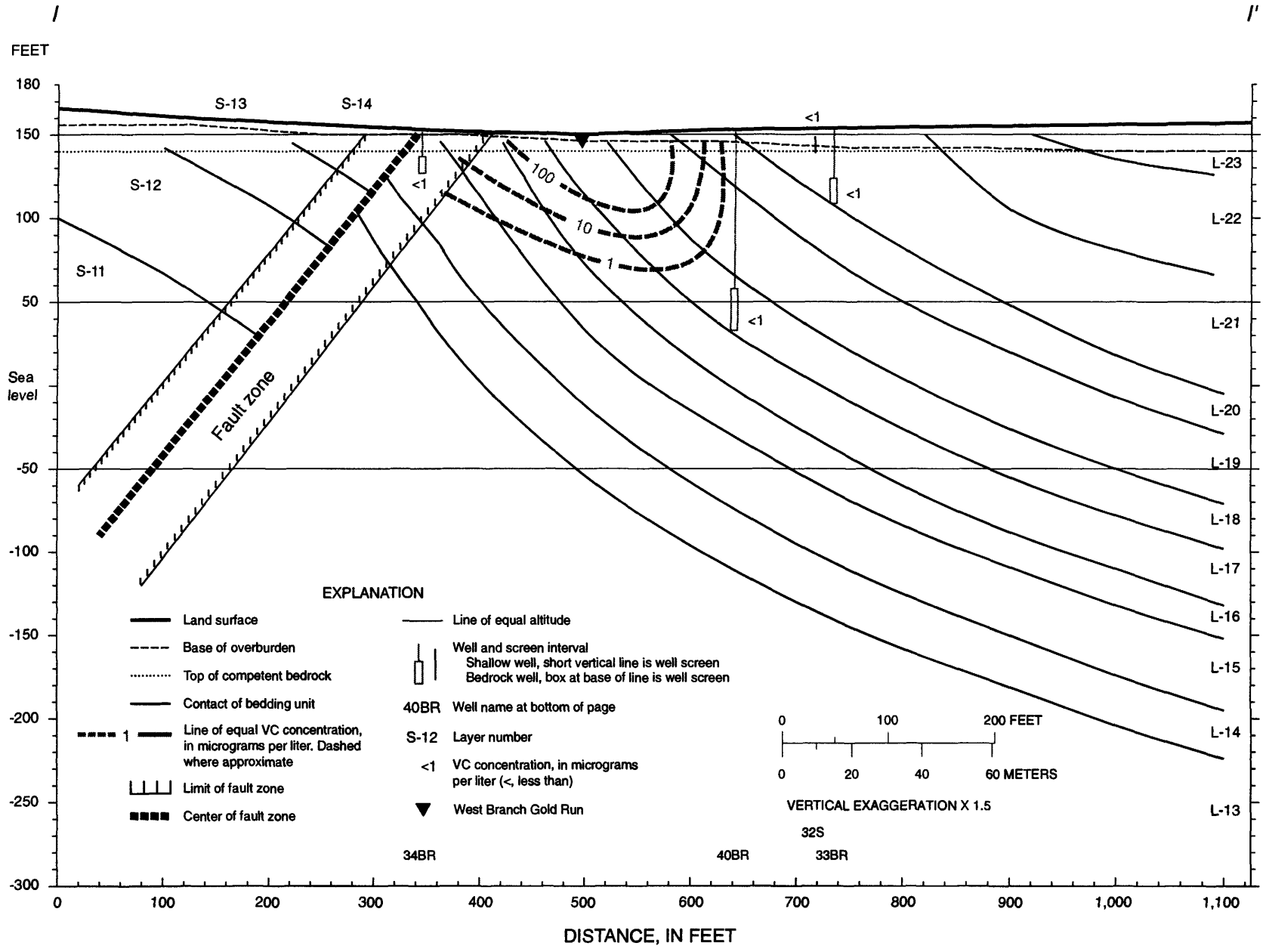

Figure 104. Section *I-I'* showing VC concentrations in water samples from bedrock wells, June 1997.

Site 3: Lagoon and Sludge Disposal Area

Concentrations in the VC plume in the Site 3 area were less than 7 µg/L in 1997. The plume is limited to the area directly below the former lagoon. The VC plume does not appear to have moved down gradient to the southwest nor was it detected under the sludge disposal area.

Area between Site 3 and Site 1

North of the Building 21 area, the concentrations of VC in wells 16BR and 41BR were 26 and 10 µg/L respectively. VC concentrations in well 16BR were 12 to 62 µg/L in three sampling events during 1993, and well 41BR was not sampled before. These concentrations indicate some degradation of cis-DCE to VC in bedding unit L-19.

Site 1: Brine-Handling Area

The maximum concentration of VC in the Site 1 area was 21,000 µg/L in well BRP2 in 1997. Wells 20BR showed VC concentrations of 9,100 µg/L. The wells are screened in bedding unit L-17. The center of the VC plume at land surface (fig. 93) is about 200 to 300 ft west of the center of the TCE plume (fig. 69) and about 100 ft west of the center of the cis-DCE plume (fig 81). The VC plume is interpreted to be moving southwestward with ground-water flow toward the West Branch of Gold Run.

Well 4BR showed a VC concentration of 250 µg/L in 1997. The well also is screened in bedding unit L-17. Wells BRP1, 16BR, and 41BR form a northeast limb of the Site 1 VC contamination area. Well BRP1 is in bedding units L-19 and L-20, whereas wells 16BR and 41BR are in bedding units L-19. This arm of the Site 1 VC plume is interpreted to be controlled by some aspect of the bedding units, but it is not understood which aspect of degradation and ground-water flow is controlling the higher concentrations of VC in this bedding.

There is very little concentration of VC at depth (fig. 95); therefore, the conditions are not optimal for degradation at depth. There is no reported VC south of the fault in 1997. Water samples collected during 1992-93 and 1995 also showed VC concentrations below detection limits.

SUMMARY AND CONCLUSION

The hydrogeologic framework was evaluated and water-level and water-quality data were analyzed as part of an investigation of trichloroethylene (TCE) contamination of ground water at two sites at the Naval Air Warfare Center (NAWC) in West Trenton, N.J.

The hydrogeologic framework consists of upper strata of the Stockton Formation and the lower strata of the Lockatong Formation with an east/west-trending fault. The Stockton Formation has been divided into 5 bedding units and the Lockatong Formation has been divided into 14 bedding units. The bedding units are based on the signature of gamma-ray logs, rock type, and rock color. The strike of the bedding units of the Stockton Formation and the Lockatong Formation are N70°E and N65°E, respectively. The general dip of each formation is about 15° to 30° NW in areas that are more than 300 ft from the fault. Close to the fault the bedrock dip increases to 70° NW. The Stockton Formation is the Stockton aquifer; the Lockatong Formation is the Lockatong aquifer. The Stockton and Lockatong aquifers are made up of a number of water-bearing zones and semi-confining zones.

The east/west-trending fault has been mapped (prior to the investigation reported here) as a gradational contact between the Stockton and the Lockatong Formations. The fault strikes roughly N70°E, similar to the strike of the bedrock, and dips about 40° SE. The fault separates the two formations-- the

Lockatong predominantly to the north, and the Stockton predominantly to the south-- and acts as a confining unit.

Static water-level maps at land surface show an apparent regional hydraulic gradient to the south. Because actual ground-water flow is within the bedding-plane partings and near-vertical partings in the bedrock, however, the true flow direction on the north side of the fault is westward toward the West Branch of Gold Run and the Delaware River. The flow direction on the south side of the fault is toward the West Branch of Gold Run. The fault inhibits the direct flow of water from the Lockatong aquifer into the Stockton aquifer. Ground water from the Lockatong aquifer discharges into the West Branch of Gold Run in a spring west of NAWC and flows overland to the Stockton aquifer.

Water-level drawdowns that resulted from aquifer tests in the Lockatong aquifer show elongate cones of depression around pumped wells; therefore, the aquifer is anisotropic. Water levels in selected water-bearing zones of the aquifer shows circular or near circular cones of depression around the pumped wells; therefore, these water-bearing zones are isotropic or nearly so. The drawdown water-levels maps and sections show that water withdrawal from one bedding unit will cause drawdown most readily in wells screened in the same unit. The same maps and sections show that the shallower part of the bedding units is probably more fractured but less permeable than the deeper part of the bedding unit. Stressed water levels, as a result of operation of the recovery well created an elongate cone of depression, but the cone does not encompass the whole TCE contamination plume of the brine handling area (Site 1).

Water-quality data from Lockatong aquifer shows that TCE flowed from the source areas downward. In the lagoon and sludge-disposal area (Site 3), the dissolved TCE flowed from the area in a southwestward direction along the north side of the fault. In the Site 1 area, dense non-aqueous phase liquid (DNAPL) trichloroethylene (TCE) flowed downward into the bedrock aquifer; however, DNPAL TCE has not been found in water samples from the aquifer. Two possible scenarios for the fate of the DNAPL TCE are (Scenario 1) that the DNAPL TCE sank to a depth of about 300 ft below land surface or (scenario 2) that the DNAPL TCE dissolved and degraded by a depth of 100 ft below land surface. In Scenario 1, the plume of DNAPL TCE is not deeper than about 300 ft below land surface because the partings are closed at those depths. The DNAPL TCE at depth dissolves very slowly because there is very limited ground-water flow. Data show there are very little cis 1,2-dichloroethylene (cis-DCE) and vinyl chloride (VC) at depth when compared to the shallow aquifer; therefore, there is little degradation of the dissolved TCE at depth.

cis-DCE and VC were not used during routine operation at NAWC, and cis-DCE and VC in the aquifer is a result of degradation of TCE. High levels of cis-DCE and VC in the shallow part of the aquifers indicate that degradation of TCE is occurring there, whereas low levels of cis-DCE and VC in the deep part of the aquifer indicates that little degradation is occurring there. The center of the cis-DCE and VC plumes are about 100 and 200 ft, respectively, west of the center of the TCE plume.This indicates that ground-water-flow direction is westward toward the West Branch of Gold Run.

REFERENCES CITED

Chappell F. H., 1993, Ground-water microbiology and geochemistry: New York, John Wiley & Sons, Inc., 424 p.

EA Engineering, Science, and Technology, Inc., 1995, Site 1 Interim action well monitoring at Naval Air Warfare Center, New Jersey. Reports 1, 2, 3, and 4: Berkeley Heights, N.J., EA Engineering, Science, and Technology, Inc., about 100 pages.

_____ February 1996, Site 1 Interim action well monitoring at Naval Air Warfare Center Trenton, New Jersey; Report 5: Berkeley Heights, N.J., EA Engineering, Science, and Technology, Inc., about 100 pages.

_____ June 1996, Draft Site 1 Focused Feasibility Study Site Safety, Health, and Emergency Response Plan for the Naval Air Warfare Center Trenton, New Jersey: Berkeley Heights, N.J., EA Engineering, Science, and Technology, Inc., about 100 pages.

_____ July 1996, Final 1995 Aquifer test report for Naval Air Warfare Center Trenton, New Jersey: Berkeley Heights, N.J., EA Engineering, Science, and Technology, Inc., about 100 pages.

_____ August 1997, Ground water sampling report NAWC Trenton (Ewing Township), New Jersey: Berkeley Heights, N.J., EA Engineering, Science, and Technology, Inc., about 100 pages.

International Technology Corporation, November 1994, Remedial Investigation Report, Installation Restoration Program, Naval Air Warfare Center Trenton, New Jersey: Edison, N.J., International Technology Corp., contract N624-86-c-1041 IT project Number 529538, 529658, 6 volumes.

Lyttle, P.T., and Epstein, J.B., 1987, Geologic map of the Newark 1° x 2° quadrangle, New Jersey, Pennsylvania and New York: U.S. Geological Survey Miscellaneous Investigations Series Map I-1715, 2 sheets.

Mercer County Highway Department, 1942, Parkway Avenue construction map, File A, Pocket 14, Folder 1 to 3 unpublished maps, available at County building, East State St., Trenton, N.J.

New Jersey Department of Environmental Protection, 1913, New Jersey Atlas Sheet 27, Original Survey 1885, principle features revised 1913: Trenton, N.J., New Jersey Department of Environmental Protection, 1 sheet.

Vecchioli, John, and Palmer, M.M., 1962, Ground-water resources of Mercer County, New Jersey: New Jersey Department of Conservation and Economic Development Special Report 19, 71 p.

U.S. Geological Survey, 1979, Aeroradioactivity map of parts of Delaware and New Jersey: U.S. Geological Survey Open-File Report 79-1683, 2 sheets.